DISSERTATION

FRACTIONAL TRANSPORT OF BED-MATERIAL LOAD IN SAND-BED CHANNELS

Submitted by

Baosheng Wu

Department of Civil Engineering

In partial fulfillment of the requirements

for the Degree of Doctor of Philosophy

Colorado State University

Fort Collins, Colorado

Spring 1999

COLORADO STATE UNIVERSITY

DECEMBER 7, 1998

WE HEREBY RECOMMEND THAT THE DISSERTATION PREPARED UNDER OUR SUPERVISION BY **BAOSHENG WU** ENTITLED **FRACTIONAL TRANSPORT OF BED-MATERIAL LOAD IN SAND-BED CHANNELS** BE ACCEPTED AS FULFILLING IN PART REQUIREMENTS FOR THE DEGREE OF DOCTOR OF PHILOSOPHY.

Committee on Graduate Work

Pierre Julien

Chester C. Watson

Freeman M. Smith

Albert Molinas

Advisor

Department Head/Director

ABSTRACT OF DISSERTATION

FRACTIONAL TRANSPORT OF BED-MATERIAL LOAD IN SAND-BED CHANNELS

This dissertation presents a new method for predicting fractional transport rates of bed-material load in sand-bed channels. The proposed method is developed based on the concept of the transport capacity fraction (TCF) approach. The bed-material concentration for a given size fraction is obtained by weighting the bed-material concentration, C_t, with a transport capacity distribution function, P_{ci}. The procedure and a detailed example problem showing the use of the proposed method are provided.

Two transport capacity distribution functions are developed. The first function is in terms of relative fall velocity. This function is derived from the unit stream power theory and the concepts of the TCF approach and the bed material fraction (BMF) approach. The second function is in terms of relative diameter. It is derived from the Engelund and Hansen's transport relations and the concepts of the TCF approach and the BMF approach. The sheltering and exposure effects are considered in both functions. The coefficients in both functions were calibrated using 118 sets of flume and field data (891 data points) falling in sand sizes. The formulations using relative diameter is suggested for practical applications because of its simplicity (no need for relative fall velocity computations).

For the computation of bed-material concentrations, the effect of size gradations on the transport of sediment mixtures is investigated in detail. First, a new relationship is proposed for predicting the median diameter, D_{50t}, of bed-material load. This equation is developed based on the 118 sets of data used for the development of transport capacity distribution functions plus 280 sets of CSU flume data. Then, the effect of size gradation on the transport of sediment mixtures is demonstrated by the use of Engelund and Hansen's transport function and Yang's unit stream power function. To account for size gradation effects, the newly developed expression for the median diameter, D_{50t}, is proposed for use as the representative size in bed-material load computations. For the existing bed-material load equations, an equivalent diameter, D_e, is proposed. This equivalent diameter, which is related to D_{50t}, is incorporated into the Engelund and Hansen, Ackers and White, and Yang formulas for the computation of bed-material concentrations.

The proposed method is compared with various existing fractional transport methods using 118 sets of measurements (891 data points) and verified using 48 sets of independent data (327 data points). Comparison and verification indicate that the proposed method provides better predictions for fractional bed-material concentrations and size fractions of sediment in transport.

Baosheng Wu
Civil Engineering Department
Colorado State University
Fort Collins, Colorado 80523
Spring, 1999

ACKNOWLEDGEMENTS

The author wishes to express his sincere gratitude and appreciation to his major advisor, Dr. Albert Molinas, for his inspiration, guidance, and encouragement he provided throughout the course of this work.

The author also wishes to express his appreciation to the members of his committee, Dr. P. Y. Julien, Dr. T. K. Gates, and Dr. F. M. Smith, for their valuable comments and review of the dissertation.

Special appreciation is extended to Mr. Yuqian Long for his help and encouragement. Also, a great deal of thanks is due to Dr. Junke Guo for his useful discussion, encouragement, and friendship.

Finally, my deepest gratitude goes to my wife, Chunying, and my son, Tuo, for their patience, sacrifice, understanding, and continual support and encouragement throughout this research. All this has made my goal possible and worthwhile.

TABLE OF CONTENTS

LIST OF TABLES

LIST OF FIGURES

Figure | Page

LIST OF SYMBOLS

The following symbols are used in the text:

A = coefficient;

AGD = average geometric deviation between computed and measured values;

B = coefficient;

C, C_1, C_2 = coefficients;

C_T = concentration of total sediment load;

C_t = concentration of bed-material load;

C_{ti} = concentration of bed-material load corresponding to the size fraction i;

C_{pi} = potential concentration of bed-material load corresponding to the size fraction i, using D_i as if it exists alone;

C_{tc}, C_{tm} = computed and measured bed-material concentrations, respectively;

C_{tci}, C_{tmi} = computed and measured bed-material concentrations, respectively, corresponding to the size fraction i;

D = diameter of bed material;

D_A = scaling size defined by White and Day;

D_a = arithmetic mean diameter of sediment mixtures;

D_w = wash load limit diameter;

D_e = equivalent diameter defined by Eq. (4.6);

D_{gr} = dimensionless grain diameter defined by Ackers and White;

D_{gri} = dimensionless grain diameter corresponding the size fraction i;

D_i = representative diameter (geometric mean) of bed material corresponding to the size fraction i;

D_m = mean diameter of bed material;

D_n = scaling size;

D_p = particle sizes for which p percent of bed material is finer by dry weight;

D_s = representative diameter for suspended load computations;

D_{50t} = median diameter of bed-material load;

d = average flow depth;

F_{gri} = mobility number corresponding to the size fraction i;

F_r = Froude number;

f = general function;

f' = friction factor defined by Engelund and Hansen;

G = size gradation coefficient of bed material = $(D_{84}/D_{50} + D_{50}/D_{16})/2$;

g = gravitational acceleration;

I = coefficient;

I_1, I_2 = integrals of Einstein's form of the suspended sediment equation;

i = size fraction number or data point number in a data set;

J = coefficient;

JN = total number of data points;

K_d = coefficient;

K_e = coefficient;

M = Kramer's uniformity coefficient for sediment mixtures;

MNE = mean normalized error;

m = coefficient;

N = number of size fractions present in a sediment mixture;

n = coefficient;

P_{ai} = areal function of bed material defined by Karim;

P_{bi} = fraction of bed material, by dry weight, corresponding to the size fraction i;

P_{ci} = fraction of bed-material transport capacity, by dry weight, corresponding to the size fraction i;

P_{cci} = percentage of computed bed-material load, by dry weight, corresponding to the size fraction i;

P_{cmi} = percentage of measured bed-material load, by dry weight, corresponding to the size fraction i;

P_{si} = fraction of suspended load, by dry weight, corresponding to the size fraction i;

q_t = bed-material load per unit width by dry weight;

q_{ti}, q_{bi}, q_{si} = bed-material load, bedload, and suspended load, respectively, per unit width by dry weight corresponding to the size fraction i;

R, R′ = hydraulic radius and hydraulic radius associated with grain roughness, respectively;

R = discrepancy ratio between computed and measured bed-material concentrations;

R_i = discrepancy ratio between computed and measured fractional bed-material concentrations corresponding to the size fraction i;

S = energy slope;

s_g = specific gravity = γ_s / γ;

T = transport stage parameter;

V = flow velocity;

V_{cr} = critical velocity at incipient motion;

V_* = shear velocity = $\sqrt{\tau / \rho} = \sqrt{gRS}$;

W_i = hiding factor introduced by Karim and Kennedy;

α, β = coefficients;

γ, γ_s = specific weight of water and sediment, respectively;

Δ = apparent roughness of the bed surface;

δ' = laminar sublayer thickness due to grain roughness;

$\varepsilon_{ti}, \varepsilon_{bi}, \varepsilon_{si}$ = correction factors for critical shear stresses to account for the sheltering and exposure effect for bed-material load, bedload, and suspended load, respectively;

ζ = coefficient;

η = sheltering parameter;

θ = dimensionless shear parameter = $\tau / [(\gamma_s - \gamma)D]$;

θ_c = critical dimensionless shear parameter = $\tau_c / [(\gamma_s - \gamma)D]$;

θ_{ci} = critical dimensionless shear parameter corresponding to the size fraction i = $\tau_c / [(\gamma_s - \gamma)D_i]$;

θ_e = dimensionless shear parameter using equivalent diameter, D_e;

θ_i = dimensionless shear parameter corresponding to the size fraction i = $\tau / [(\gamma_s - \gamma)D_i]$;

κ = von Kàrmàn constant;

ν = kinematic viscosity;

ξ_i = Einstein's sheltering parameter;

$\xi_{ti}, \xi_{bi}, \xi_{si}$ = correction factors for effective shear stresses to account for the sheltering and exposure effect for bed-material load, bedload, and suspended load, respectively;

σ_g = geometric standard deviation of bed material = $\sqrt{D_{84} / D_{16}}$;

τ, τ_0 = shear stress along the bed = $\gamma RS \approx \gamma dS$;

τ_c = critical shear stress;

τ_{ci} = critical shear stress corresponding to the size fraction i;

τ' = grain shear stress = $\gamma R' S$;

Φ_t = dimensionless sediment transport function;

Φ_e = dimensionless sediment transport function using equivalent diameter, D_e.

$\Phi_{ti}, \Phi_{bi}, \Phi_{si}$ = dimensionless sediment transport function corresponding to the size fraction i for bed-material load, bedload, and suspended load, respectively;

ϕ_i = weighting function for *i*th fraction of a sediment mixture;

$\overline{X}$ = scaling size of the sediment mixture defined by Einstein;

ω_e = equivalent fall velocity corresponding to the equivalent diameter of D_e;

ω_n = scaling fall velocity corresponding to the scaling size of D_n;

ω_i = fall velocity of sediment corresponding to the particle size of D_i; and

ω_{50} = fall velocity of sediment corresponding to the particle size of D_{50};

CHAPTER 1

INTRODUCTION

1.1 BACKGROUND

The transport of nonuniform sediment mixtures is more complicated than the transport of uniform sediment because both the condition for initiation of motion of a given size of sediment and its transport rate are affected by the presence of other sizes in the mixtures. The coarser particles on the bed are exposed more to the action of flow past them and act like isolated roughness elements. On the other hand, the finer fractions are sheltered in the wakes of the coarser fractions. These mechanisms cause the entrainment and transport of different size fractions, in the case of nonuniform mixtures, to deviate from the behavior of uniform sediments. Generally the finer fractions are transported at a relatively lower rate than if they were in a uniform sediment bed, and the coarser particles consequently are transported at a higher rate.

Transport of uniform sediments in open channels has been extensively investigated for decades and is reasonably well understood at present. However, the subject of fractional transport of nonuniform sediment mixtures is still very challenging because of its complexity. Starting from Einstein (1950), many attempts including field measurements, laboratory studies, empirical and theoretical analysis, and numerical simulations have been made in the past to understand the mechanisms of nonuniform sediment transport and to predict the bed-material transport rates by size fractions. However, prediction of sediment transport rates by size fractions has not been accomplished following a purely analytical method. All existing fractional sediment transport methods have been established relying on calibration using limited flume and field data collected under so-called steady uniform flow conditions. When different methods were applied to a given river, computed results of fractional transport rates could vary drastically from each other and from actual measurements.

In alluvial river simulation models, computation of sediment transport rates for individual size fractions is one of the key elements in the case of nonuniform sediment mixtures (Wu and Molinas, 1996). Especially for those models involved in the simulation of the change of bed material composition, sediment sorting processes, and bed armoring, accurate prediction of fractional transport rates is essential for their successful implementation in natural rivers. Unfortunately, none of the existing methods satisfactorily predicts fractional transport rates of nonuniform sediment mixtures in open channels. It is of practical importance to develop a reliable prediction method of fractional transport rate for the implementation of numerical models in more sophisticated problems encountered in natural rivers.

1.2 OBJECTIVES

The primary objective of this study is to investigate the mechanics of fractional transport and to present a procedure for predicting the fractional transport rate of bed-material sediments in sand-bed channels. The proposed methodology should be theoretically sound and practically applicable. The study also includes a comprehensive analysis of the differences and relationships between the transported sediment size composition and the bed material size composition, and an intensive investigation of the effect of size gradations on the bed-material transport of sediment mixtures.

1.3 SCOPE OF WORK

Bed-Material Load Concept

There are two common classifications of total sediment load in a stream, as shown in Fig. 1.1. By the type of movement, the total sediment load can be divided into bedload and suspended load; by the source of sediment, the total sediment load is separated into the supply-limited wash load and the capacity-limited bed-material load (Julien, 1995). Bedload refers to the transport of sediment particles that frequently maintain contact with the bed. Suspended load, by definition, moves in suspension. Wash load refers to the finest portion of sediment not found with a significant amount in the bed, for which sediment transport is limited by the upstream supply of fine particles and is generally not correlated with the hydraulic

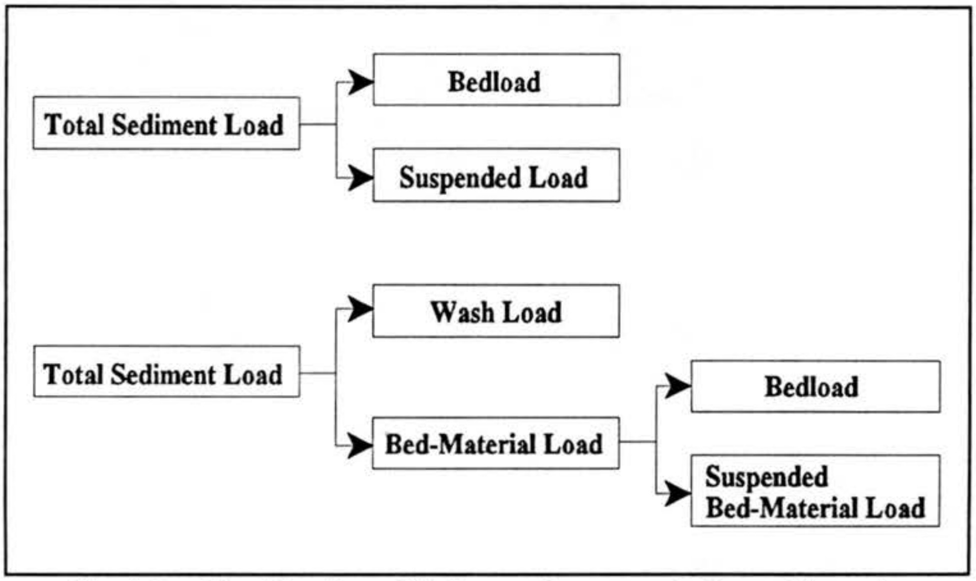

Fig. 1.1. Classification of Sediment Transport in Open Channels.

characteristics of a river. The bed-material load consists of particles generally found in the bed and can be predicted by the transport capacity of the stream. Bed-material load can also be defined as the sum of bedload and suspended bed-material load.

In flume experiments (except in special cases), wash load is almost invariably absent, and total sediment load would be the bed-material load. On the other hand, in natural rivers, wash load is invariably present, and the total sediment load is the summation of the bed-material load and the wash load. In these cases, wash load should be subtracted from the measurements for the analysis and comparison of bed-material load.

A sediment particle may be transported as bedload at one time and as suspended load at another time or location. Considering the dynamics of sediment movement, the process of suspension may be visualized as an advanced stage of traction along the bed; therefore the total sediment transport rate should be related primarily to the shear parameter, and no distinction needs to be made between bedload and suspended load (Garde and Ranga Raju, 1985). Raudkivi (1990) argued that once the suspension phase of transport has developed, the distinction is less meaningful, although there would still be particles which roll and slide on the bed as bedload. In the case of nonuniform sediments, the finer sizes of the bed material may move predominantly in suspension, while the coarser fractions of the bed material may move mostly as bedload. Distinction between bedload and suspended load becomes more difficult and unnecessary for nonuniform sediment mixtures. In practice, we are interested in the bd-material load, not in how much is transported in which mode. Therefore, the bed-material load, without dividing it into bedload and suspended bed-material load, will be considered for the determination of sediment transport capacity in natural rivers.

Sediment Size

The size of sediment particles is one of the most important physical properties in transportation. Sediment sizes, along with the flow conditions, determine the manner of sediment movement (such as the fall velocity, cohesion, initiation of motion of particles, mode of sediment movement, and so on) in a stream. Generally in mountain streams with gravel-bed, sediments are mostly transported as bedload, while in alluvial rivers with sand-bed, sediments are mainly transported as suspended load. This study focuses on the fractional transport of sediment mixtures in the sand range without cohesive effect. Most of the nonuniform sediment transport experiments which included the measurement of both bed material size distribution and bed-material load size distribution were conducted in sand-bed flumes. These experimental data are necessary for the analysis and development of a transport equation in the sand range.

Transport capacity

The sediment transport capacity is defined as the amount of sediment that is transported by a stream in equilibrium conditions for given conditions of flow and sediment. Equilibrium conditions refer to a flow for which neither erosion nor deposition occurs along the channel. Equilibrium of sediment transport is a result of the balance between the transport capacity of a flow and the sediment load carried by the flow, which can be only achieved under constant sediment supply and uniform flow or gradually-varied flow conditions. Sediment transport rate in a river is not necessarily equal to the transport capacity of the flow. If the supply of sediment is larger than the transport capacity, aggradation occurs. Conversely, if in a sand-bed river the supply of sediment is less than the transport capacity, degradation and associated fluvial processes will alter the channel until a new equilibrium condition is achieved. Throughout this study, we will consider the sediment transport capacity or sediment transport rate in equilibrium conditions, not the sediment transport during the processes of aggradation or degradation.

1.4 DISSERTATION OUTLINE

This dissertation includes six chapters. Chapter 1 presents an introduction to the dissertation, including the background, objectives, and scope of work. Chapter 2 comprises a comprehensive review of the available literature addressing the problem and theories under investigation.

Chapter 3 presents the development of new transport capacity distribution functions, including their theoretical derivation, physical consideration, and calibration.

Chapter 4 discusses the variation of sediment sizes in transport, the effect of size gradation on the transport of sediment mixtures, and the use of a representative diameter in bed-material load predictions.

Chapter 5 tests the proposed fractional bed-material load computation methodology through comparison with other fractional load computation methods based on flume and field data.

Finally, Chapter 6 summarizes the main results and conclusions drawn out of the study coupled with recommendations.

CHAPTER 2

LITERATURE REVIEW

2.1 GENERAL

In order to predict the response of mixed-size sediment to flow (initiation of motion, hydraulic sorting, bed armoring, evolution of stream bed), it is necessary to predict the transport rates of the individual size fractions in the mixture, which is essential in numerical models such as HEC-6 (U.S. Corps of Engineers, 1977; Thomas, 1982), GSTARS (Molinas and Yang, 1986), BRI-STARS (Molinas, 1990, Molinas and Trent, 1991), IALLUVIAL (Karim and Kennedy, 1982; Dorough, Holly, and Wei, 1988), CHARIMA and SEDICOUP (Holly, 1988), and other sediment transport models (Han, 1973, 1980; Ribberink, 1987; Wu, 1992b; Zhang and Wu, 1993; and Qu et al., 1994). Recently, research on the fractional transport of sediment mixtures has become very active due to its practical significance in numerical models to simulate the change of bed composition, hydraulic sorting, and bed armoring of rivers with nonuniform sediment mixtures. In 1991, a seminar on grain sorting was held at the Center Stefano Franscini on Monte Verità in Ascona, Switzerland (Vischer, 1992), which presented the progress and further needs in research concerning transport process of individual size fractions and the hiding and exposure effect between different sizes.

Fractional transport of nonuniform sediment mixtures has intrigued scientists for decades. Einstein (1950) and Einstein and Chien (1953) started the study of fractional transport of nonuniform sediment mixture in the early fifties. Following Einstein, many attempts including field observations, laboratory studies, empirical and theoretical analysis, and numerical simulations have been made to attempt to understand the mechanisms of transport process for sediment mixtures and to predict the transport rates for individual size fractions. The research has covered the fractional transport processes of both sand- and gravel-bed materials. Even though the current research of fractional load transport concentrates on the sand-bed materials, relevant works on gravel-bed materials will be also discussed in this literature review.

2.2 CLASSIFICATION

From the theoretical point of view, and based on the treatment in formulations and the physical considerations in the development, the extensive literature on fractional sediment transport can be classified into four categories (Wu and Molinas, 1996):

- Direct computation by the size fraction approach;
- Shear stress correction approach;
- Bed Material Fraction approach (BMF); and
- Transport Capacity Fraction approach (TCF).

Direct computation by the size fraction approach

Direct computation by the size fraction approach aims at computing sediment transport rates for each size fraction present in nonuniform mixtures. After the computation of transport capacities corresponding to each size group, the bed-material load is calculated by the summation of fractional sediment transport rates from

$$q_t = \sum_{i=1}^{N} q_{ti} \quad or \quad C_t = \sum_{i=1}^{N} C_{ti} \tag{2.1}$$

in which q_t = bed-material load per unit width by dry weight; C_t = concentration of bed-material load; N = number of size fractions present in the sediment mixture; and subscript i denotes the size fraction number in a mixture.

Shear stress correction approach

The shear stress correction approach focuses on extending a uniform sediment transport formula or a bed-material transport rate formula to fractional transport rate for nonuniform sediment mixtures. In doing so, the actual shear stresses acting on each size fraction or the critical shear stresses for each size fraction are corrected by introducing a correction factor. This approach may be written as

$$\Phi_{ti} = P_{bi} f(\xi_{ti} \theta_i) , \qquad q_t = \sum_{i=1}^{N} q_{ti} \tag{2.2}$$

or

$$\Phi_{ti} = P_{bi} f(\theta_i - \varepsilon_{ti} \theta_{ci}) , \qquad q_t = \sum_{i=1}^{N} q_{ti} \tag{2.3}$$

in which f = general functional relationship; P_{bi} = fraction of bed material by dry weight corresponding to size fraction i; Φ_{ti} = dimensionless sediment transport function corresponding to size fraction i; θ_i = dimensionless shear stress corresponding to size fraction i; θ_{ci} = critical dimensionless shear stress corresponding to size fraction i; and ξ_{ti}, ε_{ti} = correction factors accounting for the sheltering and exposure effect. Parameters of Φ_{ti},

θ_i, and θ_{ci} are expressed as follows, respectively

$$\Phi_{ti} = \frac{q_{ti}}{\gamma_s \sqrt{\frac{\gamma_s - \gamma}{\gamma} g D_i^3}} \tag{2.4}$$

$$\theta_i = \frac{\tau}{(\gamma_s - \gamma) D_i} \tag{2.5}$$

$$\theta_{ci} = \frac{\tau_{ci}}{(\gamma_s - \gamma) D_i} \tag{2.6}$$

in which D_i = the representative diameter of bed material corresponding to size fraction i; g = gravitational acceleration; γ, γ_s = specific weight of water and sediment, respectively; τ = shear stress along the bed; and τ_{ci} = critical shear stress along the bed corresponding to size fraction i. Note that the dimensionless sediment transport functions for bedload, Φ_{bi}, and suspended load, Φ_{si}, are obtained by replacing q_{ti} in Eq. (2.4) with q_{bi} or q_{si}, respectively. The corresponding correction factors for bedload and suspended load are referred to as ξ_{bi} and ξ_{si} in Eq. (2.2) and ε_{bi} and ε_{si} in Eq. (2.3), respectively.

The product $\xi_{ti}\theta_i$ in Eq. (2.2) is believed to be the actual or effective dimensionless shear stress acting on the particles of size fraction i in a mixture, while $\varepsilon_{ti}\theta_{ci}$ in Eq. (2.3) may be regarded as the effective critical shear parameter. Correction with ξ_{ti} is to reduce the value of shear stress for the finer fractions and to increase the value for the coarse fractions. Conversely, correction with ε_{ti} is to increase the value of critical shear stress for the finer fractions and to reduce the value for the coarse fractions. These corrections result in a similar effect, viz. a reduction of the transport rate of the smaller sizes and increase of the transport rate of the larger sizes. There is no reason to suppose $\xi_{ti} = \varepsilon_{ti}$.

The BMF approach

The BMF approach relates the fractional transport rates directly to the size distribution of bed material. It assumes that a channel bed can be considered as a hypothetical mixture of sediment particles; the mixture can be formed into class intervals by size, and a potential transport capacity can be calculated for each class interval, whether or not particles are physically present. Subsequently, particle availability can be evaluated and expressed as P_{bi}. Availability and potential transport capacity can then be combined to give transport capacity as follows

$$C_{ti} = P_{bi} C_{pi} , \quad C_t = \sum_{i=1}^{N} C_{ti} \tag{2.7}$$

in which C_{pi} = potential concentration for size fraction i in the case of uniform sediment in identical hydraulic conditions. In using the BMF approach, the potential concentration, C_{pi}, for a given size fraction i, is computed with a bed-material load formula by replacing the representative size with the average (or geometric mean) diameter, D_i, of the corresponding size fraction of the bed material. Conceptually, a stream bed can be considered as a hypothetical mixture of sediment particles, and the mixture can be formed into size groups. If it is assumed that individual size fractions have no influence on each other, then a potential transport rate can be computed for each size fraction whether or not particles are physically present on the bed surface. Consequently, P_{bi} can be visualized as the availability of sediment particles on the bed surface.

The TCF approach

The TCF approach relates the fractional transport rate to the bed-material transport rate and the transport capacity distribution function. First, the bed-material sediment concentration is computed by the use of a bed-material load equation. Then, the computed bed-material concentration is broken into fractional concentrations by a transport capacity distribution function. This concept is expressed as

$$C_{ti} = P_{ci} C_t \, , \quad \sum_{i=1}^{N} P_{ci} = 1 \tag{2.8}$$

in which P_{ci} = transport capacity distribution function corresponding to size fraction i. The TCF approach comprises two components: the computation of bed-material transport capacity, C_t, and the computation of its fraction, P_{ci}. The bed-material sediment concentration C_t can be determined by using any appropriate bed-material transport relationships available in the literature. In essence, the transport capacity distribution function P_{ci} is the size distribution of the transported sediments and does not necessarily resemble the size distribution of bed material. The availability concept and the sheltering and exposure effect are included in the consideration of P_{ci} by relating it to both hydraulic conditions and sediment properties.

2.3 DIRECT COMPUTATION BY THE SIZE FRACTION APPROACH

Direct computation by the size fraction approach includes methods of Einstein (1950), Laursen (1958), and Toffaleti (1968, 1969), which were originally developed to compute the sediment transport rates by size fractions for nonuniform sediment mixtures. Einstein (1950) presented the most extensive analysis on sediment transport of nonuniform mixtures based on fluid mechanics and probability. The sediment transport computations were made for the individual size fraction that has a representative grain size equal to the geometric mean grain diameter of each fraction. Einstein recognized the effect of the presence of one size on the transport rate of another in case of nonuniform sediment, and he proposed to account for this effect by introducing a hiding factor. Some fundamental concepts in sediment transport introduced by Einstein were later modified or simplified by others for the computation of sediment transport rate.

In Einstein's approach, the unit bed-material discharge for a given size fraction, q_{ti}, was expressed as the summation of unit bedload discharge, q_{bi}, and unit suspended load discharge, q_{si}, that is,

$$q_{ti} = q_{bi} + q_{si} = q_{bi}(1 + P_E I_1 + I_2) \tag{2.9}$$

in which $P_E = 2.303\log(30.2d/\Delta)$ is the transport parameter; and I_1 and I_2 = integrals of Einstein's form of the suspended sediment equation.

This equation relates the bedload transport to suspended load transport for all size fractions. The effects of other size fractions on the transport rate of a given size are accounted for through the treatments in bedload computation. Einstein's bedload function relates the dimensionless transport function, Φ_{*i}, to the flow intensity function, ψ_{*i}, by the following relationship (Fig. 2.1)

$$1 - \frac{1}{\sqrt{\pi}}\int_{-(1/7)\psi_{*i}-2}^{(1/7)\psi_{*i}-2} e^{-t^2}dt = \frac{43.5\Phi_{*i}}{1 + 43.5\Phi_{*i}} \tag{2.10}$$

where

$$\Phi_{*i} = \frac{q_{bi}}{P_{bi}\gamma_s\sqrt{\frac{\gamma_s-\gamma}{\gamma}gD_i^3}} \tag{2.11}$$

$$\psi_{*i} = \xi_i Y \left[\frac{\log(10.6)}{\log(10.6\overline{X}/\Delta)} \right]^2 \psi_i \tag{2.12}$$

and

$$\psi_i = \frac{(\gamma_s - \gamma) D_i}{\gamma R' S} \tag{2.13}$$

in which D_{65} = the bed material size by which 65 percent is finer; R'= the hydraulic radius associated with grain roughness; S = channel slope; ξ_i = correction factor defined by Einstein and given as a function of $D_i / \overline{X}$ (Fig. 2.2); Y = the correction factor for the lift coefficient given as a function of D_{65}/δ' (Fig. 2.3); $\overline{X}$= the characteristic grain size of the mixture, which is given by

$$\overline{X} = \begin{cases} 0.77\Delta & when\ \Delta/\delta' > 1.8 \\ 1.39\delta' & when\ \Delta/\delta' < 1.8 \end{cases} \tag{2.14}$$

in which Δ = the apparent roughness of the bed surface, which equals to D_{65}/X; δ' = the laminar sublayer thickness due to grain roughness; and X = a correction factor that accounts for the variation in flow regime in the logarithmic velocity distribution (Fig. 2.4).

Most of the concern has centered around the sheltering function ξ or hiding factor. In principle, it is intended to account for the difference in mobility of the various grain sizes in the mixture compared to their mobility in beds of respective uniform sized grains. Fig. 2.5 shows a comparison by Misri at al. of the Einstein and Hayashi et al. (1980) functions, and the function proposed by Pemberton (1972), where D_a is the average grain size of mixture. Misri's experiments on coarse sediments highlighted several important limitations of Einstein's method, including the inadequacy of his $\xi_i \sim D_i / \overline{X}$. In general, Einstein's method overpredicts the transport rates of finer sizes and underpredicts the transport rates of coarser

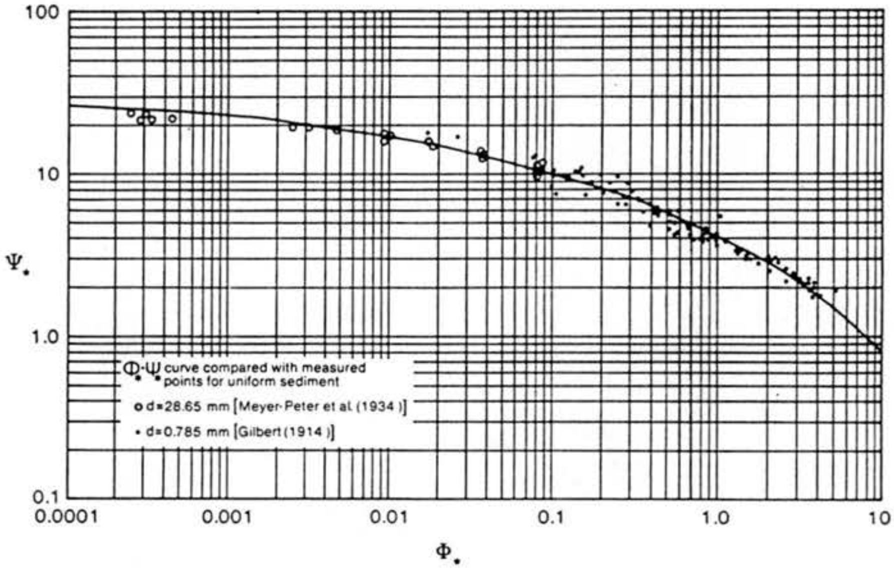

Fig.2.1. Relationship between Φ_* and Ψ_* for Einstein's Bed-Load Function (Einstein, 1950).

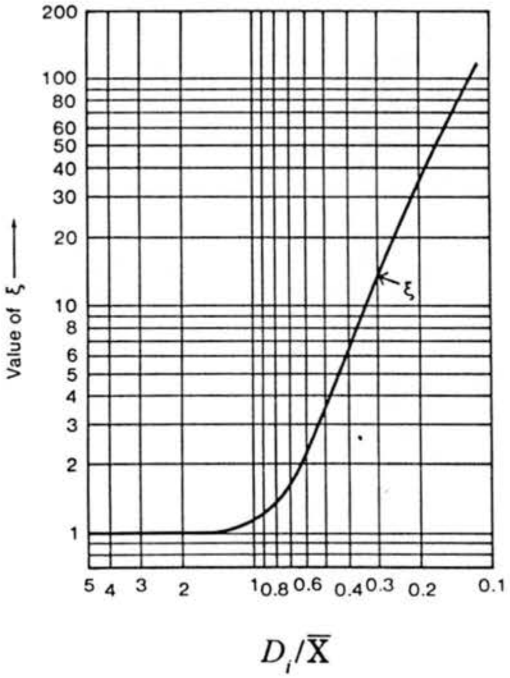

Fig. 2.2. Hiding Factor in Einstein's Bed-Load Function (Einstein, 1950).

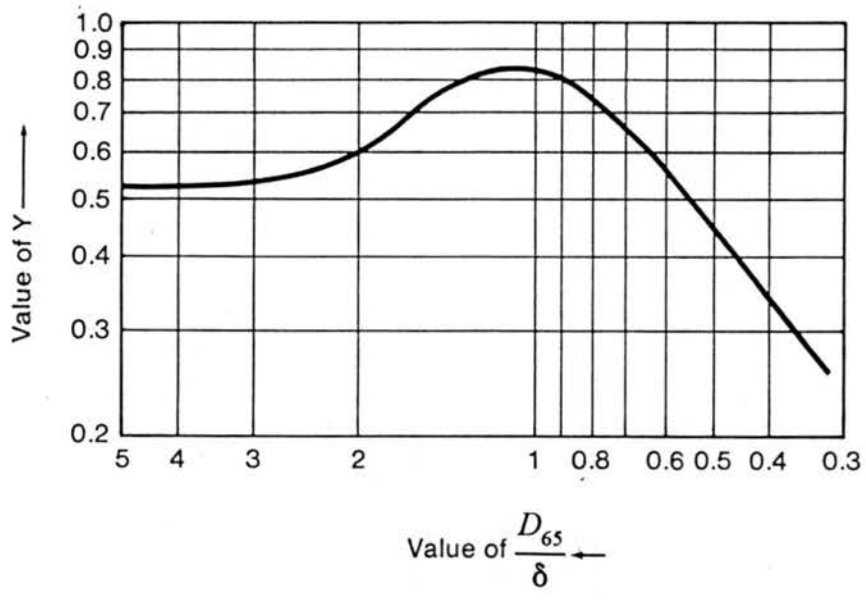

Fig. 2.3. Lifting Correction Factor (Einstein, 1950).

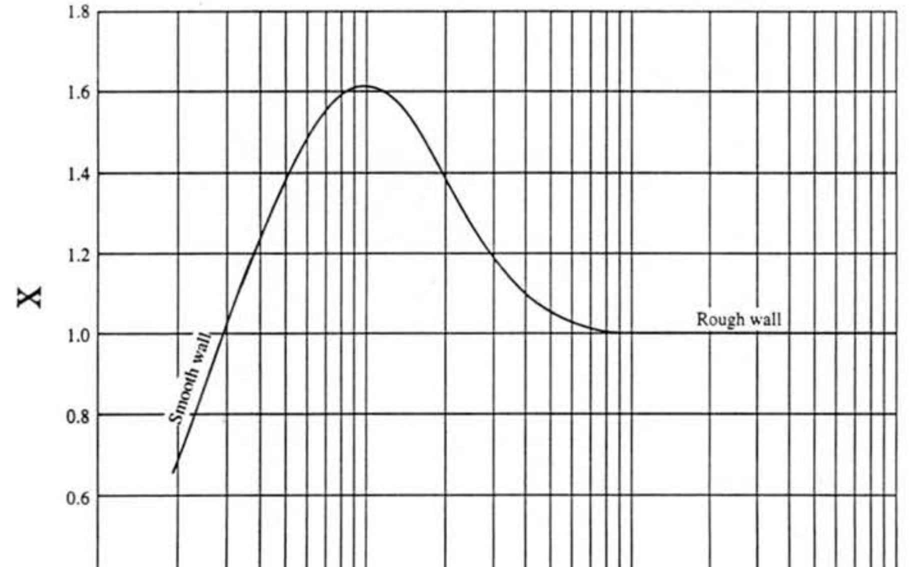

Fig. 2.4. Correction Factor in the Logarithmic Velocity Profile (Einstein, 1950).

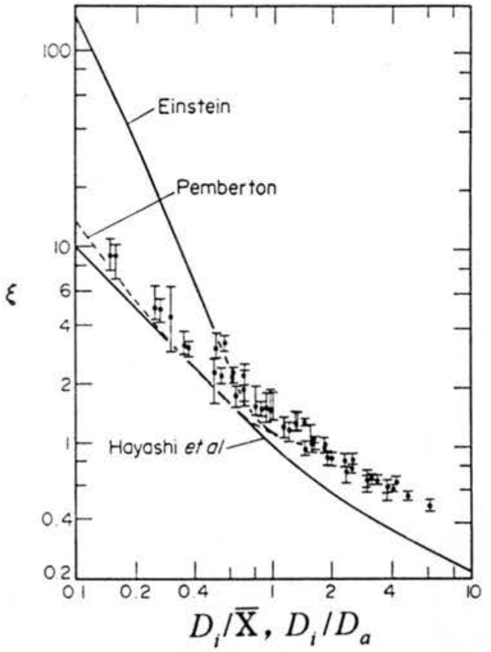

Fig. 2.5. The Sheltering Function ξ according to Misri et al. (1984).

fractions. Misri et al. also found that there was a very poor agreement with the relation for an additional correction factor, θ, introduced by Einstein and Chien (1953). These conclusions were confirmed later by the experiments and verification of Samaga el al. (1986a, b).

Laursen (1958) proposed a bed-material sediment transport formula based on his flume experimental data. His bed-material sediment concentration formula for a given size fraction may be expressed as (ASCE Task Committee, 1971)

$$C_{ti} = 0.01\gamma P_{bi}\left(\frac{D_i}{d}\right)^{7/6}\left(\frac{\tau_0'}{\tau_{ci}} - 1\right) f\left(\frac{V_*}{\omega_i}\right) \tag{2.15}$$

in which C_{ti} = bed-material sediment concentration by weight of size fraction i; V_* = shear velocity; τ_0' = bed shear stress due to grain resistance; τ_{ci} = critical shear stress for grain size of D_i as given by the Shields diagram; ω_i = fall velocity of particle of size D_i ; and

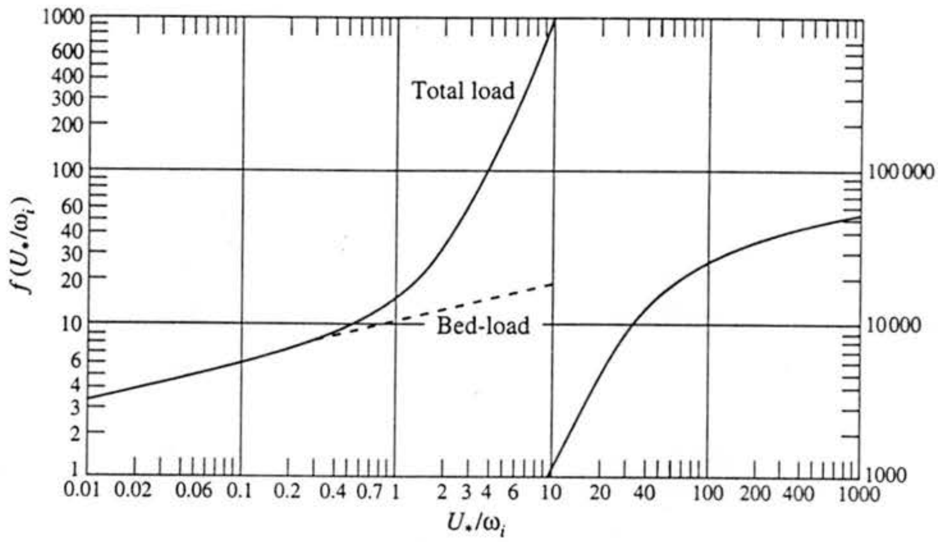

Fig. 2.6. Laursen's Sediment Transport Function (Laursen, 1958).

$f(V_*/\omega_i)$ = functional relation given in graphical form (Fig. 2.6). Laursen's shear stress due to grain resistance resulting from the use of Manning-Strickler equations is

$$\tau_0' = \frac{\rho V^2}{58}\left[\frac{D_{50}}{d}\right]^{1/3} \tag{2.16}$$

Toffaleti (1968, 1969) developed a procedure for the computation of sediment transport discharge based on the concept of Einstein (1950) and Einstein and Chien (1953). In his method, the total depth of flow is divided into four zones (Fig. 2.7), and the unit sediment discharge for each size fraction in each zone is determined individually. Then the unit bed-material load discharge for a sediment of size D_i is given by

$$q_{ti} = q_{bi} + q_{sui} + q_{smi} + q_{sli} \tag{2.17}$$

in which q_{sui}, q_{smi}, and q_{sli} = suspended load discharges per unit width in upper, middle, and

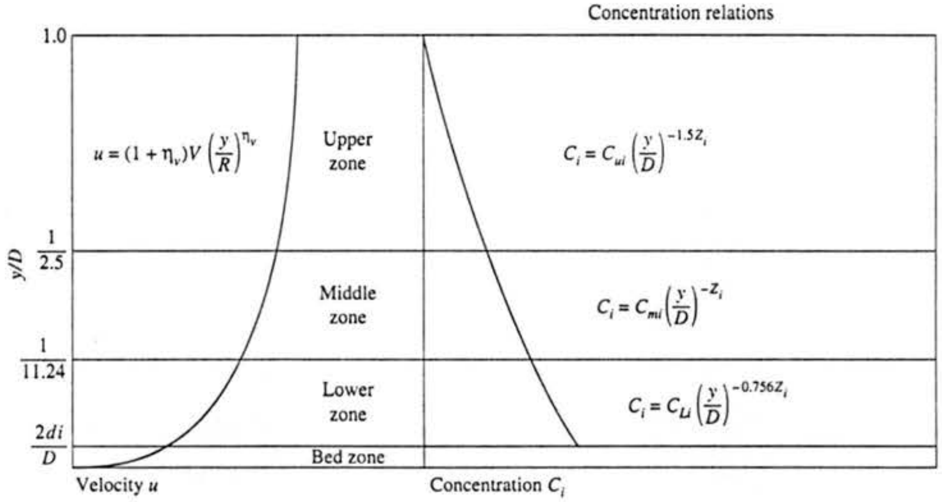

Fig. 2.7. Toffaleti's Velocity, Concentration, and Sediment Discharge Relations (Toffaleti, 1969).

lower zones, respectively, for sediment of size D_i.

Generally speaking, this group of approaches was found unsatisfactory in predicting transport rate by size fractions (Misri et al., 1984; Samaga et al., 1986b). This is due to the complexity of transport of sediment mixtures and the lack of knowledge concerning the motion of individual size and its effect on other sizes.

2.4 SHEAR STRESS CORRECTION APPROACH

Relevant contributions following the shear stress correction approach include those of the Ashida and Michiue (1973), Parker et al. (1982), White and Day (1982), Profitt and Sutherland (1983), Misri et al. (1984), Samaga et al. (1986a, 1986b), Diplas (1987), Bridge and Bennett (1992), Patel and Ranga Raju (1996), Wilcock and McArdell (1997), and Wilcock (1997).

Ashida and Michiue (1973) developed a bedload transport equation for nonuniform sediment mixtures by applying their bedload transport equation for uniform sediment. In doing so, the critical shear stress for uniform sediment was replaced by the critical shear stress for each size fraction. Ashida and Michiue found that the physical meaning for the hiding and the exposure effects of the nonuniform sediment transportation is due to the discrepancy between the critical shear stress for uniform sediment and that for nonuniform sediments. They adopted Egiazaroff's (1965) expression for critical shear stress of each individual size fraction in their bedload transport equation for nonuniform sediment mixtures. Based on a number of laboratory experiments, they also presented an empirical correction to Egiazaroff's expression in the range $D_i/D_m < 0.4$. The correction can be translated to a correction factor ε_{bi} for the critical shear stress as follows

$$\varepsilon_{bi} = \begin{cases} \left[\dfrac{\log(19)}{\log(19D_i/D_m)}\right]^2 & for\ \dfrac{D_i}{D_m} \geq 0.4 \\ 0.85\left(\dfrac{D_i}{D_m}\right)^{-1} & for\ \dfrac{D_i}{D_m} < 0.4 \end{cases} \tag{2.18}$$

in which D_m = mean diameter of bed material.

Parker et al. (1982) and Parker (1990) developed an empirical gravel transport relationship based on the equal mobility concept and the similarity transformation concept. Parker et al.'s equal mobility hypothesis states that the existence of a bed pavement regulates the entrainment of particles by stream, resulting in their mobility being approximately equal. That is, all grain sizes are entrained at about the same flow discharge and are transported at rates in proportion to their presence in the bed material. The similarity hypothesis transformation concept assumes that by choosing the proper parameter, different curves pertaining to different size fractions collapse into a single universal curve. Based on the analysis of field data from Oak Creek, the relationships between dimensionless bedload transport function W_i^* and dimensionless shear stress parameter τ_{ri}^* were given in a graphic form. These parameters are defined as

$$W_i^* = \frac{\gamma_s - \gamma}{\gamma} \frac{q_{bi}}{P_{bi}(gdS)^{1/2}dS} \tag{2.19}$$

$$\phi_i = \frac{dS}{(\gamma_s/\gamma - 1)D_i\tau_{ri}^*} \tag{2.20}$$

$$\tau_{ri}^* = 0.0876\frac{D_{50}}{D_i} \tag{2.21}$$

Because of the approximate equal mobility of all sizes, only one grain size, namely the subpavement size D_{50}, is used to characterize bedload discharge as a function of the dimensionless shear stress

$$W^* = \begin{cases} 0.0025\exp\left[14.2\,(\phi_{50} - 1) - 9.28\,(\phi_{50} -)^2\right] & for\ 0.95 < \phi_{50} < 1.65 \\ 11.2\left(1 - \dfrac{0.822}{\phi_{50}}\right)^{4.5} & for\ 1.65 < \phi_{50} \end{cases} \tag{2.22}$$

in which $\phi_{50} = \tau_{50}^* / \tau_{r50}^*$; τ_{50}^* = Shields stress for median diameter of subpavement; τ_{r50}^* = reference value of $\tau_{50}^* = 0.0876$.

Noting that Parker et al.'s approach constitutes only a first-order approximation of reality, Diplas (1987) analyzed the same data used by Parker et al. and indicated that the hiding function dependent on the average shear stress in addition to its dependence on grain size, D_i / D_{50}. An empirical expression for reduced hiding function based on Oak Creek data was proposed as follows

$$\xi_{bi} = \left[\phi_{50}^{(D_i/D_{50})^{0.3412} - 1}\right]\left[\left(\frac{D_i}{D_{50}}\right)^{-0.057}\right]^{(Di/D_{50})^{0.3214}} \tag{2.23}$$

White and Day (1982) investigated threshold conditions for individual grain sizes in a mixture in a recirculating flume. The prediction of transport rates was made by using Ackers and White's (1973) formulations by determining the initial motion parameter for each size fraction. The results led to a hiding function which is related to D_i/D_A, where D_A is the scaling size in a mixture defined by White and Day. White and Day's correction factor for mobility number can be transformed into a correction factor for effective shear stress

$$\xi_{bi} = \left(\frac{0.4}{(D_i/D_A)^{1/2}} + 0.6\right)^2 \tag{2.24}$$

and

$$\frac{D_A}{D_{50}} = 1.6\left(\frac{D_{84}}{D_{16}}\right)^{-0.28} \tag{2.25}$$

Proffitt and Sutherland (1983) studied the effect of sediment nonuniformity by comparing the transport rate of individual fractions in a mixture with that of uniform material of the same size. In the analysis they considered Paintal's (1971) and Ackers and White's (1973) transport functions as the basis for studying the effect of nonuniformity and suggested corrections to be applied to these two functions. By analyzing experimental data, they defined the following expression of ξ_{bi} for Paintal's function

$$\xi_{bi} = \begin{cases} 1.0\left(\dfrac{D_i}{D_u}\right)^{0.51} & for\ 0.60 < \dfrac{D_i}{D_u} < 10.0 \\ 1.16\left(\dfrac{D_i}{D_u}\right)^{0.81} & for\ \dfrac{D_i}{D_u} < 0.60 \end{cases} \tag{2.26}$$

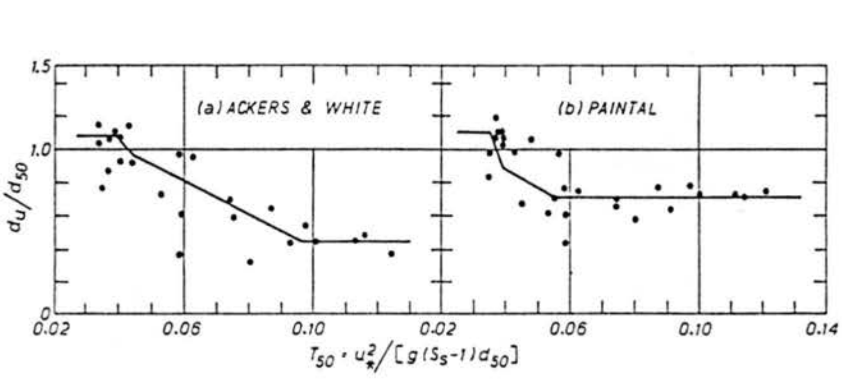

Fig. 2.8. Proffitt and Sutherland's Scaling Size (Proffitt and Sutherland, 1983).

in which D_u = scaling size which determines the roughness of the bed (Fig. 2.8).

A similar expression of ξ_{bi} was proposed by Proffitt and Sutherland for the correction of Ackers and White's function

$$\xi_{bi} = \begin{cases} 1.30 & for \quad 3.70 < \dfrac{D_i}{D_u} \\ 0.53 \log\left(\dfrac{D_i}{D_u}\right) + 1.0 & for \quad 0.075 < \dfrac{D_i}{D_u} < 3.70 \\ 0.40 & for \quad \dfrac{D_i}{D_u} < 0.075 \end{cases} \tag{2.27}$$

Proffitt and Sutherland's correction factor does not take into account all the relevant parameters, and the data used in the development of their relation for ξ_{bi} covers a relatively narrow range of flow conditions.

Misri et al. (1984) modified the Einstein type transport relationships and obtained a function for uniform sediment as follows by fitting experimental data

$$\Phi_b = \begin{cases} 4.6\times10^7 \left(\theta'\right)^8 & for\ \theta' \le 0.065 \\ \dfrac{8.5\left(\theta'\right)^{1.8}}{\left[1 + 5.95\times10^{-6} / \left(\theta'\right)^{4.7}\right]^{1.43}} & for\ \theta' > 0.065 \end{cases} \tag{2.28}$$

where

$$\theta' = \frac{\tau'}{(\gamma_s - \gamma) D} \tag{2.29}$$

in which D = sediment size; τ' = grain shear stress.

For nonuniform sediment, Misri et al. introduced a factor ξ_{bi} into Eq. (2.28) to account for the sheltering and exposure effect. Similar to Proffitt and Sutherland's method, Misri et al. conceptually related the coefficient ξ_{bi} to D_i / D_a. Then, based on dimensionless analysis, they defined the following functional relationship for ξ_{bi}

$$\xi_{bi} = \frac{D_i}{D_a} = \frac{\tau_e}{\tau'} = f\left(\theta_i', \ \frac{\tau'}{\tau_c}, \ M\right) \tag{2.30}$$

where

$$\theta_i' = \frac{\tau'}{(\gamma_s - \gamma) D_i} \tag{2.31}$$

in which τ_e = effective shear stress for transport of size fraction D_i as bedload; τ_c = critical shear stress for size D_a based on Shields' criterion; D_a = arithmetic mean diameter of sediment mixtures; M = the Kramer's uniformity coefficient for the mixture, which was defined as

$$M = \frac{\sum_0^{50} D_i \, \Delta P_{bi}}{\sum_{50}^{100} D_i \, \Delta P_{bi}} \tag{2.32}$$

in which D_i = geometric mean of size group i; and ΔP_i = percentage weight corresponding to size group i.

Through extensive analysis of their experimental data, the correction factor was given as

$$\xi_{bi} = \frac{0.038\,K_2\left(\tau'/\tau_c\right)^{0.75}}{\left(\theta'\right)^{1.2}\left[\left(1+0.0031\left(\theta'\right)^{-2.1}\right]^{1/3}} \tag{2.33}$$

in which K_2 = coefficient.

Samaga et al. (1986a, 1986b) proposed a correction factor ξ_{bi} through modifying Misri's model to calculate bedload transport rate of individual fractions for sediment mixtures. Following a line of analysis similar to that for bedload transport, Samaga et al. also defined a coefficient ξ_{si} for suspended load. The functional relationship for ξ_{si} was expressed as

$$\xi_{si} = \frac{\tau_e}{\tau'} = f\left(\theta_i',\ \frac{\tau'}{\tau_c},\ M\right) \tag{2.34}$$

The coefficients ξ_{bi} and ξ_{si} were expressed in graphical forms. Samaga et al. referred to ξ_{bi} and ξ_{si} as the sheltering-cum-exposure coefficient and sheltering-cum-exposure-cum-interference coefficient, respectively.

Samaga et al. used the coefficients defined by

$$(K_b\ ,\ K_s) = f(\tau_0'/\tau_{0c}) \tag{2.35}$$

$$(L_b\ ,\ L_s) = f(M) \tag{2.36}$$

and

$$(K_b L_b \xi_{bi}) \ , \ (K_s L_s \xi_{si}) \ = f(\theta') \tag{2.37}$$

The relationship between L_B and M is given in a table . The coefficients K_b and $(K_b L_b \xi_{bi})$ are given in graphical forms. With known ξ_{bi} θ_i' the value of dimensionless bedload Φ_{bi} can be read from a graphical relation. Following the same procedure, Φ_{si} can be obtained.

Bridge and Bennett (1992) developed a model for the bedload transport of sediment grains of different sizes, in which the shape and density were also considered.

Recently, Patel and Ranga Raju (1996) checked the performance of the relationships for the methods of Ashida and Michiue(1973), Proffitt and Sutherland (1983), and Bridge and Bennett (1992) based on a large number of bedload data from flume and fields, and indicated that none of these methods give satisfactory results. Patel and Ranga Raju (1996) thus proposed an empirical relationship for fractional bedload transport which they calibrated using both flume and field data. The exposure-cum-sheltering correction factor proposed by Patel and Ranga Raju was as follows

$$\xi_{bi} \ = \ 0.0713 \left(C_s \, \theta_i' \right)^{-0.75144} / \ C_m \tag{2.38}$$

where

$$\log(C_s) \ = \ -0.1957$$
$$- 0.9571 \left[\log\left(\frac{\tau'}{\tau_c} \right) \right] - 0.1949 \left[\log\left(\frac{\tau'}{\tau_c} \right) \right]^2 + 0.0644 \left[\log\left(\frac{\tau'}{\tau_c} \right) \right]^3 \tag{2.39}$$

and

$$C_m = \begin{cases} 0.7092\log(M) + 1.293 & for\ 0.05 < M < 0.38 \\ 1.0 & for\ \quad M > 0.38 \end{cases} \tag{2.40}$$

This new method is only applicable for fractional bed-material load.

More recently, Wilcock and McArdell (1997) and Wilcock (1997) studied partial transport and fractional transport. They expressed the fractional transport rate as the product of the spatial entrainment, displacement frequency, and displacement length. In their fractional transport expression, the partial transport of individual size fractions was emphasized. But this common feature in gravel-bed rivers is not a major concern in sand-bed rivers.

The shear stress correction approach is most commonly used for the computation of fractional bedload transport in nonuniform mixtures. Some of the concepts used in this approach, which relate the shear stress correction factor to relative diameter (D_i/D_{50}, D_i/D_A, D_i/D_u, D_i/D_a, etc.), bed material size gradation (uniformity coefficient, M), and flow intensity (average shear stress), can be expanded to the study of the transport of sediment mixtures.

2.5 BED MATERIAL FRACTION APPROACH

Among the four categories of fractional sediment transport rate computation methods, the BMF approach is the most commonly used method in numerical models, even though the shortcomings of using this approach in nonuniform sediment transport models have been pointed out in the literature (Hsu and Holly 1992). The BMF approach does not account for the interactions between different size particles present in sediment mixtures. Hsu and Holly (1992) point out that one important disadvantage of this approach is the difficulty in obtaining the correct gradation and total transport amount, and another minor disadvantage is its sensitivity to the number and distribution of class intervals. However, due to its simplicity and the fact that it may be acceptable under certain transport conditions, the BMF approach is still widely in use in numerical models such as HEC-6 (U. S. Corps of Engineers 1977; Thomas, 1982), GSTARS (Molinas and Yang, 1986), CARICHAR (Rahuel et al., 1989), and BRI-STARS (Molinas, 1990; Molinas and Trent, 1991; Molinas 1993).

Karim (1985) introduced a so-called hiding factor, W_i, into the BMF approach to reflect the influence of other sediment particles in the mixture on the transport of given size fraction i

$$C_{ti} = W_i P_{bi} C_{pi} \tag{2.41}$$

Eq. (2.41) can be visualized as a modified BMF method. They expressed W_i as a simple power function of D_i/D_{50}

$$W_i = C_1 \left(\frac{D_i}{D_{50}} \right)^{C_2} \tag{2.42}$$

in which C_1 and C_2 = coefficients, which were determined to be 1.0 and 0.8, respectively, using typical Missouri River bed material size distributions and flow data and a trial and error procedure.

Following the same procedure, Karim (1998) developed new relations for predicting sediment discharge for each size fraction

$$C_{ti} = \phi_i C_{pi} \tag{2.43}$$

in which ϕ_i = weighing function for *i*th fraction:

$$\phi_i = P_{ai} \eta \tag{2.44}$$

in which P_{ai} = areal function of bed material in ith size fraction; and η = sheltering factor. The areal function and sheltering factor proposed by Karim are

$$P_{ai} = \frac{\dfrac{P_{bi}}{D_i}}{\displaystyle\sum_{i=1}^{N} \frac{P_{bi}}{D_i}} \tag{2.45}$$

$$\eta = C_1 \left(\frac{D_i}{D_{50}} \right)^{C_2} \tag{2.46}$$

in which C_1, C_2 = coefficients determined based on experimental data from Einstein and Chien (1953):

$$C_1 = 1.15 \left(\frac{\omega_{50}}{V_*} \right), \quad C_2 = 0.60 \left(\frac{\omega_{50}}{V_*} \right) \tag{2.47}$$

Similar to Karim and Kennedy's modification [Eq. (2.41)], Wang and Zhang (1990), Wang et al. (1995), and Wang et al. (1998) introduced a modifying coefficient K_D into the BMF concept for fractional load computation

$$q_{ti} = K_D (q_{bi} + q_{si}) \tag{2.48}$$

Based on data analysis and heuristic reasoning, they expressed K_D as follows

$$K_D = D_k^m , \quad D_k = \frac{D_i}{D_p} \tag{2.49}$$

in which

$$D_p = D_m \theta^{0.5} , \quad D_m = \sum P_{bi} D_i \tag{2.50}$$

and

$$m = 0.06 + 2.55D_k - 0.863D_k^2 + 0.1088D_k^3 - 0.0046D_K^4 \tag{2.51}$$

It needs to be pointed out that all modification factors (W_i, ϕ_i, and K_D) in the use of the BMF concept were calibrated along with a specific transport equation used to compute the potential transport rate in their development. Therefore, these modification factors may not be used in conjunction with other transport equations to predict fractional transport rate.

2.6 TRANSPORT CAPACITY FRACTION APPROACH

The TCF approach comprises two components, the computation of bed-material transport capacity, C_t, and the computation of its fraction, P_{ci}. It is assumed that these two components can be treated separately in the development and application of the TCF concept. The bed-material sediment concentration, C_t, can be determined by using the available bed-material transport formulas in the literature. The key problem in the application of the TCF approach is the proper determination of the sediment transport capacity distribution function, P_{ci}.

For suspended load, a simple method was suggested by Dou et al. (1987) by relating to P_{si} / ω_i

$$P_{csi} = \frac{(P_{si} / \omega_i)^{\alpha}}{\sum_{i=1}^{N} (P_{si} / \omega_i)^{\alpha}} \tag{2.52}$$

where P_{csi} = the fraction of suspended sediment transport capacity, by dry weight, corresponding to size fraction i; P_{si} = the fraction of suspended load, by dry weight, corresponding to size fraction i, and ω_i = the fall velocity of sediment corresponding to particle size D_i. The deficiency of this method is that it is basically developed for suspended load and it does not take into account the influence of the bed material size and the hydraulic conditions.

From statistical theory, Li (1988) derived a method which related to P_{bi}, ω_i, and V_*

$$P_{csi} = \frac{P_{bi} \dfrac{1-A_i}{\omega_i} \left(1 - e^{-6\omega_i/\kappa V_*}\right)}{\sum_{i=1}^{N} P_{bi} \dfrac{1-A_i}{\omega_i} \left(1 - e^{-6\omega_i/\kappa V_*}\right)} \tag{2.53}$$

where

$$A_i = \frac{\omega_i}{\dfrac{\sigma_v}{\sqrt{2\pi}} e^{-\omega_i^2/2\sigma_v^2} + \omega_i \phi\left(\dfrac{\omega_i}{\sigma_v}\right)} \tag{2.54}$$

where κ = the universal constant of von Kármán; σ_v = the turbulence coefficient, and it was assumed that $\sigma_v = V^*$; V_* is the shear velocity; and ϕ = the standardized normal distribution frequency function. Li's method was basically developed for the computation of fractions of suspended bed-material sediment transport capacity.

Karim and Kennedy (1981) proposed an equation for P_{ci} as follows

$$P_{ci} = \frac{P_{bi} \left(\dfrac{D_{50}}{D_i}\right)^x}{\sum_{i=1}^{N} P_{bi} \left(\dfrac{D_{50}}{D_i}\right)^x} \tag{2.55}$$

where

$$x = 0.0316 \left(\frac{d}{D_{50}}\right)^{0.5} \tag{2.56}$$

As indicated by Holly and Karim (1986), this method has no theoretical basis, and it was developed through heuristic reasoning supported by data analysis of measured suspended sediment size distribution of the Missouri, the Niobrara, and the Middle Loup Rivers. Karim and Kennedy's conceptual model was also used by Holly and Rahuel (1990) for the fractional bedload transport computation in their general framework for mobile-bed modeling.

Based on observation of sediment-mixture experiments, Hsu and Holly (1992) postulated that the fraction of each size class in transported material is proportional to the joint probability of the relative mobility (Pmo_i) of each particle size and the availability (P_{bi}) of each size class on the bed surface. Therefore, they expressed the transported distribution as

$$P_{ci} = \frac{Pmo_i P_{bi}}{\sum_{i=1}^{N} (Pmo_i P_{bi})} \tag{2.57}$$

where

$$\begin{aligned} Pmo_i &= \frac{1}{\sigma\sqrt{2\pi}} \int_{(V_{ci}/V)-1}^{\infty} \exp\left(-\frac{x^2}{2\sigma} \right) dx \\ &= 0.5 - 0.5\, erf\left(\frac{\frac{V_{ci}}{V} - 1}{\sigma\sqrt{2}} \right) \end{aligned} \tag{2.58}$$

in which efr(z) = the error function; V_{ci} = the incipient velocity for a particular size class i in a mixture; V' = the absolute fluctuations of velocity; and σ = the standard deviation of V'/Vdistribution. Unfortunately, Hsu and Holly's method is limited to the transport of bedload and has not been verified with direct measurements of fractional transport data.

CHAPTER 3

TRANSPORT CAPACITY DISTRIBUTION FUNCTION

3.1 GENERAL

Presently, none of the four groups of approaches gives a satisfactory prediction of fractional transport rates of nonuniform sediment mixtures in open channels. The approach using direct computation by size fractions results in the worst prediction of fractional transport rates and is rarely used in numerical models. The shear stress correction approach is commonly used for the computation of fractional bedload transport. This approach is more suitable for flows with gravel-bed materials since the sheltering and exposure effects are more pronounced in these cases. The physical considerations and the parameters used in the shear correction approach can be incorporated into research on fractional transport of sand-bed materials. The BMF approach is widely used in numerical models due to its simplicity. But both the shear stress correction approach and the BMF concept fail to estimate the correct gradation and total amount of bed-material transport rate. The TCF concept has its advantages in avoiding additional errors in estimating the bed-material concentration by the summation of transport capacities of individual size fractions and may limit the discrepancies in computing concentrations for individual size fractions. The sheltering and exposure effect considered in the shear stress correction approach for nonuniform mixtures can be incorporated in the determination of the transport capacity distribution function, P_{ci}. Currently, most research utilizing the TCF concept is limited to fractional load transport of suspended sediments. It is desirable to develop a new method for the computation of bed-material load transport capacity by size fractions based on the TCF approach and using the concept of sheltering and exposure corrections.

The TCF approach comprises two components, the computation of bed-material transport capacity, C_t, and the computation of transport capacity distribution function, P_{ci}. It is assumed in the present study that these two components can be treated separately in development and application of the TCF concept. In this section, we focus on the computation of P_{ci}, which is the crucial component in the successful implementation of the TCF concept.

3.2 DATA SOURCES

The processes and mechanisms of nonuniform sediment transport are still not well understood in our knowledge due to their complexity. Prediction of sediment transport rates by size fractions has not been accomplished following a purely analytical method. It is a common practice to develop a fractional sediment transport procedure following semi-empirical derivation and relying on calibration using flume and field data. Therefore it is very important to collect a complete and reliable set of sediment transport data for the analysis, development, calibration, and comparison of fractional sediment transport methods. It is required that the data include measurements of size distribution for both bed material and the sediments in transport.

The flume data of Einstein (1978), Einstein and Chien (1953), and Samaga et al.

(1986a, 1986b), and field data from the Niobrara River near Cody, Nebraska (Colby and Hembree, 1955), and the Middle Loup River at Dunning, Nebraska (Hubbell and Matejka, 1959) were used to analyze the fractional transport rate of sediment mixtures. A summary of this data base is given in Table 3.1. It incorporates 118 dat sets containing a total of 891 data points. These data are limited to sand sizes with median diameter in the range of 0.10 to 0.90 mm, geometric standard deviation in the range of 1.30 to 3.0, flow discharge in the range of 0.0056 to 16.06 m^3/s, velocity in the range of 0.49 to 1.41 m/s, flow depth in the range of 0.056 to 0.58 m, and slope in the range of 0.00093 to 0.013.

For the laboratory data, the bed-material concentrations were measured directly to eliminate the uncertainty of unmeasured load near the bed surface. The bed-material concentrations for the Niobrara River near Cody, Nebraska are measured as suspended bed-material concentrations at a contracted section and are based on depth integrated samples. The bed-material concentrations reported for the Middle Loup River at Dunning, Nebraska are measured suspended bed-material concentrations with a turbulence flume and are also based on depth integrated samples. Data with unmeasured load near the bed surface determined by the use of indirect methods are not included in this study.

Detailed sediment transport data are given in Tables 3.2 - 3.6. The sediment transport data contains a complete record for flow and sediment information pertaining to each measurement. This information for each record includes:

- Flow properties,
- Bed material properties,
- Transported sediment properties, and
- Size distributions of bed material and transported sediments.

Table 3.1. Summary of Laboratory and River Data

Data Source (1)	Average Discharge (m^3/s) (2)	Average Velocity (m/s) (3)	Average Depth (m) (4)	Slope (m/m) (5)	Temperature (°C) (6)	Median Diameter (mm) (7)	Geometric Standard Deviation of Bed Size (8)	Bed-Material Conc. (PPM) (9)	No. of Data Sets (10)	No. of Size Groups (11)	No. of Data Points (12)
(a) Laboratory Data											
Einstein (IRTCES, 1978)	0.019 -0.042	0.54 -1.41	0.099 -0.139	0.00262 -0.0127	16.0 -27.2	0.108 -0.903	1.245 -2.158	1325 -39560	29	13	289
Einstein and Chien (1953)	0.043 -0.066	0.73 -1.12	0.177 -0.237	0.00157 -0.00489	8.9 -27.8	0.104 -0.381	1.414 -2.968	2115 -57970	22	15	218
Samaga et al. (1986a, b)	0.0056 -0.015	0.49 -0.78	0.056 -0.101	0.00449 -0.00693	14.0 -26.5	0.212 -0.404	1.480 -2.460	3392 -10260	33	10	258
(b) River Data											
Colby and Hembree (1955)	5.86 -16.06	0.62 -1.27	0.421 -0.576	0.00114 -0.00180	0.56 -28.3	0.215 -0.349	1.514 -2.345	257 -1600	19	8	59
Hubell and Matejka (1959)	9.34 -12.54	0.63 -1.11	0.250 -0.370	0.000928 -0.00146	1.10 -31.1	0.219 -0.424	1.651 -2.403	411 -1831	15	8	67
(c) Total of Laboratory and River Data											
Total	0.0056 -16.06	0.49 -1.41	0.056 -0.576	0.000928 -0.0127	0.56 -31.1	0.104 -0.903	1.245 -2.968	257 -57970	118		891

Table 3.2. Laboratory Data of Einstein (IRTCES, 1978)

Data No. (1)	Run ID (2)	Flow Properties: Q (m^3/s) (3)	W (m) (4)	d (m) (5)	S (m/m) (6)	T (°C) (7)	Bed Material: D_{50}^* (mm) (8)	D_{65}^* (mm) (9)	σ_g^* (10)	s_g (11)	Transported Sediment: C_T (kg/m^3) (12)	C_T (PPM) (13)	D_{50t}^* (mm) (14)	σ_{gt}^* (15)
1	10	0.0329	0.2667	0.1049	0.010330	21.0	0.150	0.173	1.529	2.65	41.33	40290.77	0.122	1.510
2	11	0.0260	0.2667	0.1390	0.002622	20.1	0.150	0.173	1.529	2.65	2.00	2001.52	0.161	1.586
3	12	0.0300	0.2667	0.1356	0.003867	21.8	0.150	0.173	1.529	2.65	3.86	3854.92	0.162	1.595
4	13	0.0343	0.2667	0.1329	0.005542	22.1	0.150	0.173	1.529	2.65	8.26	8216.38	0.148	1.637
5	14	0.0385	0.2667	0.1289	0.008750	22.7	0.150	0.173	1.529	2.65	21.84	21542.65	0.123	1.510
6	15	0.0425	0.2667	0.1277	0.011789	23.6	0.150	0.173	1.529	2.65	43.79	42623.29	0.121	1.450
7	16	0.0306	0.2667	0.0994	0.008988	25.6	0.223	0.247	1.367	2.65	16.81	16631.27	0.212	1.352
8	17	0.0271	0.2667	0.1003	0.006411	26.0	0.223	0.247	1.367	2.65	8.61	8560.20	0.219	1.406
9	18	0.0239	0.2667	0.1058	0.003975	25.9	0.223	0.247	1.367	2.65	3.55	3544.13	0.232	1.350
10	19	0.0203	0.2667	0.1052	0.002840	23.4	0.223	0.247	1.367	2.65	1.92	1916.13	0.231	1.385
11	20	0.0269	0.2667	0.1273	0.006373	20.0	0.595	0.658	1.245	2.65	3.16	3149.08	0.604	1.241
12	21	0.0220	0.2667	0.1148	0.005493	19.1	0.595	0.658	1.245	2.65	2.31	2311.38	0.593	1.229
13	22	0.0345	0.2667	0.1134	0.007631	17.4	0.595	0.658	1.245	2.65	5.65	5633.37	0.589	1.229
14	23	0.0233	0.2667	0.1350	0.003318	16.0	0.595	0.658	1.245	2.65	1.46	1456.70	0.580	1.208
15	24	0.0230	0.2667	0.1332	0.003510	18.9	0.903	1.037	1.383	2.65	1.33	1327.94	0.879	1.372
16	25	0.0226	0.2667	0.1274	0.004820	18.5	0.903	1.037	1.383	2.65	1.57	1567.34	0.891	1.379
17	26	0.0326	0.2667	0.1204	0.009433	16.4	0.903	1.037	1.383	2.65	6.01	5990.52	0.871	1.399
18	27	0.0404	0.2667	0.1075	0.012380	19.5	0.609	0.845	2.158	2.65	11.14	11058.46	0.692	1.995
19	28	0.0357	0.2667	0.1029	0.010460	21.0	0.609	0.845	2.158	2.65	9.31	9257.81	0.749	1.792
20	29	0.0357	0.2667	0.1036	0.010630	21.3	0.609	0.845	2.158	2.65	7.12	7092.39	0.756	1.775
21	31	0.0389	0.2667	0.1043	0.012720	19.2	0.609	0.845	2.158	2.65	9.72	9657.18	0.647	1.743
22	32	0.0308	0.2667	0.1014	0.008709	24.8	0.609	0.845	2.158	2.65	6.47	6444.42	0.714	1.977
23	33	0.0189	0.2667	0.1317	0.002846	26.5	0.121	0.135	1.329	2.65	2.42	2420.98	0.101	1.290
24	34	0.0227	0.2667	0.1302	0.003087	27.2	0.119	0.131	1.307	2.65	2.12	2114.97	0.109	1.326
25	35	0.0262	0.2667	0.1298	0.004418	26.3	0.119	0.131	1.320	2.65	3.91	3902.89	0.116	1.327
26	35	0.0261	0.2667	0.1307	0.004544	25.0	0.110	0.119	1.308	2.65	5.36	5338.11	0.109	1.317
27	35	0.0260	0.2667	0.1308	0.004447	22.5	0.108	0.117	1.306	2.65	5.98	5961.74	0.110	1.314
28	36	0.0299	0.2667	0.1298	0.006282	26.1	0.116	0.128	1.340	2.65	7.15	7114.17	0.120	1.311
29	37	0.0333	0.2667	0.1309	0.008513	25.5	0.114	0.123	1.323	2.65	15.94	15787.15	0.111	1.312

Note: * — Values computed from adjusted bed material size distribution (wash load materials excluded).

Table 3.2. Laboratory Data of Einstein (IRTCES, 1978) (continued)

Data No. (1)	Run ID (2)	D_c (mm) (16)	Size distribution of bed material, finer than indicated diameters: Grp1 (%) (17)	Grp2 (%) (18)	Grp3 (%) (19)	Grp4 (%) (20)	Grp5 (%) (21)	Grp6 (%) (22)	Grp7 (%) (23)	Grp8 (%) (24)	Grp9 (%) (25)	Grp10 (%) (26)	Grp11 (%) (27)	Grp12 (%) (28)	Grp13 (%) (29)
			0.061	**0.074**	**0.088**	**0.104**	**0.124**	**0.147**	**0.175**	**0.208**	**0.246**	**0.295**	**0.351**	**0.417**	**0.589mm**
1	10	0.061	3.49	6.33	13.78	20.66	35.99	49.94	67.69	77.18	88.04	94.17	97.60	98.87	100.00
2	11	0.061	3.49	6.33	13.78	20.66	35.99	49.94	67.69	77.18	88.04	94.17	97.60	98.87	100.00
3	12	0.061	3.49	6.33	13.78	20.66	35.99	49.94	67.69	77.18	88.04	94.17	97.60	98.87	100.00
4	13	0.061	3.49	6.33	13.78	20.66	35.99	49.94	67.69	77.18	88.04	94.17	97.60	98.87	100.00
5	14	0.061	3.49	6.33	13.78	20.66	35.99	49.94	67.69	77.18	88.04	94.17	97.60	98.87	100.00
6	15	0.061	3.49	6.33	13.78	20.66	35.99	49.94	67.69	77.18	88.04	94.17	97.60	98.87	100.00
7	16	0.061	0.03	0.04	0.08	0.14	0.75	4.13	21.56	39.79	64.72	81.27	91.13	95.51	100.00
8	17	0.061	0.03	0.04	0.08	0.14	0.75	4.13	21.56	39.79	64.72	81.27	91.13	95.51	100.00
9	18	0.061	0.03	0.04	0.08	0.14	0.75	4.13	21.56	39.79	64.72	81.27	91.13	95.51	100.00
10	19	0.061	0.03	0.04	0.08	0.14	0.75	4.13	21.56	39.79	64.72	81.27	91.13	95.51	100.00
			0.246	**0.295**	**0.351**	**0.417**	**0.489**	**0.589**	**0.701**	**0.833**	**0.991**	**1.168**	**1.397**	**1.981mm**	
11	20	0.417	0.01	0.09	0.71	4.29	16.63	50.61	75.68	92.15	98.30	99.80	100.00	100.00	
12	21	0.417	0.01	0.09	0.71	4.29	16.63	50.61	75.68	92.15	98.30	99.80	100.00	100.00	
13	22	0.417	0.01	0.09	0.71	4.29	16.63	50.61	75.68	92.15	98.30	99.80	100.00	100.00	
14	23	0.417	0.01	0.09	0.71	4.29	16.63	50.61	75.68	92.15	98.30	99.80	100.00	100.00	
15	24	0.417	0.08	0.13	0.25	0.46	1.34	7.19	22.30	41.40	60.37	77.75	93.92	100.00	
16	25	0.417	0.08	0.13	0.25	0.46	1.34	7.19	22.30	41.40	60.37	77.75	93.92	100.00	
17	26	0.417	0.08	0.13	0.25	0.46	1.34	7.19	22.30	41.40	60.37	77.75	93.92	100.00	
			0.089	**0.125**	**0.175**	**0.246**	**0.350**	**0.495**	**0.700**	**0.991**	**1.397**	**1.981**	**2.790**	**3.100mm**	
18	27	0.175	1.08	2.16	5.22	12.29	25.52	42.86	59.22	73.27	84.47	91.95	98.87	100.00	
19	28	0.175	1.08	2.16	5.22	12.29	25.52	42.86	59.22	73.27	84.47	91.95	98.87	100.00	
20	29	0.175	1.08	2.16	5.22	12.29	25.52	42.86	59.22	73.27	84.47	91.95	98.87	100.00	
21	31	0.175	1.08	2.16	5.22	12.29	25.52	42.86	59.22	73.27	84.47	91.95	98.87	100.00	
22	32	0.175	1.08	2.16	5.22	12.29	25.52	42.86	59.22	73.27	84.47	91.97	98.87	100.00	
			0.061	**0.074**	**0.088**	**0.104**	**0.124**	**0.147**	**0.175**	**0.208**	**0.246**	**0.351**	**0.495**	**0.701**	**0.991mm**
23	33	0.061	3.36	5.48	18.28	30.27	55.17	78.21	95.80	98.74	99.40	99.88	99.96	99.98	100.00
24	34	0.061	2.94	5.15	17.61	29.89	58.16	81.38	96.93	98.83	99.45	99.91	99.97	99.98	100.00
25	35	0.061	1.65	5.00	17.28	28.39	58.20	80.24	96.00	98.66	99.42	99.92	99.98	99.99	100.00
26	35	0.061	2.80	8.30	27.62	40.30	73.00	90.51	98.50	99.70	99.91	99.99	100.00	100.00	100.00
27	35	0.061	3.44	9.93	31.36	44.68	76.40	91.68	98.75	99.75	99.91	99.99	100.00	100.00	100.00
28	36	0.061	1.80	6.35	21.09	31.13	62.04	81.93	95.85	98.75	99.45	99.93	99.99	100.00	100.00
29	37	0.061	2.08	6.91	23.64	34.67	66.65	85.95	97.20	99.20	99.67	99.96	99.99	100.00	100.00

Table 3.2. Laboratory Data of Einstein (IRTCES, 1978) (continued)

Data No. (1)	Run ID (2)	Size distribution of sediment load, finer than indicated diameters Grp1 (%) (30)	Grp2 (%) (31)	Grp3 (%) (32)	Grp4 (%) (33)	Grp5 (%) (34)	Grp6 (%) (35)	Grp7 (%) (36)	Grp8 (%) (37)	Grp9 (%) (38)	Grp10 (%) (39)	Grp11 (%) (40)	Grp12 (%) (41)	Grp13 (%) (42)
		0.061	**0.074**	**0.088**	**0.104**	**0.124**	**0.147**	**0.175**	**0.208**	**0.246**	**0.295**	**0.351**	**0.417**	**0.589mm**
1	10	8.49	14.38	27.21	37.33	56.01	69.21	82.54	88.53	93.90	97.14	98.85	99.45	100.00
2	11	2.71	5.70	11.41	18.07	31.39	43.39	58.77	68.84	81.49	89.79	96.05	97.82	100.00
3	12	3.05	5.34	10.64	17.88	31.21	43.03	57.93	68.03	80.36	89.46	95.98	97.99	100.00
4	13	4.40	8.09	15.76	25.06	40.18	51.81	65.49	73.90	83.51	91.05	96.11	98.02	100.00
5	14	7.37	12.77	25.57	36.07	54.92	69.44	82.16	87.86	93.40	96.64	98.55	99.31	100.00
6	15	7.37	13.41	20.77	37.47	56.61	69.89	82.91	88.57	93.98	97.20	98.89	99.50	100.00
7	16	0.50	0.70	0.90	1.20	2.60	8.00	28.10	47.40	72.10	85.60	93.40	96.60	100.00
8	17	1.00	1.20	1.50	1.80	3.10	7.80	26.70	43.70	65.50	80.40	90.00	94.40	100.00
9	18	0.17	0.17	0.23	0.40	0.68	2.55	16.55	33.73	58.50	78.74	91.27	95.52	100.00
10	19	0.20	0.30	0.70	1.10	2.00	4.40	19.50	36.40	58.40	77.40	90.20	95.10	100.00
		0.246	**0.295**	**0.351**	**0.417**	**0.489**	**0.589**	**0.701**	**0.833**	**0.991**	**1.168**	**1.397**	**1.981mm**	
11	20	0.06	0.24	0.93	3.30	14.87	47.83	74.83	92.77	98.83	99.88	100.00	100.00	
12	21	0.00	0.16	1.12	4.14	16.87	51.02	78.74	94.27	99.17	99.96	100.00	100.00	
13	22	0.07	0.12	0.54	2.74	15.54	51.38	78.18	94.28	99.08	99.95	100.00	100.00	
14	23	0.07	0.20	0.93	3.93	18.85	55.05	83.15	96.20	99.53	100.00	100.00	100.00	
15	24	0.00	0.10	0.20	0.30	1.10	7.30	22.90	44.10	63.80	80.00	95.00	100.00	
16	25	0.00	0.20	0.50	0.90	1.80	8.60	22.70	42.80	62.40	78.80	95.20	100.00	
17	26	0.00	0.40	1.10	1.80	3.40	11.60	26.80	46.30	64.40	79.60	95.00	100.00	
		0.089	**0.125**	**0.175**	**0.246**	**0.350**	**0.495**	**0.700**	**0.991**	**1.397**	**1.981**	**2.790**	**3.100mm**	
18	27	0.24	0.29	0.46	1.63	9.09	27.39	50.97	70.63	76.37	96.28	100.00	100.00	
19	28	0.06	0.11	0.21	0.90	6.40	23.78	45.93	67.33	85.21	96.76	100.00	100.00	
20	29	0.05	0.07	0.18	0.95	6.77	22.56	44.91	68.19	85.59	97.19	100.00	100.00	
21	31	0.02	0.04	0.10	1.01	8.75	29.64	56.09	76.41	89.97	97.76	100.00	100.00	
22	32	0.30	0.74	2.14	6.45	16.55	31.85	49.99	68.45	84.12	94.83	100.00	100.00	
		0.061	**0.074**	**0.088**	**0.104**	**0.124**	**0.147**	**0.175**	**0.208**	**0.246**	**0.351**	**0.495**	**0.701**	**0.991mm**
23	33	16.72	20.36	44.81	61.15	82.39	94.10	98.93	99.65	99.83	99.95	99.98	100.00	100.00
24	34	7.81	11.76	32.10	46.79	72.05	88.05	97.97	99.09	99.49	99.94	99.97	99.99	100.00
25	35	2.17	6.46	21.33	31.62	62.58	83.49	96.62	98.91	99.49	99.92	99.98	99.99	100.00
26	35	3.64	9.44	30.48	43.24	73.08	90.39	98.29	99.61	99.84	99.98	100.00	100.00	100.00
27	35	3.35	8.63	30.02	41.48	73.00	90.51	98.57	99.63	99.83	99.98	100.00	100.00	100.00
28	36	1.48	4.66	17.04	26.23	56.93	81.37	96.68	98.92	99.47	99.91	99.98	99.99	100.00
29	37	3.06	8.01	29.23	40.21	71.13	91.23	98.74	99.69	99.88	99.98	100.00	100.00	100.00

Table 3.3. Laboratory Data of Einstein and Chien (1953)

		Flow Properties					Bed Material				Transported Sediment			
Data No. (1)	Run ID (2)	Q (m^3/s) (3)	W (m) (4)	d (m) (5)	S (m/m) (6)	T (°C) (7)	D_{50}^* (mm) (8)	D_{65}^* (mm) (9)	σ_g^* (10)	s_g (11)	C_T (kg/m^3) (12)	C_T (PPM) (13)	D_{50t}^* (mm) (14)	σ_{gt}^* (15)
1	A-1	0.0623	0.3048	0.1981	0.003752	18.3	0.193	0.271	2.065	2.65	19.51	19277.42	0.096	1.431
2	A-2	0.0628	0.3048	0.2003	0.004894	24.4	0.366	0.412	1.413	2.65	2.14	2136.61	0.328	1.417
3	A-3	0.0627	0.3048	0.1996	0.003520	22.2	0.187	0.254	2.071	2.65	17.86	17664.50	0.096	1.411
4	A-4	0.0629	0.3048	0.1966	0.003760	16.7	0.279	0.371	2.191	2.65	15.87	15717.37	0.095	1.462
5	B-1	0.0629	0.3048	0.1878	0.003948	12.8	0.218	0.315	2.138	2.65	12.91	12811.59	0.103	1.574
6	B-2	0.0629	0.3048	0.2009	0.004188	14.4	0.173	0.243	2.090	2.65	13.56	13450.35	0.096	1.449
7	B-3	0.0626	0.3048	0.1996	0.003328	8.9	0.145	0.197	2.030	2.65	16.38	16214.02	0.096	1.442
8	B-4	0.0629	0.3048	0.1984	0.003578	11.1	0.141	0.195	2.094	2.65	17.24	17060.36	0.093	1.420
9	B-5	0.0629	0.3048	0.1996	0.003661	10.6	0.129	0.174	2.100	2.65	18.76	18542.08	0.092	1.406
10	C-1	0.0629	0.3048	0.1932	0.003050	16.1	0.158	0.228	2.417	2.65	80.08	76281.29	0.054	1.597
11	C-2	0.0623	0.3048	0.2030	0.003931	20.6	0.151	0.218	2.491	2.65	117.94	109874.57	0.050	1.564
12	C-3	0.0623	0.3048	0.1954	0.003680	14.4	0.145	0.208	2.479	2.65	148.67	136071.28	0.048	1.572
13	C-4	0.0623	0.3048	0.1945	0.003460	15.6	0.189	0.265	2.293	2.65	35.31	34550.59	0.059	1.782
14	C-5	0.0623	0.3048	0.1942	0.003945	13.9	0.233	0.313	2.071	2.65	12.52	12425.50	0.109	1.782
15	D-1	0.0629	0.3048	0.2140	0.004448	17.8	0.161	0.217	2.163	2.65	36.15	35350.86	0.057	1.636
16	D-4	0.0430	0.3048	0.1774	0.003063	17.8	0.140	0.211	2.658	2.65	79.77	75994.43	0.045	1.445
17	D-5	0.0439	0.3048	0.1978	0.003015	22.8	0.270	0.357	2.952	2.65	78.53	74873.71	0.045	1.335
18	D-6	0.0657	0.3048	0.1945	0.003865	26.1	0.351	0.490	2.324	2.65	28.03	27548.95	0.094	1.609
19	D-7	0.0430	0.3048	0.1850	0.003000	20.0	0.307	0.438	2.573	2.65	19.71	19466.29	0.054	1.607
20	D-8	0.0620	0.3048	0.1847	0.003655	26.1	0.135	0.174	1.971	2.65	42.05	40980.71	0.060	1.850
21	D-9	0.0428	0.3048	0.1871	0.001570	27.8	0.104	0.136	2.001	2.65	30.02	29467.84	0.046	1.550
22	E-1	0.0629	0.3048	0.1847	0.003485	21.1	0.203	0.278	2.420	2.65	52.49	50827.05	0.054	1.696

Note: * — Values computed from adjusted bed material size distribution (wash load materials excluded).

Table 3.3. Laboratory Data of Einstein and Chien (1953) (continued)

Data No. (1)	Run ID (2)	D_c (mm) (16)	Grp1 (%) (17)	Grp2 (%) (18)	Grp3 (%) (19)	Grp4 (%) (20)	Grp5 (%) (21)	Grp6 (%) (22)	Grp7 (%) (23)	Grp8 (%) (24)	Grp9 (%) (25)	Grp10 (%) (26)	Grp11 (%) (27)	Grp12 (%) (28)	Grp13 (%) (29)	Grp14 (%) (30)	Grp15 (%) (31)
			Size distribution of bed material, finer than indicated diameters														
			0.061	**0.074**	**0.104**	**0.147**	**0.208**	**0.295**	**0.417**	**0.589**	**0.833**	**1.168mm**					
1	A-1	0.061	2.51	8.28	18.45	38.30	54.82	69.22	82.43	95.15	99.34	99.80					
2	A-2	0.061	0.00	0.04	0.14	0.25	2.30	23.31	66.14	93.45	99.38	99.65					
3	A-3	0.061	3.11	9.64	21.14	40.66	56.00	73.08	84.44	94.45	99.06	99.58					
4	A-4	0.061	1.69	5.33	11.75	23.60	36.31	52.90	71.00	83.52	93.42	98.89					
5	B-1	0.061	0.00	5.07	14.44	31.69	47.92	61.74	78.00	90.21	97.31	99.66					
6	B-2	0.061	0.00	6.17	21.04	41.88	59.08	71.86	84.95	93.56	98.11	99.73					
7	B-3	0.061	0.00	9.55	28.04	51.01	67.44	78.99	89.89	95.86	98.73	99.71					
8	B-4	0.061	0.00	10.67	30.68	52.41	67.59	78.25	88.66	95.43	98.90	99.79					
9	B-5	0.061	0.00	12.22	35.17	58.81	71.36	79.84	88.71	94.85	98.59	99.83					
			0.008	**0.013**	**0.02**	**0.03**	**0.045**	**0.061**	**0.074**	**0.104**	**0.147**	**0.208**	**0.295**	**0.417**	**0.589**	**0.833**	**1.168mm**
10	C-1	0.03	0.46	1.17	2.60	5.30	11.00	18.00	23.60	36.00	49.50	63.00	76.00	86.70	93.40	97.50	99.40
11	C-2	0.03	0.52	1.32	3.00	6.70	13.40	21.00	26.50	38.20	52.00	65.20	77.00	86.60	93.20	97.20	99.20
12	C-3	0.03	0.87	2.40	5.10	10.00	17.00	24.00	30.00	42.00	55.00	68.00	78.40	87.50	93.50	97.20	99.20
13	C-4	0.03	0.10	0.41	1.25	3.05	7.00	11.00	15.20	25.50	39.00	56.00	70.00	83.00	92.00	97.10	99.42
14	C-5	0.061	0.00	0.00	0.00	0.55	2.00	4.80	7.70	16.00	29.00	46.00	63.00	78.00	89.00	95.30	98.30
15	D-1	0.03	0.13	0.40	1.00	2.60	6.20	12.00	17.00	30.00	46.50	64.00	78.50	89.00	95.70	98.75	99.82
16	D-4	0.03	0.62	1.50	3.50	7.80	16.00	24.50	30.50	42.50	55.00	66.50	77.00	85.20	91.50	96.20	98.70
17	D-5	0.03	0.30	0.90	2.50	6.30	14.00	22.00	26.00	31.50	35.50	43.00	56.00	75.50	90.00	96.70	99.22
18	D-6	0.061	0.00	0.00	0.03	0.18	0.90	2.50	4.40	10.00	19.00	29.00	42.00	54.50	70.50	84.00	94.00
19	D-7	0.03	0.40	0.80	1.58	3.00	5.50	8.50	11.00	17.00	25.00	35.00	46.00	59.00	72.00	84.00	92.00
20	D-8	0.03	0.13	0.56	1.80	4.70	10.50	18.00	24.00	38.50	57.00	76.70	91.30	97.70	99.60	100.00	100.00
21	D-9	0.03	0.83	2.60	6.10	12.20	22.00	33.00	40.50	56.00	73.00	87.00	95.50	98.90	99.81	100.00	100.00
22	E-1	0.03	0.00	0.90	2.20	4.60	8.70	13.40	17.20	26.00	38.00	52.40	68.00	79.50	89.00	94.80	98.00

Table 3.3. Laboratory Data of Einstein and Chien (1953) (continued)

Data No. (1)	Run ID (2)	Grp1 (%) (32)	Grp2 (%) (33)	Grp3 (%) (34)	Grp4 (%) (35)	Grp5 (%) (36)	Grp6 (%) (37)	Grp7 (%) (38)	Grp8 (%) (39)	Grp9 (%) (40)	Grp10 (%) (41)	Grp11 (%) (42)	Grp12 (%) (43)	Grp13 (%) (44)	Grp14 (%) (45)	Grp15 (%) (46)
		Size distribution of transported sediment, finer than indicated diameters														
		0.061	**0.074**	**0.104**	**0.147**	**0.208**	**0.295**	**0.417**	**0.589**	**0.833**	**1.168mm**					
1	A-1	17.21	34.81	65.81	87.78	93.91	96.28	97.99	99.09	99.77	99.93					
2	A-2	0.91	1.45	2.40	3.04	7.30	38.25	78.29	96.65	99.69	99.85					
3	A-3	15.25	33.42	65.43	89.66	95.63	97.40	98.45	99.17	99.81	99.92					
4	A-4	22.60	39.44	69.10	87.21	92.83	95.45	97.33	98.58	99.50	99.93					
5	B-1	8.91	25.55	54.87	80.17	89.25	92.96	95.85	97.71	99.13	99.86					
6	B-2	17.26	35.04	66.37	86.55	92.84	95.29	97.00	98.35	99.33	99.86					
7	B-3	13.95	32.42	64.95	86.36	93.38	96.06	97.83	98.89	99.58	99.93					
8	B-4	14.62	34.23	68.77	88.78	94.49	96.68	98.13	99.06	99.63	99.90					
9	B-5	15.54	35.54	70.78	90.17	95.05	96.80	98.05	98.95	99.58	99.92					
		0.008	**0.013**	**0.02**	**0.03**	**0.045**	**0.061**	**0.074**	**0.104**	**0.147**	**0.208**	**0.295**	**0.417**	**0.589**	**0.833**	**1.168mm**
10	C-1	17.40	26.00	37.50	51.70	68.00	81.00	87.60	94.60	97.70	99.10	99.60	99.80	99.89	99.94	99.97
11	C-2	21.00	32.00	45.00	60.00	76.50	87.00	91.50	96.20	98.20	99.15	99.50	99.65	99.78	99.87	99.94
12	C-3	18.80	29.00	43.00	59.50	77.70	87.50	91.50	96.10	98.40	99.26	99.61	99.73	99.82	99.90	99.95
13	C-4	13.00	20.00	29.20	42.00	58.50	72.50	79.50	88.50	93.50	96.45	97.60	98.45	99.04	99.46	99.76
14	C-5	1.80	4.70	10.00	19.00	35.00	50.00	58.50	73.50	84.00	90.50	94.20	96.50	98.10	99.05	99.59
15	D-1	15.00	25.00	37.00	50.80	66.00	78.50	85.00	93.30	97.10	98.70	99.30	99.55	99.75	99.91	99.97
16	D-4	23.50	40.00	56.00	72.50	86.50	93.80	96.00	98.15	99.25	99.56	99.72	99.80	99.86	99.91	99.95
17	D-5	17.00	29.00	44.00	61.00	80.00	93.70	97.40	99.00	99.38	99.49	99.54	99.63	99.75	99.87	99.95
18	D-6	0.00	8.49	20.60	32.00	48.00	64.00	73.20	85.20	91.90	95.10	96.60	97.35	98.05	98.72	99.30
19	D-7	13.00	22.00	33.60	48.00	66.20	79.20	86.50	94.00	97.50	98.60	99.10	99.40	99.60	99.78	99.90
20	D-8	16.50	28.00	40.20	53.00	67.00	77.00	82.50	89.70	94.40	97.00	98.55	99.36	99.73	100.00	100.00
21	D-9	20.40	34.50	50.60	69.00	84.00	91.00	94.00	97.30	98.80	99.44	99.74	99.87	99.93	100.00	100.00
22	E-1	16.50	28.00	42.00	56.50	72.00	82.00	87.00	93.00	96.20	98.10	98.92	99.32	99.56	99.74	99.85

Table 3.4. Laboratory Data of Samaga et al. (1986a, b)

		Flow Properties					Bed Material				Transported Sediment			
Data No. (1)	Run ID (2)	Q (m^3/s) (3)	W (m) (4)	d (m) (5)	S (m/m) (6)	T (°C) (7)	D_{50}^* (mm) (8)	D_{65}^* (mm) (9)	σ_g^* (10)	s_g (11)	C_T (kg/m^3) (12)	C_T (PPM) (13)	D_{50t}^* (mm) (14)	σ_{gt}^* (15)
1	M1-1	0.0068	0.200	0.057	0.005760	24.5	0.403	0.639	2.458	2.65	4.6321	4618.81	0.659	2.511
2	M1-2	0.0104	0.200	0.077	0.005760	23.0	0.403	0.639	2.458	2.65	4.9910	4975.52	0.489	2.843
3	M1-3	0.0133	0.200	0.092	0.005760	22.0	0.403	0.639	2.458	2.65	5.7284	5708.03	0.639	2.559
4	M1-4	0.0081	0.200	0.064	0.006870	18.5	0.403	0.639	2.458	2.65	6.7757	6747.28	0.649	2.457
5	M1-5	0.0109	0.200	0.080	0.006870	19.5	0.403	0.639	2.458	2.65	6.9021	6872.53	0.655	2.446
6	M1-6	0.0133	0.200	0.091	0.006870	20.2	0.403	0.639	2.458	2.65	7.0541	7023.30	0.709	2.386
7	M1-7	0.0056	0.200	0.057	0.005047	20.5	0.403	0.639	2.458	2.65	3.4479	3440.48	0.551	2.443
8	M1-8	0.0114	0.200	0.089	0.005047	17.5	0.403	0.639	2.458	2.65	6.4285	6402.85	0.629	2.551
9	M1-9	0.0146	0.200	0.101	0.005047	17.0	0.403	0.639	2.458	2.65	6.1268	6103.51	0.745	2.263
10	M2-1	0.0075	0.200	0.072	0.004960	16.0	0.316	0.514	2.373	2.65	3.7577	3748.93	0.315	2.301
11	M2-2	0.0108	0.200	0.080	0.004960	16.0	0.316	0.514	2.373	2.65	5.0442	5028.39	0.552	2.830
12	M2-3	0.0124	0.200	0.092	0.004960	14.5	0.316	0.514	2.373	2.65	6.0750	6052.15	0.606	2.752
13	M2-4	0.0083	0.200	0.069	0.006048	14.5	0.316	0.514	2.373	2.65	7.2608	7228.17	0.596	2.652
14	M2-5	0.0116	0.200	0.083	0.006048	14.5	0.316	0.514	2.373	2.65	7.4719	7437.30	0.552	2.826
15	M2-6	0.0144	0.200	0.100	0.006048	15.3	0.316	0.514	2.373	2.65	8.3955	8351.81	0.654	2.747
16	M2-7	0.0091	0.200	0.070	0.006926	14.0	0.316	0.514	2.373	2.65	7.4258	7391.61	0.692	2.454
17	M2-8	0.0118	0.200	0.084	0.006926	16.3	0.316	0.514	2.373	2.65	9.2762	9222.98	0.722	2.433
18	M2-9	0.0143	0.200	0.093	0.006926	16.5	0.316	0.514	2.373	2.65	9.1903	9138.02	0.659	2.709
19	M3-1	0.0109	0.200	0.078	0.006926	18.5	0.281	0.439	2.196	2.65	10.3286	10262.65	0.597	2.266
20	M3-2	0.0129	0.200	0.087	0.006926	23.0	0.281	0.439	2.196	2.65	9.0970	9045.75	0.591	2.260
21	M3-3	0.0088	0.200	0.068	0.006926	23.5	0.281	0.439	2.196	2.65	8.3844	8340.87	0.605	2.197
22	M3-4	0.0075	0.200	0.066	0.005415	24.5	0.281	0.439	2.196	2.65	7.3982	7364.32	0.409	2.310
23	M3-5	0.0101	0.200	0.077	0.005415	22.1	0.281	0.439	2.196	2.65	7.1173	7085.94	0.568	2.245
24	M3-6	0.0134	0.200	0.091	0.005415	25.0	0.281	0.439	2.196	2.65	5.8694	5847.99	0.598	2.203
25	M3-7	0.0081	0.200	0.064	0.006097	23.5	0.281	0.439	2.196	2.65	7.5946	7558.90	0.560	2.239
26	M3-8	0.0063	0.200	0.056	0.006097	25.0	0.281	0.439	2.196	2.65	6.1781	6154.41	0.373	2.212
27	M3-9	0.0129	0.200	0.086	0.006097	24.5	0.281	0.439	2.196	2.65	7.7749	7737.44	0.566	2.201
28	M4-1	0.0081	0.200	0.062	0.006097	24.5	0.212	0.249	1.481	2.65	5.8615	5840.15	0.301	1.771
29	M4-2	0.0121	0.200	0.080	0.006097	25.5	0.212	0.249	1.481	2.65	7.5698	7534.28	0.320	1.772
30	M4-3	0.0083	0.200	0.068	0.005268	26.0	0.212	0.249	1.481	2.65	5.6843	5664.25	0.304	1.983
31	M4-4	0.0132	0.200	0.087	0.005268	26.0	0.212	0.249	1.481	2.65	6.4086	6383.09	0.296	1.950
32	M4-5	0.0085	0.200	0.068	0.004487	26.0	0.212	0.249	1.481	2.65	4.3627	4350.91	0.304	1.888
33	M4-6	0.0135	0.200	0.091	0.004487	26.5	0.212	0.249	1.481	2.65	4.5958	4582.71	0.298	1.902

Note: * — Values computed from adjusted bed material size distribution (wash load materials excluded).

Table 3.4. Laboratory Data of Samaga et al. (1986a, b) (continued)

Data No. (1)	Run ID (2)	D_c (mm) (16)	Size distribution of bed material, finer than indicated diameters Grp1 (%) (17)	Grp2 (%) (18)	Grp3 (%) (19)	Grp4 (%) (20)	Grp5 (%) (21)	Grp6 (%) (22)	Grp7 (%) (23)	Grp8 (%) (24)	Grp9 (%) (25)	Grp10 (%) (26)
			0.0849	**0.158**	**0.170**	**0.265**	**0.329**	**0.539**	**0.927**	**1.502**	**1.856**	**3.000** mm
1	M1-1	0.158	1.00	6.20	10.80	39.20	47.21	61.45	79.58	89.38	94.76	100.00
2	M1-2	0.158	1.00	6.20	10.80	39.20	47.21	61.45	79.58	89.38	94.76	100.00
3	M1-3	0.158	1.00	6.20	10.80	39.20	47.21	61.45	79.58	89.38	94.76	100.00
4	M1-4	0.158	1.00	6.20	10.80	39.20	47.21	61.45	79.58	89.38	94.76	100.00
5	M1-5	0.158	1.00	6.20	10.80	39.20	47.21	61.45	79.58	89.38	94.76	100.00
6	M1-6	0.158	1.00	6.20	10.80	39.20	47.21	61.45	79.58	89.38	94.76	100.00
7	M1-7	0.158	1.00	6.20	10.80	39.20	47.21	61.45	79.58	89.38	94.76	100.00
8	M1-8	0.158	1.00	6.20	10.80	39.20	47.21	61.45	79.58	89.38	94.76	100.00
9	M1-9	0.158	1.00	6.20	10.80	39.20	47.21	61.45	79.58	89.38	94.76	100.00
10	M2-1	0.158	0.50	6.30	14.60	45.34	54.90	68.51	82.48	91.86	96.00	100.00
11	M2-2	0.158	0.50	6.30	14.60	45.34	54.90	68.51	82.48	91.86	96.00	100.00
12	M2-3	0.158	0.50	6.30	14.60	45.34	54.90	68.51	82.48	91.86	96.00	100.00
13	M2-4	0.158	0.50	6.30	14.60	45.34	54.90	68.51	82.48	91.86	96.00	100.00
14	M2-5	0.158	0.50	6.30	14.60	45.34	54.90	68.51	82.48	91.86	96.00	100.00
15	M2-6	0.158	0.50	6.30	14.60	45.34	54.90	68.51	82.48	91.86	96.00	100.00
16	M2-7	0.158	0.50	6.30	14.60	45.34	54.90	68.51	82.48	91.86	96.00	100.00
17	M2-8	0.158	0.50	6.30	14.60	45.34	54.90	68.51	82.48	91.86	96.00	100.00
18	M2-9	0.158	0.50	6.30	14.60	45.34	54.90	68.51	82.48	91.86	96.00	100.00
19	M3-1	0.0849	2.60	12.40	19.30	48.66	58.20	71.42	88.70	99.31	100.00	100.00
20	M3-2	0.0849	2.60	12.40	19.30	48.66	58.20	71.42	88.70	99.31	100.00	100.00
21	M3-3	0.0849	2.60	12.40	19.30	48.66	58.20	71.42	88.70	99.31	100.00	100.00
22	M3-4	0.0849	2.60	12.40	19.30	48.66	58.20	71.42	88.70	99.31	100.00	100.00
23	M3-5	0.0849	2.60	12.40	19.30	48.66	58.20	71.42	88.70	99.31	100.00	100.00
24	M3-6	0.0849	2.60	12.40	19.30	48.66	58.20	71.42	88.70	99.31	100.00	100.00
25	M3-7	0.0849	2.60	12.40	19.30	48.66	58.20	71.42	88.70	99.31	100.00	100.00
26	M3-8	0.0849	2.60	12.40	19.30	48.66	58.20	71.42	88.70	99.31	100.00	100.00
27	M3-9	0.0849	2.60	12.40	19.30	48.66	58.20	71.42	88.70	99.31	100.00	100.00
28	M4-1	0.0849	4.80	20.50	32.90	72.37	84.02	95.50	99.89	100.00	100.00	100.00
29	M4-2	0.0849	4.80	20.50	32.90	72.37	84.02	95.50	99.89	100.00	100.00	100.00
30	M4-3	0.0849	4.80	20.50	32.90	72.37	84.02	95.50	99.89	100.00	100.00	100.00
31	M4-4	0.0849	4.80	20.50	32.90	72.37	84.02	95.50	99.89	100.00	100.00	100.00
32	M4-5	0.0849	4.80	20.50	32.90	72.37	84.02	95.50	99.89	100.00	100.00	100.00
33	M4-6	0.0849	4.80	20.50	32.90	72.37	84.02	95.50	99.89	100.00	100.00	100.00

Table 3.4. Laboratory Data of Samaga et al. (1986a, b) (continued)

Data No. (1)	Run ID (2)	Size distribution of sediment load, finer than indicated diameters									
		Grp1 (%) (27)	Grp2 (%) (28)	Grp3 (%) (29)	Grp4 (%) (30)	Grp5 (%) (31)	Grp6 (%) (32)	Grp7 (%) (33)	Grp8 (%) (34)	Grp9 (%) (35)	Grp10 (%) (36)
		0.0849	**0.158**	**0.170**	**0.265**	**0.329**	**0.539**	**0.927**	**1.502**	**1.856**	**3.000 mm**
1	M1-1	0.95	3.69	8.60	20.17	30.90	39.79	72.31	78.93	97.57	100.00
2	M1-2	1.34	2.25	13.46	32.61	44.87	52.70	78.37	83.45	98.23	100.00
3	M1-3	1.12	2.27	8.34	20.09	30.86	41.81	71.58	78.42	98.43	100.00
4	M1-4	0.89	1.91	3.61	18.24	28.79	39.36	73.22	80.50	98.57	100.00
5	M1-5	0.93	2.49	7.87	17.92	31.23	40.57	70.32	80.26	95.45	100.00
6	M1-6	0.82	1.45	5.46	14.44	22.56	33.66	67.32	75.98	98.33	100.00
7	M1-7	1.14	1.40	4.24	19.17	33.75	49.48	79.87	84.27	98.04	100.00
8	M1-8	0.92	1.64	7.03	20.13	32.30	41.97	73.04	80.25	98.97	100.00
9	M1-9	0.71	1.41	5.70	9.44	18.42	29.88	64.70	75.59	96.89	100.00
10	M2-1	0.72	3.01	13.31	40.38	54.20	62.04	83.89	88.85	98.29	100.00
11	M2-2	0.91	3.97	12.74	32.63	46.32	51.03	74.56	80.64	97.59	100.00
12	M2-3	0.62	2.73	10.18	26.64	37.75	45.82	71.42	78.98	96.81	100.00
13	M2-4	0.31	2.15	7.71	25.88	37.07	45.07	77.35	83.24	97.05	100.00
14	M2-5	0.49	2.32	11.40	30.85	42.09	50.11	74.12	80.85	96.33	100.00
15	M2-6	0.37	1.90	9.31	24.37	32.11	40.73	69.52	76.42	95.84	100.00
16	M2-7	0.21	1.47	5.35	15.93	26.04	35.87	68.13	76.34	95.07	100.00
17	M2-8	0.20	0.91	5.34	15.47	24.25	32.69	65.57	76.66	97.79	100.00
18	M2-9	0.70	1.86	11.38	23.34	31.64	39.45	70.50	80.64	97.71	100.00
19	M3-1	2.44	5.84	13.70	25.38	35.27	44.54	80.08	100.00	100.00	100.00
20	M3-2	3.33	6.39	13.74	26.25	37.31	45.91	79.70	100.00	100.00	100.00
21	M3-3	2.65	5.08	12.68	23.62	34.55	43.57	80.08	100.00	100.00	100.00
22	M3-4	3.63	6.71	19.88	37.48	48.07	56.53	86.03	100.00	100.00	100.00
23	M3-5	3.58	6.41	14.16	27.71	38.99	48.55	81.47	100.00	100.00	100.00
24	M3-6	2.90	5.60	13.54	24.76	34.81	44.27	81.54	100.00	100.00	100.00
25	M3-7	3.32	6.06	16.55	28.67	39.76	49.07	84.61	100.00	100.00	100.00
26	M3-8	1.99	3.80	15.42	34.69	48.49	58.37	87.35	100.00	100.00	100.00
27	M3-9	3.45	6.63	14.46	26.61	38.23	48.61	82.99	100.00	100.00	100.00
28	M4-1	3.44	9.41	18.11	38.58	60.76	84.39	100.00	100.00	100.00	100.00
29	M4-2	3.15	9.09	12.71	31.87	54.55	79.71	100.00	100.00	100.00	100.00
30	M4-3	2.47	6.34	19.55	38.68	58.72	74.83	100.00	100.00	100.00	100.00
31	M4-4	3.55	8.77	21.45	42.27	60.89	77.68	100.00	100.00	100.00	100.00
32	M4-5	3.55	8.32	17.93	36.70	60.20	79.07	100.00	100.00	100.00	100.00
33	M4-6	3.71	8.67	17.76	39.31	62.50	78.16	100.00	100.00	100.00	100.00

Table 3.5. Niobrara River Data of Colby and Hembree (1955)

Data No. (1)	Survey Date (yymmdd) (2)	Flow Properties: Q (m^3/s) (3)	W (m) (4)	d (m) (5)	S (m/m) (6)	T (°C) (7)	Bed Material: D_{50}^* (mm) (8)	D_{65}^* (mm) (9)	σ_g^* (10)	s_g (11)	Transported Sediment: C_T (kg/m^3) (12)	C_T (PPM) (13)	D_{50t}^* (mm) (14)	σ_{gt}^* (15)
1	490713	7.56	21.49	0.47	0.001345	23.9	0.304	0.363	1.619	2.65	0.9706	970.00	0.248	1.679
2	500303	11.35	21.34	0.49	0.001705	5.0	0.307	0.411	2.345	2.65	1.8922	1890.00	0.209	1.618
3	500414	11.72	21.64	0.49	0.001705	6.7	0.286	0.348	1.643	2.65	2.0025	2000.00	0.242	1.645
4	500511	16.05	21.95	0.58	0.001799	11.7	0.215	0.256	1.573	2.65	2.2231	2220.00	0.227	1.650
5	500607	7.64	21.34	0.48	0.001269	18.3	0.286	0.355	1.687	2.65	0.7804	780.00	0.237	1.649
6	500613	6.65	21.49	0.44	0.001288	23.3	0.292	0.347	1.594	2.65	0.7904	790.00	0.240	1.647
7	500709	7.16	21.18	0.46	0.001288	22.2	0.337	0.403	1.660	2.65	0.9105	910.00	0.237	1.652
8	500802	7.22	21.34	0.44	0.001174	17.2	0.306	0.366	1.625	2.65	1.0006	1000.00	0.230	1.646
9	500830	9.74	21.34	0.47	0.001420	15.6	0.262	0.327	1.653	2.65	1.7820	1780.00	0.263	1.657
10	500920	9.42	21.03	0.48	0.001402	16.1	0.327	0.380	1.514	2.65	1.4914	1490.00	0.223	1.655
11	510427	12.88	21.64	0.53	0.001686	14.4	0.314	0.382	1.669	2.65	1.9023	1900.00	0.236	1.670
12	520619	6.62	21.34	0.47	0.001250	20.6	0.285	0.350	1.663	2.65	0.7544	754.00	0.223	1.625
13	520704	7.78	21.34	0.49	0.001288	22.8	0.314	0.374	1.609	2.65	0.9345	934.00	0.268	1.650
14	520720	6.57	21.34	0.43	0.001136	24.4	0.280	0.341	1.638	2.65	0.5032	503.00	0.230	1.632
15	520731	5.91	21.03	0.42	0.001250	28.3	0.320	0.384	1.631	2.65	0.3921	392.00	0.235	1.636
16	520816	7.53	21.34	0.49	0.001155	22.2	0.299	0.378	1.824	2.65	0.8204	820.00	0.238	1.625
17	520829	5.86	21.34	0.44	0.001212	22.8	0.349	0.428	1.956	2.65	0.4291	429.00	0.219	1.596
18	520926	6.65	21.18	0.47	0.001136	16.1	0.300	0.362	1.638	2.65	0.7363	736.00	0.218	1.603
19	521211	9.40	21.34	0.43	0.001610	0.6	0.334	0.395	1.575	2.65	1.2209	1220.00	0.223	1.611

Note: * — Values computed from adjusted bed material size distribution (wash load materials excluded).

Table 3.5. Niobrara River Data of Colby and Hembree (1955) (continued)

Data No. (1)	Survey Date (yymmdd) (2)	D_c (mm) (16)	Size distribution of bed material, finer than indicated diameters: Grp1 (%) (17)	Grp2 (%) (18)	Grp3 (%) (19)	Grp4 (%) (20)	Grp5 (%) (21)	Grp6 (%) (22)	Grp7 (%) (23)	Grp8 (%) (24)
			0.062	**0.125**	**0.25**	**0.5**	**1**	**2**	**4**	**8** mm
1	490713	0.125	0.0	2.0	35.0	92.0	98.0	99.0	100.0	100.0
2	500303	0.125	0.0	4.0	42.0	76.0	86.0	92.0	98.0	100.0
3	500414	0.125	0.0	4.0	42.0	93.0	99.0	100.0	100.0	100.0
4	500511	0.125	0.0	6.0	66.0	100.0	100.0	100.0	100.0	100.0
5	500607	0.125	0.0	2.0	42.0	89.0	95.0	98.0	100.0	100.0
6	500613	0.125	0.0	1.0	37.0	97.0	99.0	100.0	100.0	100.0
7	500709	0.125	0.0	1.0	26.0	83.0	95.0	98.0	99.0	100.0
8	500802	0.125	0.0	1.0	34.0	91.0	97.0	99.0	100.0	100.0
9	500830	0.125	0.0	4.0	49.0	94.0	99.0	100.0	100.0	100.0
10	500920	0.125	0.0	23.0	41.0	94.0	98.0	99.0	100.0	100.0
11	510427	0.125	0.0	2.0	34.0	86.0	96.0	99.0	100.0	100.0
12	520619	0.125	0.0	1.0	41.0	91.0	99.0	100.0	100.0	100.0
13	520704	0.125	0.0	1.0	31.0	90.0	97.0	99.0	100.0	100.0
14	520720	0.125	0.0	1.0	42.0	94.0	98.0	99.0	100.0	100.0
15	520731	0.125	0.0	2.0	31.0	87.0	97.0	99.0	100.0	100.0
16	520816	0.125	0.0	2.0	40.0	83.0	92.0	95.0	99.0	100.0
17	520829	0.125	1.0	2.0	27.0	77.0	90.0	96.0	99.0	100.0
18	520926	0.125	0.0	1.0	36.0	91.0	99.0	100.0	100.0	100.0
19	521211	0.125	0.0	1.0	25.0	86.0	96.0	98.0	99.0	100.0

Table 3.5. Niobrara River Data of Colby and Hembree (1955) (continued)

Data No. (1)	Survey Date (yymmdd) (2)	Size distribution of sediment load, finer than indicated diameters							
		Grp1 (%) (25)	Grp2 (%) (26)	Grp3 (%) (27)	Grp4 (%) (28)	Grp5 (%) (29)	Grp6 (%) (30)	Grp7 (%) (31)	Grp8 (%) (32)
		0.062	**0.125**	**0.25**	**0.5**	**1**	**2**	**4**	**8 mm**
1	490713	7.0	15.0	58.0	93.0	99.0	100.0	100.0	100.0
2	500303	13.0	33.0	78.0	96.0	97.0	100.0	100.0	100.0
3	500414	7.0	20.0	62.0	96.0	100.0	100.0	100.0	100.0
4	500511	15.0	33.0	72.0	96.0	100.0	100.0	100.0	100.0
5	500607	10.0	26.0	66.0	96.0	100.0	100.0	100.0	100.0
6	500613	8.0	23.0	64.0	96.0	100.0	100.0	100.0	100.0
7	500709	14.0	30.0	68.0	96.0	100.0	100.0	100.0	100.0
8	500802	10.0	26.0	68.0	96.0	100.0	100.0	100.0	100.0
9	500830	27.0	40.0	68.0	96.0	100.0	100.0	100.0	100.0
10	500920	9.0	25.0	70.0	95.0	100.0	100.0	100.0	100.0
11	510427	12.0	32.0	69.0	95.0	100.0	100.0	100.0	100.0
12	520619	11.0	25.0	70.0	97.0	100.0	100.0	100.0	100.0
13	520704	9.0	20.0	56.0	95.0	100.0	100.0	100.0	100.0
14	520720	12.0	26.0	68.0	97.0	100.0	100.0	100.0	100.0
15	520731	13.0	29.0	68.0	97.0	100.0	100.0	100.0	100.0
16	520816	14.0	33.0	69.0	98.0	100.0	100.0	100.0	100.0
17	520829	23.0	40.0	77.0	99.0	100.0	100.0	100.0	100.0
18	520926	9.0	23.0	71.0	98.0	100.0	100.0	100.0	100.0
19	521211	9.0	23.0	69.0	98.0	100.0	100.0	100.0	100.0

Table 3.6. Middle Loup River Data of Hubbell and Matejka (1959)

Data No. (1)	Survey Date (yymmdd) (2)	Flow Properties: Q (m^3/s) (3)	W (m) (4)	d (m) (5)	S (m/m) (6)	T (°C) (7)	Bed Material: D_{50}^* (mm) (8)	D_{65}^* (mm) (9)	σ_g^* (10)	s_g (11)	Transported Sediment: C_T (kg/m^3) (12)	C_T (PPM) (13)	D_{50t}^* (mm) (14)	σ_{gt}^* (15)
1	500301	12.23	43.89	0.30	0.000928	3.9	0.278	0.347	1.684	2.65	2.3133	2310.00	0.241	1.769
2	500321	11.61	42.98	0.29	0.001439	4.4	0.292	0.364	1.707	2.65	2.4437	2440.00	0.248	1.709
3	500425	11.72	44.20	0.30	0.001023	10.6	0.335	0.420	1.976	2.65	1.4814	1480.00	0.223	1.691
4	500509	11.30	44.20	0.34	0.001250	16.1	0.382	0.471	1.926	2.65	1.3411	1340.00	0.223	1.772
5	500606	10.31	43.89	0.32	0.001458	24.4	0.317	0.399	1.980	2.65	0.6322	632.00	0.245	1.698
6	500706	10.45	43.28	0.36	0.001250	21.7	0.424	0.586	2.403	2.65	0.6873	687.00	0.250	1.862
7	501108	12.54	45.11	0.25	0.001345	2.8	0.219	0.268	1.651	2.65	1.4213	1420.00	0.230	1.721
8	510330	10.22	44.20	0.33	0.001345	10.0	0.339	0.416	1.849	2.65	1.4112	1410.00	0.237	1.758
9	510726	10.39	44.81	0.37	0.001288	31.1	0.383	0.476	2.301	2.65	0.5482	548.00	0.259	1.721
10	511031	12.09	46.33	0.31	0.001307	3.9	0.351	0.428	1.877	2.65	1.6417	1640.00	0.272	2.176
11	511205	11.30	37.49	0.33	0.001174	1.1	0.351	0.435	1.952	2.65	2.0225	2020.00	0.240	1.805
12	520718	9.34	44.81	0.33	0.001420	30.6	0.282	0.365	1.808	2.65	0.8525	852.00	0.278	2.048
13	520813	10.93	45.11	0.33	0.001326	26.1	0.334	0.424	2.095	2.65	0.6863	686.00	0.277	1.869
14	520911	9.46	45.42	0.31	0.001288	20.0	0.351	0.440	2.153	2.65	1.0407	1040.00	0.350	2.237
15	520924	10.36	45.11	0.33	0.001307	18.3	0.274	0.344	1.687	2.65	1.0206	1020.00	0.302	1.961

Note: * — Values computed from adjusted bed material size distribution (wash load materials excluded).

Table 3.6. Middle Loup River Data of Hubbell and Matejka (1959) (continued)

Data No. (1)	Survey Date (yymmdd) (2)	D_c (mm) (16)	Size distribution of bed material, finer than indicated diameters							
			Grp1 (%) (17)	Grp2 (%) (18)	Grp3 (%) (19)	Grp4 (%) (20)	Grp5 (%) (21)	Grp6 (%) (22)	Grp7 (%) (23)	Grp8 (%) (24)
			0.062	**0.125**	**0.25**	**0.5**	**1**	**2**	**4**	**8 mm**
1	500301	0.125	0.0	2.0	44.0	90.0	97.0	99.0	99.0	100.0
2	500321	0.125	0.0	4.0	42.0	87.0	96.0	98.0	99.0	100.0
3	500425	0.125	0.0	2.0	32.0	77.0	92.0	96.0	98.0	100.0
4	500509	0.125	0.0	2.0	21.0	70.0	90.0	94.0	96.0	100.0
5	500606	0.125	0.0	2.0	36.0	80.0	90.0	95.0	99.0	100.0
6	500706	0.125	0.0	1.0	17.0	61.0	80.0	88.0	94.0	100.0
7	501108	0.125	1.0	11.0	66.0	94.0	97.0	98.0	100.0	100.0
8	510330	0.125	0.0	2.0	29.0	79.0	94.0	98.0	99.0	100.0
9	510726	0.125	1.0	2.0	22.0	69.0	83.0	90.0	96.0	100.0
10	511031	0.125	0.0	1.0	25.0	77.0	92.0	96.0	99.0	100.0
11	511205	0.125	0.0	1.0	27.0	75.0	92.0	97.0	99.0	100.0
12	520718	0.125	0.0	5.0	46.0	84.0	94.0	97.0	98.0	100.0
13	520813	0.125	0.0	2.0	33.0	76.0	89.0	94.0	97.0	100.0
14	520911	0.125	0.0	2.0	29.0	74.0	87.0	94.0	98.0	100.0
15	520924	0.125	0.0	2.0	45.0	90.0	96.0	98.0	100.0	100.0

Table 3.6. Middle Loup River Data of Hubbell and Matejka (1959) (continued)

Data No. (1)	Survey Date (yymmdd) (2)	Size distribution of sediment load, finer than indicated diameters							
		Grp1 (%) (25)	Grp2 (%) (26)	Grp3 (%) (27)	Grp4 (%) (28)	Grp5 (%) (29)	Grp6 (%) (30)	Grp7 (%) (31)	Grp8 (%) (32)
		0.062	**0.125**	**0.25**	**0.5**	**1**	**2**	**4**	**8 mm**
1	500301	14.0	30.0	67.0	90.0	96.0	99.0	100.0	100.0
2	500321	7.0	25.0	63.0	92.0	98.0	100.0	100.0	100.0
3	500425	7.0	25.0	70.0	93.0	98.0	100.0	100.0	100.0
4	500509	9.0	35.0	74.0	91.0	98.0	100.0	100.0	100.0
5	500606	10.0	28.0	65.0	93.0	98.0	100.0	100.0	100.0
6	500706	10.0	30.0	65.0	88.0	95.0	98.0	100.0	100.0
7	501108	8.0	28.0	69.0	92.0	99.0	100.0	100.0	100.0
8	510330	9.0	26.0	66.0	90.0	97.0	100.0	100.0	100.0
9	510726	12.0	25.0	61.0	91.0	98.0	100.0	100.0	100.0
10	511031	4.0	18.0	56.0	81.0	91.0	97.0	100.0	100.0
11	511205	4.0	19.0	62.0	87.0	95.0	99.0	100.0	100.0
12	520718	10.0	24.0	58.0	84.0	93.0	98.0	100.0	100.0
13	520813	12.0	28.0	60.0	87.0	96.0	100.0	100.0	100.0
14	520911	5.0	15.0	40.0	76.0	88.0	97.0	100.0	100.0
15	520924	6.0	20.0	51.0	84.0	93.0	98.0	100.0	100.0

Flow properties for each record include the measurements of flow discharge, channel width, flow depth, water surface/energy slope, and water temperature. Bed material properties include the measured value of median diameter and D_{65}, size gradation coefficient, and specific gravity of sediment particles. Transported sediment properties include measured values of sediment concentration, median diameter, and size gradation coefficient of sediment in transport. Size distribution data include both the bed material size distribution and the transported sediment size distribution.

3.3 TRANSPORT CAPACITY DISTRIBUTION FUNCTION BASED ON RELATIVE FALL VELOCITY

The fraction of sediment transport capacity, P_{ci}, is analogous to the bed material size fraction, P_{bi}. However, rather than the size distribution of bed material it denotes the size distribution of transported material. The fraction, P_{bi}, of bed material may be visualized as the availability of size class i on the bed surface. It is implied in the BMF concept that the fractional transport rates are directly proportional to the availability of sediment particles on the bed surface. This is also the case for the shear stress correction approach given by Eqs. (2.2) and (2.3). The critical shear stress for incipient motion, the particle entrainment, and transport mechanism for a single size fraction are all affected by the other sizes existing in a sediment mixture. The effective shear stress acting on a particle or the unit stream power expenditure for the entrainment of a given size particle is different for a nonuniform sediment mixture than for uniform material. The resulting fractional transport rates are greatly affected by the so-called sheltering and exposure effect.

Since the fractional transport rates are directly proportional to the availability of sediment particles on the bed surface, the concept of the BMF approach may be adopted as a first approximation in the development of a method to predict the transport capacity distribution function. Further development may introduce appropriate modification factors or terms accounting for the sheltering and exposure effects. In doing so, Yang's dimensionless unit stream power equation may be simplified into (Yang and Molinas 1982)

$$C_t = I\left(\frac{VS}{\omega_{50}}\right)^J \tag{3.1}$$

in which I, J = coefficients, which are related to flow and sediment properties, and ω_{50}= fall velocity of sediment corresponding to particle size D_{50}. Applying the BMF concept [Eq. (2.6)], the bed-material concentration of size fraction i can be expressed as

$$C_{ti} = P_{bi}\left[I\left(\frac{VS}{\omega_i}\right)^J\right] \tag{3.2}$$

Using the conceptual equation of the TCF approach [Eq. (2.7)], the bed-material concentration, C_{ti}, can be also expressed as

$$C_{ti} = P_{ci}\left[I\left(\frac{VS}{\omega_{50}}\right)^J\right] \tag{3.3}$$

From Eqs. (3.2) and (3.3), the following relation is obtained

$$\frac{P_{ci}}{P_{bi}} = \left(\frac{\omega_i}{\omega_{50}}\right)^{-J} \tag{3.4}$$

This equation is similar to Dou et al.'s equation (1987) for suspended load transport capacity. It is a first approximation for the transport capacity fraction in the case of nonuniform sediment mixtures. Figs. 3.1 and 3.2 show the variation of P_{cmi}/P_{bi} with D_i/D_{50} and the variation of P_{cmi}/P_{bi} with ω_i/ω_{50}, respectively, where P_{cmi} is the measured size fraction of bed-material load for size group i. The data shown in Figs. 3.1 and 3.2 include the 118 sets of measurements (891 points) given in Table 3.1. Except for the Samaga et al. data which approximated the surface layer composition with the original mixture composition, it can be seen that a trend exists between P_{cmi}/P_{bi} and D_i/D_{50} or between P_{cmi}/P_{bi} and ω_i/ω_{50}. It should be noted that the relationship between P_{cmi}/P_{bi} and D_i/D_{50} or between P_{cmi}/P_{bi} and ω_i/ω_{50} is not a simple power relationship. The smaller particles are sheltered by the larger ones and are therefore transported at a relatively smaller rate. On the other hand, the larger particles experience larger fluid dynamic forces then they would if they were in a uniform sediment bed and are consequently transported at a higher rate. At low stream powers and low shear stresses the coarse fractions may not move at all, resulting in a state of partial transport.

The theoretical analysis presented earlier in this study indicates that the effect of sheltering on smaller sizes and the effect of exposure on coarse sizes are primarily dependent on the relative diameters (Einstein, 1950; Karim and Kennedy, 1981; White and Day, 1982; Proffitt and Sutherland, 1983; Misri et al., 1984; Wang and Zhang, 1990; Wang et al. 1995; Karim, 1998), such as D_i/X, D_i/D_{50}, D_i/D_A, D_i/D_u, D_i/D_a, and D_i/D_p, of the bed material. Instead of using relative diameters, it is assumed that the ratio ω_i/ω_{50} can also be used to express the sheltering and exposure effect on a size fraction due to the presence of other fractions in sediment mixtures. Retaining the basic form of Eq. (3.4) but introducing a second term to accommodate the sheltering and exposure effect results in

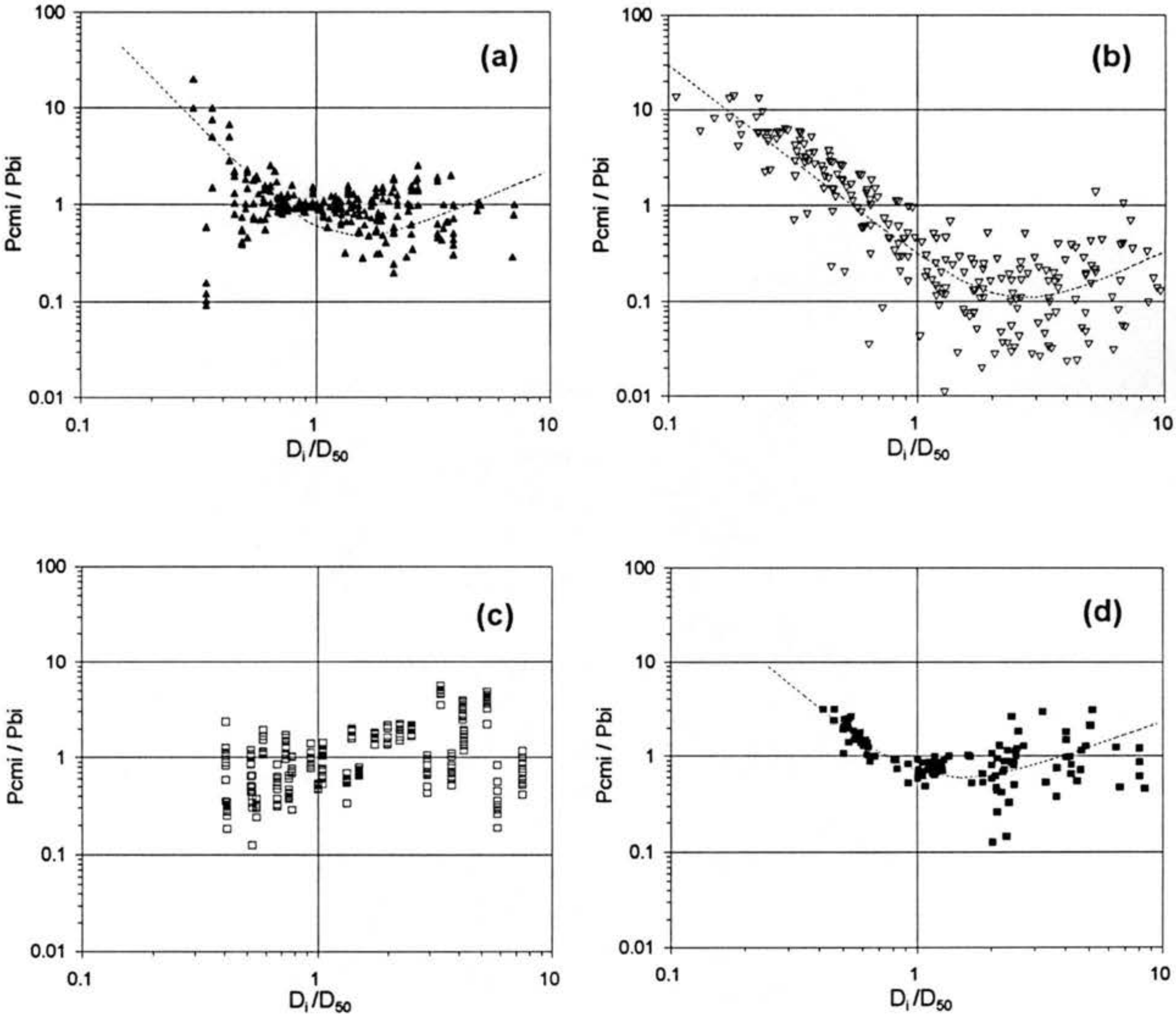

Fig. 3.1 Variation of P_{cmi} / P_{bi} with D_i / D_{50}: (a) Einstein Data; (b) Einstein and Chien Data; (c) Samaga et al. Data; (d) Niobrara River and Middle Loup River Data.

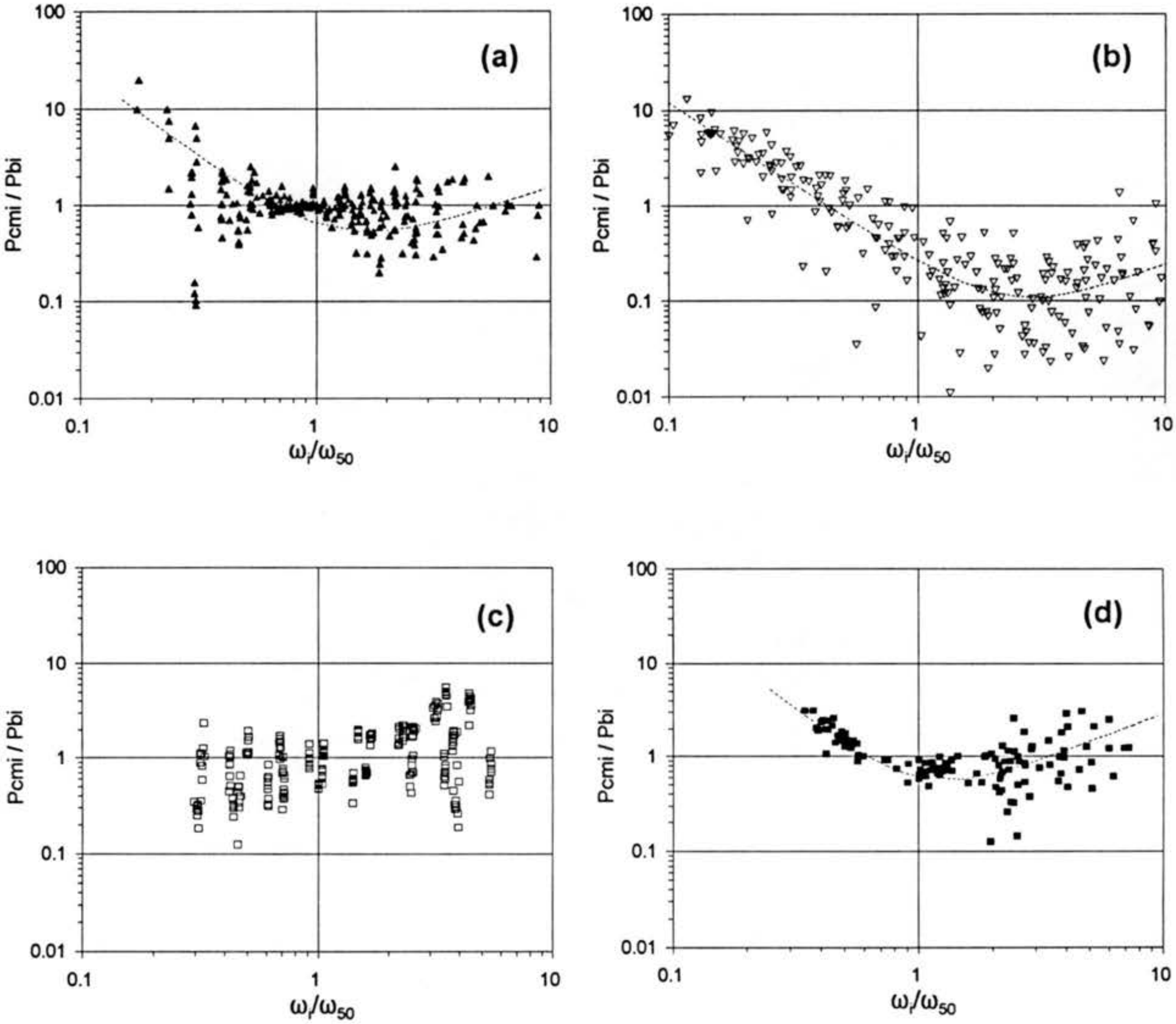

Fig. 3.2 Variation of P_{cmi} / P_{bi} with ω_i / ω_{50}: (a) Einstein Data; (b) Einstein and Chien Data; (c) Samaga et al. Data; (d) Niobrara River and Middle Loup River Data.

$$\frac{P_{ci}}{P_{bi}} = C_1\left(\frac{\omega_i}{\omega_{50}}\right)^{\alpha} + C_2\left(\frac{\omega_i}{\omega_{50}}\right)^{\beta} \tag{3.5}$$

in which C_1, C_2, α, β = coefficients which will be analyzed in the following.

In Eq. (3.5), the fall velocity ω_{50} may be regarded as a scaling or normalizing factor. Particles having a fall velocity smaller than this scaling factor (size) experience sheltering effects, and those particles having a fall velocity larger than this size experience exposure effects. In more general terms, Eq. (3.5) may be expressed as

$$\frac{P_{ci}}{P_{bi}} = C_1\left(\frac{\omega_i}{\omega_n}\right)^{\alpha} + C_2\left(\frac{\omega_i}{\omega_n}\right)^{\beta} \tag{3.6}$$

or

$$P_{ci} = P_{bi}\left[C_1\left(\frac{\omega_i}{\omega_n}\right)^{\alpha} + C_2\left(\frac{\omega_i}{\omega_n}\right)^{\beta}\right] \tag{3.7}$$

in which ω_n = fall velocity corresponding to a scaling size of bed material. According to Eq. (2.7), the summation of P_{ci} should be equal to 1. Applying this as a constraint for Eq. (3.7) gives the following relation

$$1 = \sum_{i=1}^{N} P_{bi}\left[C_1\left(\frac{\omega_i}{\omega_n}\right)^{\alpha} + C_2\left(\frac{\omega_i}{\omega_n}\right)^{\beta}\right] \tag{3.8}$$

Dividing Eq. (3.7) by Eq. (3.8) results in the following basic form of equation for the determination of P_{ci}

$$P_{ci} = \frac{P_{bi}\left[\left(\frac{\omega_i}{\omega_n}\right)^{\alpha} + \zeta\left(\frac{\omega_i}{\omega_n}\right)^{\beta}\right]}{\sum_{i=1}^{N} P_{bi}\left[\left(\frac{\omega_i}{\omega_n}\right)^{\alpha} + \zeta\left(\frac{\omega_i}{\omega_n}\right)^{\beta}\right]} \tag{3.9}$$

in which $\zeta = C_2/C_1$. In this study, D_{50} is taken as the scaling size of bed material. Correspondingly, the scaling fall velocity is expressed as

$$\omega_n = \omega_{50} = f(D_{50}) \tag{3.10}$$

The sheltering and exposure effect experienced by the particles on the bed is dependent upon the amplitude and speed of bed form, and on the different size ranges present on the bed. As the strength of the flow increases, the sheltering and exposure effect becomes secondary since the intensity of turbulence becomes more dominant. This indicates that the coefficients in Eq. (3.9) are not constant but are related to flow and sediment properties and can be defined by the following general function

$$\alpha,\ \beta,\ \zeta = f\left(F_r,\ \frac{V}{V_*},\ \frac{d}{D_{50}},\ \sigma_g,\ \ldots\right) \tag{3.11}$$

in which f = general function; d = average flow depth; V = average flow velocity; and F_r = Froude number. Detailed procedure to determine the three coefficients in Eq. (3.9) is given in the following:

Step 1. Analyze qualitatively the variability of each coefficient in Eq. (3.9) from its theoretical derivation and physical considerations. For example, α is mainly a representative of (-J) appeared in Eq. (3.4) by comparing Eq. (3.5) with Eq. (3.4).

Therefore, α must be a negative value since J is always a positive value. The order of magnitude of α should be roughly between 0-3 because J has a value between 0.5-2.0 for bed-material transport in sand-bed channels.

Step 2. Choose relevant flow and sediment parameters based on previous studies, data analysis, and general understanding of the problem.

Step 3. Choose a functional relationship for each coefficient, including linear and nonlinear relations based on previous studies and use parsimony.

Step 4. Determine the constant values contained in the functional relationship chosen for each coefficient based on the data analysis.

Step 5. Optimize the constant values in the functional relationship for each coefficient by comparing the goodness-of-fit between the computed and measured size fractions of bed-material load.

Step 6. Repeat the trial and error process from step 2 to step 5 until a satisfactory set of coefficients is obtained.

Following the procedure outlined above and through linear and nonlinear analysis of 118 sets of data given in Table 3.1, the expressions of α , β, and ζ are determined as

$$\alpha = -2.2\exp\left[-1000\left(\frac{V}{V_*}\right)^2\left(\frac{d}{D_{50}}\right)^{-2}\right] \tag{3.12}$$

$$\beta = 0.2\sigma_g \tag{3.13}$$

$$\zeta = 2.8F_r^{-1.2}\sigma_g^{-3} \tag{3.14}$$

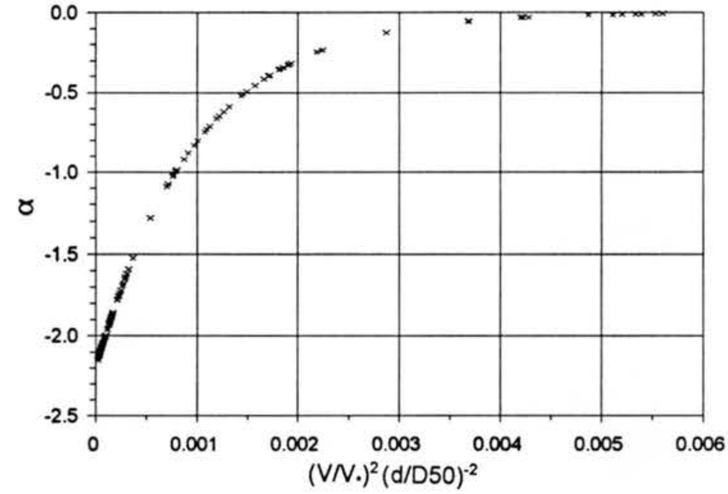

(a)

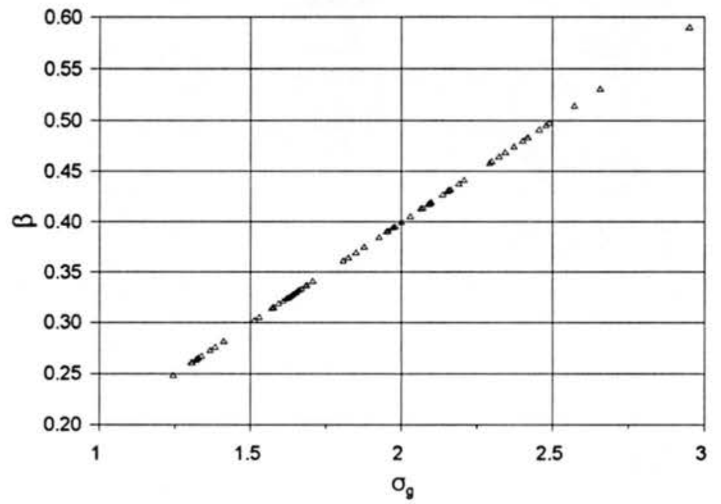

(b)

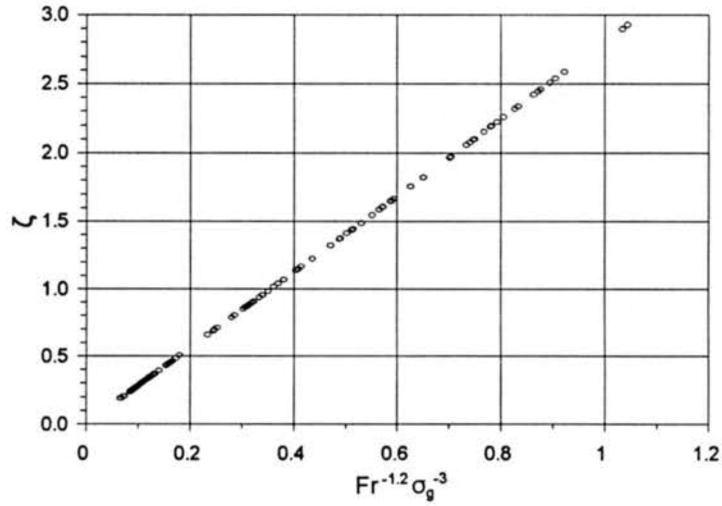

(c)

Fig. 3.3. Variations of the Coefficients Used in Eq. (3.9): (a) α from Eq. (3.12); (b) β from Eq. (3.13); and (c) ζ from Eq. (3.14).

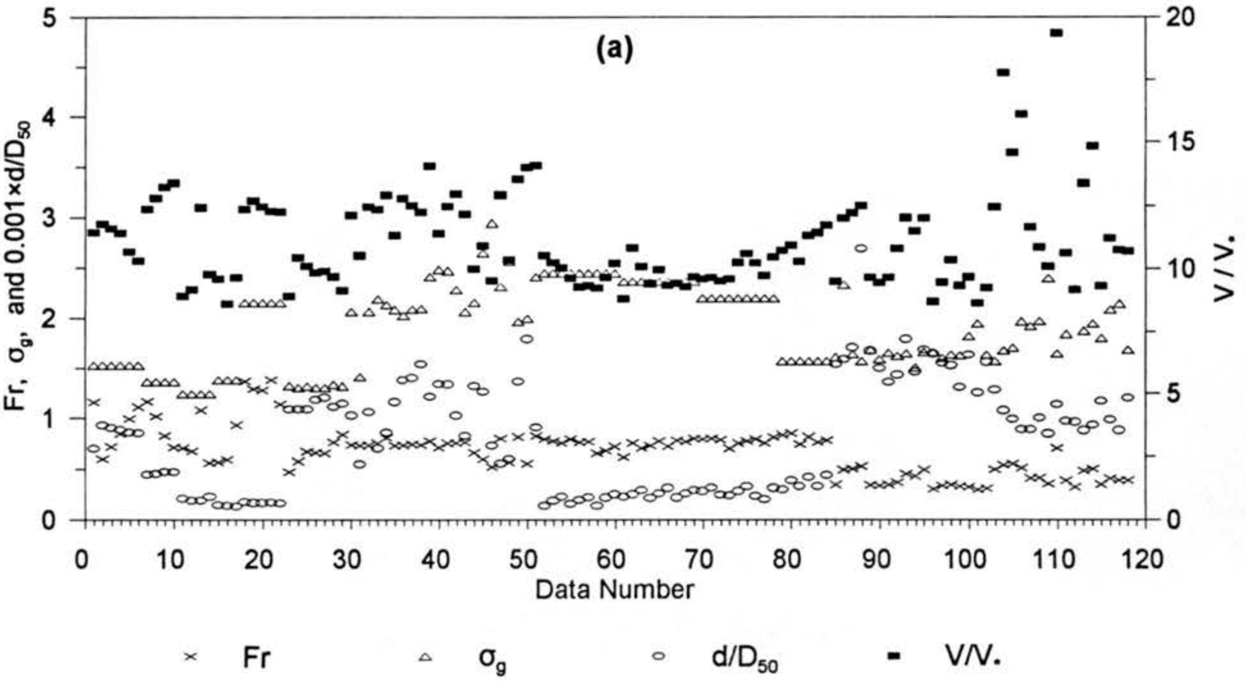

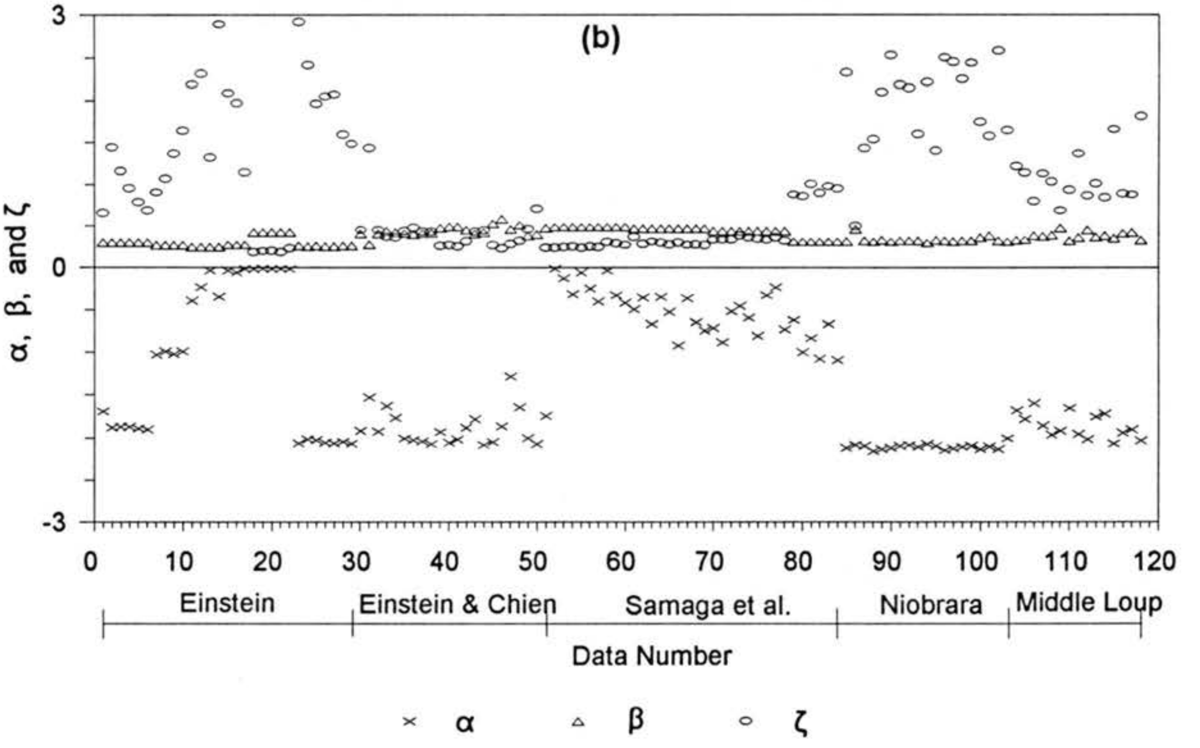

Fig. 3.4. Variability of the Coefficients Used in Eq. (3.9): (a) Variations of the Variables Used in the Computation of α, β, and ζ; (b) Variations of α, β, and ζ.

Corresponding to the above set of coefficients for Eq. (3.9), the fall velocities of the sediment particles are determined from Fig. 2 presented in the U. S. Inter-Agency Committee on Water Resources, Subcommittee on Sedimentation (1957).

Variations of the coefficients of α, β, and ζ expressed by Eqs. (3.12)-(3.14) are plotted in Figs. 3.3 and 3.4. Fig .3.3 shows the variation of the coefficients with corresponding parameters, while Fig. 3.4 shows the variation with data number or data sources. Values of α, β, and ζ for the 118 sets of data given in Table 3.1 are in the ranges of $\alpha = -2.153 \sim -0.008$, $\beta = 0.249 \sim 0.590$, and $\zeta = 0.189 \sim 2.926$.

3.4 TRANSPORT CAPACITY DISTRIBUTION FUNCTION BASED ON RELATIVE DIAMETER

Following the same procedure, P_{ci} can be expressed in terms of D_i / D_{50} starting from Engelund and Hansen's function (1967). An energy approach was used by Engelund and Hansen for bed-material load over a dune bed. The moving sediment particle is lifted over the height of the dune; thus, energy is required. The relationship obtained is

$$f' \Phi_t = 0.1\,\theta^{2.5} \tag{3.15}$$

where

$$\Phi_t = \frac{q_t}{\gamma_s \sqrt{\dfrac{\gamma_s - \gamma}{\gamma} g D_{50}^3}} \tag{3.16}$$

$$\theta = \frac{\tau}{(\gamma_s - \gamma) D_{50}} \tag{3.17}$$

$$f' = \frac{2\,g\,S\,d}{V^2} \tag{3.18}$$

Applying the conceptual equation of BMF and TCF approaches, the unit bed-material load of size fraction i can be expressed as

$$q_{ti} = P_{bi}\,\frac{\theta_i^{2.5}}{\gamma_s\sqrt{\dfrac{\gamma_s-\gamma}{\gamma}gD_i^3}} \tag{3.19}$$

and

$$q_{ti} = P_{ci}\,\frac{\theta^{2.5}}{\gamma_s\sqrt{\dfrac{\gamma_s-\gamma}{\gamma}gD_{50}^3}} \tag{3.20}$$

Eqs. (3.19) and (3.20) yields

$$\frac{P_{ci}}{P_{bi}} = \frac{\dfrac{\theta_i^{2.5}}{\gamma_s\sqrt{\dfrac{\gamma_s-\gamma}{\gamma}gD_i^3}}}{\dfrac{\theta^{2.5}}{\gamma_s\sqrt{\dfrac{\gamma_s-\gamma}{\gamma}gD_{50}^3}}} = \left(\frac{D_i}{D_{50}}\right) \tag{3.21}$$

Similar to Eq. (3.5), introducing a second term to accommodate the sheltering and exposure effect results in

$$\frac{P_{ci}}{P_{bi}} = C_1\left(\frac{D_i}{D_{50}}\right) + C_2\left(\frac{D_i}{D_{50}}\right) \tag{3.22}$$

Eq. (3.22) can be written as the following general form of equation

$$\frac{P_{ci}}{P_{bi}} = C_1\left(\frac{D_i}{D_{50}}\right)^{\alpha} + C_2\left(\frac{D_i}{D_{50}}\right)^{\beta} \tag{3.23}$$

As indicated earlier, the scaling size D_n is chosen to D_{50} of the bed material in this study. Repeating the procedure outlined by Eqs. (3.6)-(3.9) results in

$$P_{ci} = \frac{P_{bi}\left[\left(\frac{D_i}{D_{50}}\right)^{\alpha} + \zeta\left(\frac{D_i}{D_{50}}\right)^{\beta}\right]}{\sum_{i=1}^{N} P_{bi}\left[\left(\frac{D_i}{D_{50}}\right)^{\alpha} + \zeta\left(\frac{D_i}{D_{50}}\right)^{\beta}\right]} \tag{3.24}$$

Using the data sets given in Table 3.1, the coefficients in Eq. (3.24) are determined as

$$\alpha = -2.9\exp\left[-1000\left(\frac{V}{V_*}\right)^2\left(\frac{d}{D_{50}}\right)^{-2}\right] \tag{3.27}$$

$$\beta = 0.2\sigma_g \tag{3.25}$$

$$\zeta = 2.8\,F_r^{-1.2}\,\sigma_g^{-3} \tag{3.26}$$

Variations of the coefficients of α, β, and ζ expressed by Eqs. (3.25)-(3.27) are plotted in Figs. 3.5 and 3.6. Fig .3.5 shows the variation of the coefficients with corresponding parameters, while Fig. 3.6 shows the variation with data number or data sources. Values of α, β, and ζ for the 118 sets of data given in Table 3.1 are in the ranges of $\alpha = -2.839 \sim -0.011$, $\beta = 0.249 \sim 0.590$, and $\zeta = 0.189 \sim 2.926$.

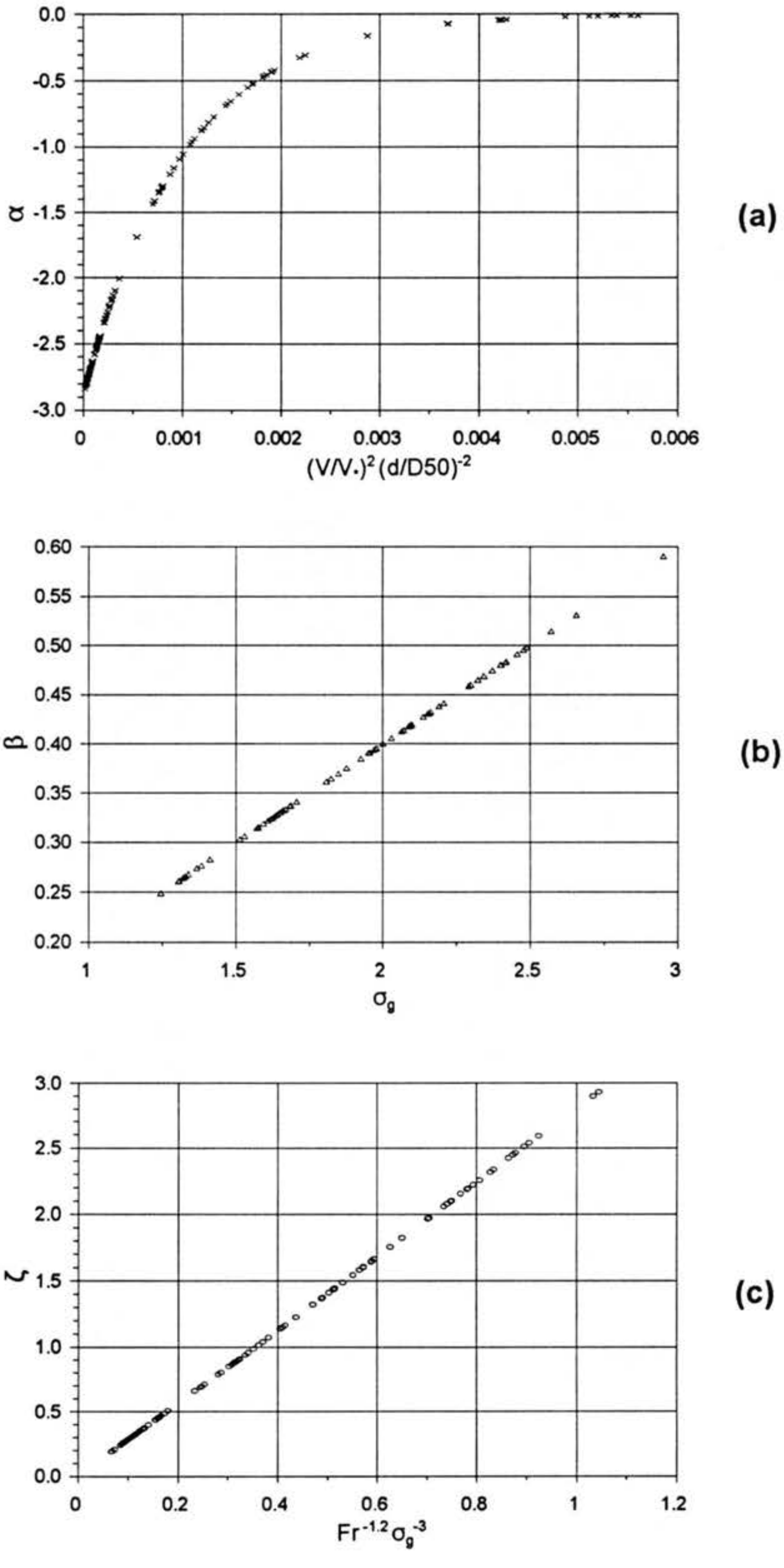

Fig. 3.5. Variations of the Coefficients Used in Eq. (3.24): (a) α from Eq. (3.25); (b) β from Eq. (3.26); and (c) ζ from Eq. (3.27).

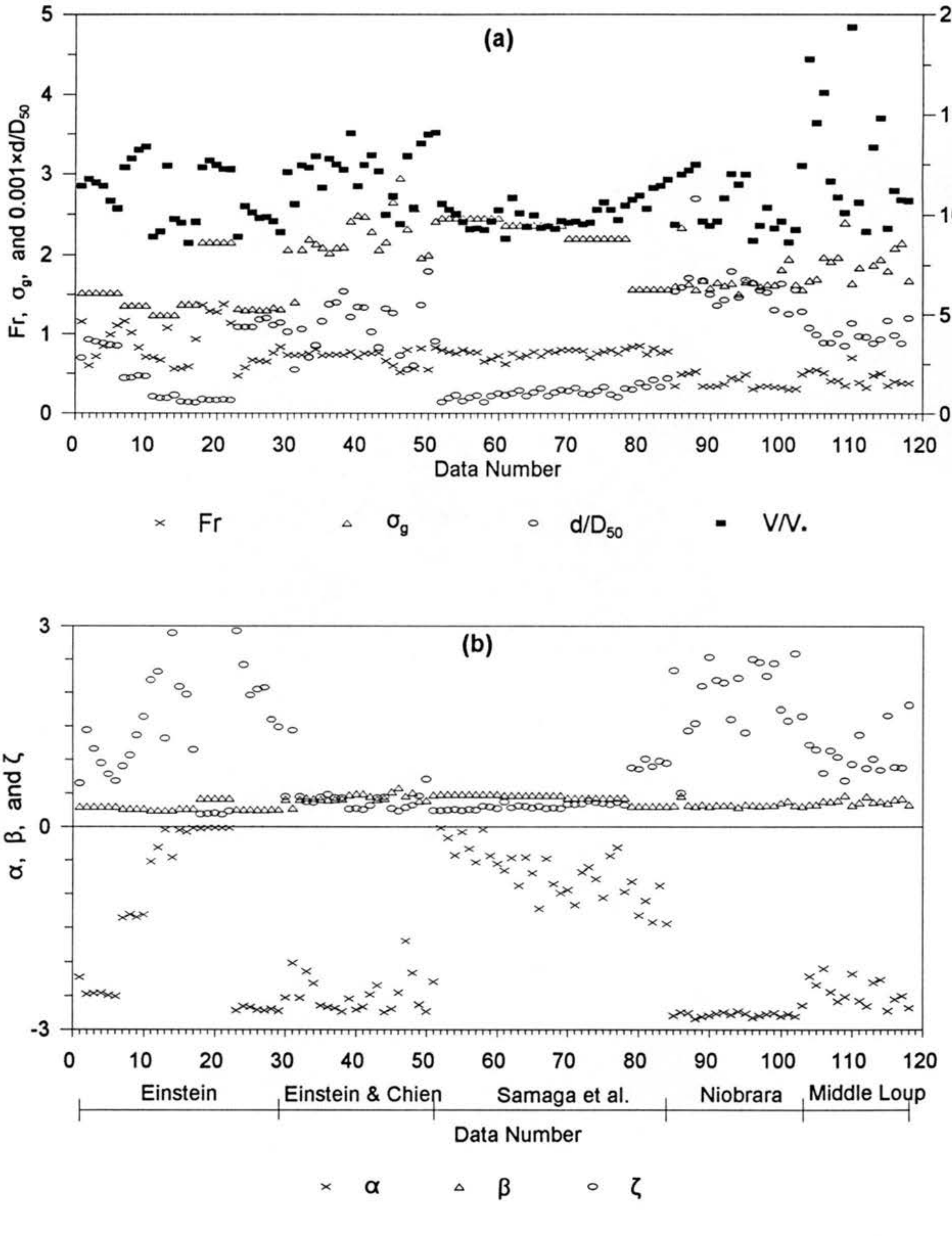

Fig. 3.6. Variability of the Coefficients Used in Eq. (3.24): (a) Variations of the Variables Used in the Computation of α, β, and ζ; (b) Variations of α, β, and ζ.

3.5 EVALUATION OF THE NEW TRANSPORT CAPACITY DISTRIBUTION FUNCTIONS

The size fractions of bed-material transport capacity are computed by using both Eqs. (3.9) and (3.24) with the 118 sets of data. The correlation coefficients between the computed and measured size fractions is 0.856 for Eq. (3.9), and 0.852 for Eq. (3.24). In Figs. 3.7 and 3.8, the ratio of computed size fractions to the measured size fractions of bed-material load are plotted against D_i/D_{50} for Eqs. (3.9) and (3.24), respectively. In these figures, values of P_{cci}/P_{cmi} equal to 1 indicate the perfect agreement of computed fractions to measured transport capacity fractions. It is seen that most of the points fall near the perfect agreement line of P_{cci}/P_{cmi} equal to 1, especially for data points around D_i/D_{50} equal to 1. However, some scatter can be observed for both finer and coarser fractions (data points with smaller and larger values of D_i/D_{50}). This is understandable because the movement of finer and coarser particles in a sediment mixture has higher uncertainty, and is greatly affected by the sheltering and exposure effects.

Figs. 3.9 and 3.10 show comparisons between computed and measured size fractions of bed-material load for Eqs. (3.9) and (2.24), respectively. A close agreement is obtained at the whole range of P_{cmi}, especially at larger values, by the use of Eqs. (3.9) and (3.24).

A earlier version of Eq. (3.24) was presented by Wu and Molinas (1996) and Molinas and Wu (1997). Chapter 5 presents more detailed comparison and an independent test of the transport capacity distribution functions proposed in this Chapter [Eqs. (3.9) and (3.24)]. The fractional bed-material load predictions using different methods will be conducted, and the computed results will be evaluated.

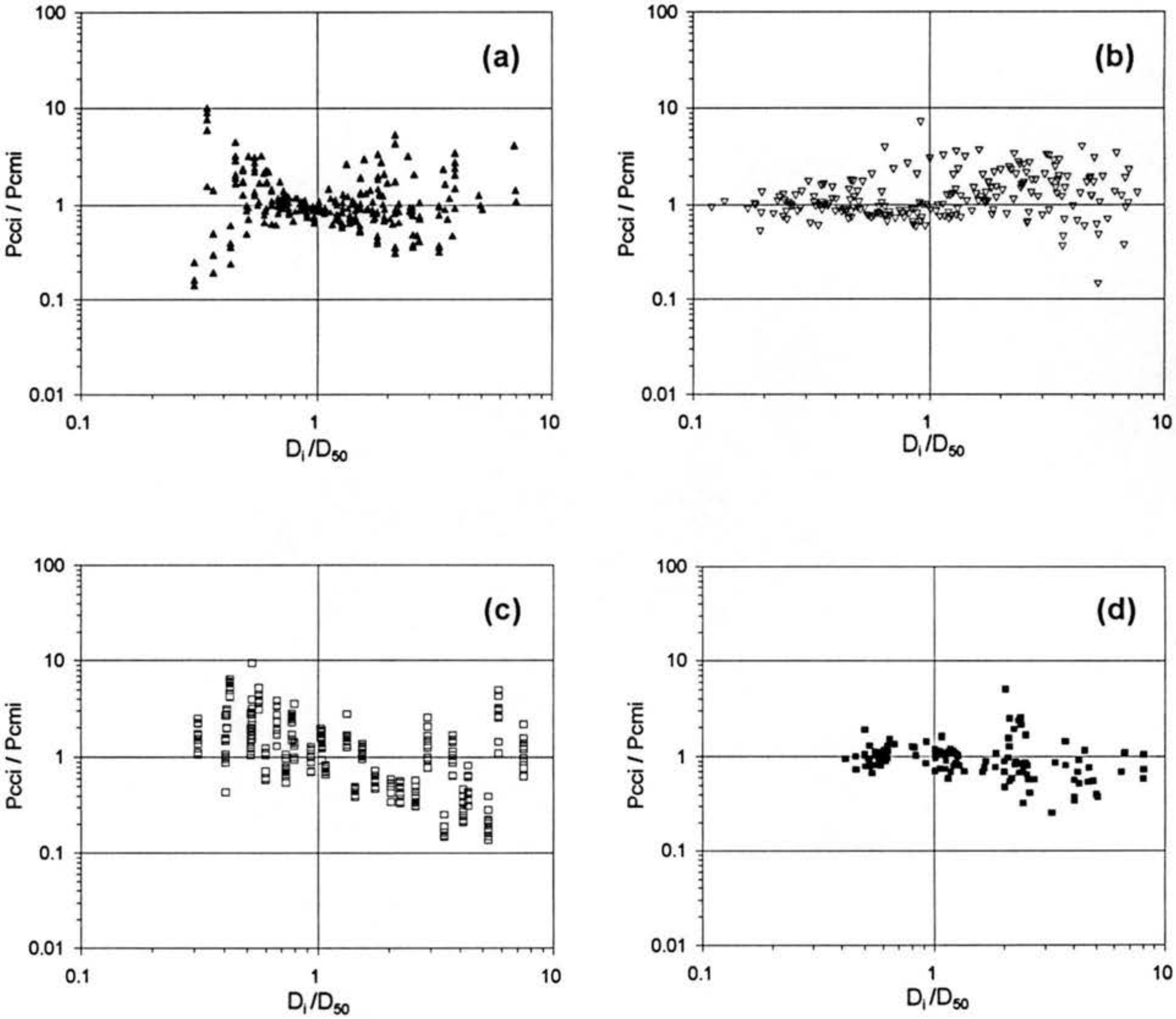

Fig. 3.7. Variation of P_{cci} / P_{cmi} with D_i / D_{50} by the Use of the Transport Capacity Distribution Function of Eq. (3.9) Derived from the TCF Concept: (a) Einstein Data; (b) Einstein and Chien Data; (c) Samaga et al. Data; (d) Niobrara River and Middle Loup River Data.

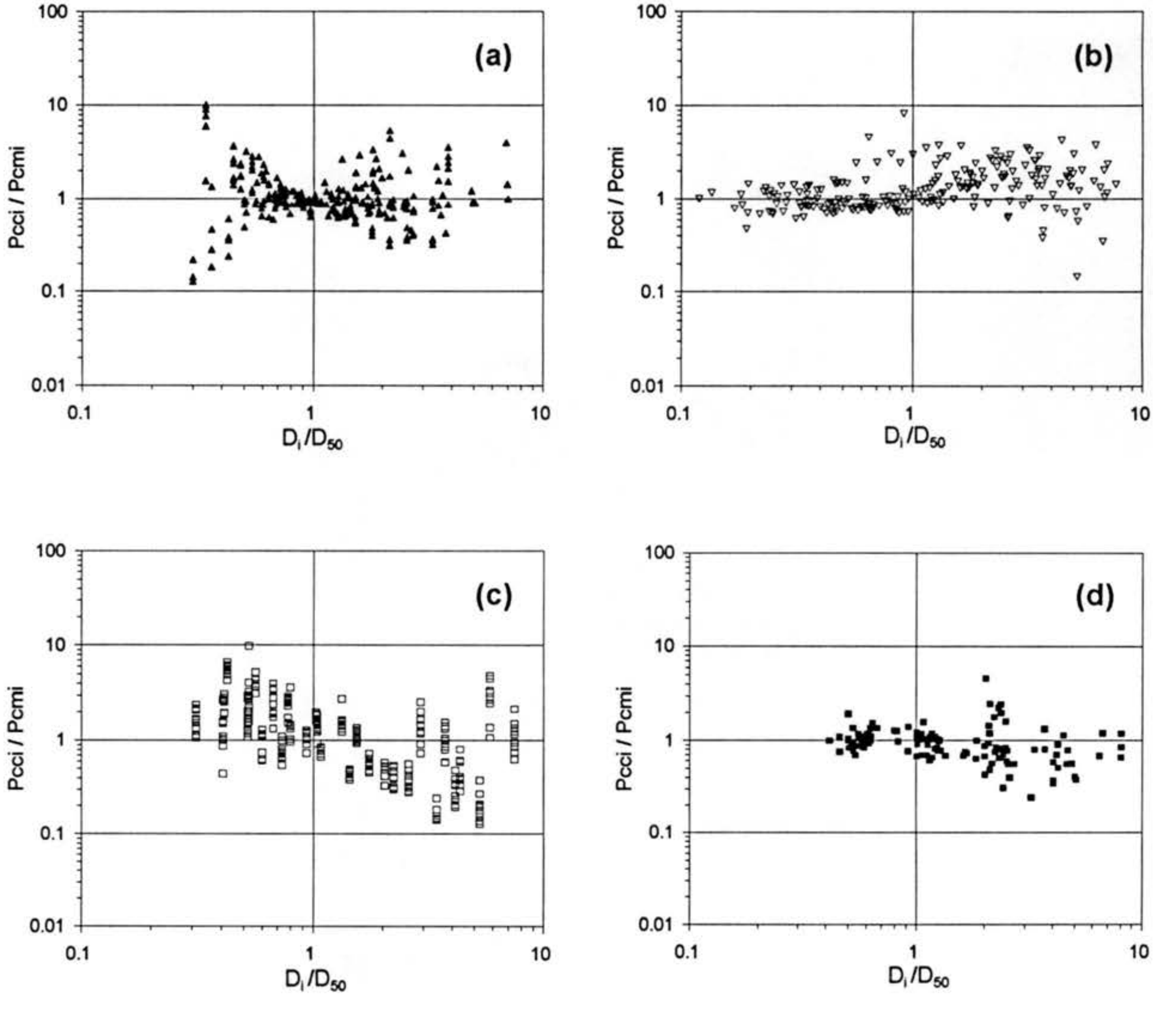

Fig. 3.8. Variation of P_{cci} / P_{cmi} with D_i / D_{50} by the Use of the Transport Capacity Distribution Function of Eq. (3.24) Derived from the TCF Concept: (a) Einstein Data; (b) Einstein and Chien Data; (c) Samaga et al. Data; (d) Niobrara River and Middle Loup River Data.

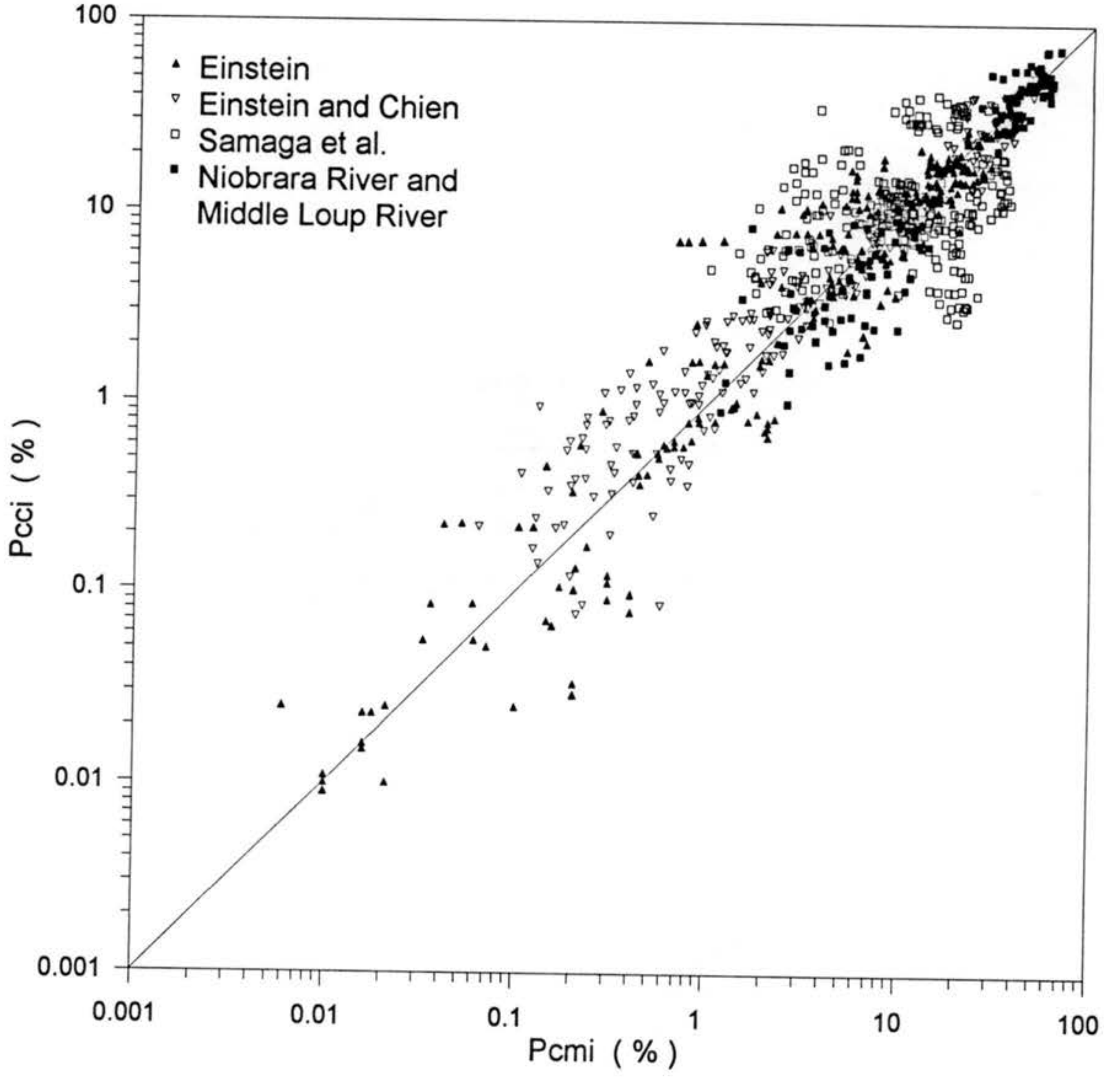

Fig. 3.9. Comparison between Percentages of Computed and Measured Bed-Material Concentrations for Individual Size Fractions in Sediment Mixtures by the Use of the Transport Capacity Distribution Function of Eq. (3.9) Derived from the TCF Concept.

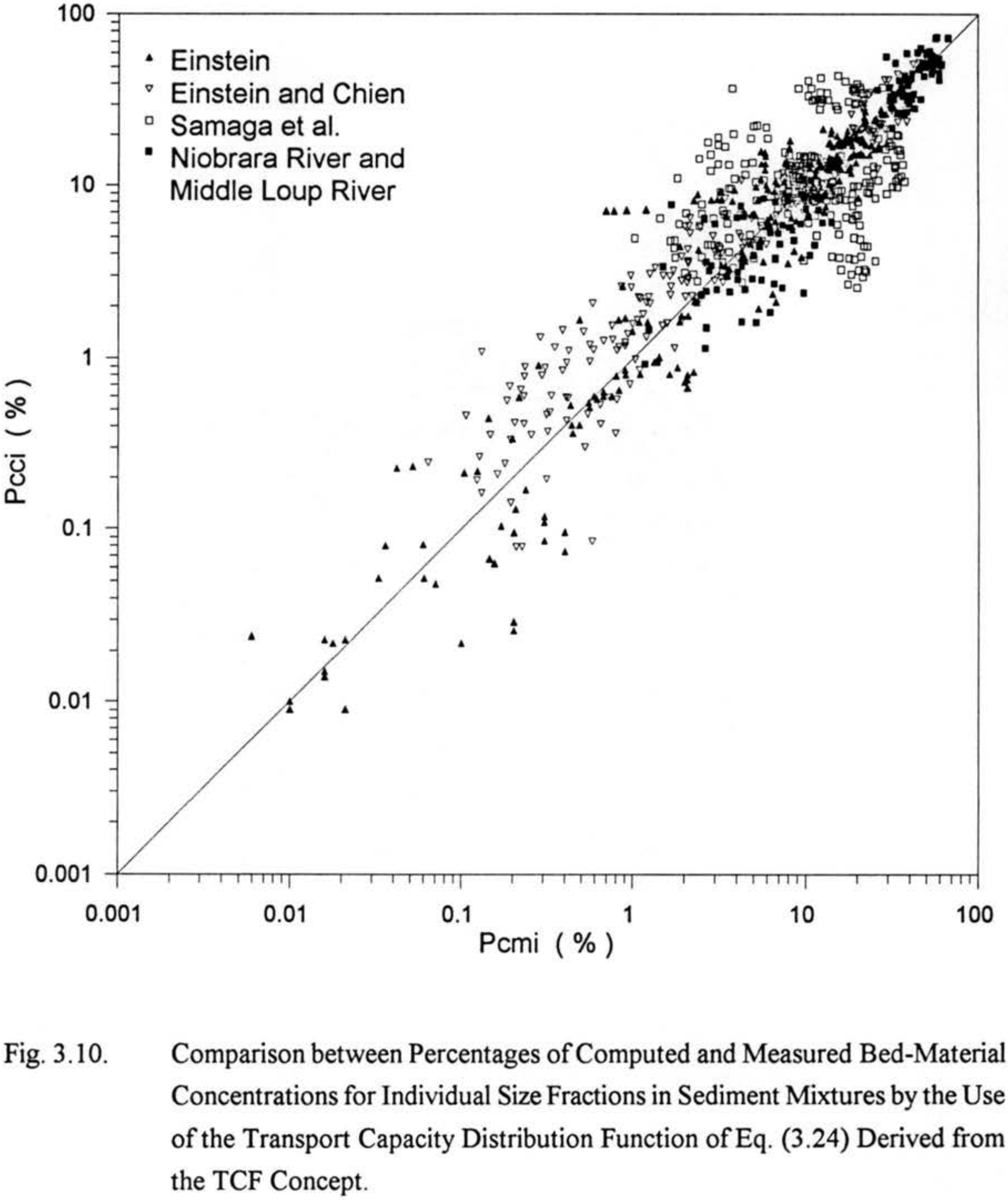

Fig. 3.10. Comparison between Percentages of Computed and Measured Bed-Material Concentrations for Individual Size Fractions in Sediment Mixtures by the Use of the Transport Capacity Distribution Function of Eq. (3.24) Derived from the TCF Concept.

CHAPTER 4

BED-MATERIAL TRANSPORT RATE

4.1 GENERAL

According to the concept of the TCF approach, C_t can be determined using any appropriate bed-material load equations available in the literature. However, the performance of a particular equation selected for the computation of C_t affects the absolute magnitude of fractional transport rates. One should be aware of the limitations and the applicability of those equations developed based on uniform sediments, and choose reliable equations, possibly those considering the effects of the size gradation.

Of the commonly used sediment transport relations, only Einstein (1950), Laursen (1958), and Toffaleti (1969) seek to take the grading of sediment into account by directly computing sediment transport rates for each size fraction. The bed-material load is obtained from the summation of transport rates for each size fraction. Other relations use an "equivalent, effective, or significant" particle size which may be D_{35}, D_{50}, or another characteristic size. It is assumed that the chosen equivalent size will produce the correct sediment transport rate for the whole mixture when used with the equations derived from uniform sediments.

In principle, those relations which directly compute transport rate for each size fraction are supposed to produce a more reliable and accurate prediction of total sediment transport rate for sediment mixtures. Unfortunately, it is not the case in practice. Even though the bed-material load formulas of Engelund and Hansen (1967), Ackers and White (1973), and Yang (1973) were developed based on a single fixed representative bed material size (D_{35} or D_{50}), they have gained increasing acceptance. However, even when they are applied to nonuniform sediment mixtures, these methods yield a relatively large scatter of computed results.

Various representative sizes of bed material have been used for the computation of transport rate for sediment mixtures. Einstein (1944) proposed D_{35} as the representative diameter in transport computations. Meyer-Peter and Müller (1948) suggested that the weighted mean diameter of bed material should be used as the representative size for nonuniform sediment mixtures. For graded sediment mixtures, Ackers and White (1973) suggested the use of D_{35} in their equation. Han (1973) proposed a weighted average fall velocity for nonuniform sediment mixtures. In additional to D_{50}, a size distribution parameter, D_{90}/D_{30}, was used by Smart and Jaeggi (1983) to develop their sediment transport equation for steep-slope rivers. Smart and Jaeggi compensated the effect due to sediment gradation by a weak power function of D_{90}/D_{30}. In applying the Engelund and Hansen equation to sediment mixtures, Nordin (1989) stated that a weighted representative diameter of bed material should be used. The gradation coefficient, G, defined as the arithmetic mean of D_{84}/D_{50} and D_{50}/D_{16}, was used by Shen and Rao (1991) to compute transport rate in sediment mixtures. In their regression equation for sediment transport, Shen and Rao showed the improvement due to the inclusion of G.

Different investigators suggesting different representative sizes of bed material for nonuniform sediment mixtures points out the fact that a single fixed size, such as D_{50}, is inadequate in representing the various sizes present in sediment mixtures. In computing the transport rate for mixtures, the representative sediment size should reflect the different bed material size distributions. This is clearly of significance since grading curves with differing shapes will have different effects on the transport process. Considering the physical processes affecting the sediment transport in the flow, D_{90}/D_{30}, G, or other factors representing the gradation of mixtures are all believed to be significant in the transport of sediment mixtures. These parameters aim to represent the range of particle sizes which are significantly present in the bed material. For a given flow condition, even if D_{50} of bed material remains the same, the resistance to flow, incipient motion, sand wave movement, and transport of sediment mixtures are different for different size distributions.

Instead of using a single fixed size or a single fixed size with a size gradation parameter as the representative property of bed material, van Rijn (1984) and Hsu and Holly (1992) suggested the use of variable representative sizes for the computation of sediment transport rate for nonuniform mixtures. The variable representative size is analogous to the median or mean size of sediments in transport. It is believed that the variable representative size is a better representation of the sediment load than a fixed particle diameter such as D_{35}, D_{50}, or D_{65} of the bed material.

In the development of the suspended load transport equation, van Rijn (1984) proposed an empirical equation to estimate the representative diameter, D_s, for suspended sediment load. The equation that gave the same value for the suspended load as that computed with Einstein's method was determined by trial and error. This equation was expressed as

$$\frac{D_s}{D_{50}} = 1 + 0.011\,(G - 1)(T - 25) \tag{4.1}$$

in which T = transport stage parameter. van Rijn stated that the D_s is a better representation of the suspended load than a fixed particle diameter such as D_{35}, D_{50}, or D_{65} of the bed material. Fig. 4.1 is a plot showing a comparison of Eq. (4.1) with some experiment data given by Guy et al. (1966).

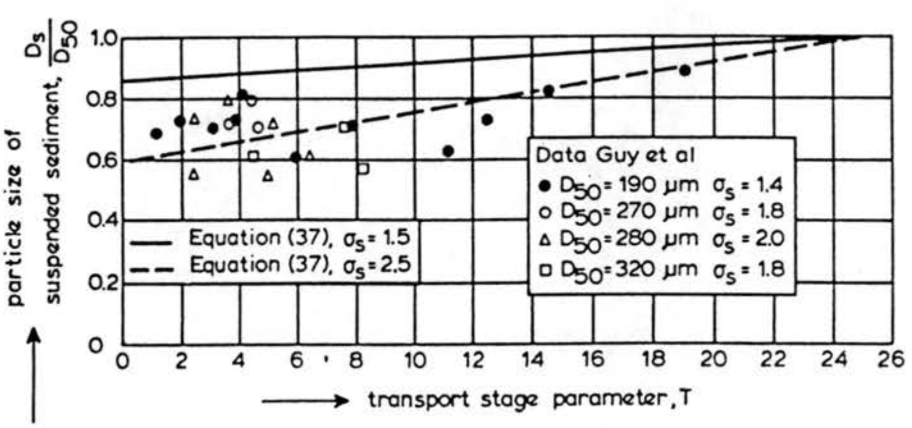

Fig. 4.1. Representative Particle Diameter of Suspended Sediment (after van Rijn, 1984).

Hsu and Holly (1992) suggested the use of a mean size of transported material (bedload), D_{mt}, as the representative diameter in their bedlaod computations. First they proposed a method to compute the size distribution of the transport material [see Eqs. (2.57)-(2.58)]. Then they determined the mean size, D_{mt}, from the computed size distribution. Hsu and Holly argued that if D_{mt} was visualized as the representative property of a uniform sediment, the bedload discharge could be evaluated using any appropriate bedload equations.

The use of a variable representative size is an interesting attempt for the prediction of sediment transport rate. Unfortunately, the representative size of Eq. (4.1) is developed based on the results computed with Einstein's method; and it is limited to suspended load. The representative size proposed by Hsu and Holly is limited to bedload; and it is not verified with measurements. In this chapter, the variation of median diameter, D_{50t}, of bed-material sediments in transport is studied. An equation for the prediction of D_{50t} is proposed. The use of D_{50t} as representative size for the computation of bed-material load is presented.

4.2 MEDIAN DIAMETER OF SEDIMENT IN TRANSPORT

The size distribution of sediment in transport is directly related to the size distribution of bed material and to the effective shear stress acting on each size group and does not necessarily resemble the gradation of bed material. Hsu and Holly (1992) pointed out that one must distinguish not only between parent-bed material composition and bed-surface material composition (or active-layer material) but also between bed-surface material composition and transported-material composition. The size gradation of transported material is generally different from the gradation of bed-surface material and should be treated as a new unknown variable.

Fig. 4.2 shows the relationship between the median diameter of transported material (bed-material load), D_{50t}, and the median diameter of bed material, D_{50}. The data shown in Fig. 4.2 include 85 sets of flume and field data given in Table 3.1 and 280 sets of Colorado State University flume data (Guy, Simons, and Richardson, 1966). Those 33 sets of flume data from Samaga et al. (1986a, b) listed in Table 3.1 are not plotted in Fig. 4.2 because the bed material composition data reported by Samaga et al. are composition of parent-bed material. As indicated earlier, the composition of bed-surface layer is different from the composition of parent-bed material. The composition of sediment in transport is directly

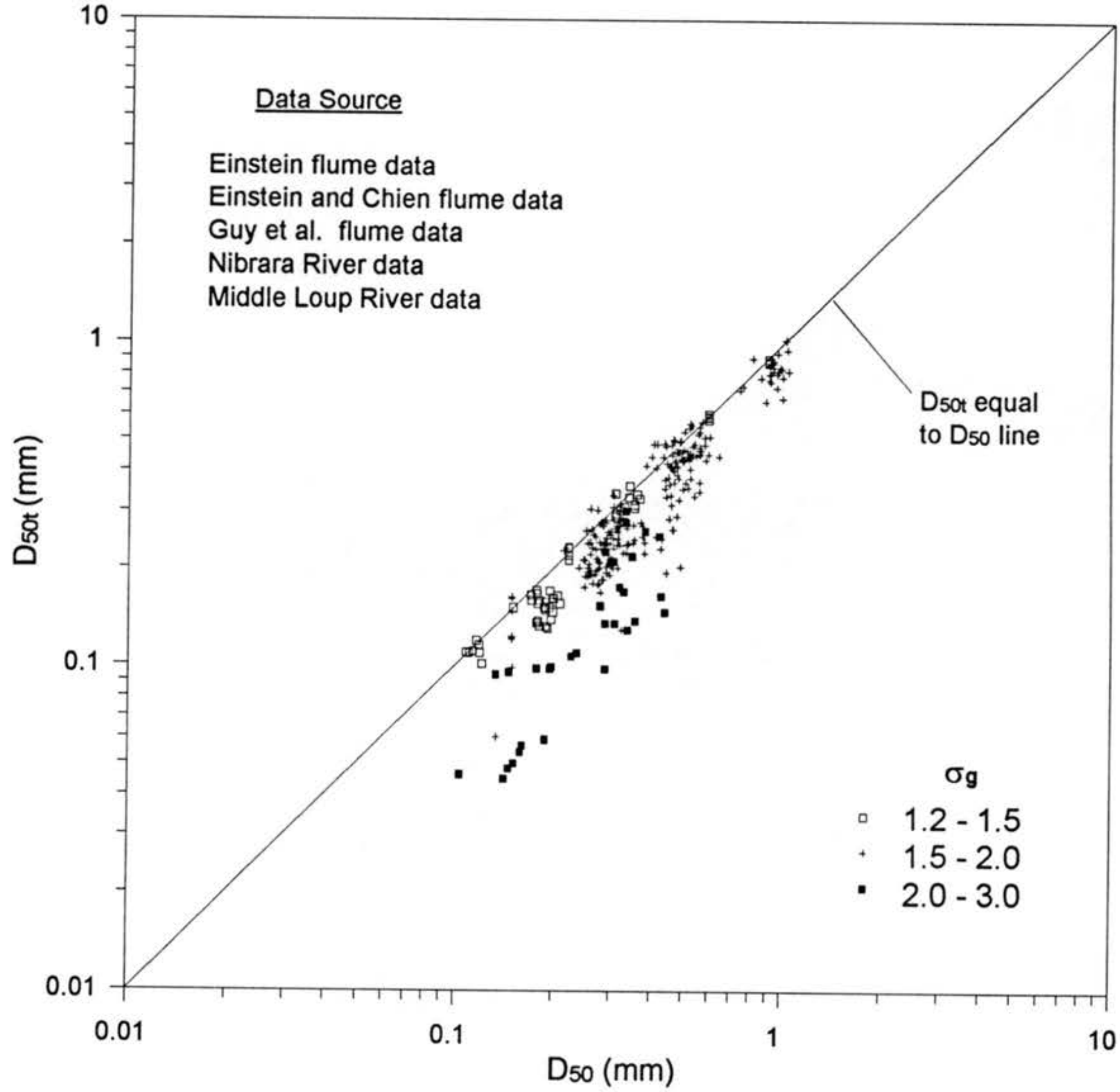

Fig. 4.2. Relationship between the Median Diameter of Bed-Material Load Sediment in Transport, D_{50t}, and the Median Diameter of Bed Material, D_{50}.

related to the composition of bed-surface layer, not the parent-bed material. From Fig. 4.2 it can be seen that, for the majority of the data, the D_{50t} corresponding to the sediment in transport is finer than the D_{50} corresponding to the bed material. This is due to the fact that the finer sizes in sediment mixtures are more readily transported by flow, which is commonly referred as the selective transport of grains by flow or hydraulic sorting. It can also be seen that for a given bed material size, for larger gradations the size of sediment in transport is finer (i.e., the larger the σ_g, the finer the sediment in transport).

The median diameter of bed-material load sediment in transport, D_{50t}, may be related to bed (bed-surface) material composition through a functional relationship of the form

$$D_{50t} = f\left(D_{50},\ \sigma_g,\ V_*/\omega_{50}\ ,\ \ldots\right) \tag{4.2}$$

In order to reflect the physical processes related to the variation of sediment size in transport, as σ_g increases, D_{50t} should decrease. Following extensive comparisons of linear and nonlinear functional relationships, the following expression was determined for D_{50t}

$$D_{50t} = \frac{D_{50}}{1 + B(V_*/\omega_{50})^m(\sigma_g - 1)^n} \tag{4.3}$$

in which B, m, and n = coefficients, which are equal to 0.8, 0.1, and 2.2, respectively.

Fig. 4.3 shows a comparison between the computed median diameter, D_{50t}, of bed-material load sediment in transport using Eq. (4.3) and the measured values. It is seen that the computed median diameters, D_{50t}, are in good agreement with the measured values.

Since the value of exponent m in Eq. (4.3) is very small (0.1), the resulting value of $(V_*/\omega_{50})^{0.1}$ is close to unity. Therefore, the flow intensity term, V_*/ω_{50}, may be neglected. This results in the following simplified equation

$$\frac{D_{50t}}{D_{50}} = \frac{1}{1 + 0.8\,(\sigma_g - 1)^{2.2}} \tag{4.4}$$

which represents the variation of relative size of sediment in transport with bed size gradation.

The value of relative median diameter, D_{50t}/D_{50}, is plotted against the geometric standard deviation, σ_g, of bed material in Fig. 4.4 for the same data shown in Fig. 4.2. It is clearly demonstrated that as σ_g increases, the value of D_{50t}/D_{50} decreases, and it generally follows the equation line given by Eq. (4.4). The variation of D_{50t}/D_{50} versus σ_g results from the selective transport of nonuniform sediment mixtures, which is a significant phenomenon in the transport process of nonuniform sediments.

Fig. 4.5 shows the variation of D_{50t}/D_{50} versus σ_g for another 124 sets of flume and field data, including flume data of Nonicos (Vanoni and Brooks, 1957; 12 sets), Taylor and Vanoni (1972, 6 sets), Vanoni and Brooks (1957, 15 sets), Vanoni and Huang (1967, 16 sets), and Wang and Zhang (1990, 27 sets), field data from the Platte River (Kircher, 1983, 20 sets), Rio Grande Conveyance Canal (Culbertson, Scott, and Bennett, 1972; 9 sets), and Yellow River at Tuchengzi (Long and Liang, 1994; 19 sets). These data cover wider ranges of variations of flow and sediment conditions with median diameter of 0.055-2.10 mm, geometric standard deviation of 1.25-4.06, discharge of 0.0037-3980, velocity of 0.19-2.81, depth of 0.062-1.91, and slope of 0.000078-0.0039. Since these 124 sets of data were not used in the development of Eq. (4.3) and its simplified relationship of Eq. (4.4), Fig. 4.5 is an independent test for the relationship given by Eq. (4.4).

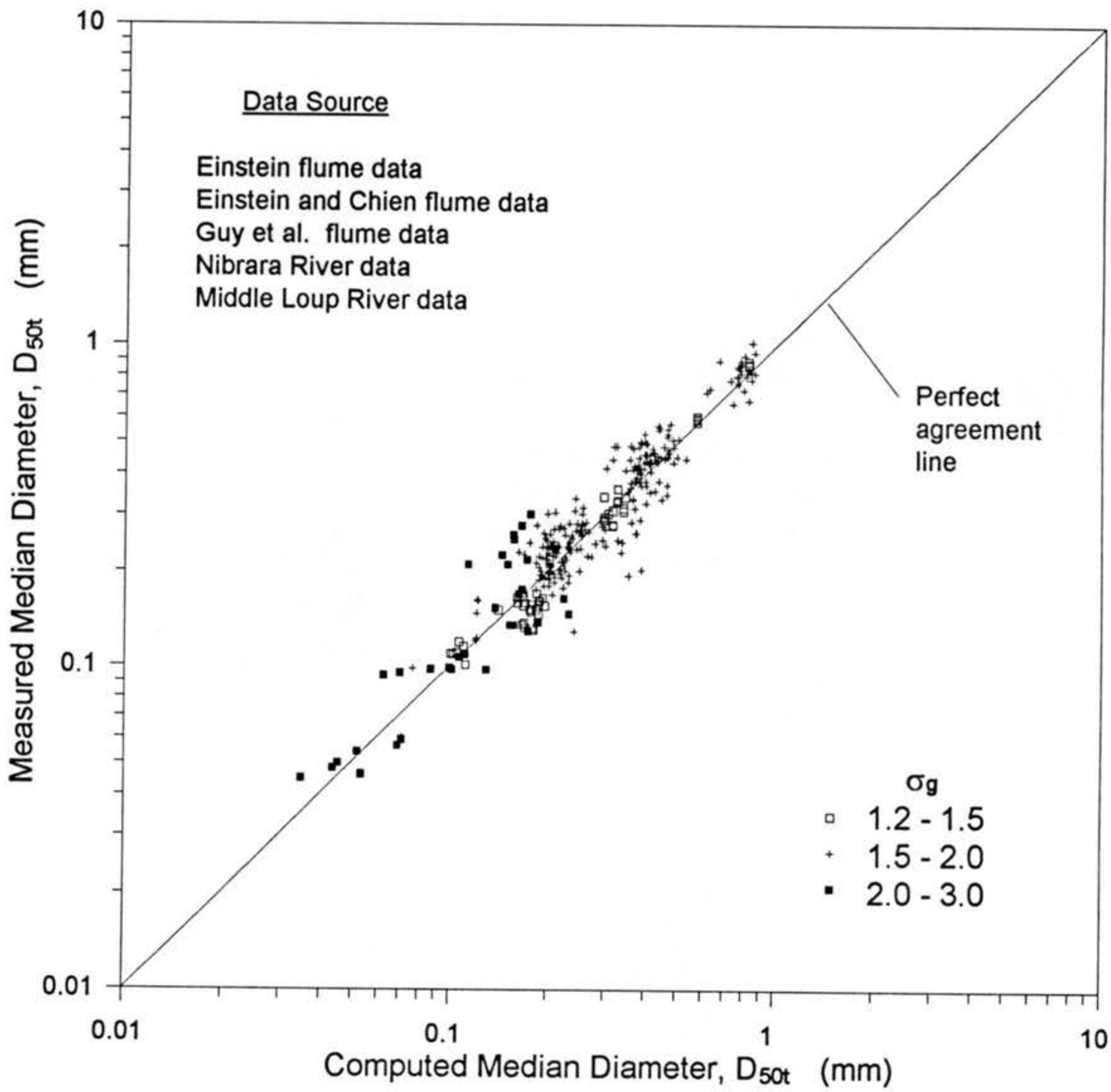

Fig. 4.3. Comparison between the Computed and Measured Median Diameter of Bed-Material Load.

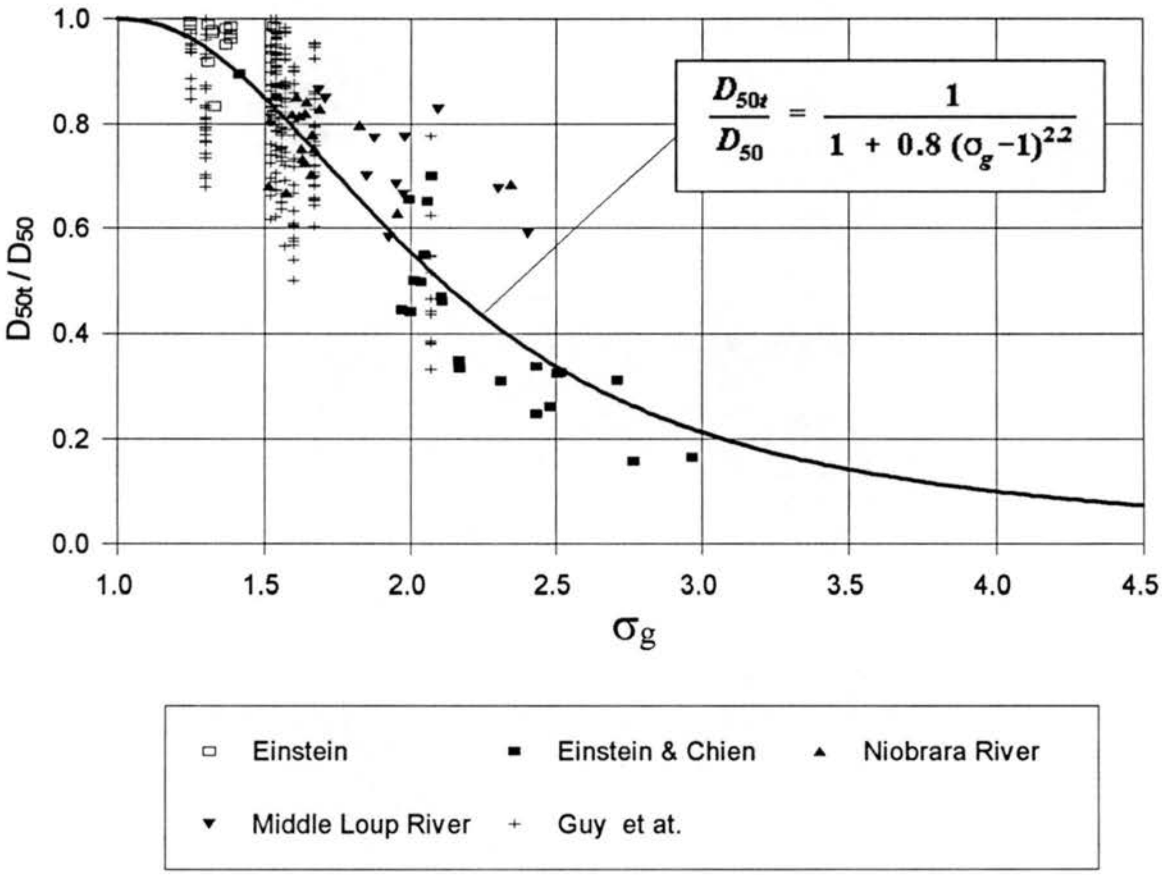

Fig. 4.4. Relationship between Relative Diameter, D_{50t} / D_{50}, and Geometric Standard Deviation, σ_g, for the 85 Sets of Flume and Field Data Derived from Table 3.1 and the 280 Sets of Data from Guy et al. (1966).

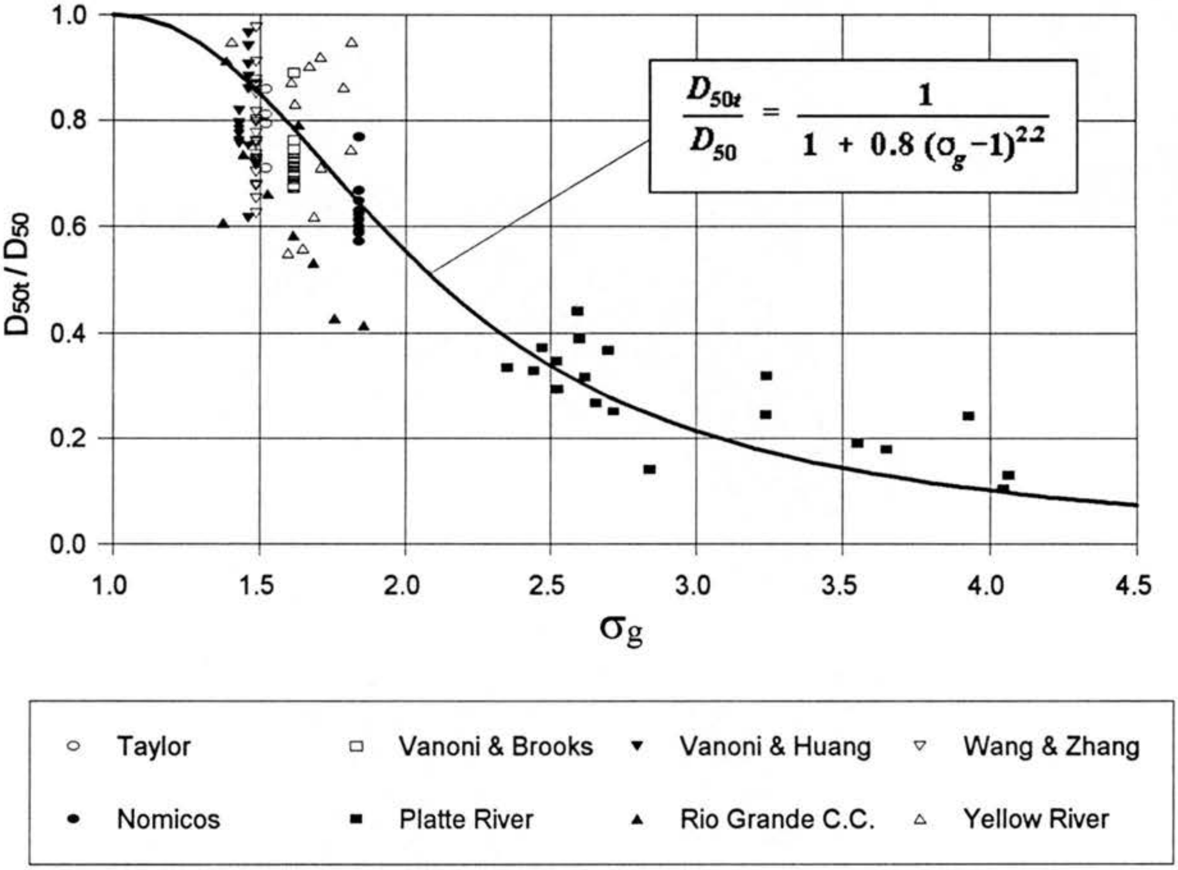

Fig. 4.5. Relationship between Relative Diameter, D_{50t}/D_{50}, and Geometric Standard Deviation, σ_g, for Another 124 Sets of Flume and Field Data (Independent Verification Data).

4.3 EFFECT OF SIZE GRADATION ON TRANSPORT OF SEDIMENT MIXTURES

The function of Engelund and Hansen (1967) can be used to demonstrate the effect of size gradation on the transport of sediment mixtures. This equation is given as

$$f'\Phi_t = 0.1\,\theta^{2.5} \tag{4.5}$$

in which Φ_t = dimensionless sediment transport function; and θ = dimensionless shear parameter. Their definitions are given by Eqs. (3.16) and (3.17), respectively.

For the 118 sets of data given in Table 3.1, $f'\Phi_t$ versus θ is plotted in Fig. 4.6. The Engelund and Hansen equation given by Eq. (4.5) is shown by a solid line, and the experimental data are sorted by sediment size ranges. Engelund and Hansen's function represents the transport phenomenon adequately, on the average, and Φ_t is inversely proportional to D_{50}. However, for a given flow condition and sediment size, a considerable scatter exists around the equation line.

The functional relationship of Engelund and Hansen given by Eq. (4.5) is replotted in Fig. 4.7 for three ranges of σ_g values using the same data. This shows that sediment transport is significantly affected by σ_g. For a given D_{50}, the dimensionless sediment transport function, Φ_t, is larger for larger σ_g values. This indicates that the combination of D_{50} and σ_g is a more effective measure for quantifying the effect of bed material size on the transport of sediment mixtures than D_{50} alone. From Fig. 4.7 it can be seen that the scatter in the relation is also related to the θ value. This implies that the adjustment is not fixed but varies with the flow conditions as well as with σ_g.

Similar to those representative diameters of sediment in transport used by van Rijn (1984) and Hsu and Holly (1992), the median diameter estimated by Eq. (4.3) can be used

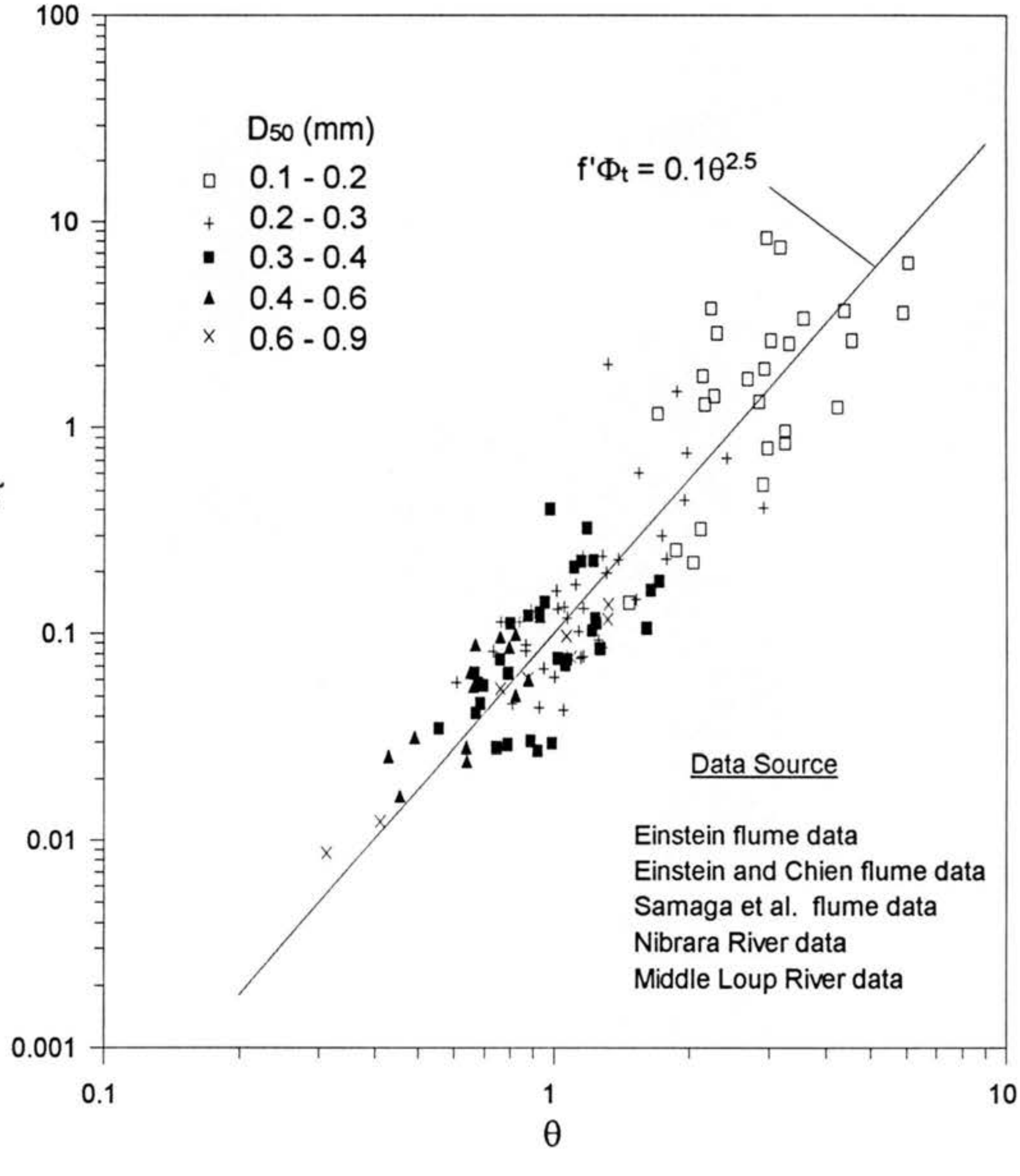

Fig. 4.6. Relationship between $f'\Phi_t$ and θ Sorted by Bed Material Size.

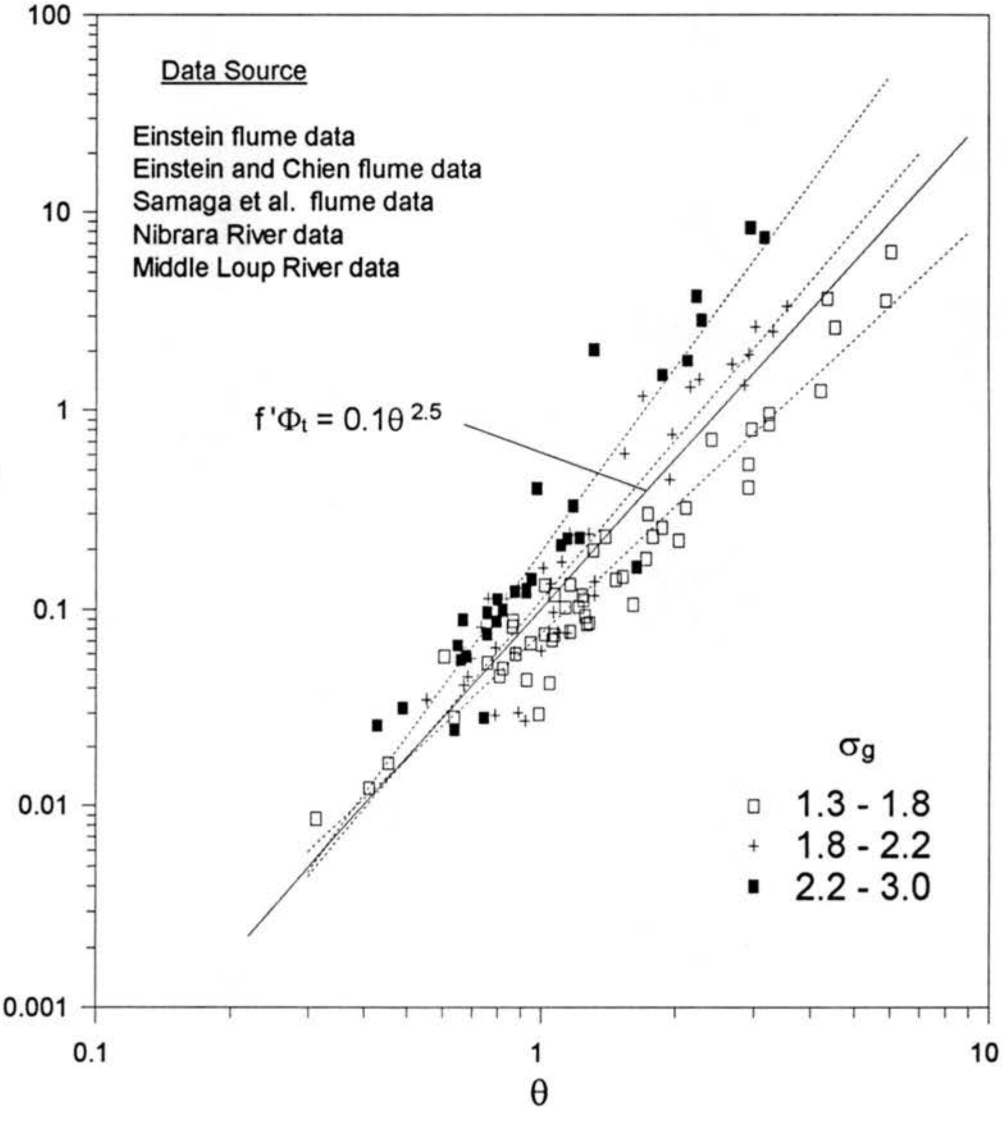

Fig. 4.7. Relationship between $f'\Phi_t$ and θ Sorted by Size Gradation (σ_g values).

as representative size in estimating the transport discharge for nonuniform sediment mixtures. It is assumed that this representative diameter will produce the correct sediment transport rate for the whole mixture when used with the equations derived from uniform sediments. As discussed earlier, D_{50t} decreases as σ_g increases. A smaller representative diameter is thus corresponding to a larger computed transport rate. This is consistent with previous results (e.g., Einstein, 1944; Ackers and White, 1973).

Considering that the existing transport equations were calibrated with data including nonuniform sediment mixtures, the coefficients in these equations implicitly include certain gradation effects. As a result, they overestimate sediment loads for uniform material and underestimate the transport rate for highly graded mixtures. To apply the representative diameter defined by Eq. (4.3), an equivalent diameter, D_e, is defined as follows

$$D_e = K_e D_{50t} = \frac{K_e D_{50}}{1 + B(V_* / \omega_{50})^m (\sigma_g - 1)^n} \tag{4.6}$$

in which K_e = a coefficient to compensate the bias in the existing transport equations, which is determined to be 1.8 in this study. The use of D_e to compensate the nonuniformity effect was recently presented in a study by Molinas and Wu (1998).

By replacing the representative size, D_{50}, in Eq. (4.5) with D_e, Engelund and Hansen's function can be transformed into

$$f' \Phi_e = 0.1\, \theta_e^{2.5} \tag{4.7}$$

where

$$\Phi_e = \frac{q_t}{\gamma_s \sqrt{\frac{\gamma_s - \gamma}{\gamma} g D_e^3}} \tag{4.8}$$

$$\theta_e = \frac{\tau}{(\gamma_s - \gamma)D_e} \tag{4.9}$$

The use of an equivalent diameter determined from Eq. (4.6) is to compensate for size gradation in existing formulas. It should not be confused with a representative size for the transported sediments even though the two are related. For example, for uniform mixtures (σ_g equal to 1), the D_e obtained from Eq. (4.6) is equal to $1.8D_{50}$, which results in smaller transport values than the values obtained using D_{50}. On the other hand, for highly graded sediment mixtures, the value of D_e is smaller than the D_{50} size of the mixture (e.g., for $\theta = 3.0$ and $\sigma_g = 3$, $D_e = 0.35D_{50}$). The effect is to increase the computed sediment transport rate.

The data shown in Fig. 4.7 are replotted in Fig. 4.8 utilizing the functional relationship give by Eq.(4.7). The relationship between $f' \Phi_e$ and θ_e shows a definite improvement; the use of D_e reduces scatters. The largest effects of the correction are observed on larger concentration values for high gradation factors. At small concentrations, and therefore lower flow intensities, the correction effects are minor.

Similar to Engelund and Hansen's function, the dimensionless unit stream power (VS/ω_{50}) relationship for bed-material concentration developed by Yang (1973), and Yang and Molinas (1982) may also be used to demonstrate the effect of size gradation on the transport of sediment mixtures. Yang's dimensionless unit stream power relationship can be simply expressed as

$$C_t = I\left(\frac{VS}{\omega_{50}}\right)^J \tag{4.10}$$

in which I and J are coefficients which are related to flow and sediment properties.

C_t versus the dimensionless unit stream power is plotted in Fig. 4.9. It can be seen

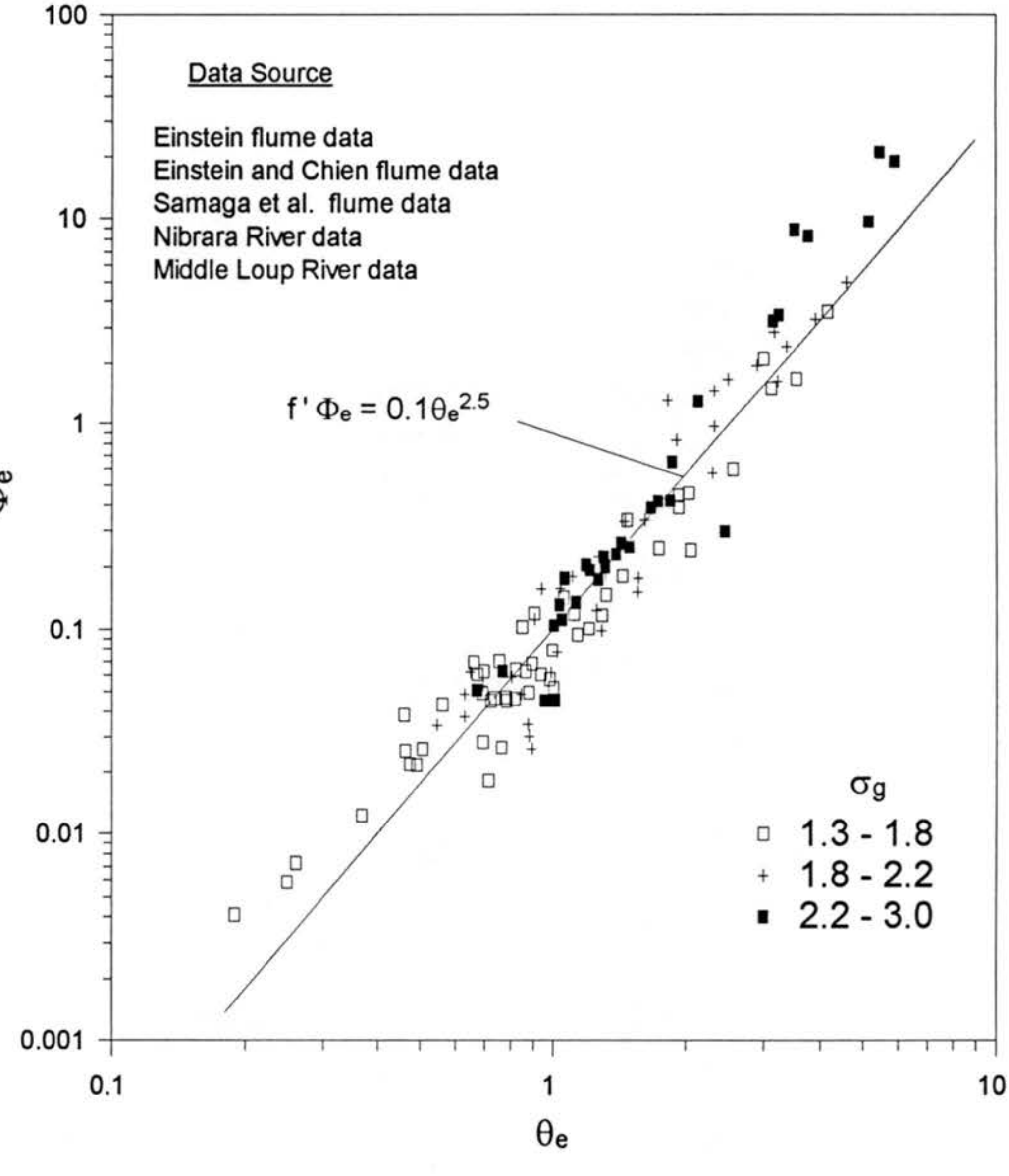

Fig. 4.8. Relationship between $f'\Phi_e$ and θ_e Using the Equivalent Representative Diameter, D_e.

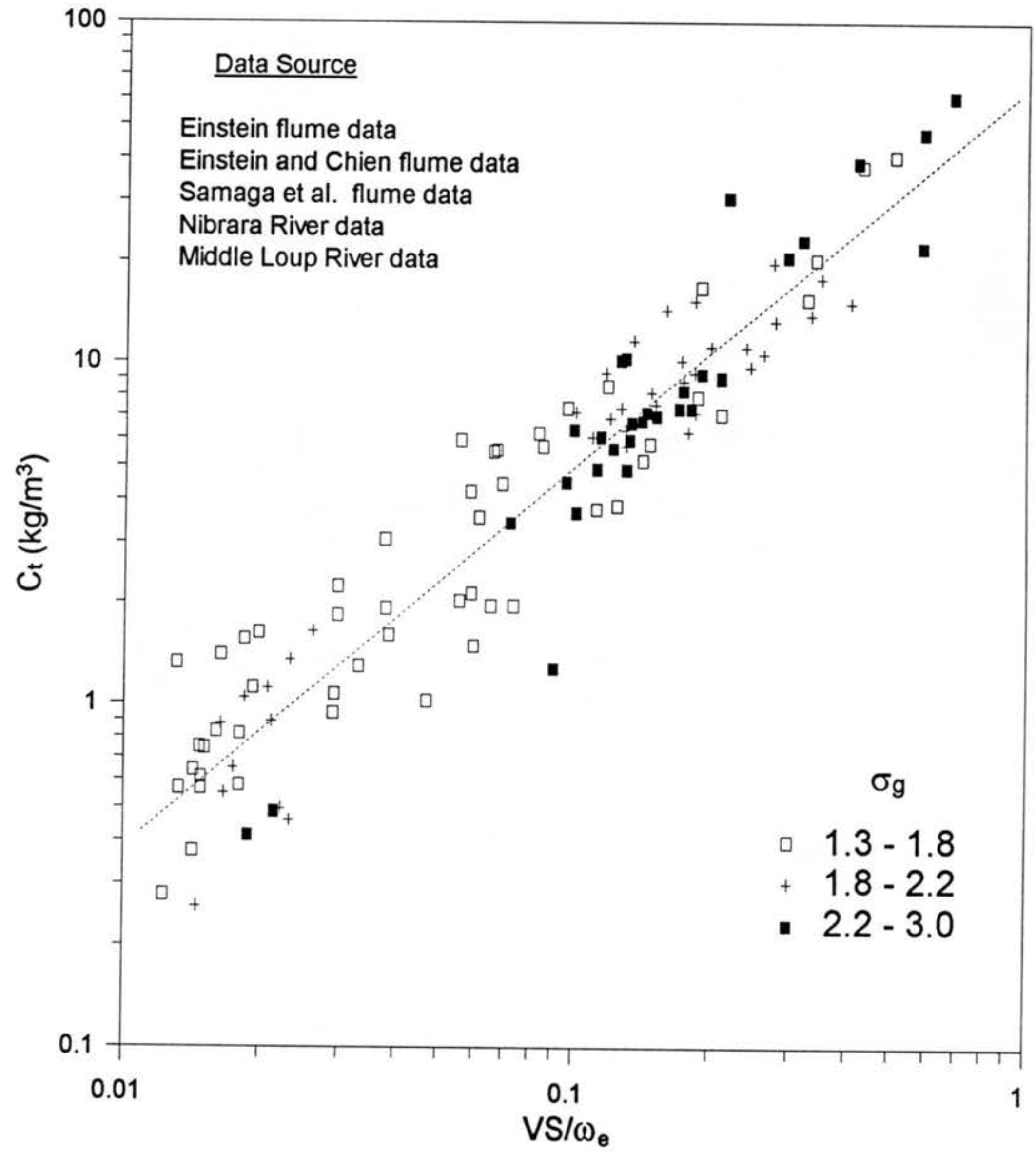

Fig. 4.11. Relationship between the Bed-Material Concentration, C_t, and the Dimensionless Unit Stream Power, VS/ω_e, Using the Equivalent Representative Diameter, D_e .

that on the average C_t is correlated with VS/ω_{50} and the size gradation effect on the transport cannot be observed. When the same data are replotted in Fig. 10 for three ranges of σ_g values, it indicates that the transport relationship is clearly a function of size gradation.

Using the equivalent diameter, D_e, defined by Eq. (4.6), the corresponding fall velocity can be expressed as

$$\omega_e = f(D_e) \tag{4.11}$$

Replacing ω_{50} in Eq. (4.10) with ω_e given by Eq. (4.11) results in

$$C_t = I\left(\frac{VS}{\omega_e}\right)^J \tag{4.12}$$

Fig. 4.11 shows the functional relationship given Eq. (4.12) using D_e (ω_e) as the representative size. It demonstrates that using D_e, the series of curves (for different σ_g values) are reduced to a single relationship.

4.4 BED-MATERIAL TRANSPORT RATE COMPUTATION

The equivalent diameter, D_e, defined in Eq. (4.6) is introduced into the Engelund and Hansen, Ackers and White, and Yang formulas to account for the effects of nonuniformity of bed material size in sediment mixtures. First, the bed-material concentrations for the 118 sets of laboratory and river data given in Table 3.1 are computed in the normal manner. Then, the representative size is replaced by the equivalent diameter defined in Eq. (4.6). In the Ackers and White formula, the term D used to define the dimensionless grain diameter, D_{gr}, is not replaced by D_e, because D_{gr} was specifically defined for sediment mixtures. All other occurrences of the sediment size are replaced to be D_e.

The comparison between computed bed-material concentrations using the Engelund and Hansen, Ackers and White, and Yang formulas and the measured values is summarized in Table 4.1 and in Figs.4.12-14. In Table 4.1, three different statistical methods are used to indicate the goodness of fit between the computed and measured results:

(i) the discrepancy ratio

$$R = \frac{C_{tc}}{C_{tm}} \tag{4.13}$$

in which C_{tc}, C_{tm} = computed and measured bed-material concentrations, respectively. For a perfect fit, R = 1.

(ii) the Average Geometric Deviation between computed and measured bed material concentrations

$$AGD = \left(\prod_{j=1}^{J} RR_j \right)^{1/J}, \quad RR_j = \begin{cases} C_{tc}/C_{tm} & for\ C_{tc} \geq C_{tm} \\ C_{tm}/C_{tc} & for\ C_{tc} < C_{tm} \end{cases} \tag{4.14}$$

in which j = data set number, j = 1, 2, . . . , J; and J = total number of data sets. For a perfect fit, AGD =1.

(iii) the Mean Normalized Error

$$MNE = \frac{100}{J} \sum_{j=1}^{J} \left| \frac{C_{tc}-C_{cm}}{C_{cm}} \right| \tag{4.15}$$

for a perfect fit, MNE = 0.

Table 4.1 and Figs. 4.12-14 show that, on the average, selected formulas predict the sediment transport adequately. However, without using D_e, considerable scatter between computed and measured sediment concentrations exists.

Use of D_e reduced the average geometric deviation between computed and measured

Table 4.1. Summary of Comparison between Computed and Measured Total Bed-Material Concentrations

Author of Formula (1)	Representative Size of Bed Material (3)	Data in Range of Discrepancy Ratio, R (%)				Average Geometric Deviation, AGD (8)	Mean Normalized Error, MNE (%) (9)	Number of Data Sets (10)
		0.75-1.25 (4)	0.5-1.5 (5)	0.25-1.75 (6)	0.5-2.0 (7)			
Engelund and Hansen (1967)	D_{50}	22	57	73	74	1.74	59.6	118
	D_e	37	77	89	86	1.47	40.4	118
Ackers and White (1973)	D_{35}	34	64	74	80	1.61	59.9	118
	D_e	44	71	82	87	1.45	43.8	118
Yang (1973)	D_{50} (ω_{50})	29	64	83	72	1.68	51.0	118
	D_e (ω_e)	48	84	98	94	1.37	29.7	118

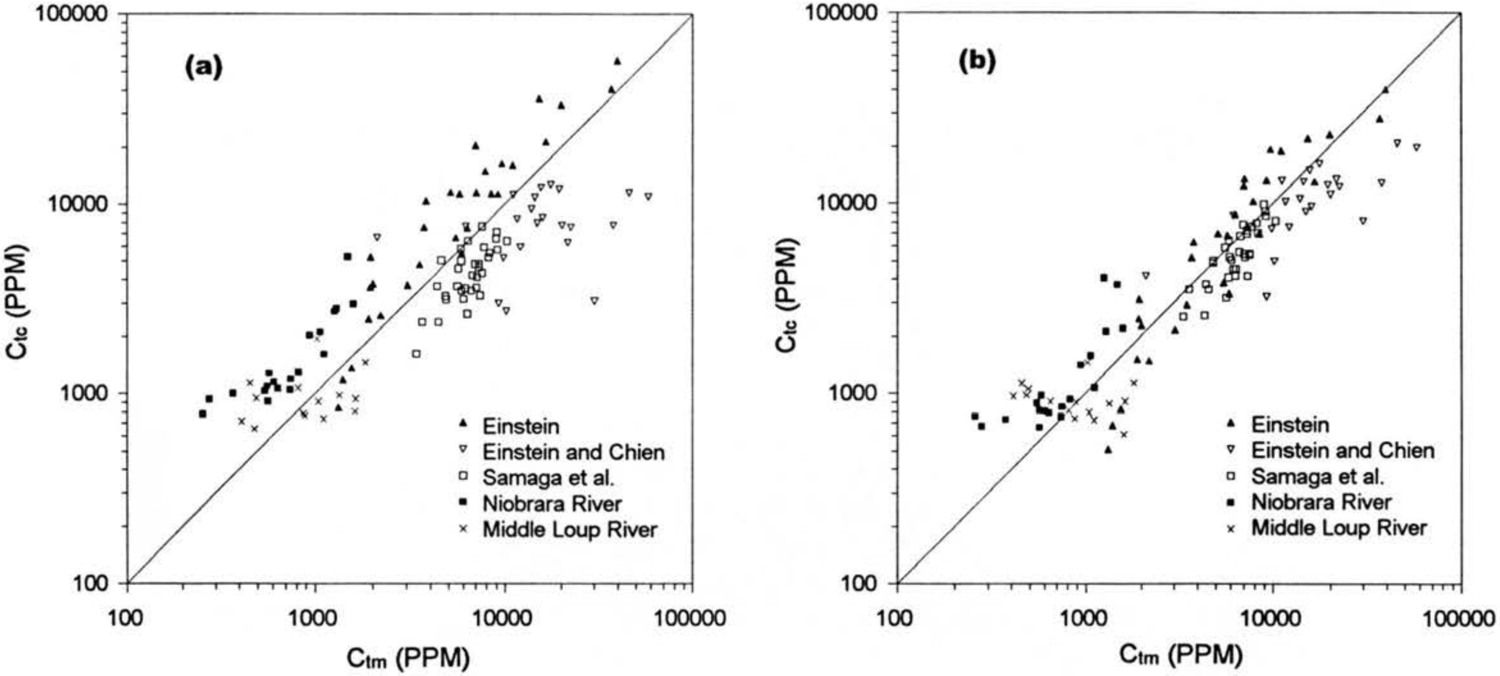

Fig. 4.12. Comparison between Computed and Measured Bed-Material Concentrations for the Engelund and Hansen Formula: (a) Using D_{50} as Representative Size; (b) Using D_e as Representative Size.

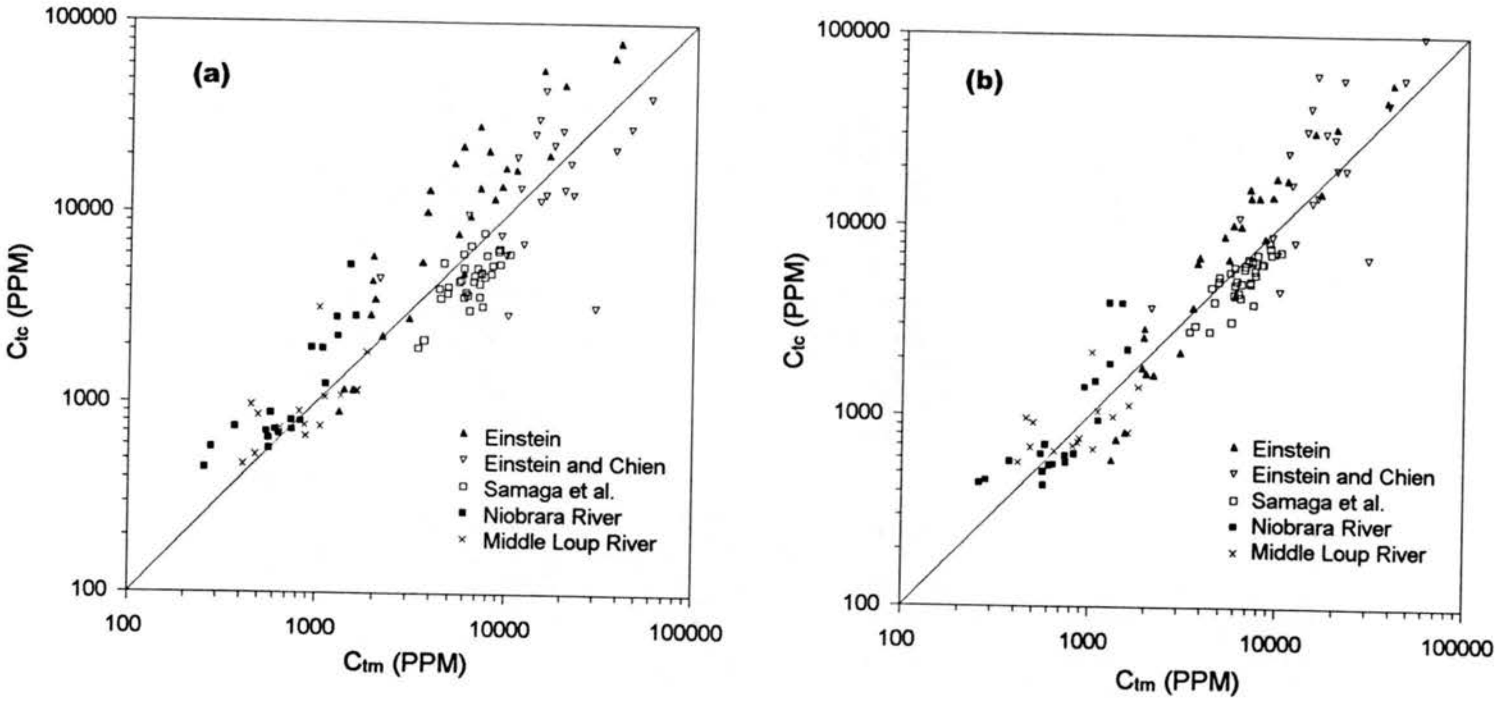

Fig. 4.13. Comparison between Computed and Measured Bed-Material Concentrations for the Akers and White Formula: (a) Using D_{35} as Representative Size; (b) Using De as Representative Size.

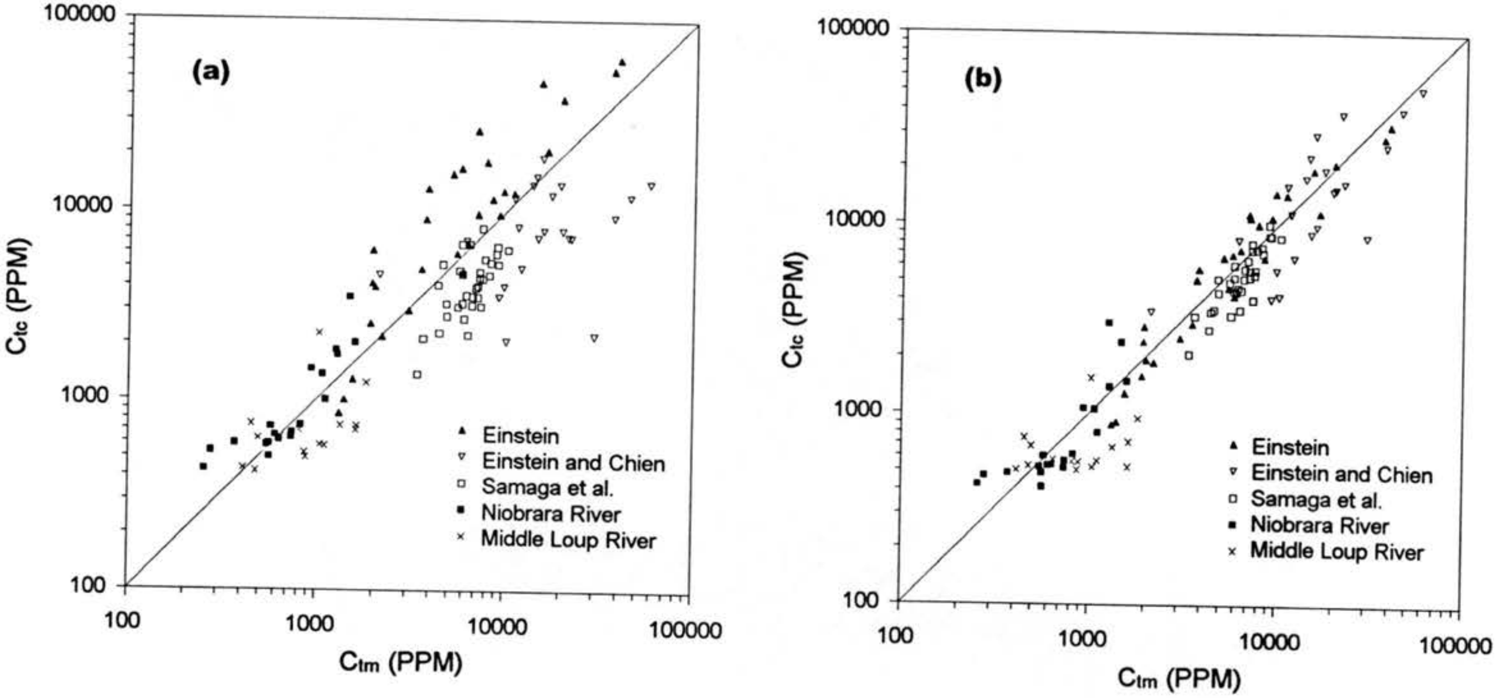

Fig. 4.14. Comparison between Computed and Measured Bed-Material Concentrations for the Yang Formula: (a) Using D_{50} as Representative Size; (b) Using D_e as Representative Size.

bed-material concentrations for the Engelund and Hansen, Ackers and White, and Yang formulas significantly from 1.74, 1.61, and 1.68 to 1.47, 1.45, and 1.37, respectively. The mean normalized error was also significantly reduced from 59.6%, 59.9%, and 51.0% to 40.4%, 43.8%, and 29.7%, respectively. The discrepancy ratios given in Table 4.1 also reflect these findings. The improvement in the range ±50% was from 57% to 77% for the Engelund and Hansen formula, from 64% to 71% for the Ackers and White formula, and from 64% to 84% for the Yang formula. Through the use of D_e, 89% of the data could be accounted for within the range ±75% (up from 73%) for the Engelund and Hansen formula, 82% (up from 74%) for the Ackers and White formula, and 98% (up from 83%) for the Yang formula.

For the Ackers and White formula, since the D_{35} of bed material was already used by the authors to accommodate the effects of size gradation on the transport of sediment mixtures, the additional improvement made by using D_e is not as significant as the improvement in the other two formulas.

4.5 VERIFICATION OF THE USE OF EQUIVALENT DIAMETER, D_e

A group of 54 sets of flume data from Colorado State University (Guy et al., 1966) was chosen to verify the use of D_e for computing bed-material load. These data were chosen since they specifically include three different gradations (σ_g = 1.25, 1.57, and 2.07) for the same median sediment size of 0.33 mm.

The statistical results for the computed sediment concentrations using D_{50} and D_e as representative size are given in Table 4.2. The comparisons between computed and measured bed-material concentrations are also shown in Figs. 4.15-4.17 for the Engelund and Hansen,

Table 4.2. Summary of Comparison between Computed and Measured Total Bed-Material Concentrations for the CSU Flume Data with Particle Size of 0.33mm

Author of Formula (1)	Representative Size of Bed Material (3)	Data in Range of Discrepancy Ratio, R (%)				Average Geometric Deviation, AGD (8)	Mean Normalized Error, MNE (%) (9)	Number of Data Sets (10)
		0.75-1.25 (4)	0.5-1.5 (5)	0.25-1.75 (6)	0.5-2.0 (7)			
Engelund and Hansen (1967)	D_{50}	18.5	44.4	57.4	64.8	1.92	136.8	54
	D_e	29.6	61.1	81.5	74.1	1.65	88.1	54
Ackers and White (1973)	D_{35}	22.2	46.3	61.1	79.6	1.64	70.7	54
	D_e	40.7	68.5	83.3	85.2	1.49	43.1	54
Yang (1973)	D_{50} (ω_{50})	33.3	63.0	77.8	81.5	1.58	61.2	54
	D_e (ω_e)	48.2	66.7	92.6	79.6	1.51	48.8	54

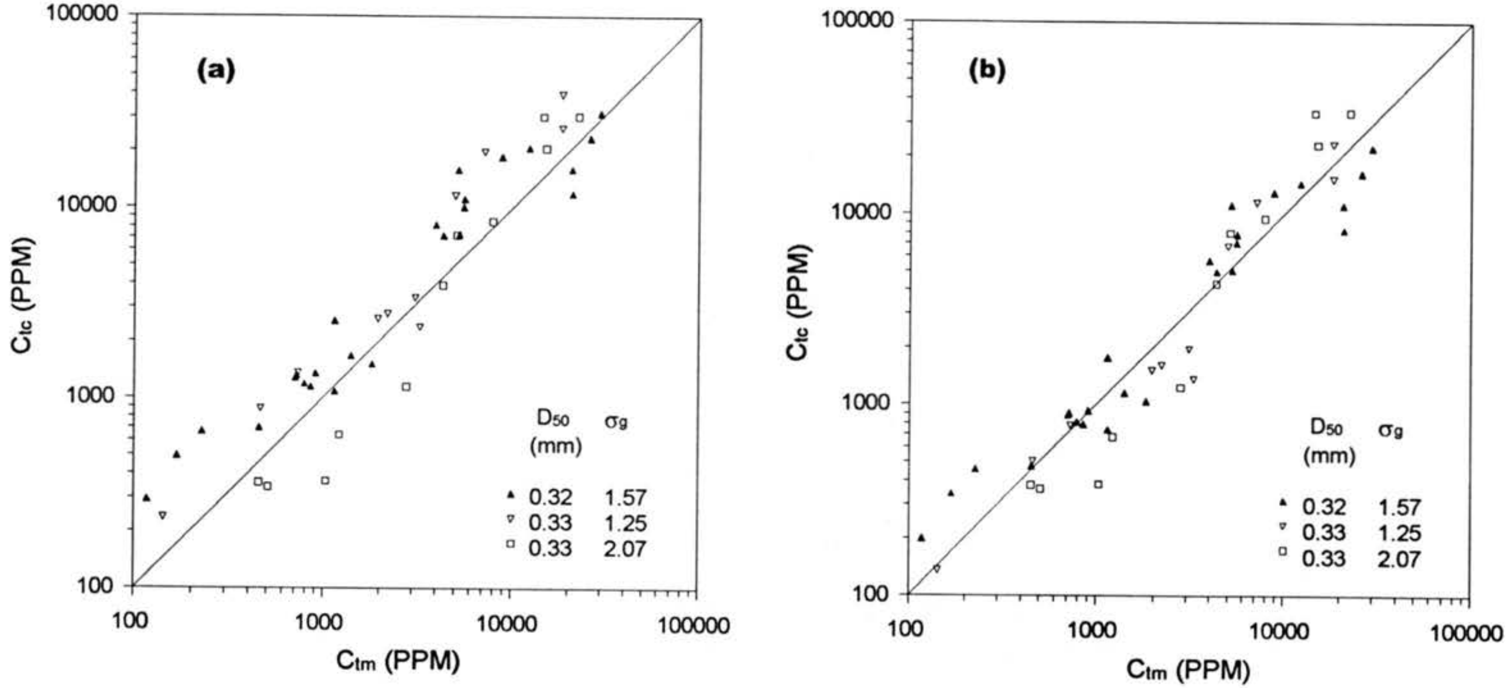

Fig. 4.15. Comparison between Computed and Measured Bed-Material Concentrations for the CSU Data with Particle Size of 0.33mm by the Engelund and Hansen Formula: (a) Using D_{50} as Representative Size; (b) Using D_e as Representative Size.

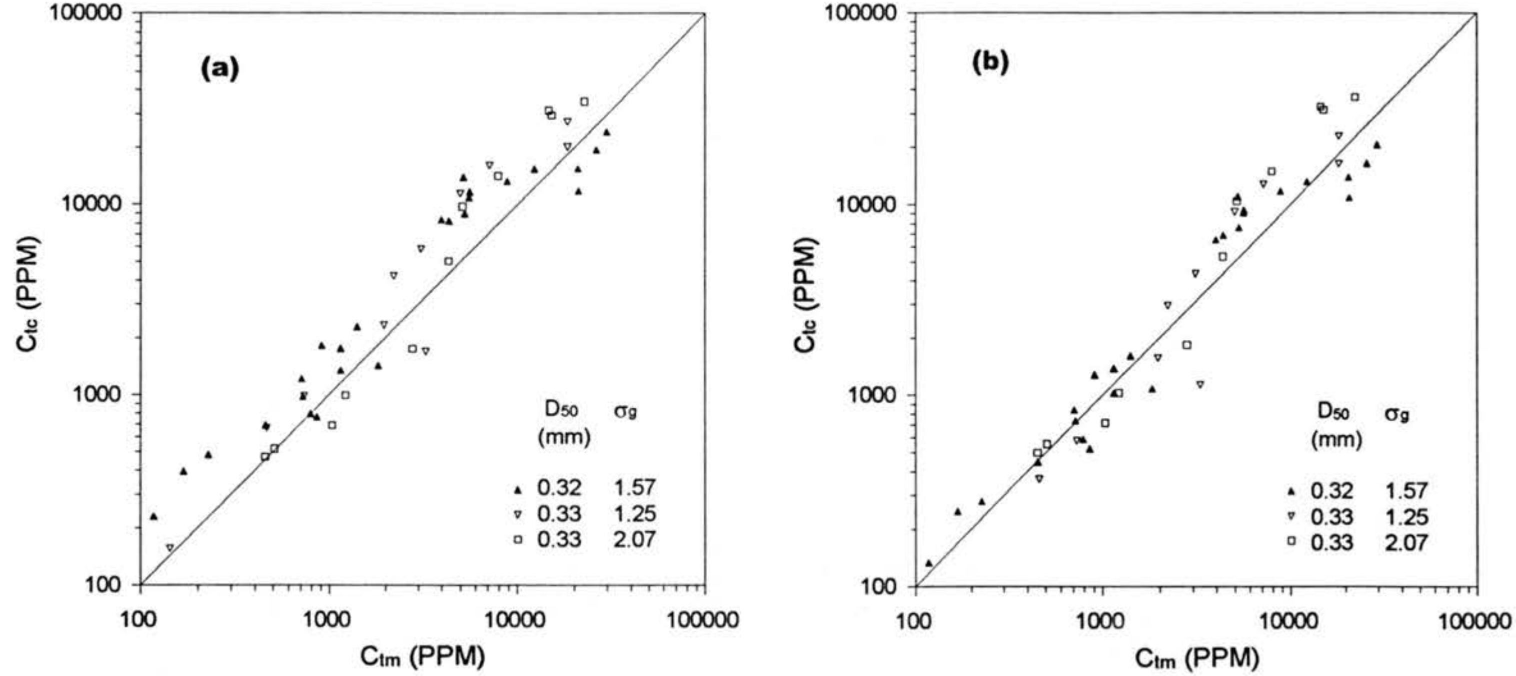

Fig. 4.16. Comparison between Computed and Measured Bed-Material Concentrations for the CSU Data with Particle Size of 0.33mm by the Ackers and White Formula: (a) Using D_{50} as Representative Size; (b) Using D_e as Representative Size.

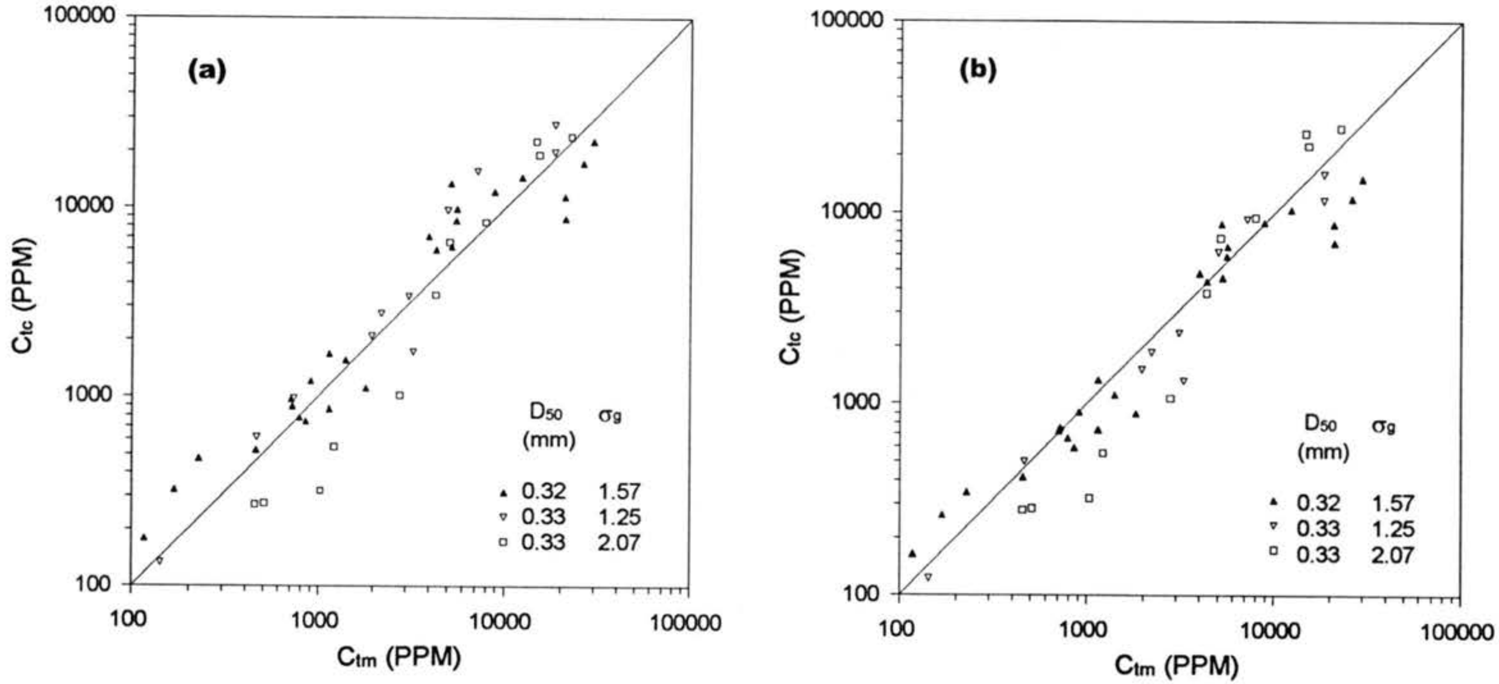

Fig. 4.17. Comparison between Computed and Measured Bed-Material Concentrations for the CSU Data with Particle Size of 0.33mm by the Yang Formula: (a) Using D_{50} as Representative Size; (b) Using D_e as Representative Size.

Ackers and White, and Yang formulas, respectively. The Engelund and Hansen formula predicts the transport rate adequately on the average. By using D_e, even though the range of σ_g variation is small, the scatter around the mean is reduced. Similar results were obtained also for the Ackers and White formula and Yang formula. The improvement in the range ±50% was from 44.4% to 61.1% for the Engelund and Hansen formula, from 46.3% to 68.57% for the Ackers and White formula, and from 63.0% to 66.7% for the Yang formula. Also 81.5% of data fell in the range ±75% (up from 57.4%) for the Engelund and Hansen formula, 83.3% (up from 61.1%) for the Ackers and White formula, and 92.6% (up from 77.8%) for the Yang formula. The average geometric deviation was reduced from 1.92 to 1.65 for the Engelund and Hansen formula, from 1.64 to 1.49 for the Ackers and White formula, and from 1.58 to 1.51 for the Yang formula. The mean normalized error also reduced from 136.8% to 88.8% for the Engelund and Hansen formula, from 70.7% to 43.1% for the Ackers and White formula, and from 61.2% to 48.8% for the Yang formula.

4.6 SUMMARY

The variation of sediment sizes in transport and the effect of size gradation on the transport of sediment mixtures were studied extensively. The data used are limited to the sand size range, and to standard deviations, σ_g, in the range of 1.30 to 3.0. The findings in this chapter can be summarized as follows

1. The size composition of sediment in transport is different from the size composition of bed-surface material. The median diameter of sediment in transport is generally finer than the median diameter of bed material, which is resulting from selective transport of grains by flow. Eq. (4.3) is developed to estimate the median size of

bed-material load. This equation relates D_{50t} to median size of bed material, the size gradation of bed material, and flow intensity. The relative median size of sediment in transport, D_{50t}/D_{50}, decreases as size gradation increases, and the relationship between them can be presented by Eq. (4.4).

2. The effects of bed material size gradation on transport of sediment mixtures cannot be reflected appropriately by a single fixed size, such as D_{35} or D_{50}. Bed-material load formulas such as those developed by Engelund and Hansen, Ackers and White, and Yang are based on a single representative size of bed material and may generate considerable scatter when applied to nonuniform sediment mixtures.

3. Considering the physical processes governing the transport of sediment mixtures, the geometric standard deviation, σ_g, which represents the range of particle sizes present in the bed material, is found to be a significant additional parameter. For the same flow condition and the same D_{50}, the sediment size in transport and the transport rate of sediment mixtures are different for different sediment size gradations. For a given flow condition and median bed-material size, as the size gradation increases, the size of sediment in transport decreases resulting in higher sediment transport rates.

4. The median diameter, D_{50t}, predicted using Eq. (4.3) (equivalent diameter, D_e, for the existing bed-material load formulas), is a better indicator for nonuniform bed material. The median diameter, D_{50t}, is a function of the geometric standard deviation, σ_g, of the bed material and the flow conditions, in conjunction with the D_{50} of the bed material. Using D_{50t} (D_e) will produce a more accurate prediction of bed-material sediment transport discharge for nonuniform sediment mixtures.

5. By incorporating D_e in the Engelund and Hansen, Ackers and White, and Yang

formulas, the accuracy of these functions is improved significantly. The equivalent diameter, D_e, does not change the overall functional behavior of the existing sediment transport functions, but it reduces the scatter due to the secondary effects of size gradations.

CHAPTER 5

APPLICATION OF THE PROPOSED METHOD

In this chapter, a general procedure for the computation of fractional bed-material concentrations using the proposed method is given. This procedure is illustrated through a detailed example problem.

5.1 GENERAL PROCEDURE

The general procedure for the computation of fractional be-material concentrations using the proposed method can be summarized as:

a) Adjustment of the size distributions of the bed material and the sediment in transport

Measured Sediment concentrations are the total sediment concentrations and may include the wash load. As pointed out earlier in Chapter 1, for the analysis and comparison of bed-material load, the wash load portion of total load should be excluded from the measurements. Correspondingly, the size distributions of the bed material and the sediment in transport need to be adjusted.

b) Computation of bed-material concentration, C_t

For the computation of bed-material concentration, an appropriate bed-material transport equation should be selected for the problem. The Engelund and Hansen, Ackers and White, and Yang formulas are commonly used for sand-bed channels. In using these equations, the equivalent diameter, D_e, proposed in Chapter 4 should be used for nonuniform sediment mixtures to compensate for the nonuniformity effect. First, the median diameter, D_{50t}, of bed-material sediment in transport is computed by

$$D_{50t} = \frac{D_{50}}{1 + B(V_*/\omega_{50})^m(\sigma_g - 1)^n} \tag{4.3}$$

in which B, m, and n = 0.8, 0.1, and 2.2, respectively.

Then, the equivalent diameter is determined by

$$D_e = K_e D_{50t} \tag{4.6}$$

in which $K_e = 1.8$.

c) Computation of transport capacity distribution function, P_{ci}

The transport capacity distribution function, P_{ci}, can be computed by either Eq. (3.9) or Eq. (3.24) which were derived in Chapter 3. From practical consideration, the use of Eq. (3.24) is suggested since it dose not require the computation of relative fall velocity, and since it provides the same accuracy as Eq. (3.9). This equation is expressed as follows

$$P_{ci} = \frac{P_{bi}\left[\left(\frac{D_i}{D_{50}}\right)^{\alpha} + \zeta\left(\frac{D_i}{D_{50}}\right)^{\beta}\right]}{\sum_{i=1}^{N} P_{bi}\left[\left(\frac{D_i}{D_{50}}\right)^{\alpha} + \zeta\left(\frac{D_i}{D_{50}}\right)^{\beta}\right]} \tag{3.24}$$

The coefficients are given by

$$\alpha = -2.9\exp\left[-1000\left(\frac{V}{V_*}\right)^2\left(\frac{d}{D_{50}}\right)^{-2}\right] \tag{3.25}$$

$$\beta = 0.2\sigma_g \tag{3.26}$$

$$\zeta = 2.8\,F_r^{-1.2}\,\sigma_g^{-3} \tag{3.27}$$

d) Computation of fractional bed-material concentrations, C_{ti}

After the bed-material concentration, C_t, and the transport capacity distribution function, P_{ci}, are determined, the fractional bed-material concentrations, C_{ti}, can be computed according to the TCF concept, i.e.

$$C_{ti} = P_{ci}C_t \tag{2.8}$$

5.2 EXAMPLE PROBLEM

An example problem showing the detailed steps in using the proposed method for the computation of fractional bed-material concentrations is presented. This example problem is derived from the measurements on July 7, 1949 at the Niobrara River (see Table 3.5). The measured flow and sediment properties are as follows:

Q	= 7.56 m^3/s	S	= 0.001345
V	= 0.7485 m/s	T	= 23.9 °C ($\nu = 9.28\times10^{-7}$ m^2/s)
W	= 21.49 m	s_g	= 2.65
d	= 0.47 m	C_T	= 970.0 PPM

The detailed size distribution of bed material (including the sizes corresponding to wash load) and the size distribution of sediment in transport (total sediment load) are given in the following tabulation:

k	1	2	3	4	5	6	7	8
$D_k^/$(mm)	0.062	0.125	0.25	0.5	1	2	4	8
$P_{bk}^/$ (%)	0.0	2.0	35.0	92.0	98.0	99.0	100.0	100.0
$P_{tk}^/$ (%)	7.0	15.0	58.0	93.0	99.0	100.0	100.0	100.0

In the above tabulation for size distributions, k is the size fraction number; $D_k^/$ is the upper bound diameter; $P_{bk}^/$ is the percentage of bed material finer than the indicated sizes by weight; and $P_{tk}^/$ is the percentage of total sediment load finer than the indicated sizes by weight.

The detailed steps for the computation of fractional bed-material concentration for the given problem are as follows:

a) Adjustment of bed material size distribution

Step 1. Wash load limit diameter, D_w

There are various methods to determine the wash load limit diameter in the literature. For simplicity, the wash load limit diameter for the given problem is determined to be

$$D_w = 0.125\,(mm) \tag{5.1}$$

since there is no significant quantity (2%) of bed material finer than this size. The corresponding size fraction number, k_w, is

$$k_w = 2 \tag{5.2}$$

The corresponding percentages of the bed material and the total sediment load finer than D_w are

$$P_b^/(D_w) = 2.0(\%) \tag{5.3}$$

and

$$P_t^{\prime}(D_w) = 15.0(\%) \tag{5.4}$$

Step 2. Adjusted size distributions

The size distributions of bed material and the sediment in transport are adjusted by subtracting sizes corresponding to the wash load. The computed results are given in

Table 5.1 Adjusted Size Distributions of Bed Material and the Sediment in Transport

i	1	2	3	4	5	6	7
$D_i^{\prime\prime}$(mm)	0.125	0.25	0.5	1	2	4	8
D_i (mm)	0.177	0.354	0.707	1.414	2.828	5.657	
$P_{bi}^{\prime\prime}$ (%)	0	33.67	91.84	97.96	98.98	100.0	100.0
P_{bi}	0.3367	0.5817	0.0612	0.0102	0.0102	0	
$P_{ti}^{\prime\prime}$ (%)	0	50.59	91.97	98.82	100.0	100.0	100.0
P_{ti}	0.5059	0.4117	0.0706	0.0118	0	0	

Table 5.2 Computations of Size Fractions of the Bed-Material Transport Capacity

i	1	2	3	4	5	6	$\sum$
D_i (mm)	0.177	0.354	0.707	1.414	2.828	5.657	
P_{tempi}	2.336	1.797	0.193	0.039	0.049	0	4.4152
P_{ci}	0.529	0.407	0.044	0.009	0.011	0	1.000
C_{ti} (PPM)	493.0	379.3	40.7	8.3	10.4	0	931.7
C_{tmi} (PPM)	417.1	339.4	58.2	9.7	0	0	824.4

Table 5.1. The variables used in this table are determined by the following relations

$$D_i^{\prime\prime} = D_{i+k_w-1}^{\prime} \quad (i = 1, 2, ..., 7) \tag{5.5}$$

$$D_i = \sqrt{D_i^{\prime\prime} D_{i+1}^{\prime\prime}} \quad (i = 1, 2, ..., 6) \tag{5.6}$$

$$P_{bi}^{\prime\prime} = \frac{P_{b\,i+k_w-1}^{\prime} - P_b^{\prime}(D_w)}{100 - P_b^{\prime}(D_w)} \times 100 \quad (i = 1, 2, ..., 7) \tag{5.7}$$

$$P_{ti}^{\prime\prime} = \frac{P_{t\,i+k_w-1}^{\prime} - P_t^{\prime}(D_w)}{100 - P_t^{\prime}(D_w)} \times 100 \quad (i = 1, 2, ..., 7) \tag{5.8}$$

$$P_{bi} = \frac{P_{b\,i+1}^{\prime\prime} - P_{bi}^{\prime\prime}}{100} \quad (i = 1, 2, ..., 6) \tag{5.9}$$

$$P_{ti} = \frac{P_{t\,i+1}^{\prime\prime} - P_{ti}^{\prime\prime}}{100} \quad (i = 1, 2, ..., 6) \tag{5.10}$$

Step 3. Characteristic sizes of bed material

Assuming that the adjusted bed material size follows a logarithmic normal distribution, the characteristic diameters can be interpolated as follows

$$D_{16} = 10^{\left(log 0.125 \, + \, \frac{log 0.25 \, - \, log 0.125}{33.67 \, - \, 0.0} (16.0 \, - \, 0.0) \right)} = 0.1738 \, (mm) \tag{5.11}$$

$$D_{50} = 10^{\left(log 0.25 \, + \, \frac{log 0.5 \, - \, log 0.25}{91.84 \, - \, 33.67} (50.0 \, - \, 33.67) \right)} = 0.3037 \, (mm) \tag{5.12}$$

$$D_{84} = 10^{\left(log0.25 + \frac{log0.5 - log0.25}{91.84 - 33.67}(84.0 - 33.67)\right)} = 0.4554\,(mm) \tag{5.13}$$

and

$$\sigma_g = \sqrt{D_{84}/D_{16}} = \sqrt{0.4554/0.1738} = 1.619 \tag{5.14}$$

b) Computation of bed-material concentration, C_t

Step 4. Shear velocity and fall velocity of D_{50}

Assuming R ≈ d:

$$V_* = \sqrt{gdS} = \sqrt{9.81\times0.47\times0.001345} = 0.0787\,(m/s) \tag{5.15}$$

The fall velocity is determined using the method presented by the U. S. Inter-Agency Committee on Water Resources, Subcommittee on Sedimentation (1957), which gives

$$\omega_{50} = 0.0432\,(m/s) \tag{5.16}$$

Step 5. D_{50t} from Eq. (4.3) and D_e from Eq. (4.6)

$$\begin{aligned} D_{50t} &= \frac{D_{50}}{1 + B(V_*/\omega_{50})^m(\sigma_g - 1)^n} \\ &= \frac{0.3037}{1 + 0.8(0.0787/0.0432)^{0.1}(1.619-1)^{2.2}} \\ &= 0.2344\,(mm) \end{aligned} \tag{5.17}$$

$$D_e = K_e D_{50t} = 1.8\times0.2344 = 0.4219\,(mm) \tag{5.18}$$

Step 6. Bed-material concentration by Engelund and Hansen formula

The Engelund and Hansen (1967) formula for bed-material concentration can be expressed as

$$C_v = \frac{0.05\, V d^{1/2} S^{3/2}}{(s_g - 1)^2 g^{1/2} D_{50}} \tag{5.19}$$

in which C_v = concentration of bed-material load by volume. Using D_e as the representative diameter gives

$$\begin{aligned} C_v &= \frac{0.05\, V d^{1/2} S^{3/2}}{(s_g - 1)^2 g^{1/2} D_e} \\ &= \frac{0.05 \times 0.7485 \times 0.47^{1/2} \times 0.001345^{3/2}}{(2.65 - 1)^2 \times 9.81^{1/2} \times 0.0004219} = 3.5179 \times 10^{-4} \end{aligned} \tag{5.20}$$

The concentration by volume can be transferred into concentration in the unit of PPM through

$$C_t = \frac{10^6 s_g C_v}{1 + (s_g - 1) C_v} = \frac{10^6 \times 2.65 \times C_v}{1 + (2.65 - 1) \times C_v} = 931.7\ (PPM) \tag{5.21}$$

c) Computation of transport capacity distribution function, P_{ci}

Step 7. Coefficients in Eq. (3.24)

$$\begin{aligned} \alpha &= -2.9 \exp\left[-1000\left(\frac{V}{V_*}\right)^2 \left(\frac{d}{D_{50}}\right)^{-2}\right] \\ &= -2.9 \exp\left[-1000\left(\frac{0.7485}{0.0787}\right)^2 \left(\frac{0.47}{0.0003037}\right)^{-2}\right] \\ &= -2.7925 \end{aligned} \tag{5.22}$$

$$\beta = 0.2\sigma_g = 0.2 \times 1.619 = 0.3238 \tag{5.23}$$

$$\begin{aligned}\zeta &= 2.8\, F_r^{-1.2}\, \sigma_g^{-3} \\ &= 2.8 \times \left(\frac{0.7485}{\sqrt{9.81 \times 0.47}} \right)^{-1.2} \times 1.619^{-3} \\ &= 2.3369\end{aligned} \tag{5.24}$$

Step 8. Size fractions of the bed-material transport capacity

The computed size fractions of the bed-material transport capacity are given in Table 5.2, which are computed using Eq. (3.24), i.e.

$$\begin{aligned}P_{ci} &= \frac{P_{bi}\left[\left(\dfrac{D_i}{D_{50}}\right)^{\alpha} + \zeta\left(\dfrac{D_i}{D_{50}}\right)^{\beta}\right]}{\sum_{i=1}^{N} P_{bi}\left[\left(\dfrac{D_i}{D_{50}}\right)^{\alpha} + \zeta\left(\dfrac{D_i}{D_{50}}\right)^{\beta}\right]} \\ &= \frac{P_{bi}\left[\left(\dfrac{D_i}{0.3037}\right)^{-2.7925} + 2.3369\left(\dfrac{D_i}{0.3037}\right)^{0.3238}\right]}{\sum_{i=1}^{6} P_{bi}\left[\left(\dfrac{D_i}{0.3037}\right)^{-2.7925} + 2.3369\left(\dfrac{D_i}{0.3037}\right)^{0.3238}\right]}\end{aligned} \tag{5.25}$$

in which D_i is expressed in mm; and P_{bi} is given in Table 5.1. The numerator in Eq. (5.25) is denoted as P_{tempi}, i.e.

$$P_{tempi} = P_{bi}\left[\left(\frac{D_i}{0.3037}\right)^{-2.7925} + 2.3369\left(\frac{D_i}{0.3037}\right)^{0.3238}\right] \tag{5.26}$$

First, the values of P_{tempi} corresponding to each size fraction are computed for various size groups, and the summation of P_{tempi} are obtained. Then, the capacity fractions for each size group are obtained by dividing P_{tempi} with $\sum P_{tempi}$ according to Eq. (5.25).

d) Computation of fractional bed-material concentrations, C_{ti}

Step 9. Fractional bed-material concentrations

The computed fractional bed-material concentrations are given in Table 5.2. The value of C_{ti} is computed according to the TCF concept, i.e.

$$C_{ti} = P_{ci} C_t = P_{ci} \times 931.7 \, (PPM) \tag{5.27}$$

Step10. Measured fractional bed-material concentrations

$$C_{tmi} = P_{ti} C_{tm} \, (PPM) \tag{5.28}$$

in which P_{ti} = given in Table 5.1; and C_{tm} = the measured bed-material concentration, which is computed by

$$C_{tm} = [100 - P_t^{\prime}(D_w)] \times C_T = (100-15)/100 \times 970.0 = 824.0 \, (PPM) \tag{5.29}$$

The measured fractional bed-material concentrations presented in Table 5.2 can be used for comparison with computed results.

CHAPTER 6

COMPARISON AND EVALUATION

6.1 GENERAL

Comparison and evaluation of existing transport functions generally limit the analyses to comparisons of bed-material sediment transport rate in the literature (American Society of Civil Engineering, 1982; White et al., 1975; Alonso, 1980; Brownlie, 1981; Yang and Molinas, 1982; Vetter, 1989; Yang and Wan, 1991; Wu, 1992a; and Wu and Long, 1992, 1993). Along with the application of the transport capacity distribution functions proposed in Chapter 3, an extensive evaluation on the fractional load computations is conducted using flume and field data. This evaluation is necessary to qualitatively and quantitatively demonstrate the performance of the newly developed fractional load computation method, and to show the limitations and variations of different methods.

In the four groups of fractional load computation methods, those of direct computation by the size fraction approach, the BMF approach, and the TCF approach will be evaluated in this chapter. Since most of the methods derived following the shear stress correction approach are only applicable for the predictions of fractional transport rates of gravel bed materials, methods in this group are excluded from this comparison.

For the computation of fractional load using different methods, Hydrau-Tech, Inc.'s SedWin (Visually Interactive Sediment Transport Computation Model for Windows 95/98)

(Wu and Molinas, 1998) is applied in this study. This program is developed for the computations of sediment transport rate by selected transport equations. Both bed-material transport rate and fractional bed-material transport rate can be computed. The new transport capacity distribution functions, P_{ci}, developed in Chapter 3 and the use of the equivalent diameter, D_e, proposed in Chapter 4 for the computation of bed-material load are incorporated in the program.

6.2 FRACTIONAL LOAD COMPUTATIONS

6.2.1 Fractional Load Using the Direct Computation by Size Fraction Approach

Even though the equations of Einstein (1950), Laursen (1958), and Toffaleti (1968, 1969) were developed based on the computations of sediment transport rates for each individual size fraction of sediment mixtures, accuracy of their predictions as to the distribution by different sediment size fractions is not known.

The bed-material concentrations of individual size fractions are computed for these three methods using the SedWin program. Eqs. (2.9), (2.15), and (2.17) are the basic transport relations of Einstein, Laursen, and Toffaleti, respectively. Detailed computation procedures for these methods can be found in Stevens and Yang (1989), Raudkivi (1990), Simons and Sentürk (1992), Julien (1995), and Yang (1996).

6.2.2. Fractional Load Using the Bed Material Fraction Approach

In the four groups of methods for the computation of fractional sediment transport rates, the BMF approach is still the most commonly used one in numerical models, even though the shortcomings of using this approach in nonuniform sediment transport models have been recognized in the literature (Karim and Kennedy, 1982; Hsu and Holly, 1992). This fact indicates that the basic concept of the BMF approach may be acceptable to some extent. According to the concept of the BMF approach, the potential concentration, C_{pi}, for a given size fraction, i, is computed by replacing the representative size used in an equation with the average diameter, D_i. Then the fractional transport rates are ready to be determined as the product of P_{bi} and C_{pi}. In the present study, the potential concentration is obtained by applying the transport formulas developed by Engelund and Hansen (1967), Ackers and White (1973), and Yang (1973) to laboratory and river data.

Engelund and Hansen's Method. Engelund and Hansen (1967) used the similarity principle to obtain the sediment transport function [see Eq. (3.15)]. In using the BMF approach to compute the bed-material concentrations of individual size fractions for sediment mixtures, the Engelund and Hansen formula can be transferred into

$$C_{pi} = \frac{0.05\, V d^{1/2} S^{3/2}}{\left(\frac{\gamma_s - \gamma}{\gamma}\right)^2 g^{1/2} D_i} \tag{6.1}$$

in which C_{pi} = potential concentration of bed-material load by volume corresponding to the size fraction i.

Ackers and White's Method. Ackers and White (1973) developed their transport functions based on the mobility theory. In using the BMF approach, their transport function can be transferred into

$$C_{pi} = C \, \frac{\gamma_s}{\gamma} \, \frac{D_i}{d} \left(\frac{V}{V_*} \right)^n \left(\frac{F_{gri}}{A} - 1 \right)^m \tag{6.2}$$

where

$$F_{gri} = \frac{V_*^n}{\sqrt{g D_i \left(\frac{\gamma_s - \gamma}{\gamma} \right)}} \left[\frac{V}{\sqrt{32} \log\left(\frac{\alpha d}{D_i} \right)} \right]^{1-n} \tag{6.3}$$

$$D_{gri} = D_i \left[\frac{g \left(\frac{\gamma_s - \gamma}{\gamma} \right)}{\nu^2} \right]^{1/3} \tag{6.4}$$

in which A, C, m, and n = parameters as function of D_{gri}; D_{gri} = dimensionless grain diameter corresponding to the size fraction, i; F_{gri} = mobility number for sediment corresponding to the size fraction, i; α = coefficient; and ν = kinematic viscosity. In the use of Ackers and White equation, the modified coefficients of m and C_A (White and Wang[1]) are used:

$$m = 6.38 / D_{gr} + 1.67 \tag{6.5}$$

$$C_A = 2.79 / \log(D_{gr}) - 0.97 \left[\log(D_{gr}) \right]^2 - 3.46 \tag{6.6}$$

Yang's Method. Yang (1973) sediment transport formula is based on unit stream power theory. In using the BMF approach, his dimensionless unit stream power formula can be transferred into

---

[1]) Private communication.

$$\log(C_{pi}) = 5.435 - 0.286\log\left(\frac{\omega_i D_i}{\nu}\right) - 0.457\log\left(\frac{V_*}{\omega_i}\right)$$
$$+ \left[1.799 - 0.409\log\left(\frac{\omega_i D_i}{\nu}\right) - 0.314\log\left(\frac{V_*}{\omega_i}\right)\right]\log\left(\frac{VS}{\omega_i} - \frac{V_{cr}S}{\omega_i}\right) \tag{6.7}$$

where

$$\frac{V_{cr}}{\omega_i} = \begin{cases} \dfrac{2.05}{\log\left(\dfrac{V_* D_i}{\nu}\right) - 0.06} & for \quad 1.2 < \dfrac{V_* D_i}{\nu} < 70 \\ 2.05 & for \quad 70 \le \dfrac{V_* D_i}{\nu} \end{cases} \tag{6.8}$$

in which C_{pi} = potential concentration of bed-material load in PPM, by weight, corresponding to the size fraction i; and V_{cr} = critical velocity at incipient motion.

Karim's Modified BMF Method. Recently, Karim (1998) developed a new method for the prediction of fractional loads, which can be classified as the modified BMF method. This relation is proposed for sand-bed flows and can be expressed as

$$q_{ti} = 0.00139\sqrt{g(s_g-1)D_i^3}\left(\frac{V}{\sqrt{g(s_g-1)D_i}}\right)^{2.97}\left(\frac{V_*}{\omega_i}\right)^{1.47}\phi_i \tag{6.9}$$

in which q_{ti} = volumetric sediment discharge per unit width for *i*th fraction; and ϕ_i = weighing function for *i*th fraction, which is the function of an areal function (P_{ai}) and a sheltering factor (η). Formulations for the weighing function were given in Chapter 2 [Eqs. (2.44)-(2.47)].

6.2.3 Fractional Load Using the Transport Capacity Fraction Approach

To obtain transport capacities for individual size fractions based on the TCF approach, both the bed-material concentration, C_t, and the fractions of bed-material transport capacity, P_{ci}, are needed. As pointed out earlier, C_t can be determined using any appropriate bed-material load equations. For this purpose, the Yang (1973) formula, along with the equivalent diameter, D_e, proposed in Chapter 4, can be used to determine the bed-material transport rate. For the computation of P_{ci}, both Karim and Kennedy's (1981) method and the new transport capacity distribution functions proposed in Chapter 3 can be used.

Karim and Kennedy's Function. The transport capacity distribution function proposed by Karim and Kennedy (1981) is applicable to flows in which total sediment discharge mainly consists of suspended load. This function was used in their numerical river simulation model IALLUVIAL (Karim and Kennedy, 1982; and Karim, 1985). Formulations for this method are given by Eqs. (2.55) and (2.56) in Chapter 2.

Li's Function. The transport capacity distribution function proposed by Li (1988) was developed for suspended load. Thus, it is applicable to flows in which total sediment discharges are composed mainly of suspended load. Formulations for Li's method are given by Eqs. (2.53) and (2.54) in Chapter 2.

Proposed Functions. The transport capacity distribution functions proposed in Chapter 3 were derived from the basic concept of the BMF approach in conjunction with the consideration of the sheltering and exposure effect introduced in the shear stress correction approach. The formulation of Eq. (3.9) is a function of relative fall velocity, while the formulation of Eq. (3.24) is a function of relative diameter. Both equations are used as weighting functions to calculate fractional load for sediment mixtures, and their performance will be compared with other fractional load methods. The general procedure and a detailed example problem showing how to use the proposed method are given in Chapter 5.

6.3 COMPARISON OF COMPUTED RESULTS

The fractional bed-material concentrations computed using various methods are compared in this section. Sediment transport data used in this comparison are those 112 sets of flume and field data given in Table 3.1, which contain a total of 891 data points. Methods used in comparisons, and their classifications are summarized as follows:

a) Direct computation by size fraction approach

   1) Einstein's equation (1950);

   2) Laursen's equation (1958);

   3) Toffaleti's equation (1968);

b) BMF approach using:

   4) Engelund and Hansen's equation (1967);

   5) Ackers and White's equation (1973);

   6) Yang's equation (1973);

   7) Karim's modified BMF method (1998);

c) TCF approach using the Yang (1973) equation with D_e and

   8) Transport capacity distribution function of Karim and Kennedy (1981);

   9) Transport capacity distribution function of Li (1988);

10) Proposed transport capacity distribution function of Eq. (3.9); and

11) Proposed transport capacity distribution function of Eq. (3.24).

For fractional transport of sediment mixtures, not only the absolute values of transport sediment concentration need to be predicted accurately, but also the size compositions need to be estimated correctly. From computed fractional bed-material concentrations, the size fraction of bed-material transport capacity (in percent) for a given size group can be obtained by

$$P_{cci} = 100 \frac{C_{tci}}{C_{tc}} = 100 \frac{C_{tci}}{\sum_{i=1}^{N} C_{tci}} \tag{6.10}$$

6.3.1 Statistical Analysis

In the statistical analysis, three different statistical methods are adopted to indicate the goodness of fit between the computed and measured results. These statistical methods are similar to those used in Chapter 4. However, the statistics conducted in this section are for the fractional bed-material concentrations in a sediment mixture, rather than the bed-material concentrations. These statistical methods are as follows:

1) the discrepancy ratio, R_i

$$R_i = \frac{C_{tci}}{C_{tmi}} \tag{6.11}$$

in which C_{tci}, C_{tmi} = computed and measured bed-material concentrations corresponding to size fraction i, respectively; and i = size fraction number or data point number in a data set. For a perfect fit, $R_i = 1$.

2) the Average Geometric Deviation between computed and measured fractional bed-material concentrations, AGD

$$AGD = \left(\prod_{j=1}^{J} \prod_{i=1}^{N_j} RR_i \right)^{1/JN} , \quad RR_i = \begin{cases} C_{tci} / C_{tmi} & for\ C_{tci} \geq C_{tmi} \\ C_{tmi} / C_{tci} & for\ C_{tci} < C_{tmi} \end{cases} \tag{6.12}$$

in which j = data set number, j = 1, 2, . . . , J; J = total number of data sets; N_j = number of points in a given data set; and JN = the total number of data points. For a perfect fit, AGD = 1.

3) the Mean Normalized Error, MNE

$$MNE = \frac{100}{JN} \sum_{j=1}^{J} \sum_{i=1}^{N_j} \left| \frac{C_{tci} - C_{tmi}}{C_{tmi}} \right| \tag{6.13}$$

for a perfect fit, MNE = 0.

Detailed statistical results for the comparison between the computed and measured bed-material concentrations of individual size fractions are given in Table 6.1. It can be seen that the mean normalized errors for the direct computation by size fraction approach of Einstein, Laursen, and Toffaleti were in the range of 84.0-156.1%; for the BMF approach using Engelund and Hansen, Ackers and White, and Yang were in the range of 110.3-222.9%; and for the TCF approach using the Yang equation with D_e and the transport distribution functions of Karim and Kennedy, and Li were in the range of 89.9-135.0%.

By using the Yang equation with D_e and the newly proposed transport capacity distribution functions of Eqs. (3.9) and (3.24), the mean normalized errors were significantly reduced to 65.6% and 68.5% (up from range of 84.0-222.9% for other methods), respectively. The average geometric deviations were also considerably reduced to 1.80 and

1.81 (down from 2.15-8.76 for other methods) by Eqs. (3.9) and (3.24), respectively.

The percentages of data falling within the range of discrepancy ratios between 0.25 and 1.75 were in the range of 36.0-62.2% for the direct computation by the size fraction approach of Einstein, Laursen, and Toffaleti. They were in the range of 44.2-57.8% for the BMF approach using Engelund and Hansen, Ackers and White, and Yang. Also they were in the range of 44.7-68.5% by using the Yang equation with D_e and the transport capacity distribution functions of Karim and Kennedy and Li. By using the Yang equation with D_e and the newly proposed transport capacity distribution functions of Eqs. (3.9) and (3.24), the percentages of data falling within the range of discrepancy ratios between 0.25 and 1.75 were increased to 77.7% and 77.0% (up from the range of 36.0-68.5% for other methods), respectively.

Statistical results for the comparison between the computed and measured size fractions of bed-material load sediment in transport are given in Table 6.2. The mean normalized errors were reduced significantly to 60.8% and 61.8% (down from the range of 96.1-252.0% for other methods) by using the newly proposed transport capacity distribution functions of Eqs. (3.9) and (3.24), respectively. The average geometric deviations were also considerably reduced to 1.64 and 1.65 (down from the range of 2.04-8.26 for other methods) by Eqs. (3.9) and (3.24), respectively. The percentage of data falling within the range of discrepancy ratios between 0.25 and 1.75 were improved to 78.7% and 78.7% (up from the range of 46.1-70.2% for other methods) by Eqs. (3.9) and (3.24), respectively.

Table 6.1 Comparison between Computed and Measured Fractional Bed-Material Concentrations for the 118 Sets of Flume and Field Data Given in Table 3.1

Fractional Bed-Material Load Computation Method (1)	Data in Range of Discrepancy Ratio, R_i (%) 0.75-1.25 (2)	0.5-1.5 (3)	0.25-1.75 (4)	0.5-2.0 (5)	Mean Normalized Error, MNE (%) (6)	Average Geometric Deviation, AGD (7)	No. of Data Points (8)
a) Direct computation by size fraction approach							
Einstein's equation (1950)	19.4	43.3	62.2	55.3	84.0	2.71	891
Laursen's equation (1958)	14.6	30.2	52.9	36.8	156.1	4.01	891
Toffaleti's equation (1968)	13.9	23.2	36.0	30.8	120.7	5.59	891
b) BMF approach using							
Engelund and Hansen's equation (1967)	19.0	38.2	55.9	48.4	111.8	2.45	891
Ackers and White's equation (1973)	20.0	39.8	57.8	51.9	222.9	2.69	891
Yang's equation (1973)	19.3	40.6	57.7	52.8	138.8	2.41	891
Karim's modified BMF method (1998)	12.1	24.8	44.2	29.1	110.3	6.07	891
c) TCF approach using Yang eq. (1973) with D_e and							
Function of Karim and Kennedy (1981)	24.1	49.5	68.5	58.5	89.9	2.15	891
Function of Li (1988)	14.4	27.8	44.7	35.1	135.0	8.76	891
Proposed function of Eq. (3.9)	31.3	59.2	77.7	68.4	65.6	1.80	891
Proposed function of Eq. (3.24)	29.7	58.6	77.0	68.5	66.2	1.81	891

Table 6.2 Comparison between Computed and Measured Size Fractions of Sediment in Transport (*Bed-Material Load*) for the 118 Sets of Flume and Field Data Given in Table 3.1

Fractional Bed-Material Load Computation Method	Data in Range of Discrepancy Ratio, R_i (%)				Mean Normalized Error, MNE (%)	Average Geometric Deviation, AGD	No. of Data Points
	0.75-1.25	0.5-1.5	0.25-1.75	0.5-2.0			
(1)	(2)	(3)	(4)	(5)	(6)	(7)	(8)
a) Direct computation by size fraction approach							
Einstein's equation (1950)	29.9	46.1	59.7	55.2	252.0	2.55	891
Laursen's equation (1958)	22.2	39.0	55.2	43.2	123.0	3.75	891
Toffaleti's equation (1968)	18.6	33.1	49.7	40.4	134.1	4.19	891
b) BMF approach using							
Engelund and Hansen's equation (1967)	28.5	48.0	65.1	55.2	117.8	2.27	891
Ackers and White's equation (1973)	21.7	39.3	58.8	44.1	99.2	2.88	891
Yang's equation (1973)	32.7	53.1	70.2	58.4	96.1	2.19	891
Karim's modified BMF method (1998)	17.0	33.3	48.5	39.1	131.2	4.68	891
c) TCF approach using							
Function of Karim and Kennedy (1981)	32.3	52.5	70.2	60.6	105.3	2.04	891
Function of Li (1988)	16.5	30.3	46.1	37.3	139.5	8.26	891
Proposed function of Eq. (3.9)	42.3	65.1	78.8	74.2	60.8	1.64	891
Proposed function of Eq. (3.24)	41.1	64.5	78.7	73.7	61.8	1.65	891

6.3.2 Graphical Comparison

Comparisons between computed and measured fractional bed-material concentrations and size fractions are graphically displayed in four different types of plots for the fractional transport methods discussed above. These plots are intended to show the agreement between predicted and measured values.

1) Plots showing the comparison between computed and measured fractional bed-material concentrations

Figs. 6.1-6.9 show the comparisons between computed and measured fractional bed-material concentrations for various fractional load methods. A large scatter of computed results from the measured values can be noticed for the direct computation by size fraction approach of Einstein, Laursen, and Toffaleti; the BMF approach using the Engelund and Hansen, Ackers and White, and Yang equations; and the TCF approach using the Yang equation with D_e and the transport distribution functions of Karim and Kennedy, and Li. The scatter is mostly in the range of two logarithmic scales for these 9 methods.

It can also be seen that the Einstein method predicts his own data very well, but it fails to predict the fractional transport rate for data from other sources. The TCF approach using the Yang equation with D_e and the transport distribution functions of Karim and Kennedy gives slightly better results, even though Karim and Kennedy treated their transport capacity distribution function in a very simple manner.

Figs. 6.10-6.11 show the results computed from the TCF approach using the Yang equation with D_e and the newly proposed transport distribution functions of Eqs. (3.9) and (3.24), respectively. A close agreement between the computed fractional bed-material concentrations and measured values can be observed.

2) Plots showing discrepancy ratio distribution

The discrepancy ratio distributions of computed fractional bed-material concentrations are plotted in Figure 6.12-6.22. It can be seen that there are 32.8% of data with discrepancy ratio $R_i < 1/7.5$ for Toffaleti, 30.8% for the Karim method, and 30.1% for the Li method, respectively. This indicates that these three methods greatly underestimate the fractional transport rates. There are also large percentages (11% and 17%) of data with a discrepancy ratio $R_i < 1/7.5$ for Einstein and Laursen methods.

The discrepancy ratio distributions are close to normal for the BMF approach using the Engelund and Hansen, Ackers and White, and Yang equations, even though the predictions are not highly concentrated around perfect agreement ($C_{tci}/C_{tmi}=1$). Overall, the discrepancy ratios resulting from the Karim and Kennedy method are normally distributed and are more concentrated around the perfect agreement.

The discrepancy ratios for the predictions using the newly developed transport capacity distribution functions of Eqs. (3.9) and (3.24) are normally distributed and have higher density close to the perfect agreement than all other methods. Predictions with extreme discrepancy ratios ($R_i < 1/7.5$ or $R_i > 7.5$) are very limited.

3) Plots showing the comparison between computed and measured size fractions of bed-material load

Figs. 6.23-6.31 and Figs. 3.9-3.10 show the comparison between computed and measured size fractions of bed-material load. In general, Figs. 6.23-6.31 show that the computed size fractions of bed-material load sediment in transport deviate significantly from actual measurements for the direct computation by the size fraction approach of Einstein, Laursen, and Toffaleti; the BMF approach using the Engelund and Hansen, Ackers and White, and Yang equations; and the TCF approach using the Yang equation with D_e and the transport distribution functions of Karim and Kennedy, and Li. As a contrast, Figs. 3.9-3.10 show that a close agreement between computed and measured values is obtained at the whole range of P_{cmi} and especially at larger values of P_{cmi} by the use of the proposed transport capacity distribution functions of Eqs. (3.9) and (3.24).

4) *Plots showing variations of the ratio of computed to measured size fractions of bed-material load with relative diameter of bed material size*

The ratio of computed size fractions of bed-material load to the measured fraction of bed-material load against the relative diameter of the bed material are shown in Fig. 6.32-6.40 and Figs. 3.7-3.8. Values of P_{cci}/P_{cmi} equal to 1 indicate perfect agreement. It can be seen from Figs. 3.7-3.8. that most of the points fall near the perfect agreement line of P_{cci}/P_{cmi} equal to 1 for the newly developed transport capacity distribution functions. The plots shown in Fig. 6.32-6.40 for other methods indicate that the values of P_{cci}/P_{cmi} are generally near perfect agreement at values of D_i/D_{50} around 1; and the values of P_{cci}/P_{cmi} diverge from the perfect agreement at smallest and largest values of D_i/D_{50}. Overall, the Einstein method underpredicts the transport rate for finer sizes and overpredicts for the coarser sizes, while the other methods overestimate the finer fractions and underestimate the coarser fractions.

In the modified BMF method, the weighting function of Eq. (2.44) proposed by Karim (1998) may be expressed as

$$\phi_i = P_{ai}\,\eta = \left[\frac{C_1\left(\dfrac{1}{D_{50}}\right)^{C_2}}{\displaystyle\sum_{i=1}^{N}\frac{P_{bi}}{D_i}}\right]\left[\frac{P_{bi}}{D_i^{\,1-C_2}}\right] \tag{6.14}$$

It can be seen that the first term in Eq. (6.14) is a constant value for a given data set, and the weighting function varies only with P_{bi} and D_i for different size fractions. In general, due to the sheltering and exposure effect in a sediment mixture, the finer fractions are transported at a relatively lower rate than they would be if they were in a uniform sediment bed. The coarser particles consequently are transported faster. To reflect this phenomenon, the exponent $(1\text{-}C_2)$ in Eq. (6.14) should be a negative value. A positive value of $(1\text{-}C_2)$ will result in unrealistic results by increasing the transport rate for finer fractions and decreasing the transport rate for coarser sizes.

As an example, the flume data of Einstein and Chien (1953) can be used to evaluate the variation of C_2. Since the values of ω_{50} / V_* are in the range of 0.13-0.61 for Einstein and Chien's data, the value of exponent C_2 [Eq. (2.47)]will vary as

$$C_2 = 0.60\left(\frac{\omega_{50}}{V_*}\right) = 0.60\,(0.13 \sim 0.61) = 0.078 \sim 0.366 \tag{6.15}$$

and the value of exponent $(1\text{-}C_2)$ will be 0.634-0.922. As a result, this produced the unreasonable results for the data of Einstein and Chien shown in Fig. 6.38. Similar results can be seen for data derived from other sources.

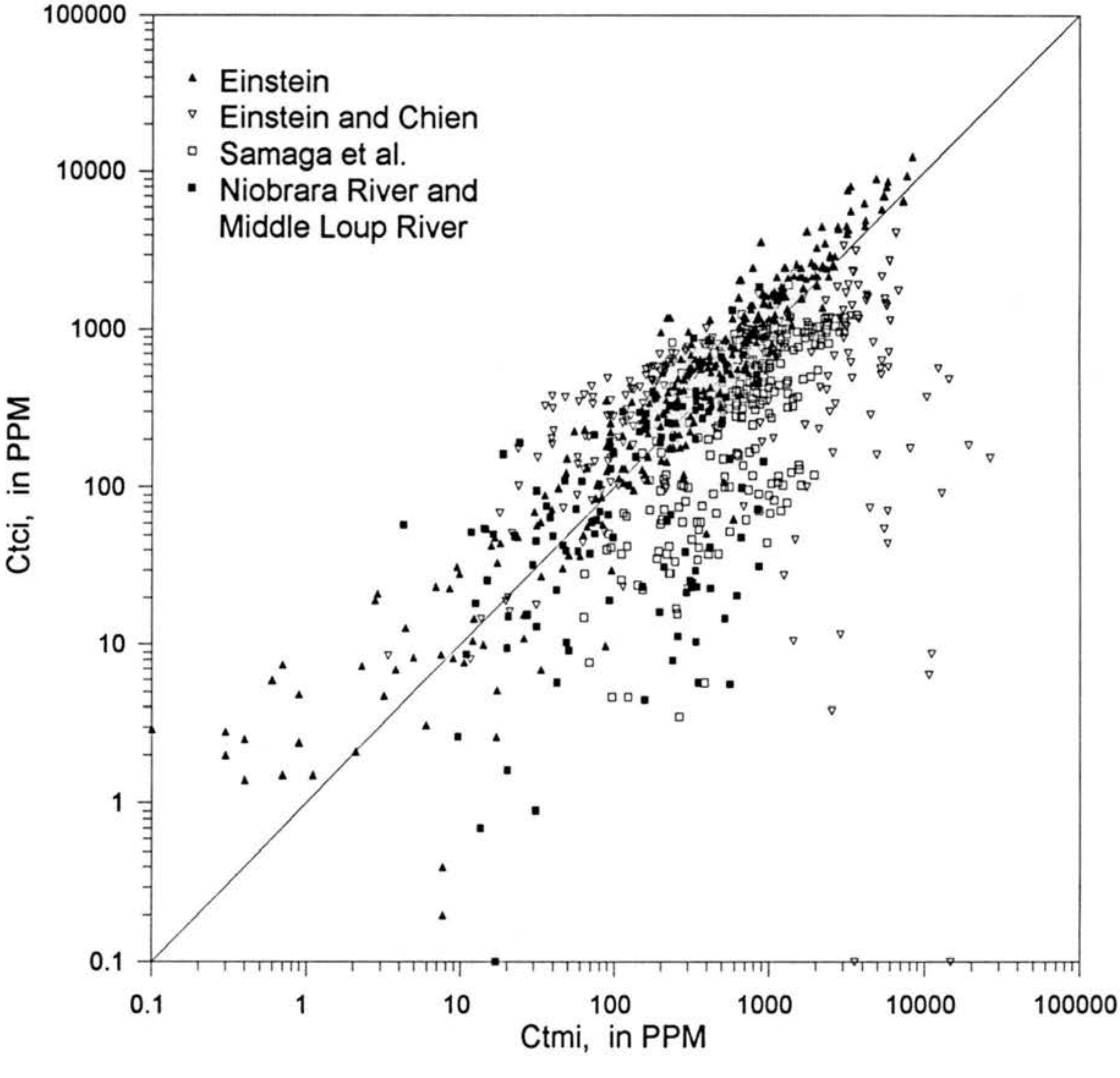

Fig. 6.1. Comparison between Computed and Measured Fractional Bed-Material Concentrations for the Einstein Equation (1950).

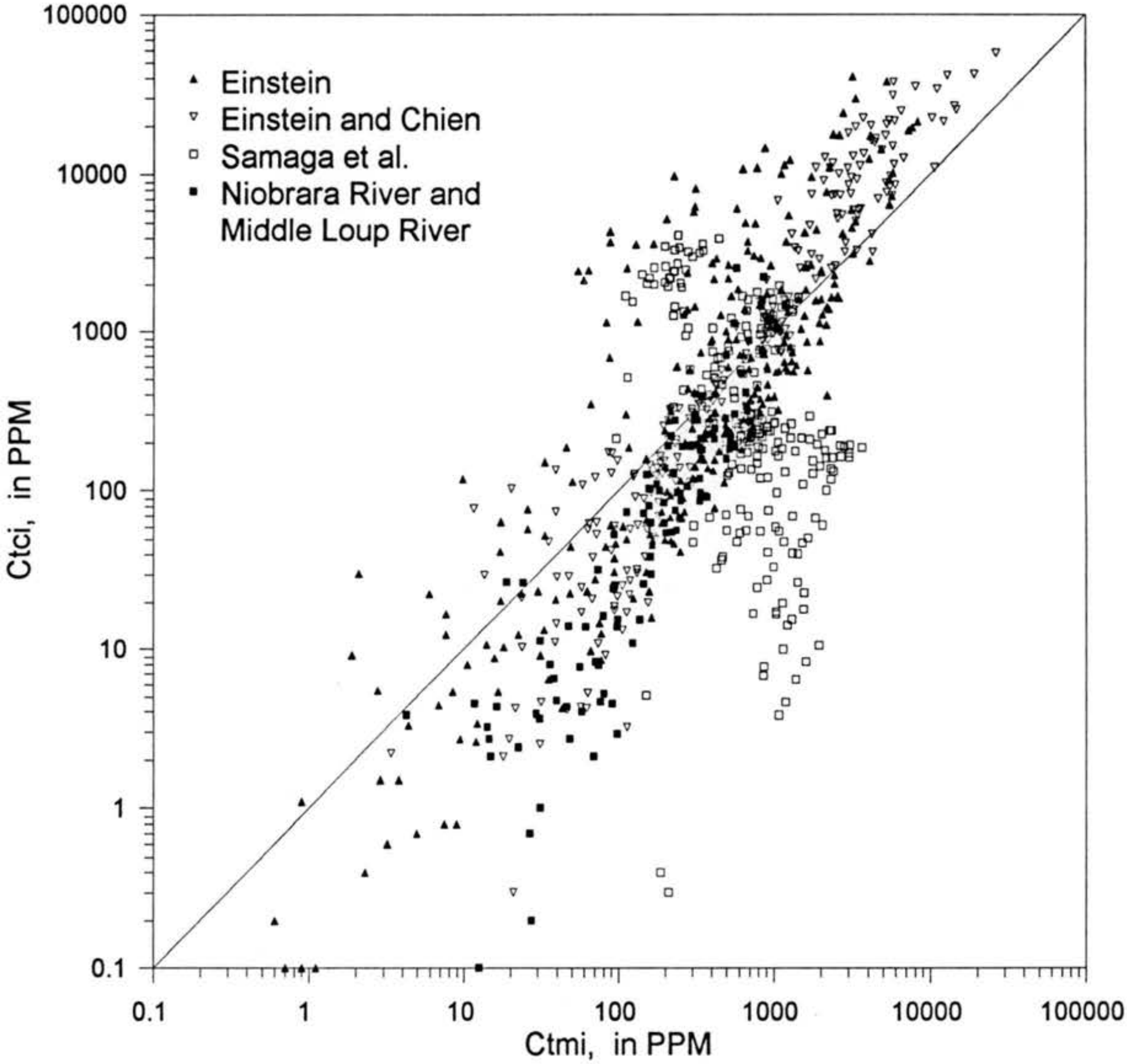

Fig. 6.2. Comparison between Computed and Measured Fractional Bed-Material Concentrations for the Laursen Equation (1958).

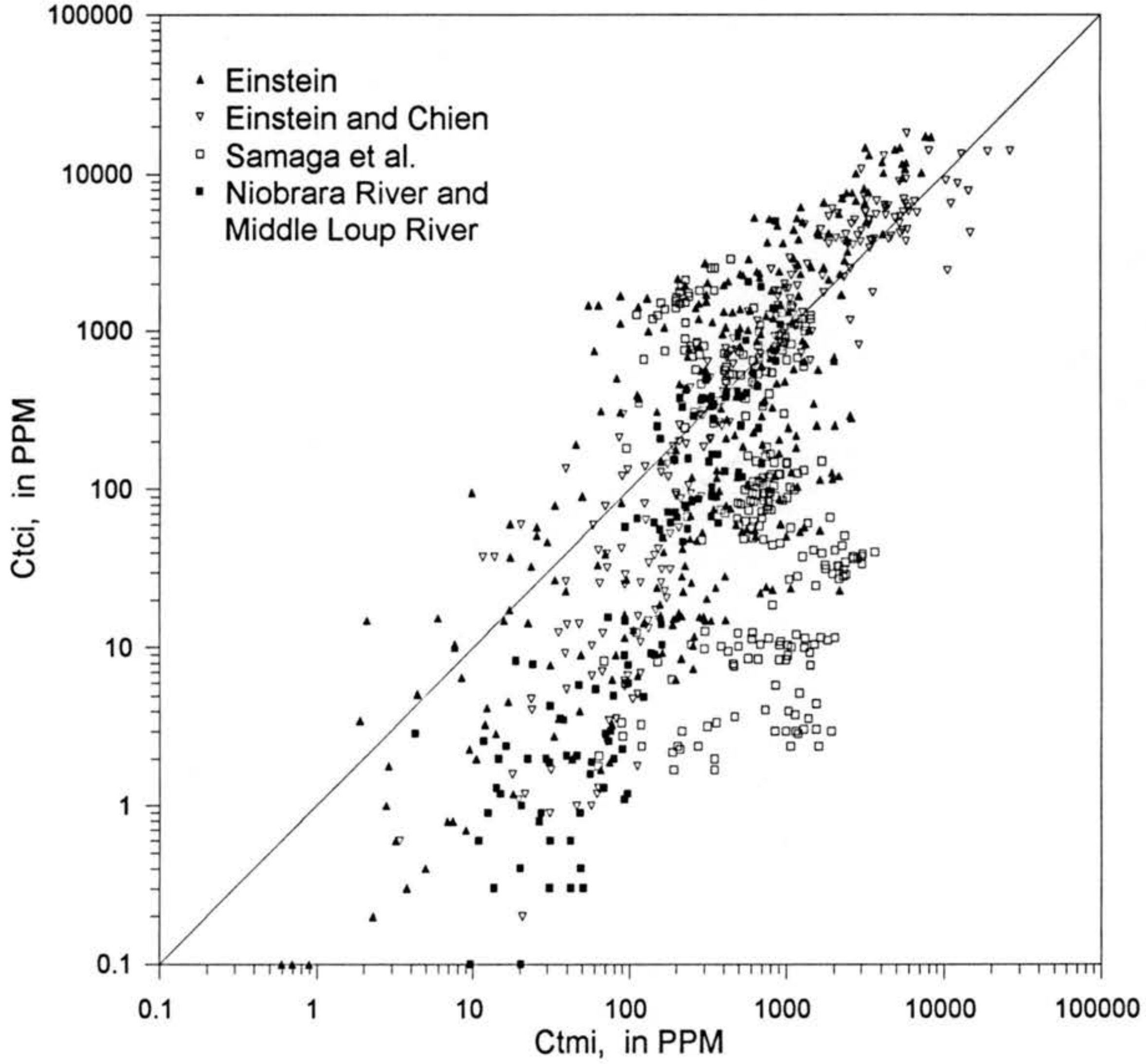

Fig. 6.3. Comparison between Computed and Measured Fractional Bed-Material Concentrations for the Toffaleti Equation (1968).

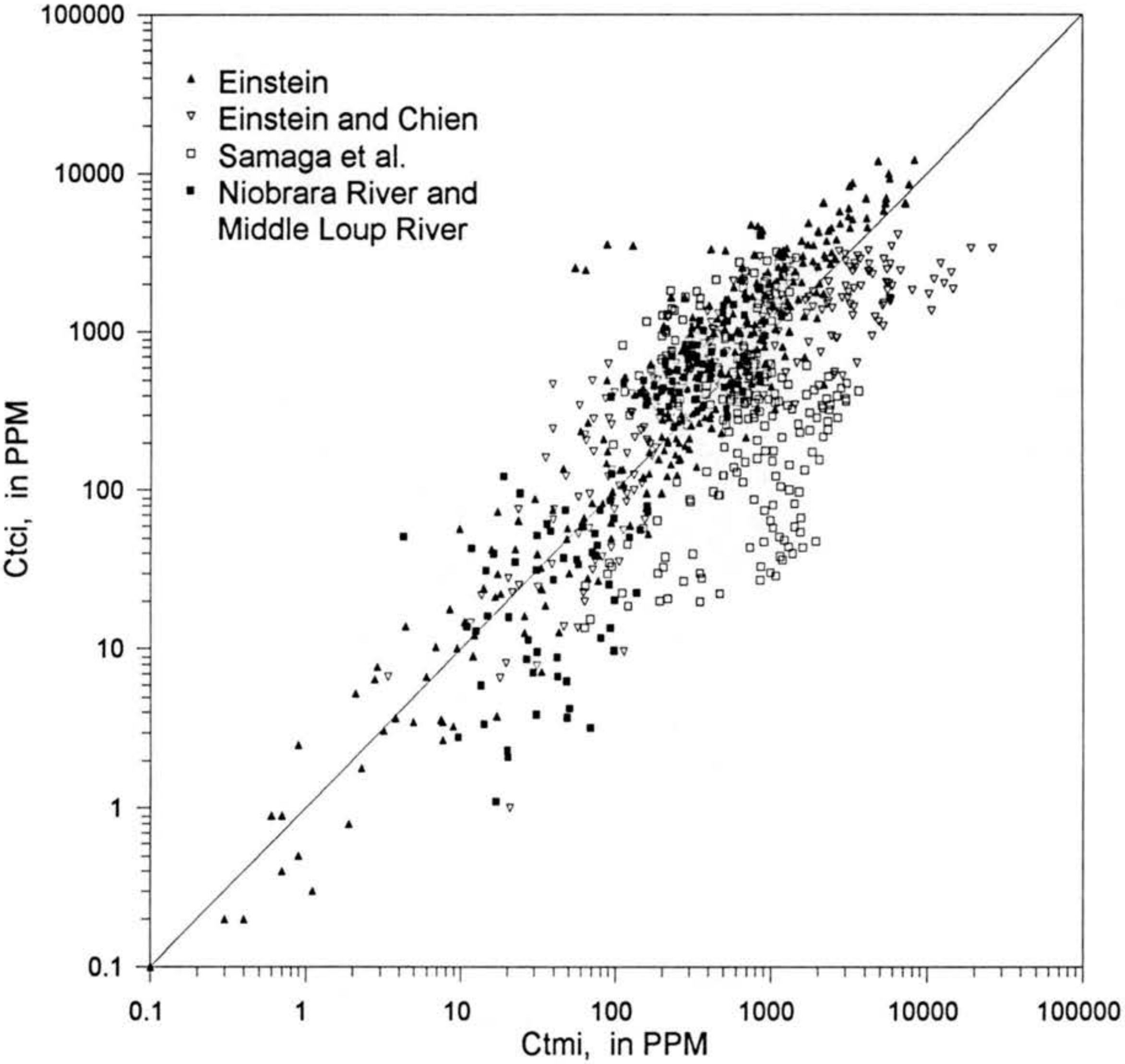

Fig. 6.4. Comparison between Computed and Measured Fractional Bed-Material Concentrations for the BMF Approach Using the Engelund and Hansen Transport Equation (1967).

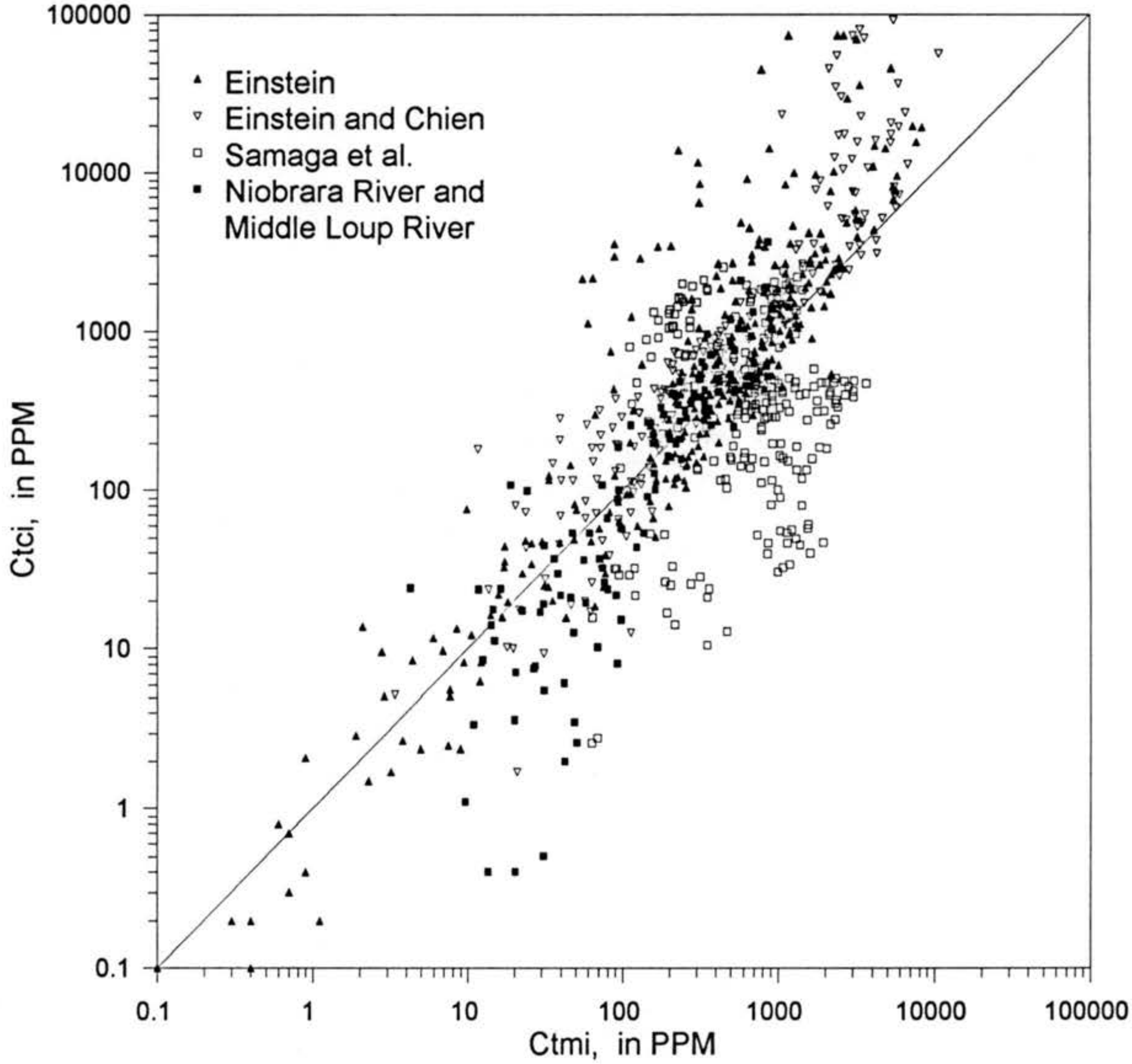

Fig. 6.5. Comparison between Computed and Measured Fractional Bed-Material Concentrations for the BMF Approach Using the Ackers and White Transport Equation (1973).

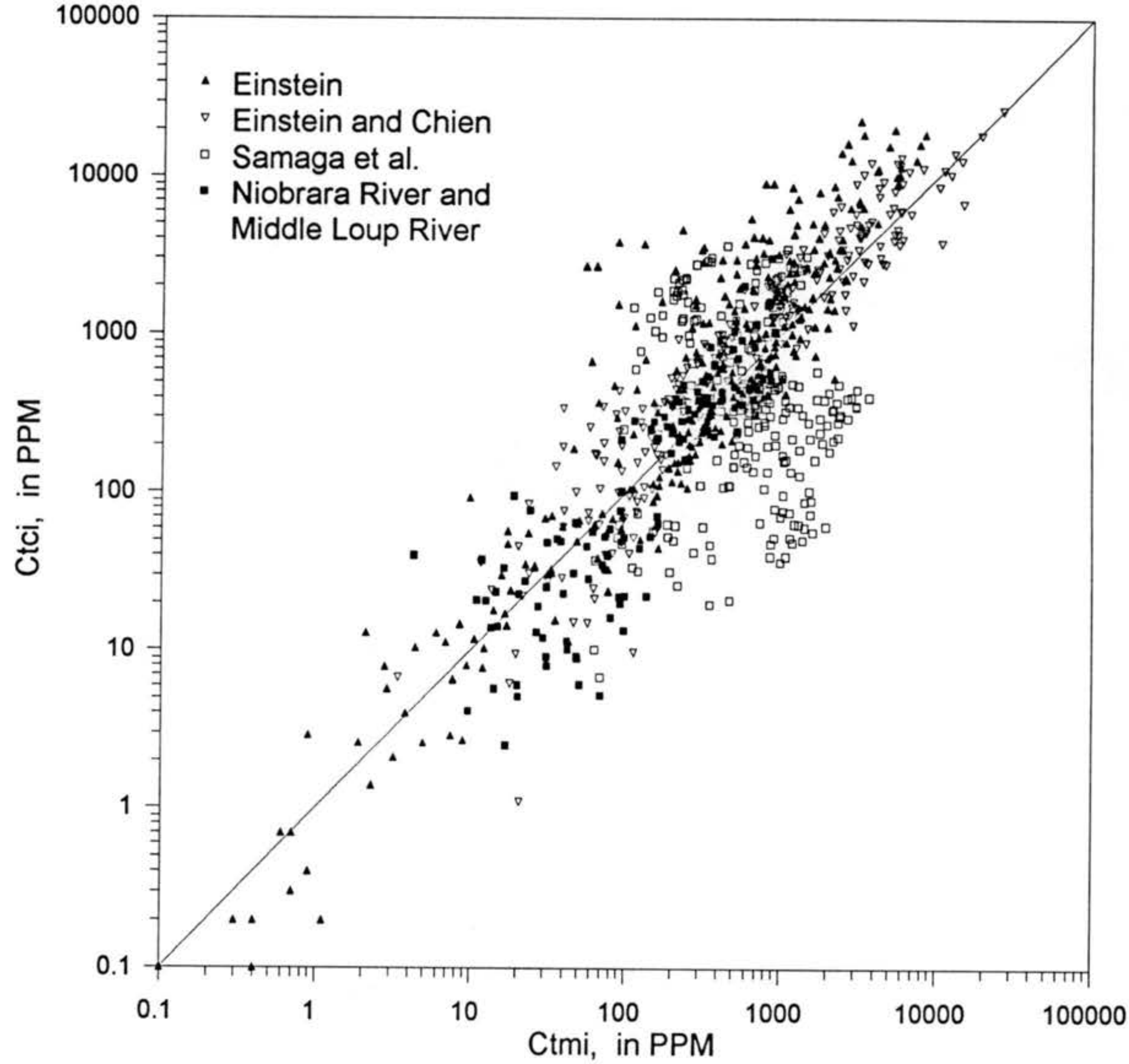

Fig. 6.6. Comparison between Computed and Measured Fractional Bed-Material Concentrations for the BMF Approach Using the Yang Transport Equation (1973).

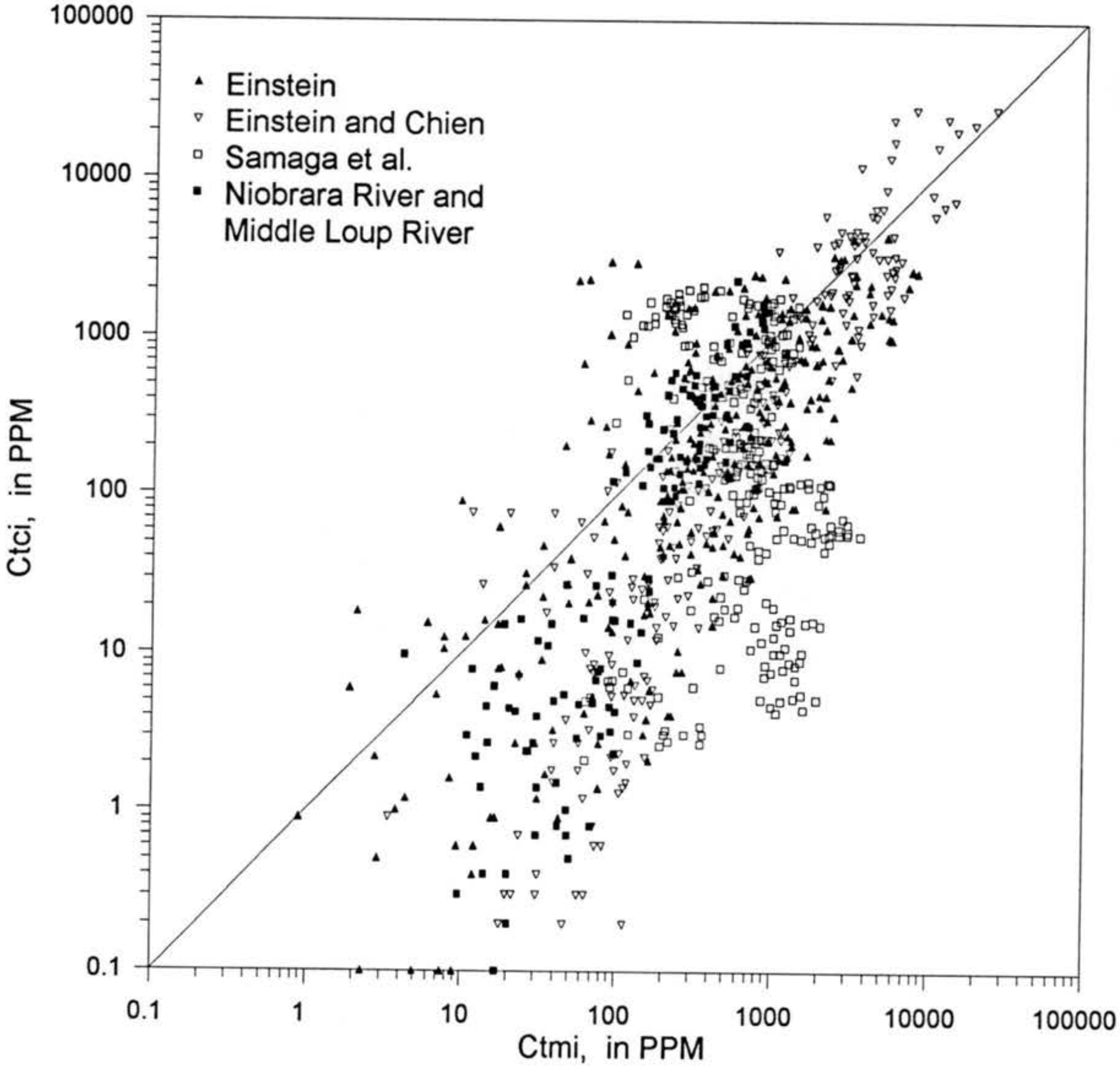

Fig. 6.7. Comparison between Computed and Measured Fractional Bed-Material Concentrations for Karim's Modified BMF Approach (1998).

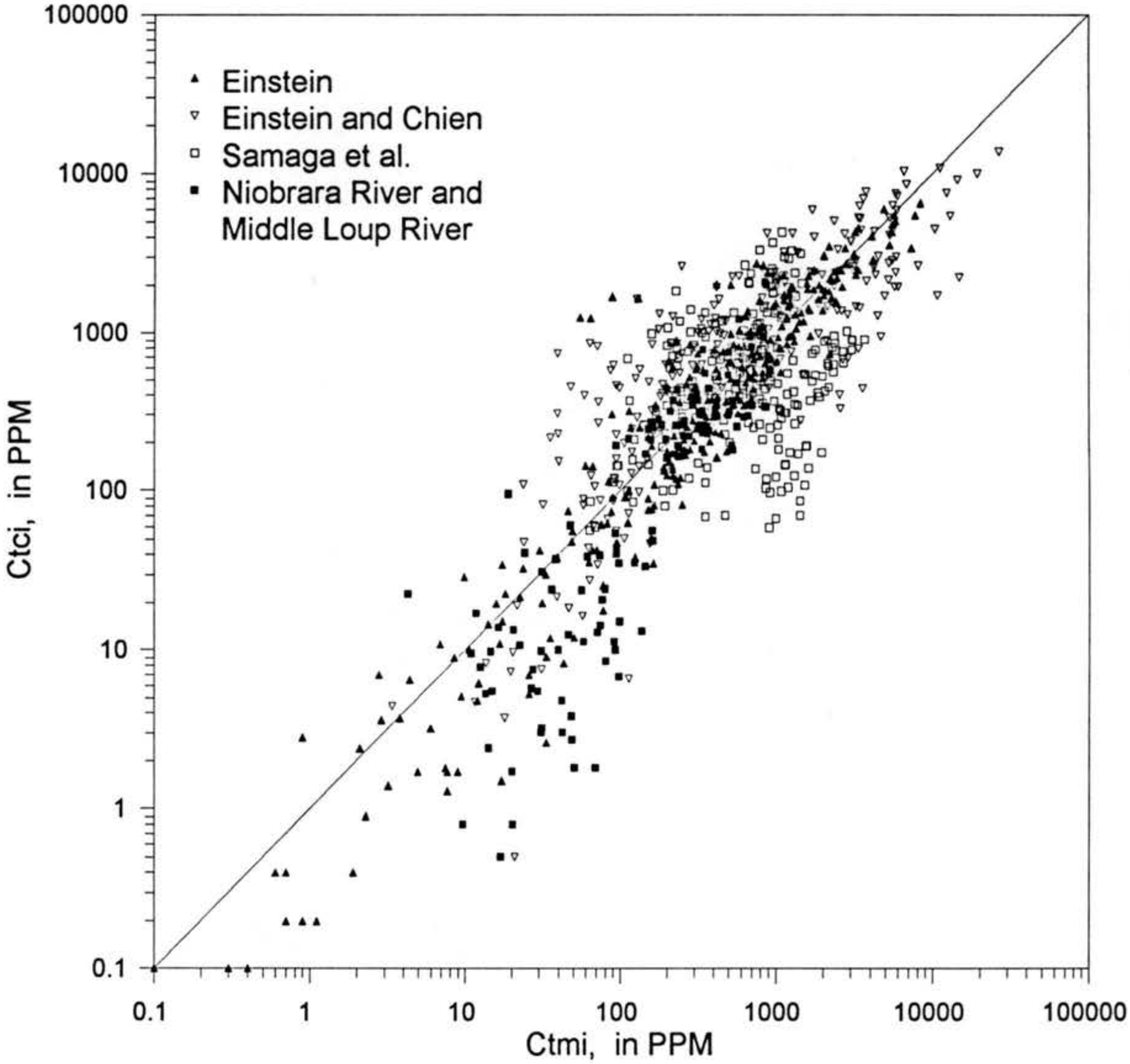

Fig. 6.8. Comparison between Computed and Measured Fractional Bed-Material Concentrations for the TCF Approach Using the Yang Equation (1973) with D_e and the Transport Capacity Distribution Function of Karim and Kennedy (1981).

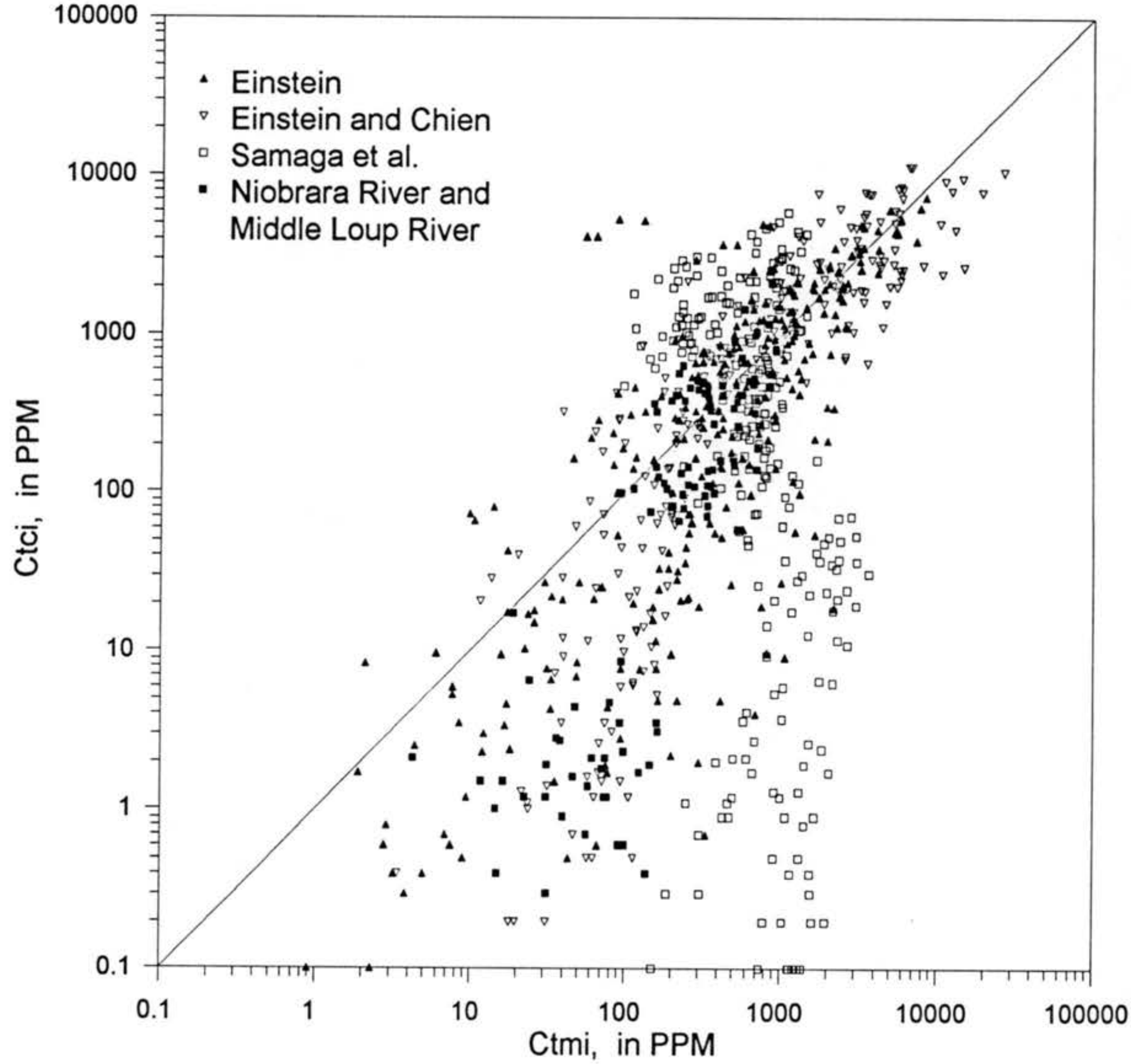

Fig. 6.9. Comparison between Computed and Measured Fractional Bed-Material Concentrations for the TCF Approach Using the Yang Equation (1973) with D_e and the Transport Capacity Distribution Function of Li (1988).

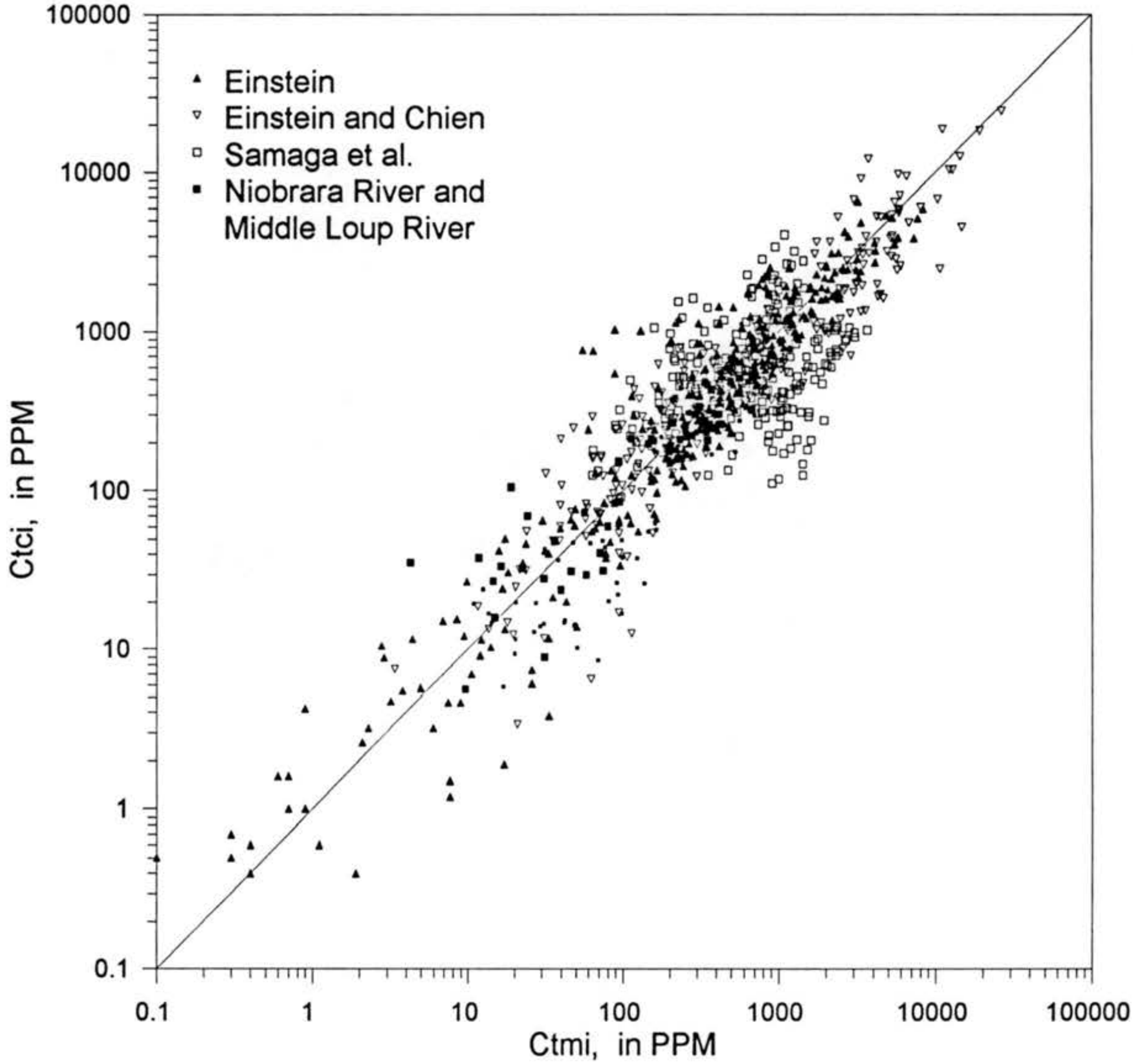

Fig. 6.10. Comparison between Computed and Measured Fractional Bed-Material Concentrations for the TCF Approach Using the Yang Equation (1973) with D_e and the Proposed Transport Capacity Distribution Function of Eq. (3.9).

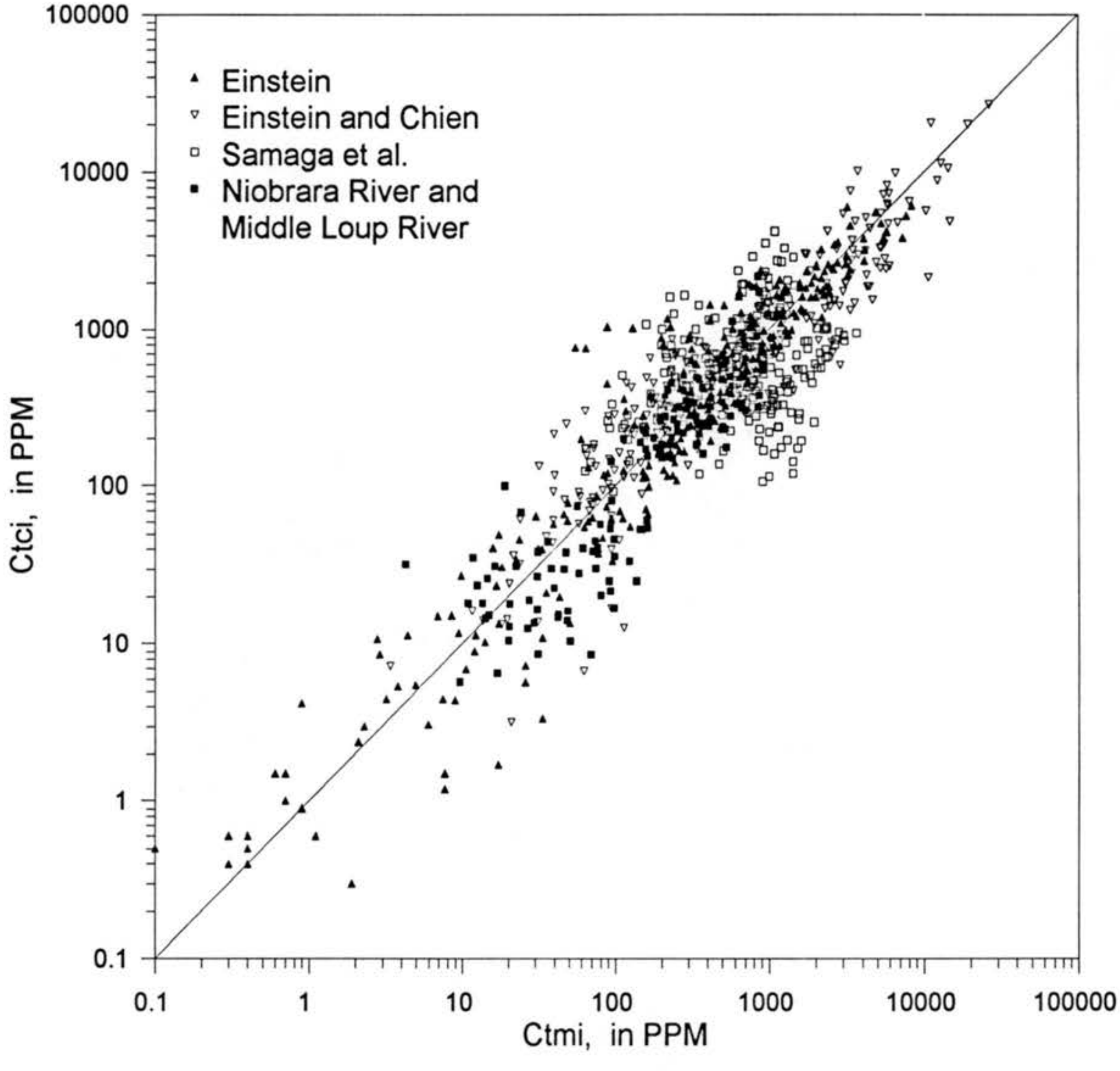

Fig. 6.11. Comparison between Computed and Measured Fractional Bed-Material Concentrations for the TCF Approach Using the Yang Equation (1973) with D_e and the Proposed Transport Capacity Distribution Function of Eq. (3.24).

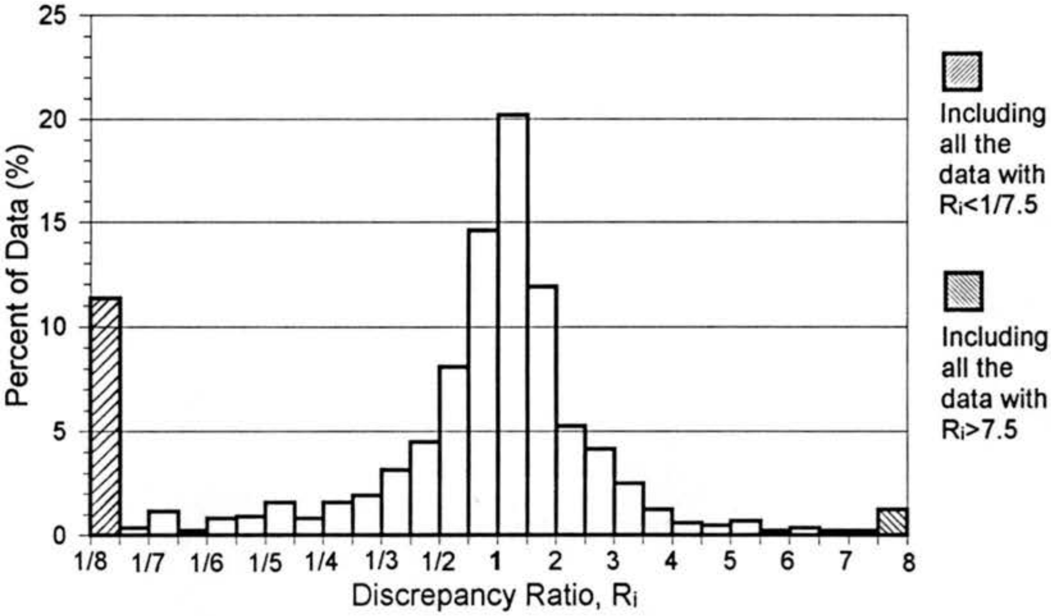

Fig. 6.12. Discrepancy Ratio Distribution of Fractional Bed-Material Concentrations for the Einstein Equation (1950).

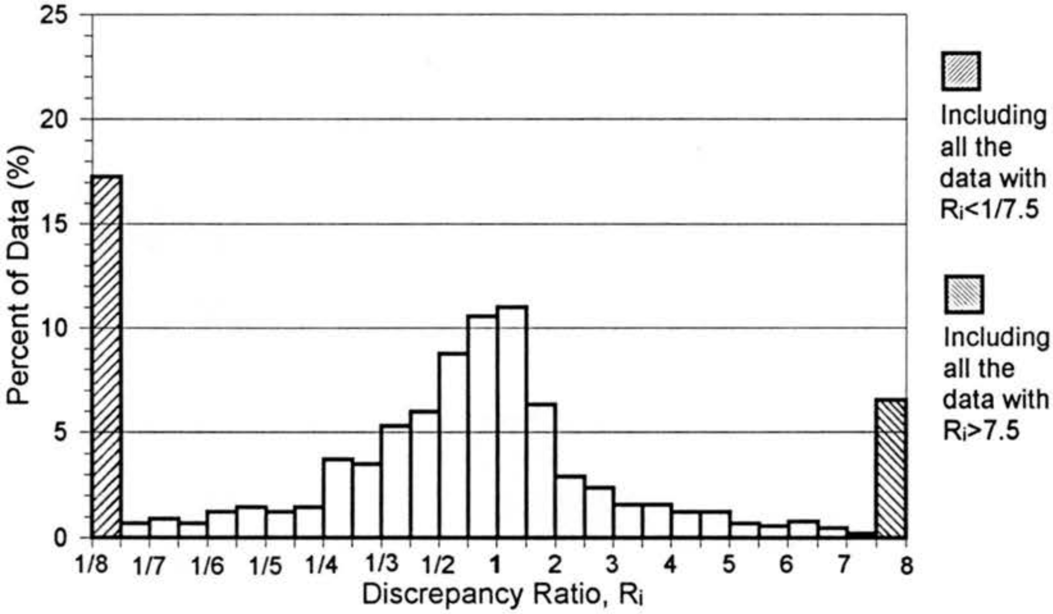

Fig. 6.13. Discrepancy Ratio Distribution of Fractional Bed-Material Concentrations for the Laursen Equation (1958).

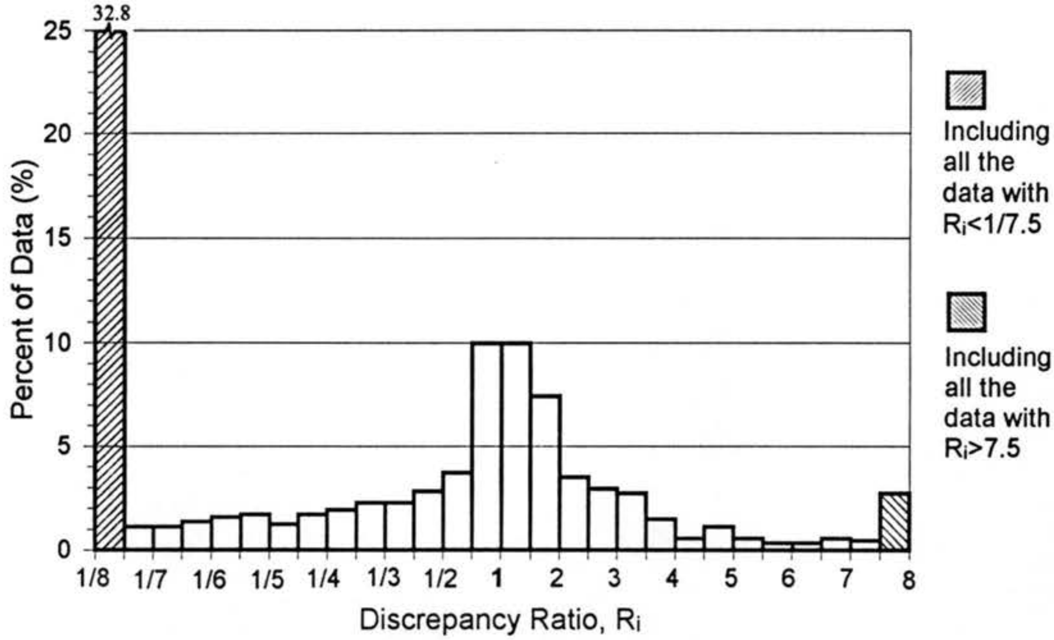

Fig. 6.14. Discrepancy Ratio Distribution of Fractional Bed-Material Concentrations for the Toffaleti Equation (1968).

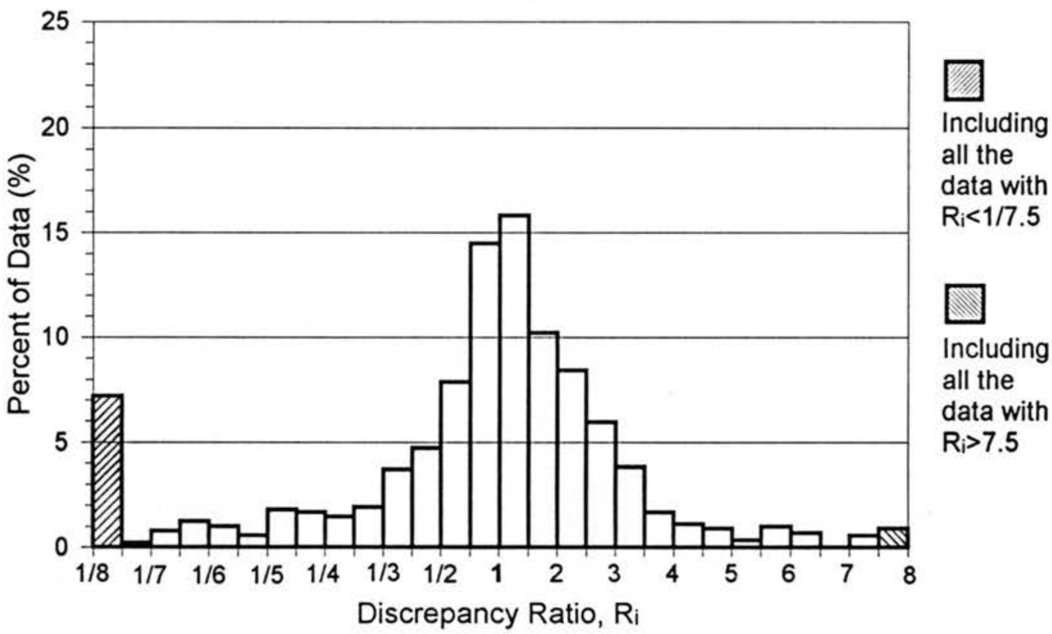

Fig. 6.15. Discrepancy Ratio Distribution of Fractional Bed-Material Concentrations for the BMF Approach Using the Engelund and Hansen Equation (1967).

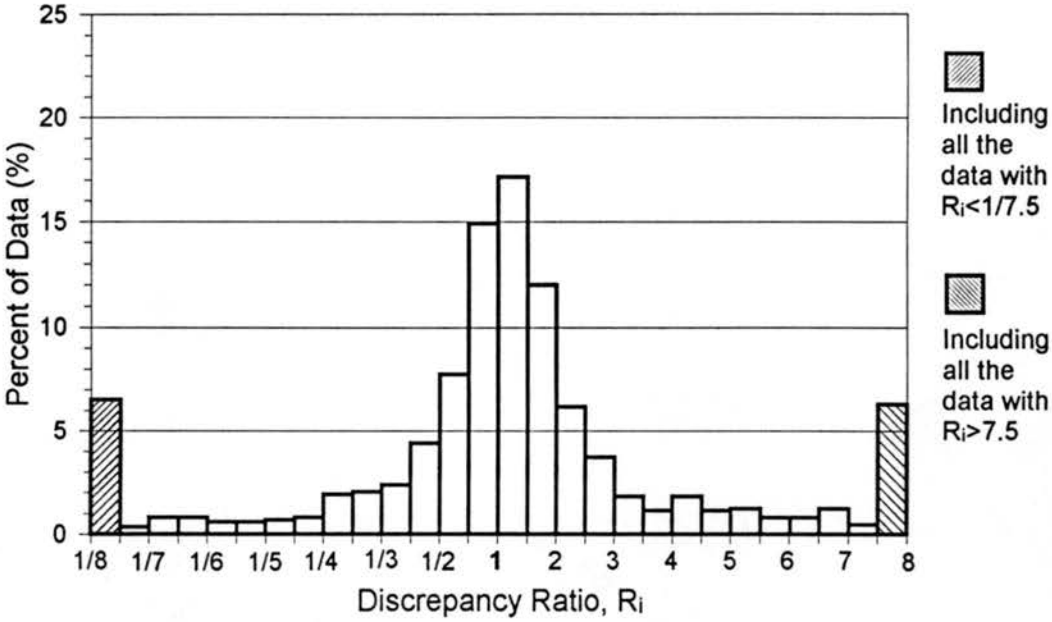

Fig. 6.16. Discrepancy Ratio Distribution of Fractional Bed-Material Concentrations for the BMF Approach Using the Ackers and White Equation (1973).

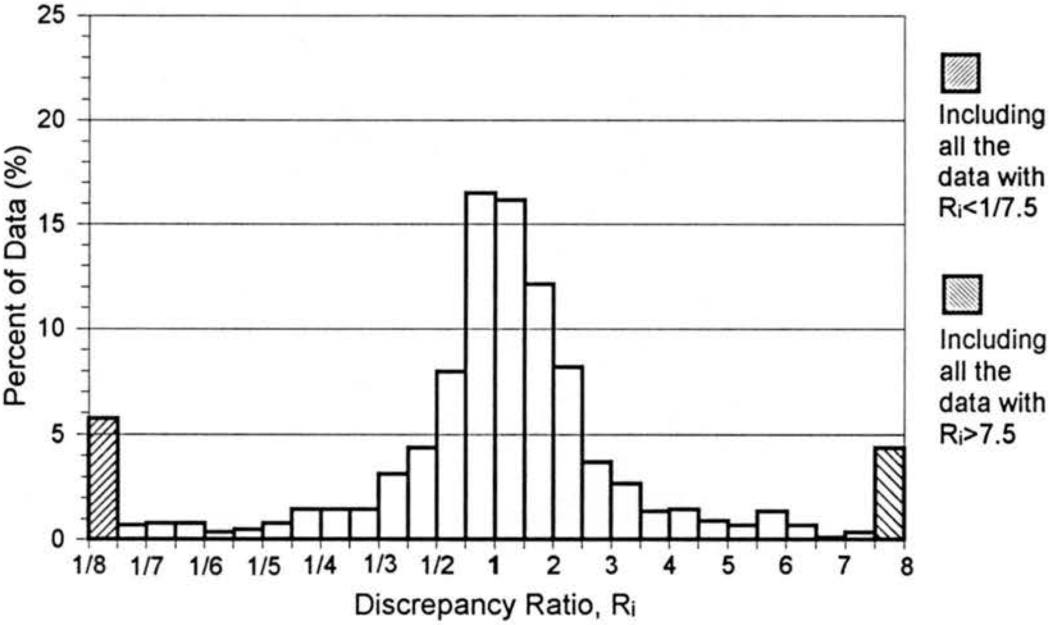

Fig. 6.17. Discrepancy Ratio Distribution of Fractional Bed-Material Concentrations for the BMF Approach Using the Yang Sand Equation (1973).

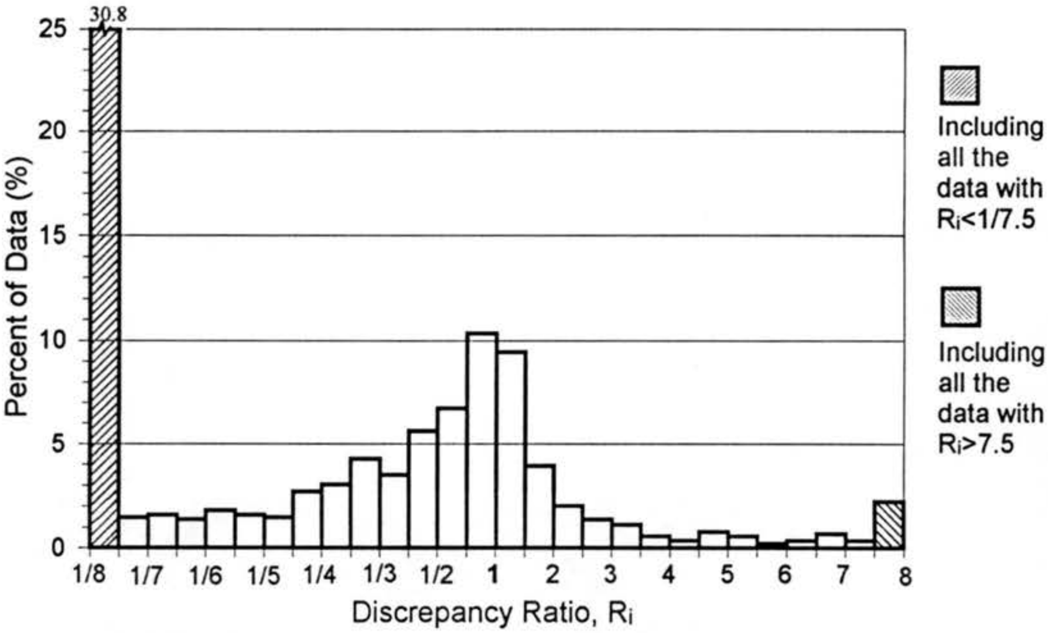

Fig. 6.18. Discrepancy Ratio Distribution of Fractional Bed-Material Concentrations for Karim's Modifed BMF Method (1998).

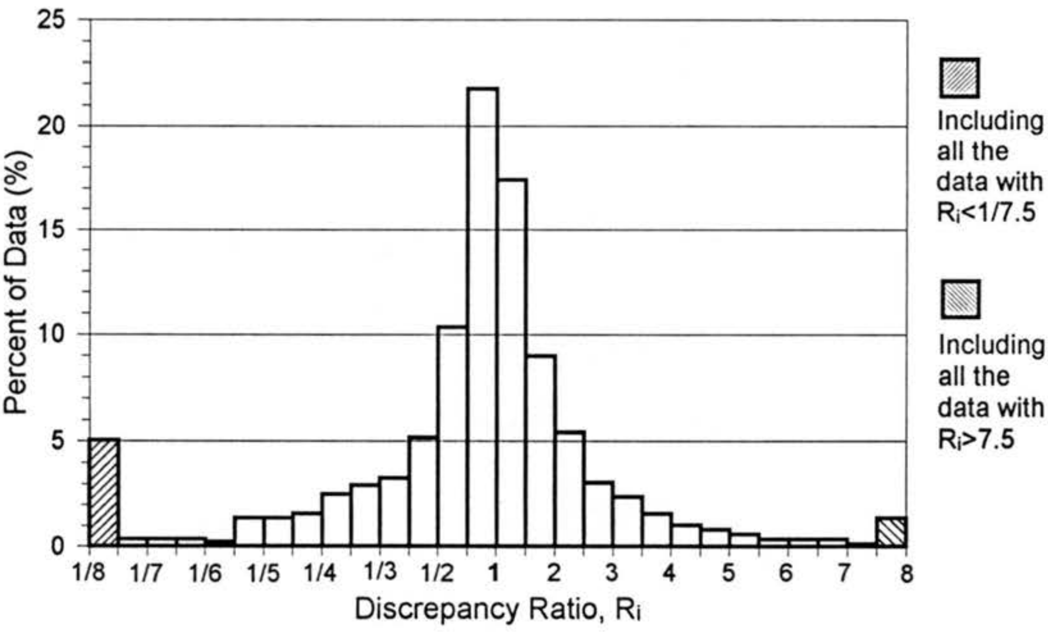

Fig. 6.19. Discrepancy Ratio Distribution of Fractional Bed-Material Concentrations for the TCF Approach Using the Yang Equation (1973) with D_e and the Transport Capacity Distribution Function of Karim and Kennedy (1981).

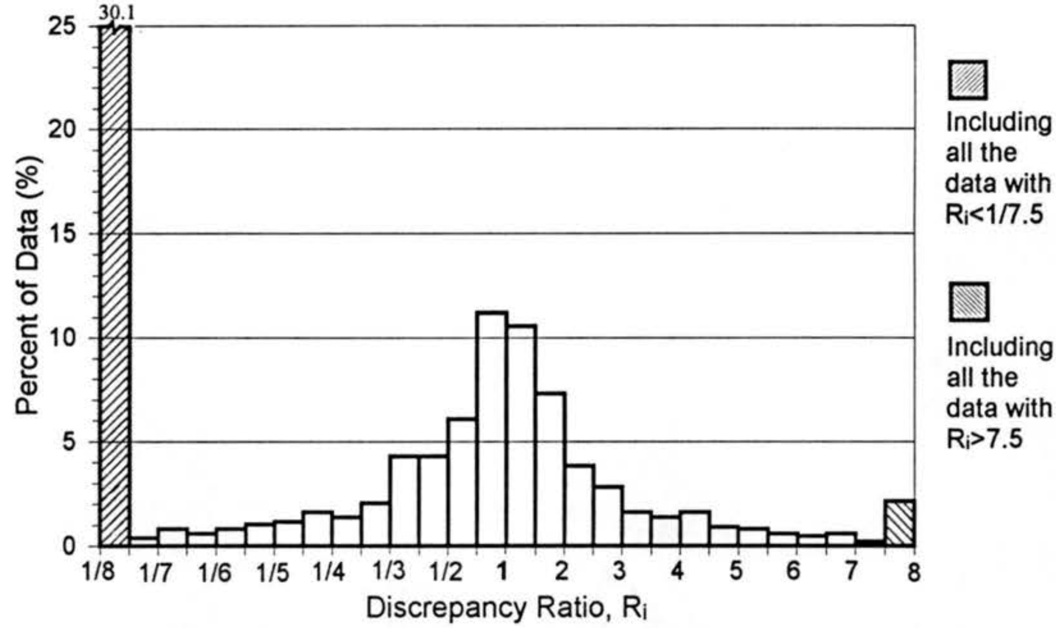

Fig. 6.20. Discrepancy Ratio Distribution of Fractional Bed-Material Concentrations for the TCF Approach Using the Yang Equation (1973) with D_e and the Transport Capacity Distribution Function of Li (1988).

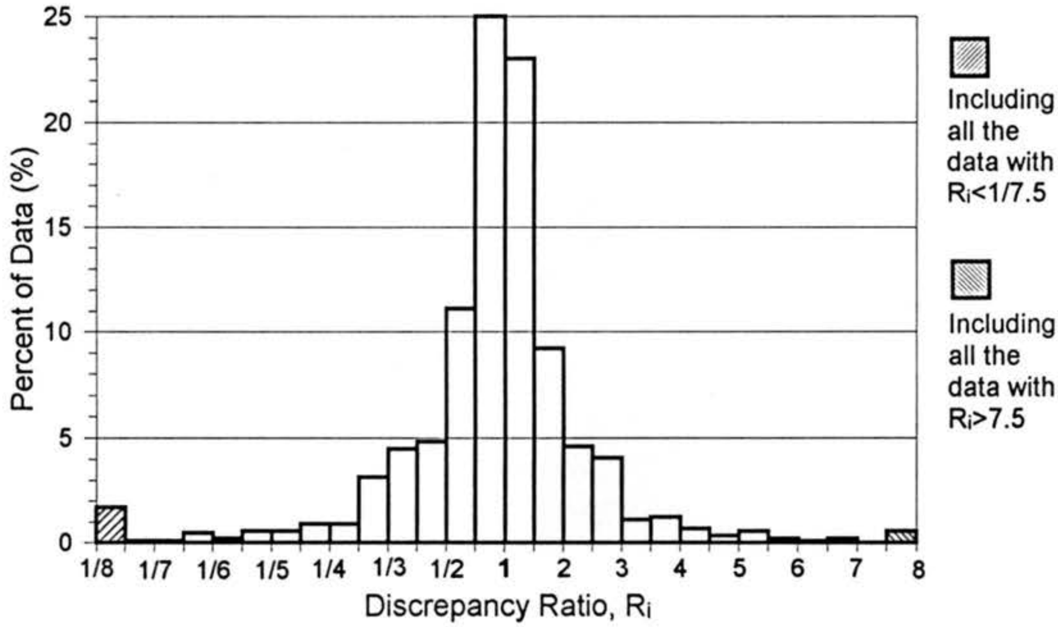

Fig. 6.21. Discrepancy Ratio Distribution of Fractional Bed-Material Concentrations for the TCF Approach Using the Yang Equation (1973) with D_e and the Proposed Transport Capacity Distrbution Function of Eq.(3.9).

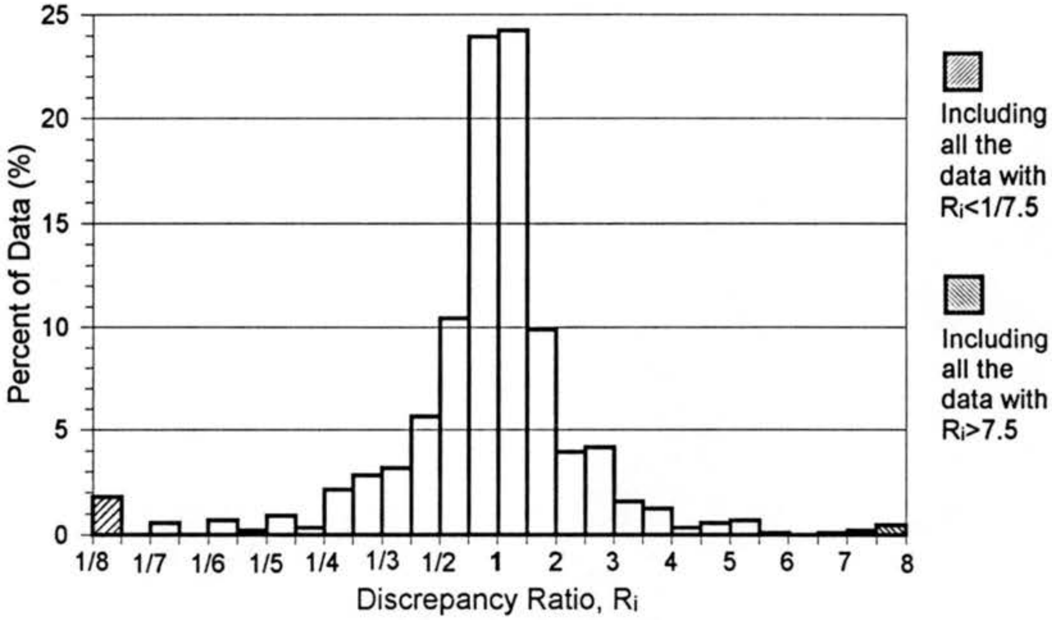

Fig. 6.22. Discrepancy Ratio Distribution of Fractional Bed-Material Concentrations for the TCF Approach Using the Yang Equation (1973) with D_e and the Proposed Transport Capacity Distribution Function of Eq.(3.24).

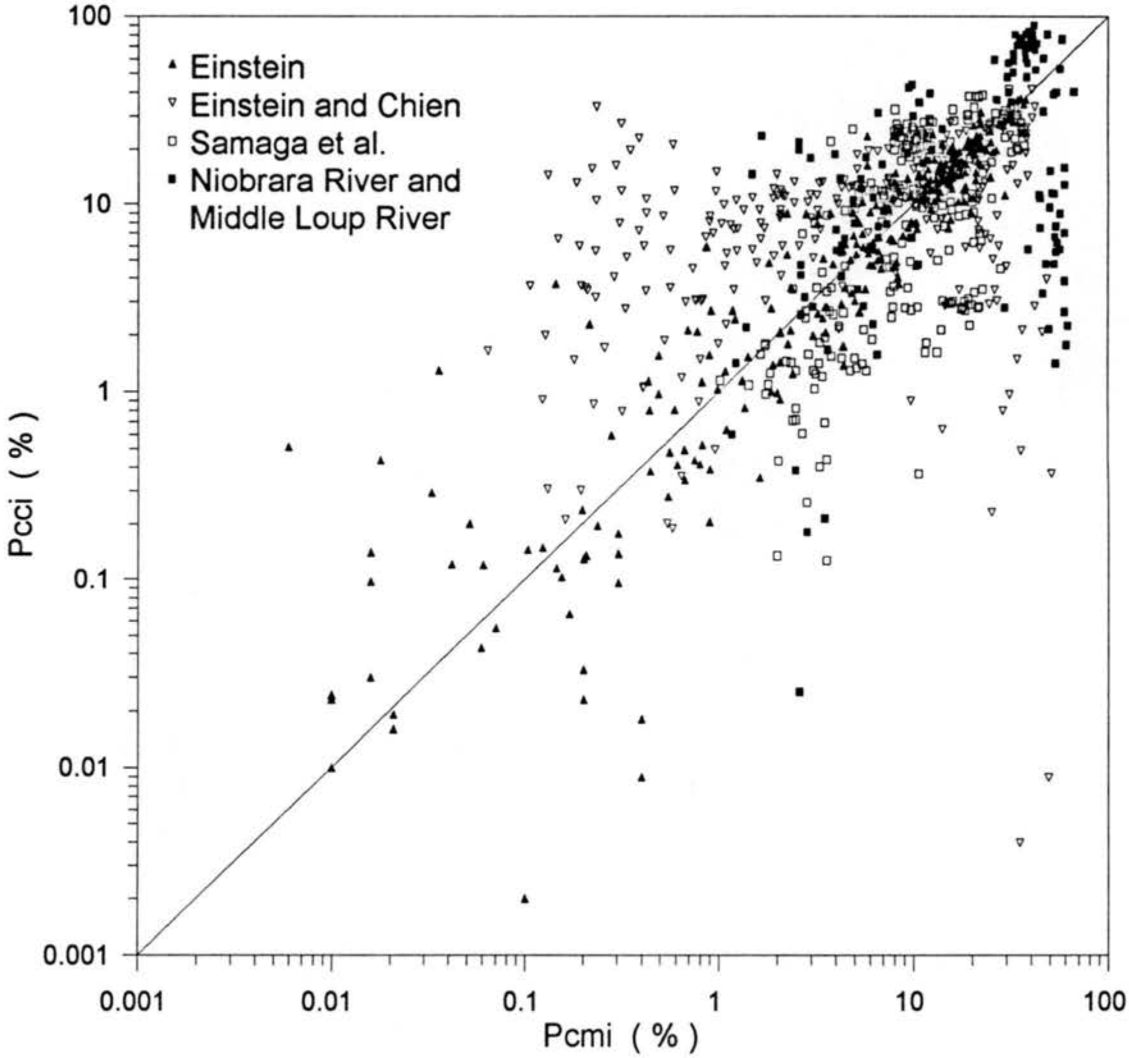

Fig. 6.23. Comparison between Computed and Measured Size Fractions of Bed-Material Load Sediment in Transport for the Einstein Equation (1950).

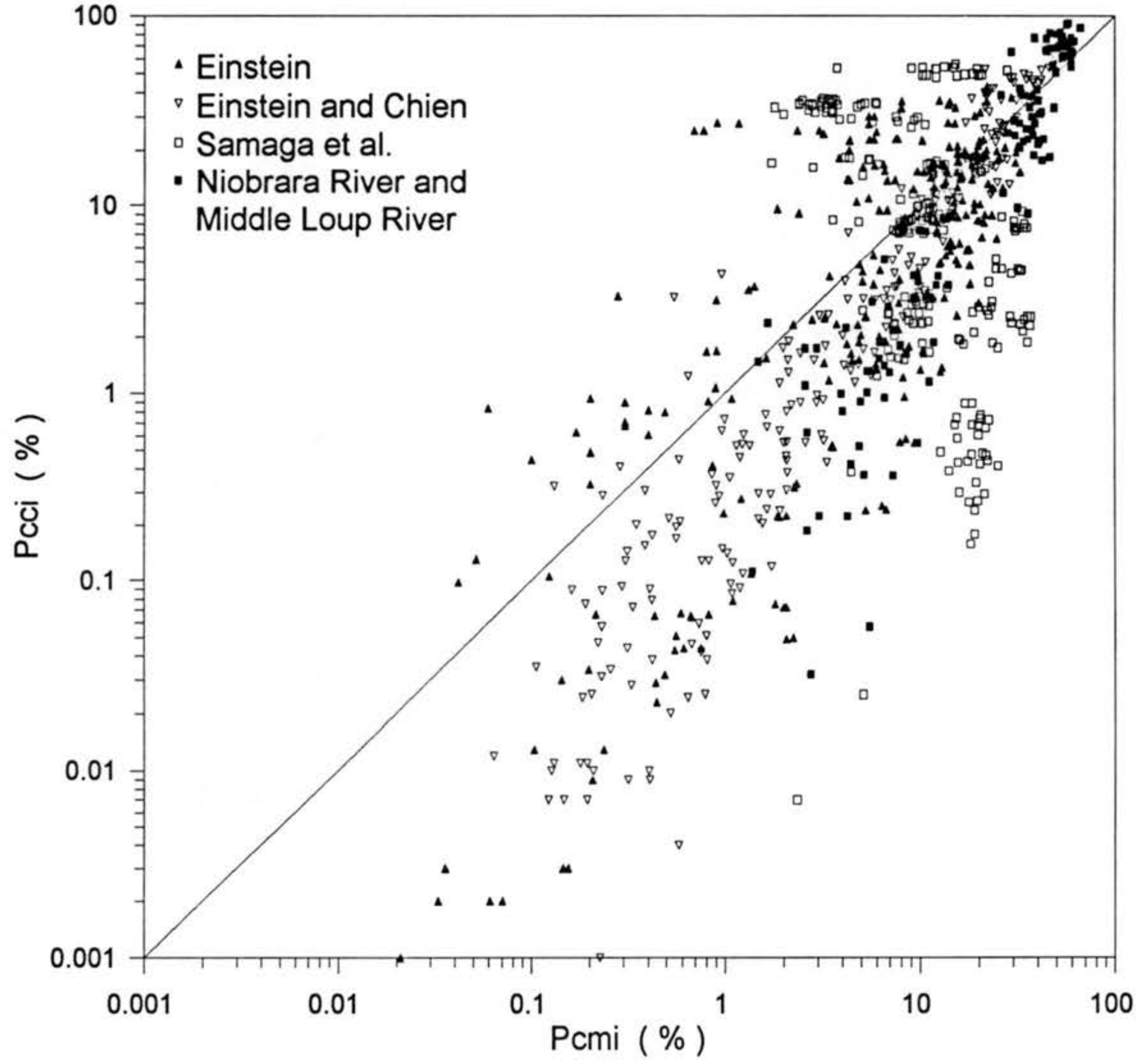

Fig. 6.24. Comparison between Computed and Measured Size Fractions of Bed-Material Load Sediment in Transport for the Laursen Equation (1958).

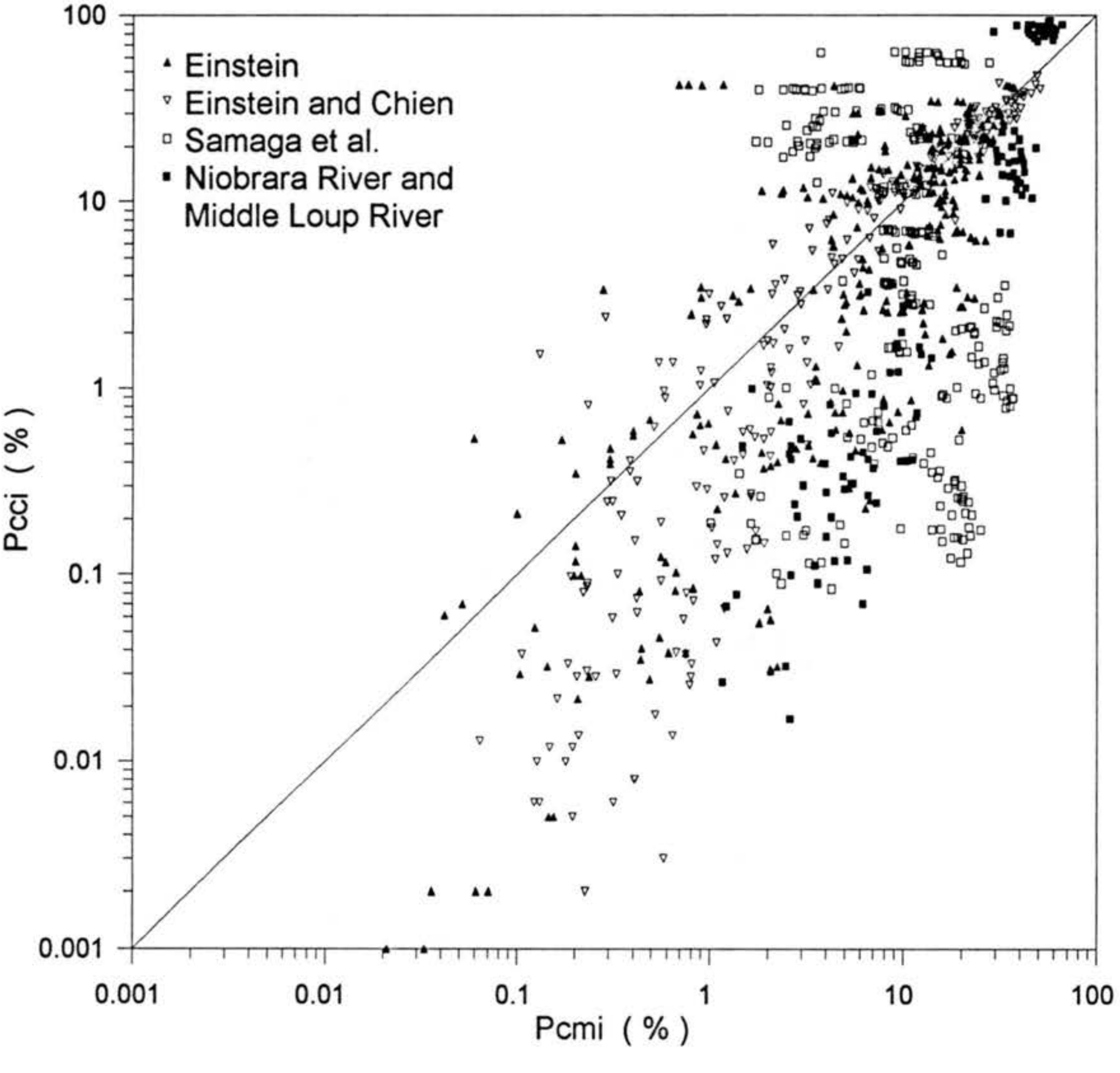

Fig. 6.25. Comparison between Computed and Measured Size Fractions of Bed-Material Load Sediment in Transport for the Toffaleti Equation (1968).

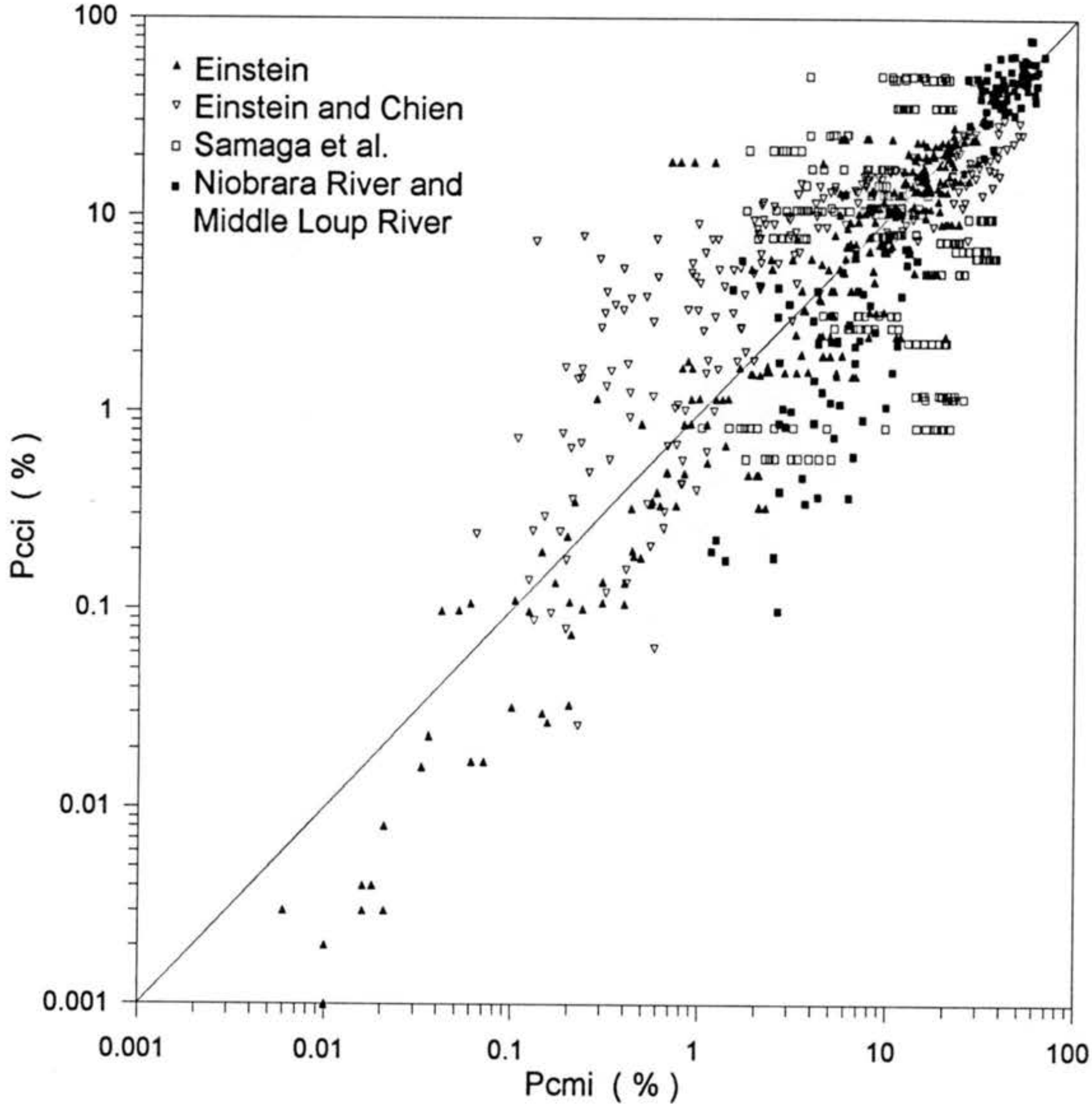

Fig. 6.26. Comparison between Computed and Measured Size Fractions of Bed-Material Load Sediment in Transport for the BMF Approach Using the Engelund and Hansen Transport Equation (1967).

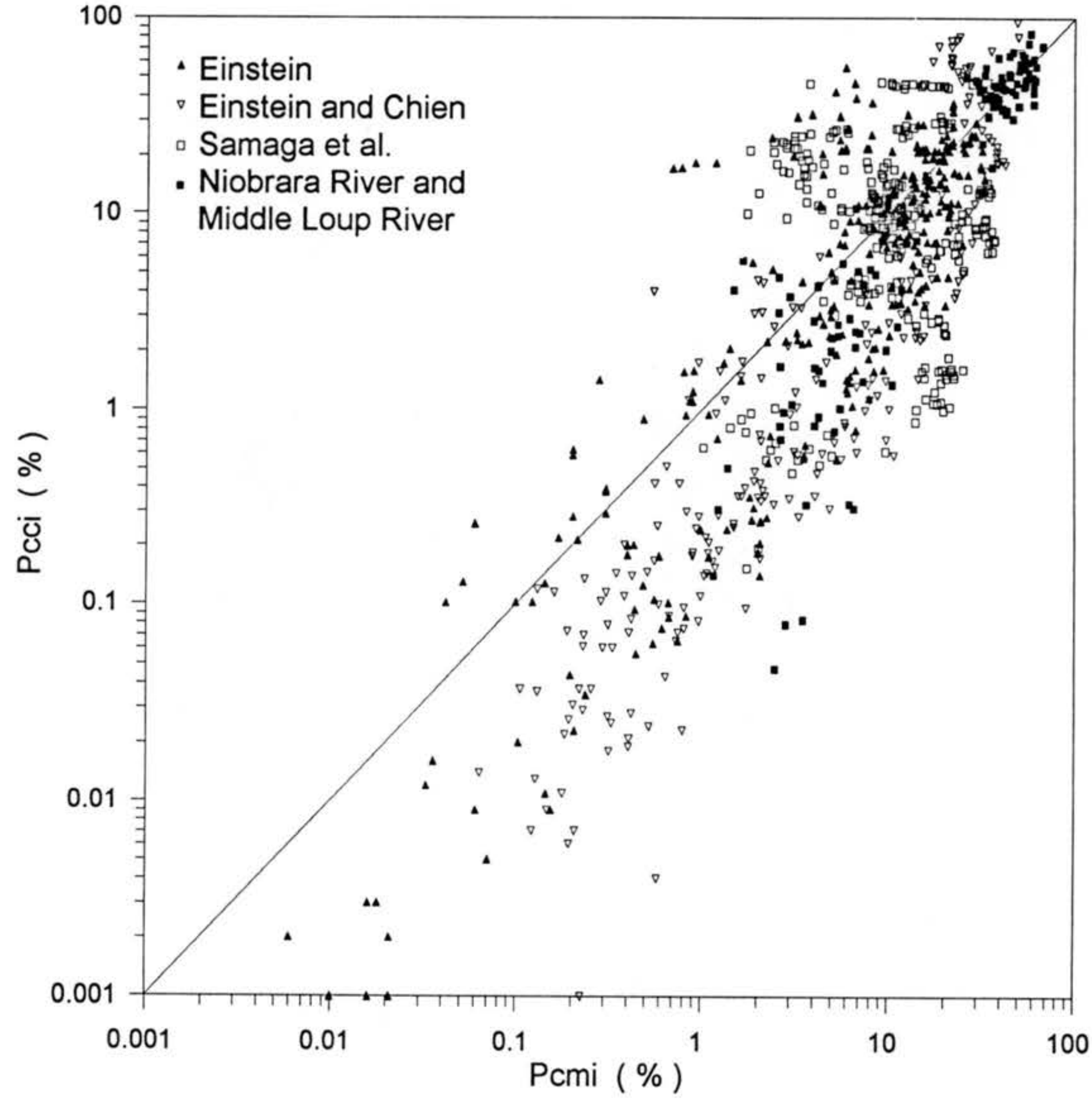

Fig. 6.27. Comparison between Computed and Measured Size Fractions of Bed-Material Load Sediment in Transport for the BMF Approach Using the Ackers and White Transport Equation (1973).

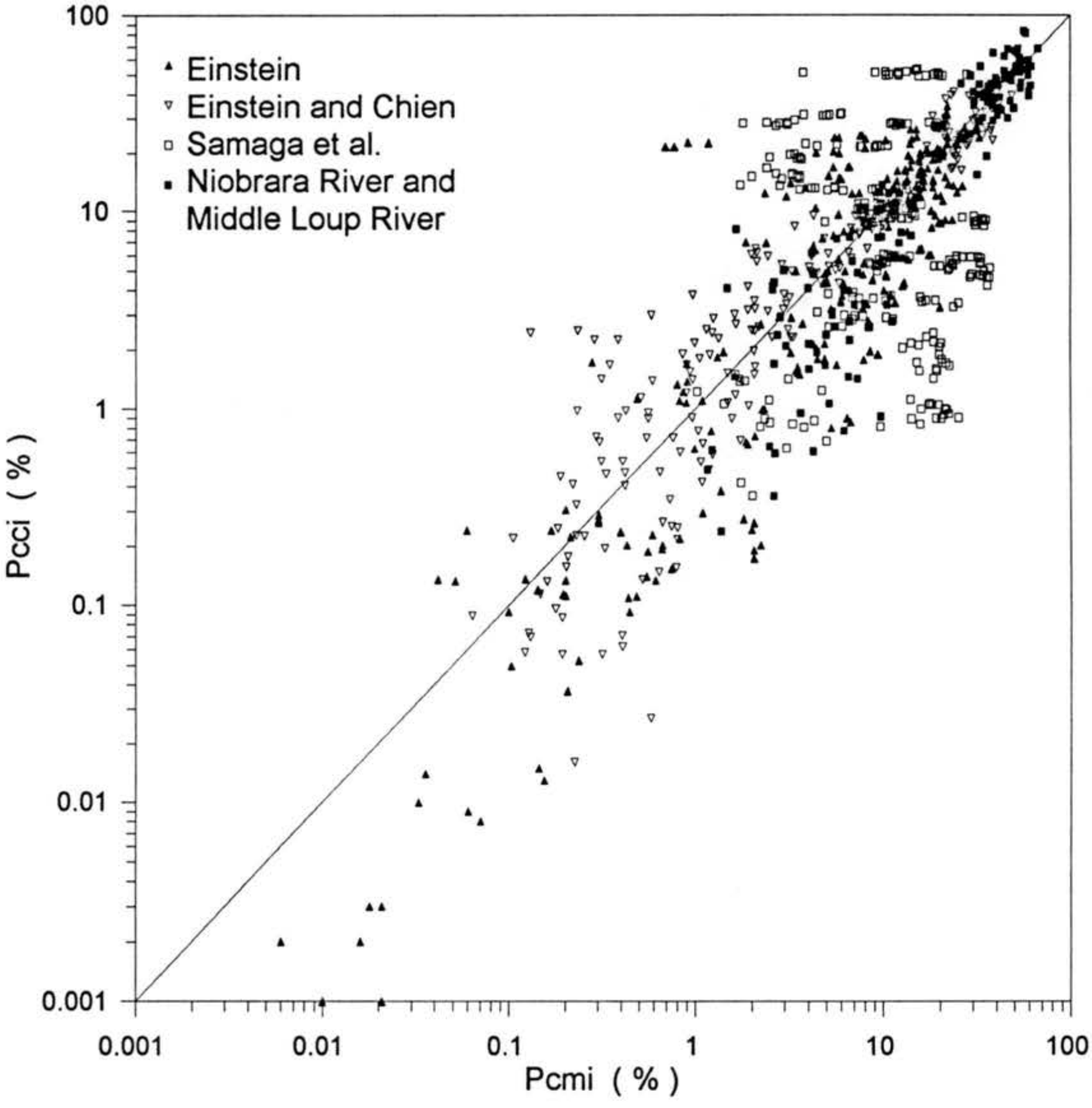

Fig. 6.28. Comparison between Computed and Measured Size Fractions of Bed-Material Load Sediment in Transport for the BMF Approach Using the Yang Transport Equation (1973).

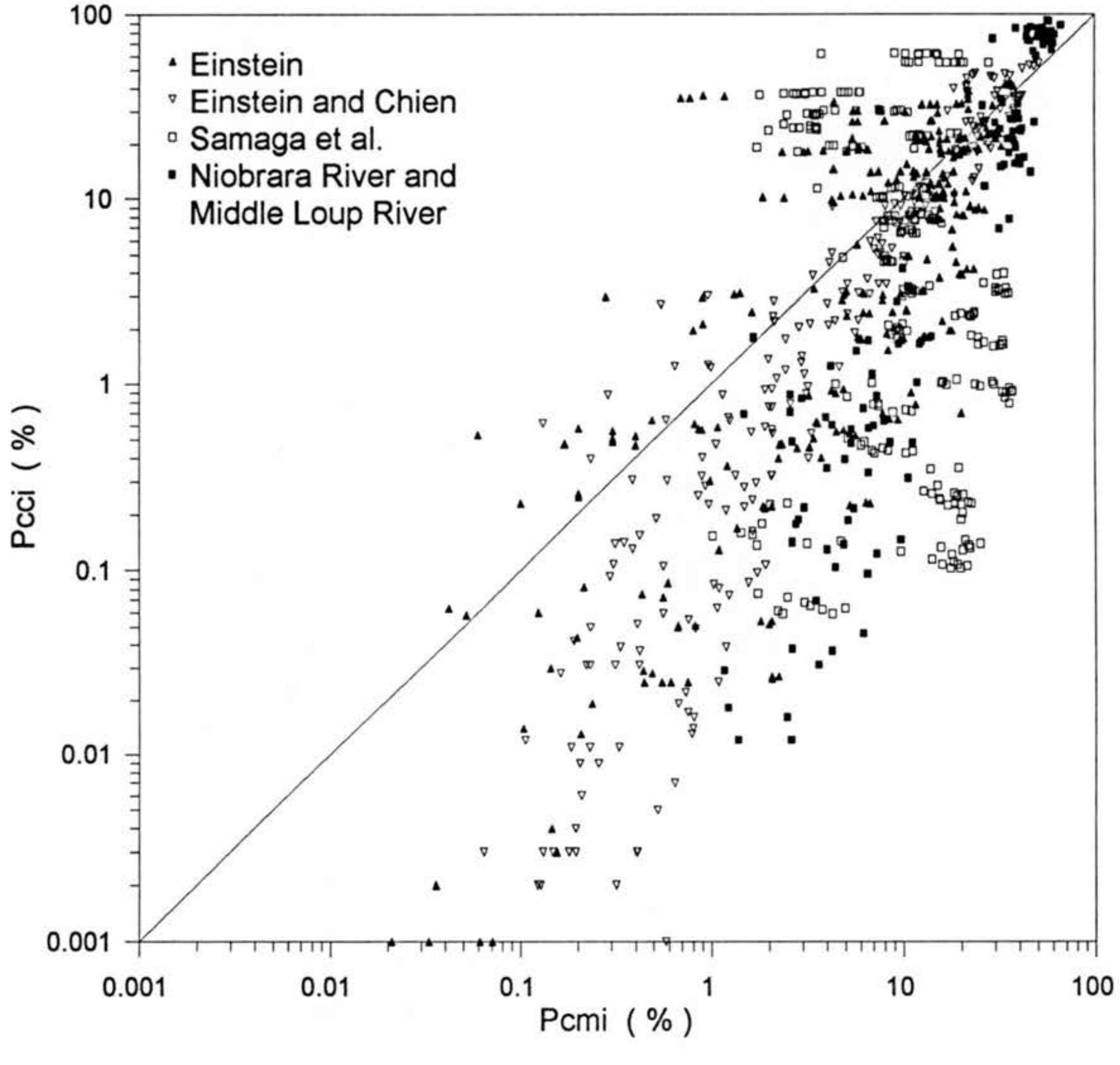

Fig. 6.29. Comparison between Computed and Measured Size Fractions of Bed-Material Load Sediment in Transport for Karim's Modified BMF Approach (1998).

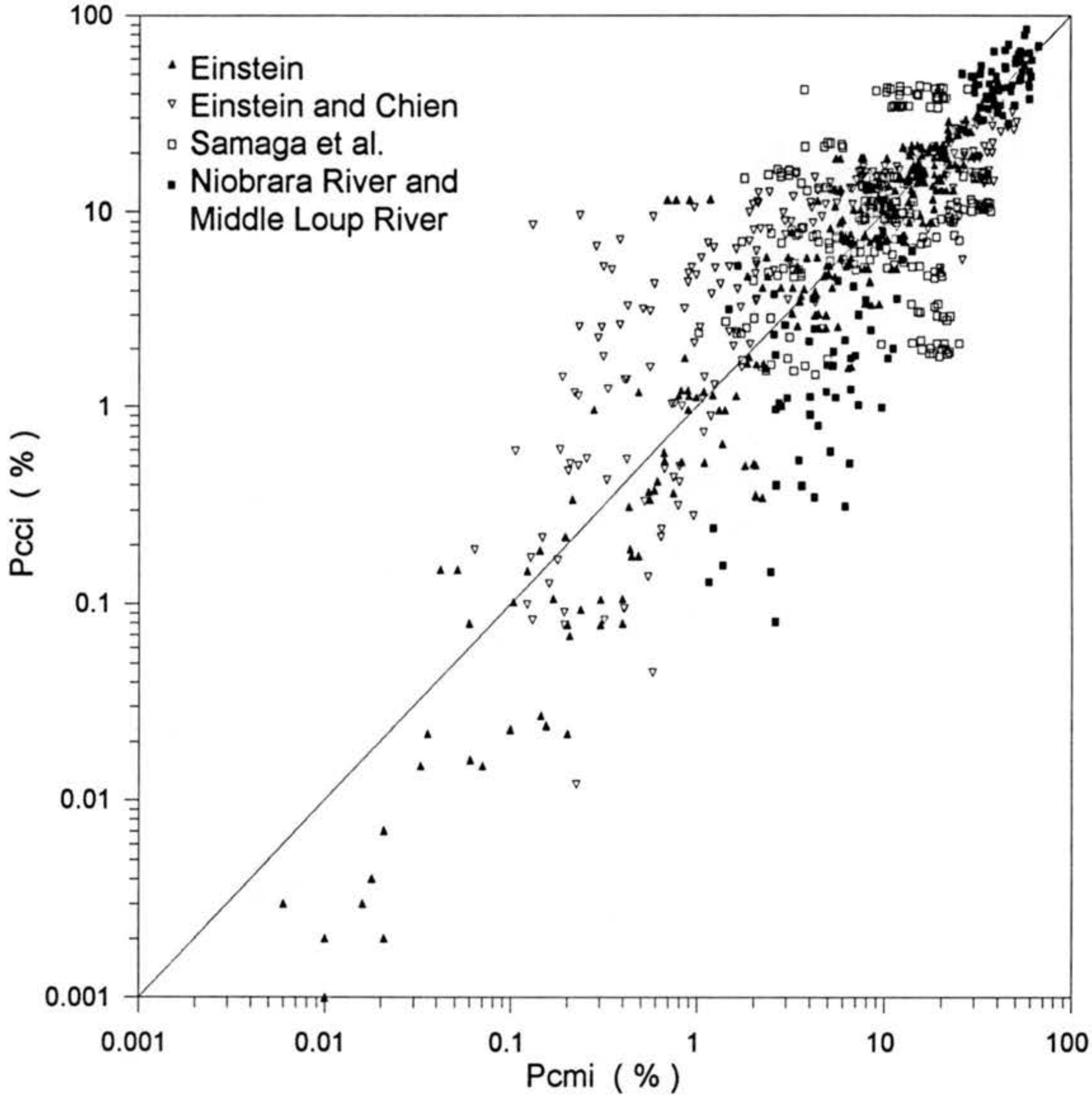

Fig. 6.30. Comparison between Computed and Measured Size Fractions of Bed-Material Load Sediment in Transport for the TCF Approach Using the Transport Capacity Distribution Function of Karim and Kennedy (1981).

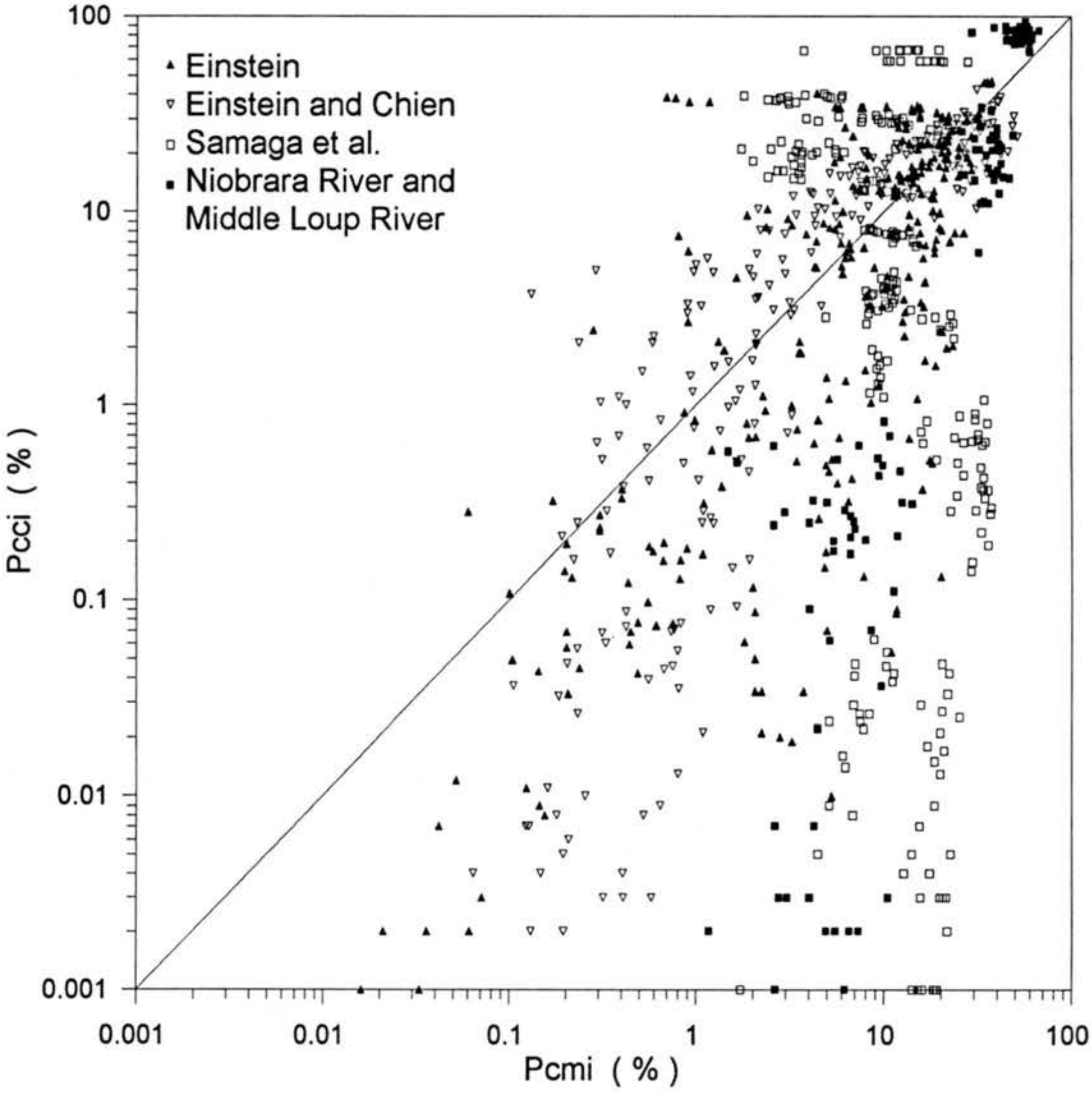

Fig. 6.31. Comparison between Computed and Measured Size Fractions of Bed-Material Load Sediment in Transport for the TCF Approach Using the Transport Capacity Distribution Function of Li (1988).

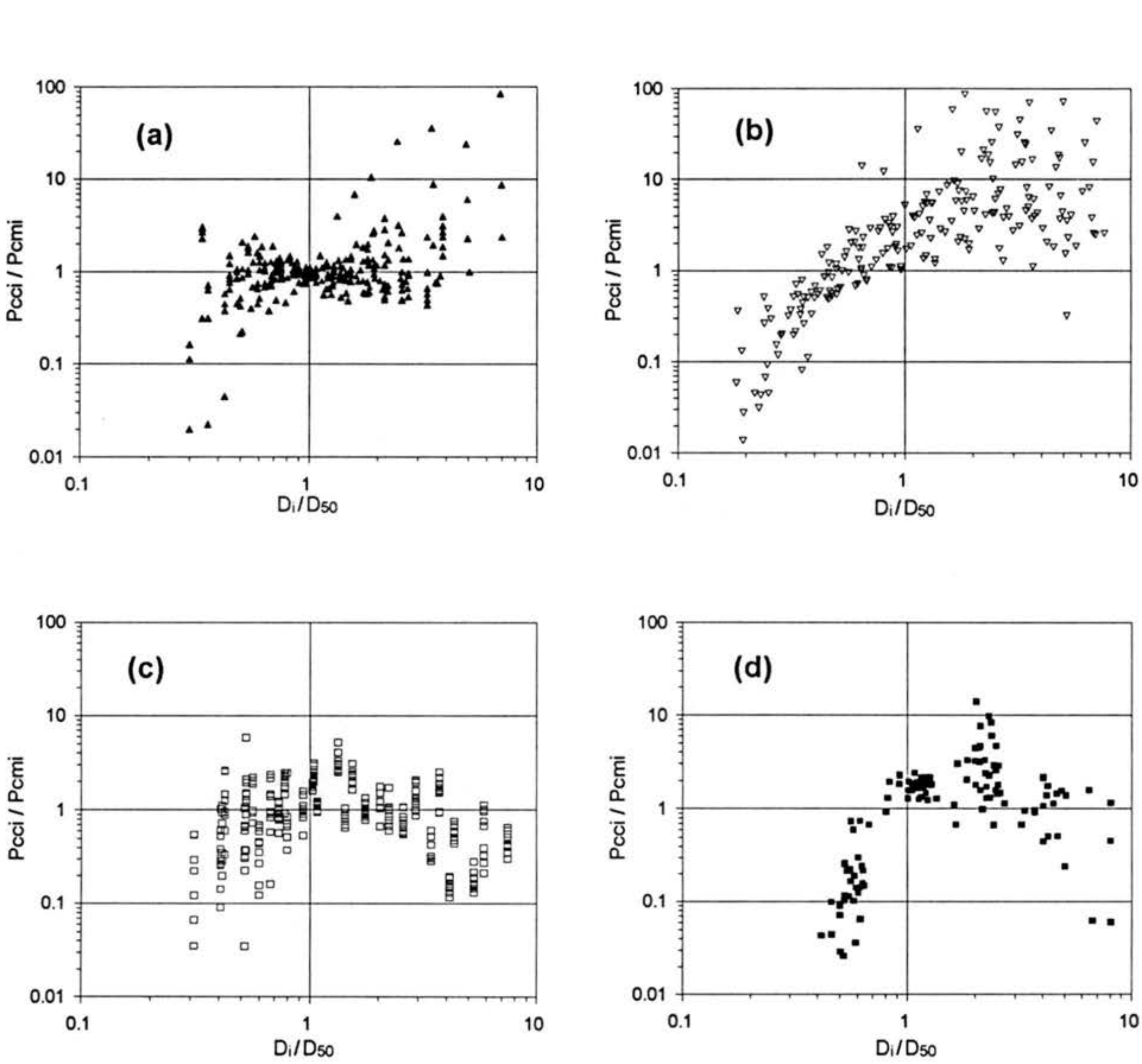

Fig. 6.32. Variation of P_{cci} / P_{cmi} versus D_i / D_{50} for the Einstein Equation (1950): (a) Einstein Data; (b) Einstein and Chien Data; (c) Samaga et al. Data; (d) Niobrara River and Middle Loup River Data.

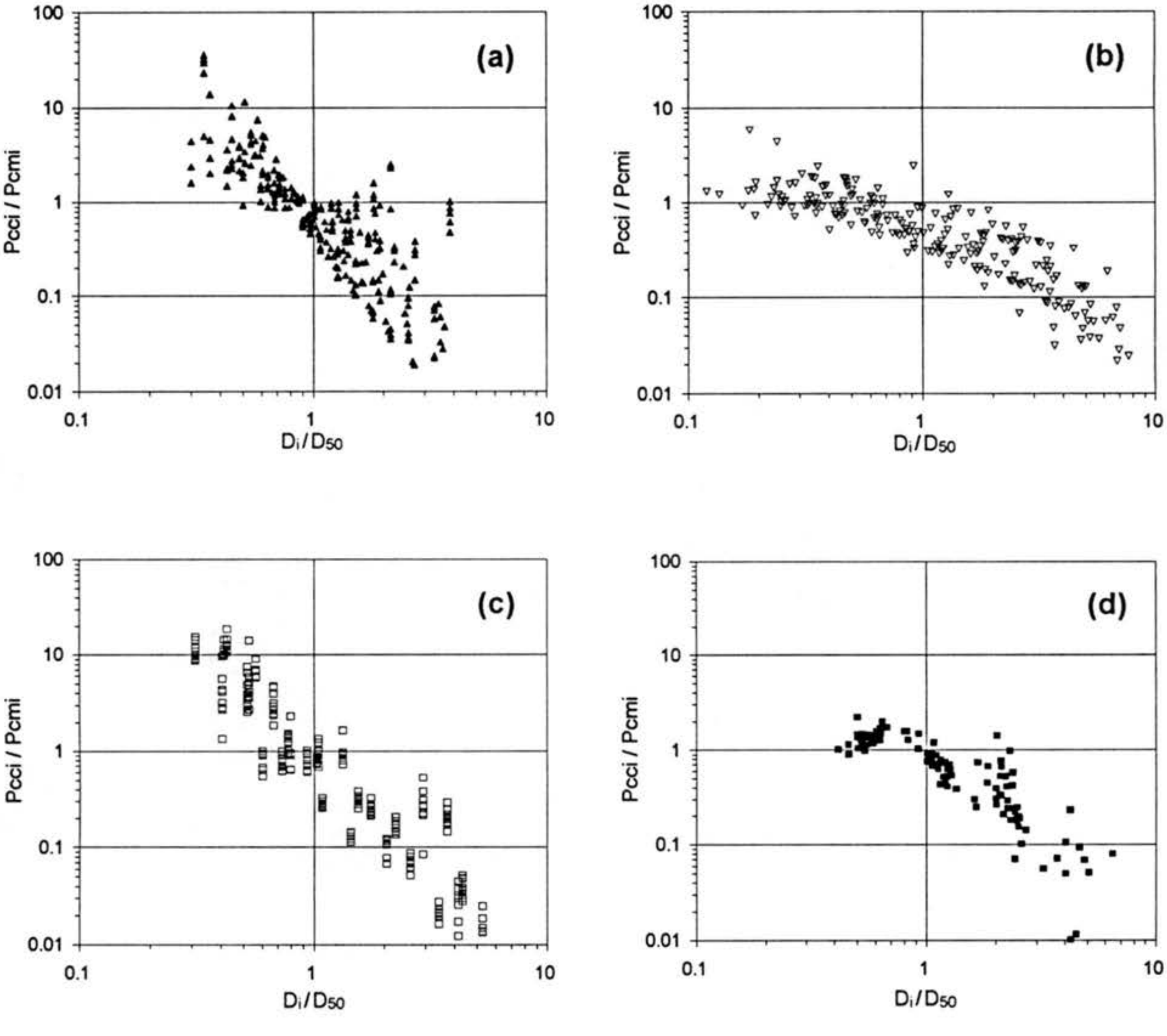

Fig. 6.33. Variation of P_{cci} / P_{cmi} versus D_i / D_{50} for the Laursen Equation (1958): (a) Einstein Data; (b) Einstein and Chien Data; (c) Samaga et al. Data; (d) Niobrara River and Middle Loup River Data.

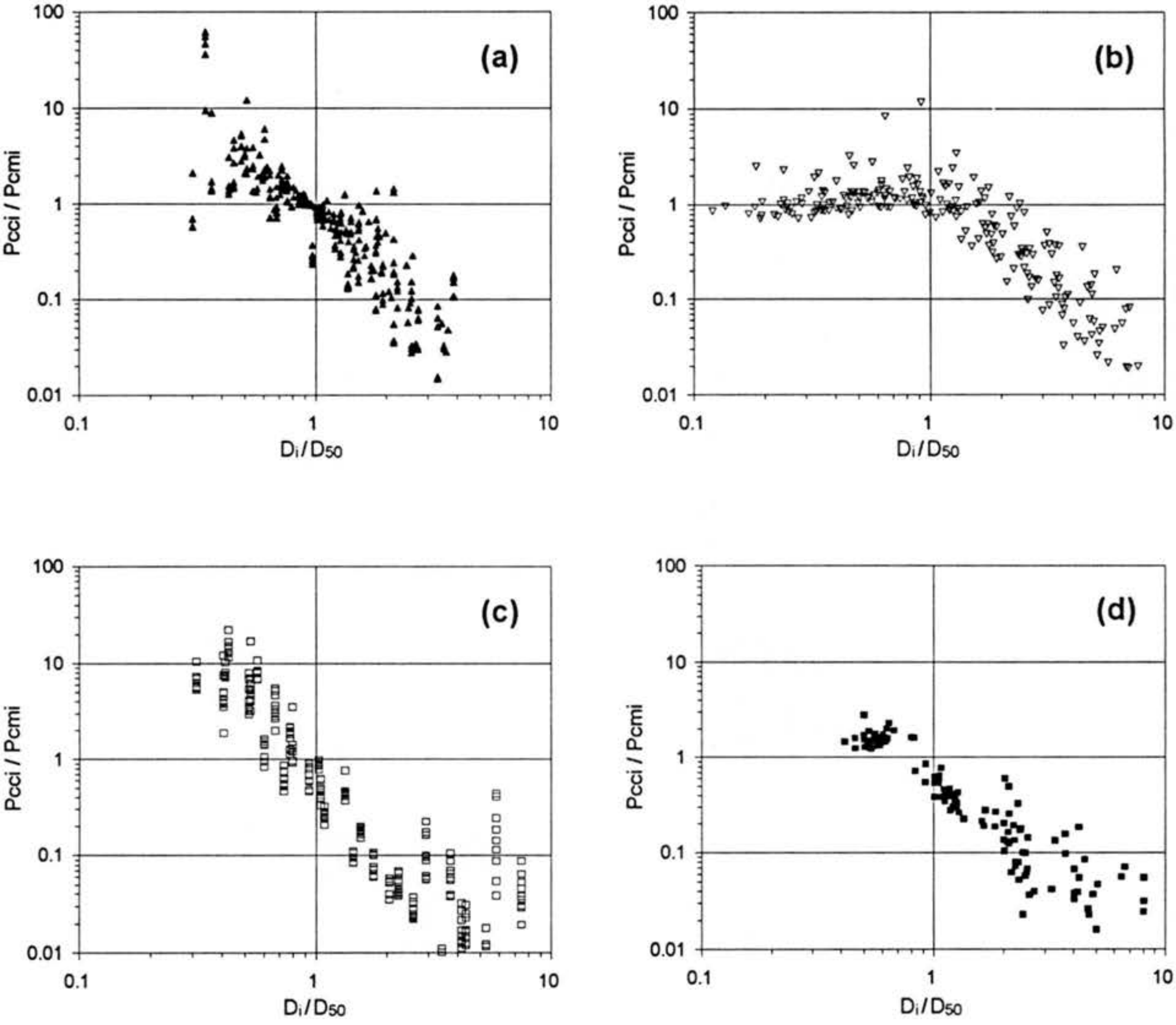

Fig. 6.34. Variation of P_{cci} / P_{cmi} versus D_i / D_{50} for the Toffaleti Equation (1968): (a) Einstein Data; (b) Einstein and Chien Data; (c) Samaga et al. Data; (d) Niobrara River and Middle Loup River Data.

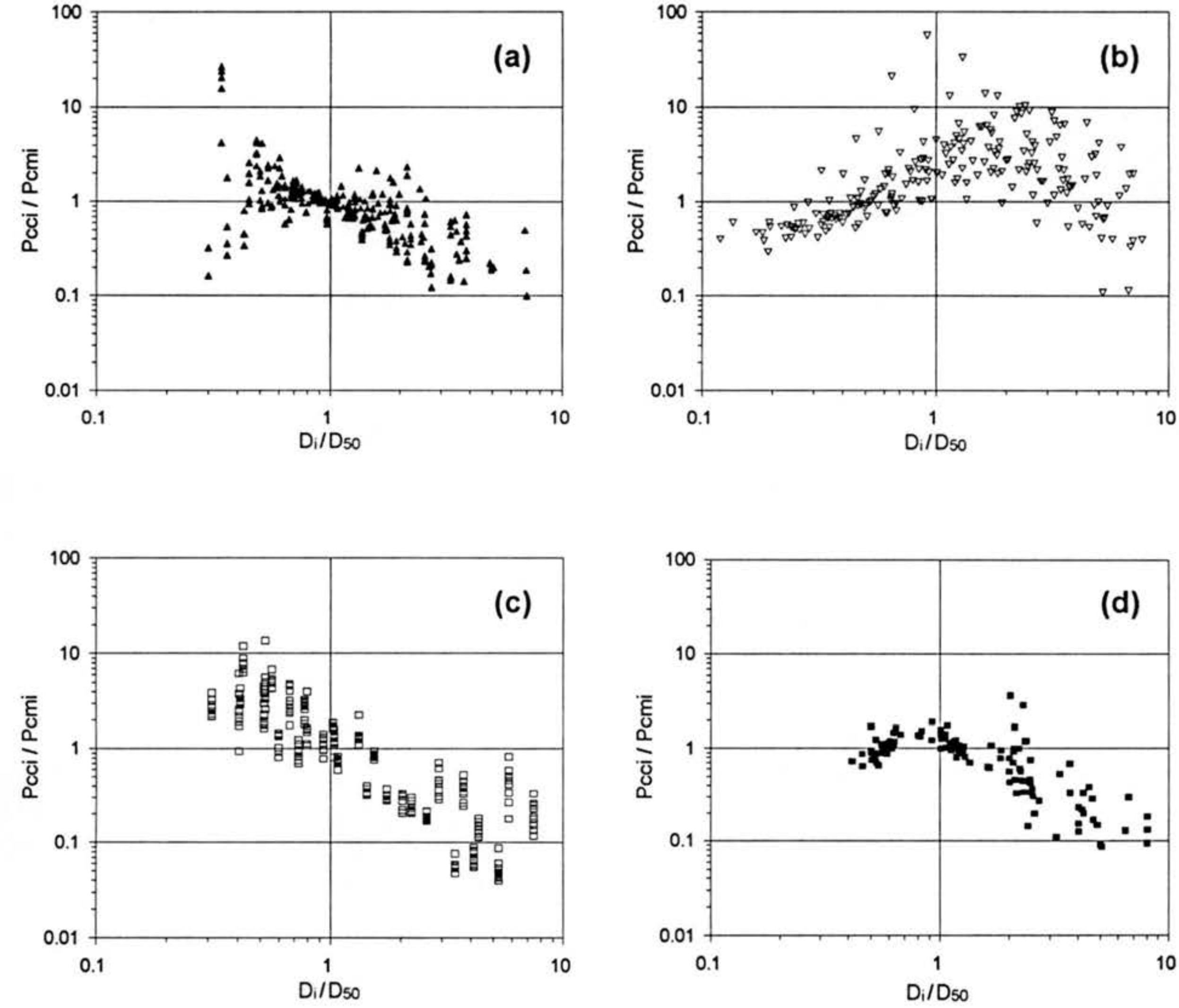

Fig. 6.35. Variation of P_{cci} / P_{cmi} versus D_i / D_{50} for the BMF Approach Using the Engelund and Hansen Transport Equation (1967): (a) Einstein Data; (b) Einstein and Chien Data; (c) Samaga et al. Data; (d) Niobrara River and Middle Loup River Data.

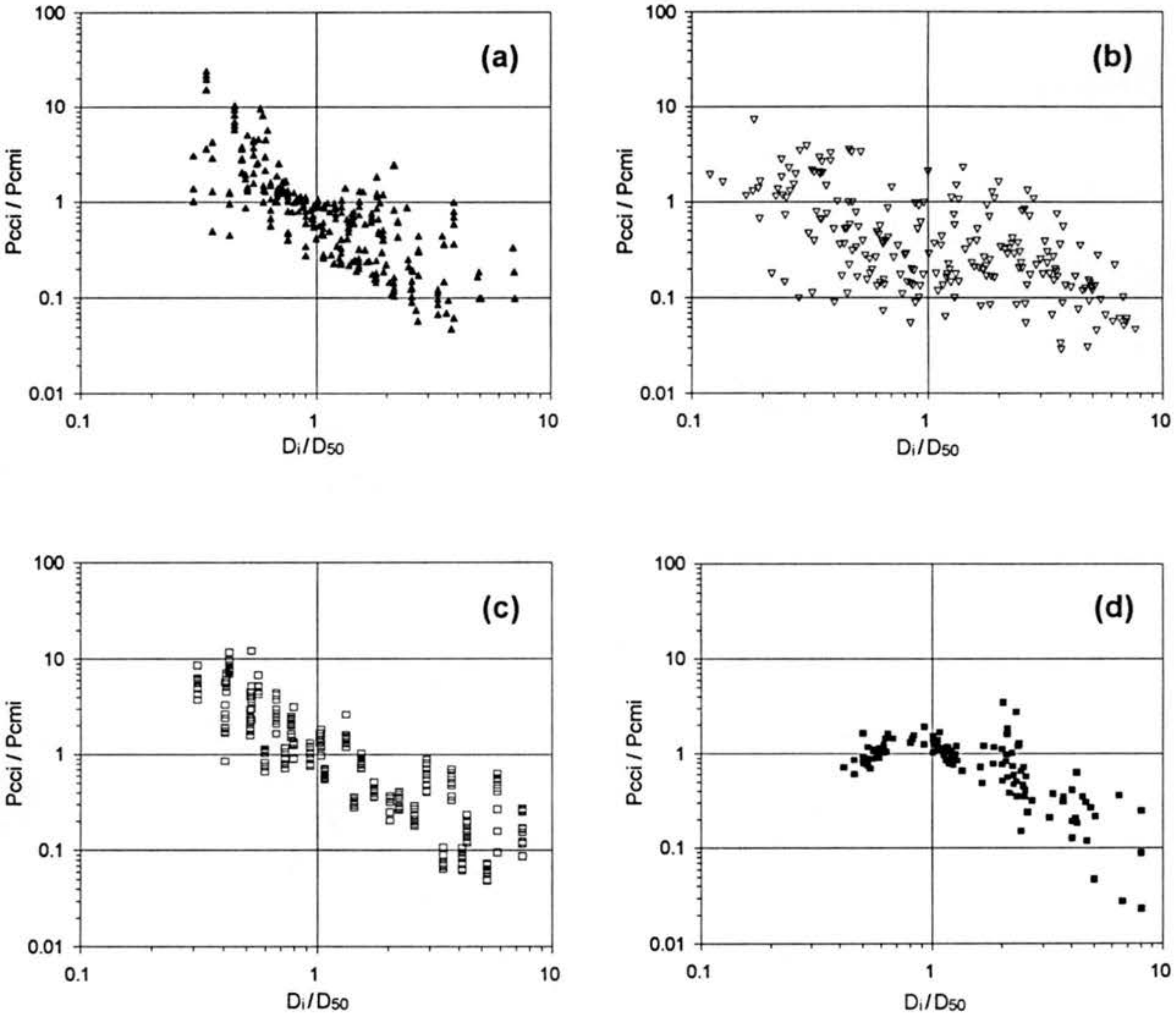

Fig. 6.36. Variation of P_{cci} / P_{cmi} versus D_i / D_{50} for the BMF Approach Using the Ackers and White Transport Equation (1973): (a) Einstein Data; (b) Einstein and Chien Data; (c) Samaga et al. Data; (d) Niobrara River and Middle Loup River Data.

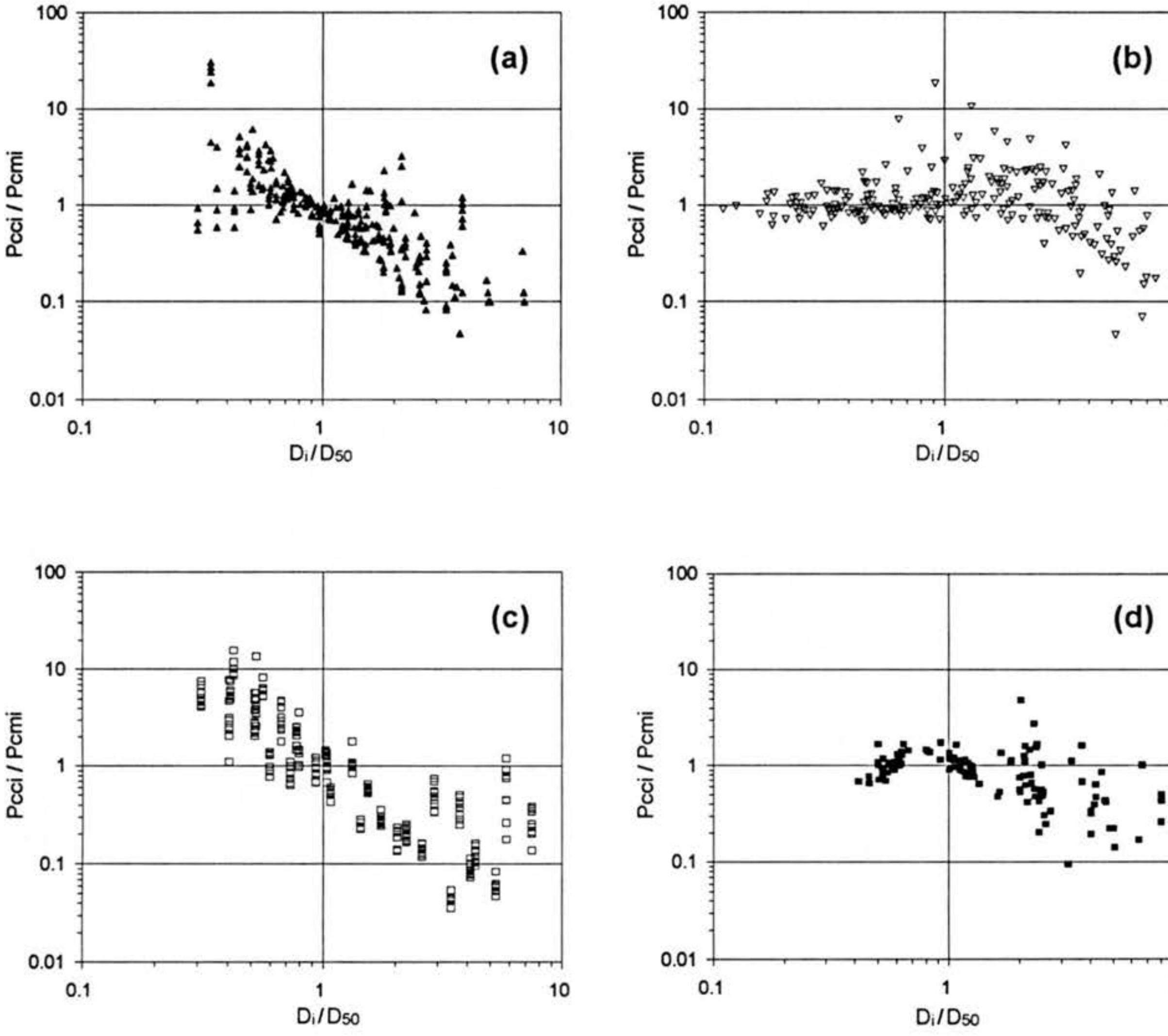

Fig. 6.37. Variation of P_{cci} / P_{cmi} versus D_i / D_{50} for the BMF Approach Using the Yang Transport Equation (1973): (a) Einstein Data; (b) Einstein and Chien Data; (c) Samaga et al. Data; (d) Niobrara River and Middle Loup River Data

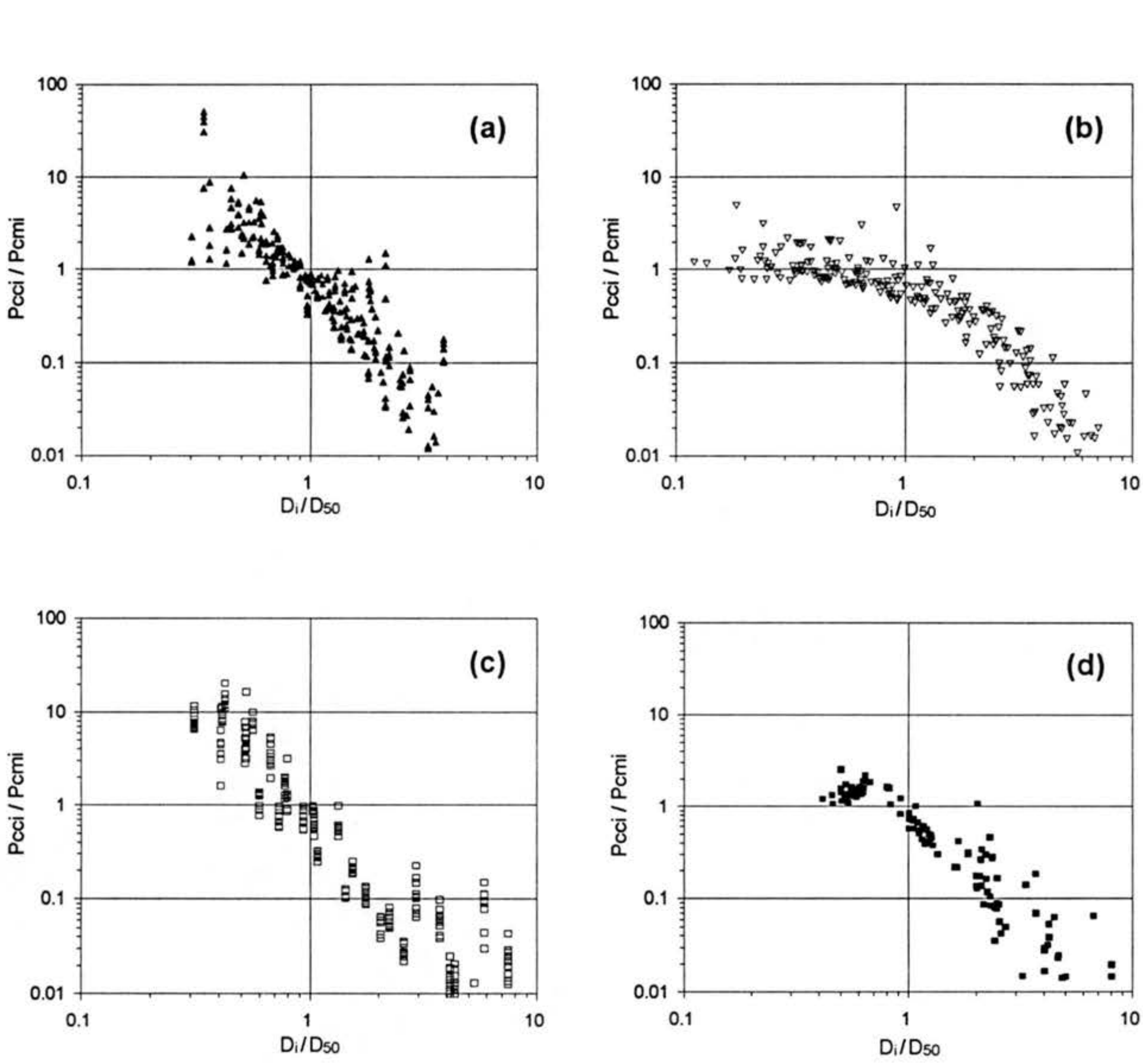

Fig. 6.38. Variation of P_{cci} / P_{cmi} versus D_i / D_{50} for Karim's Modified BMF Approach (1998): (a) Einstein Data; (b) Einstein and Chien Data; (c) Samaga et al. Data; (d) Niobrara River and Middle Loup River Data.

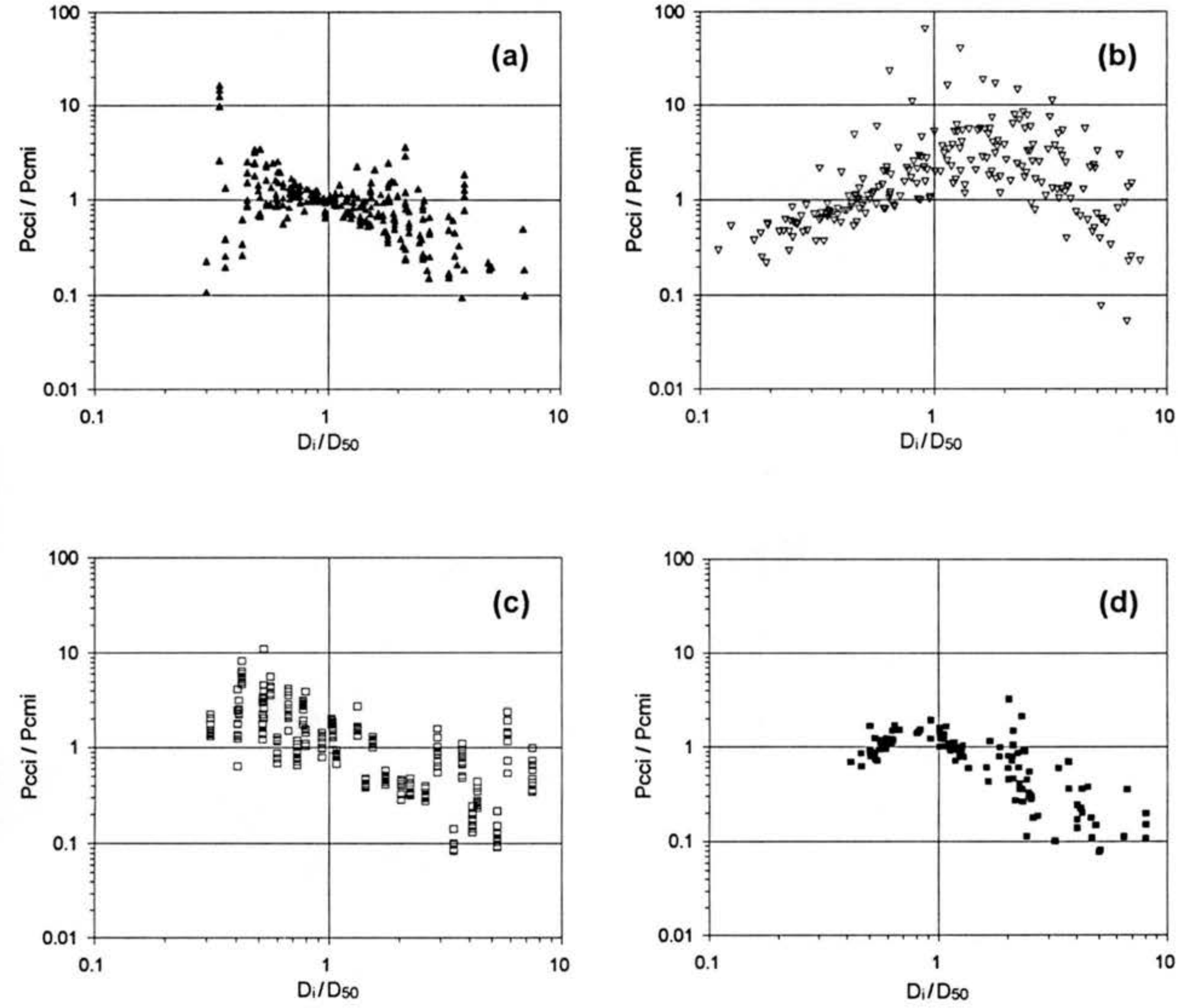

Fig. 6.39. Variation of P_{cci} / P_{cmi} versus D_i / D_{50} for the TCF Approach Using the Transport Capacity Distribution Function of Karim and Kennedy (1981): (a) Einstein Data; (b) Einstein and Chien Data; (c) Samaga et al. Data; (d) Niobrara River and Middle Loup River Data.

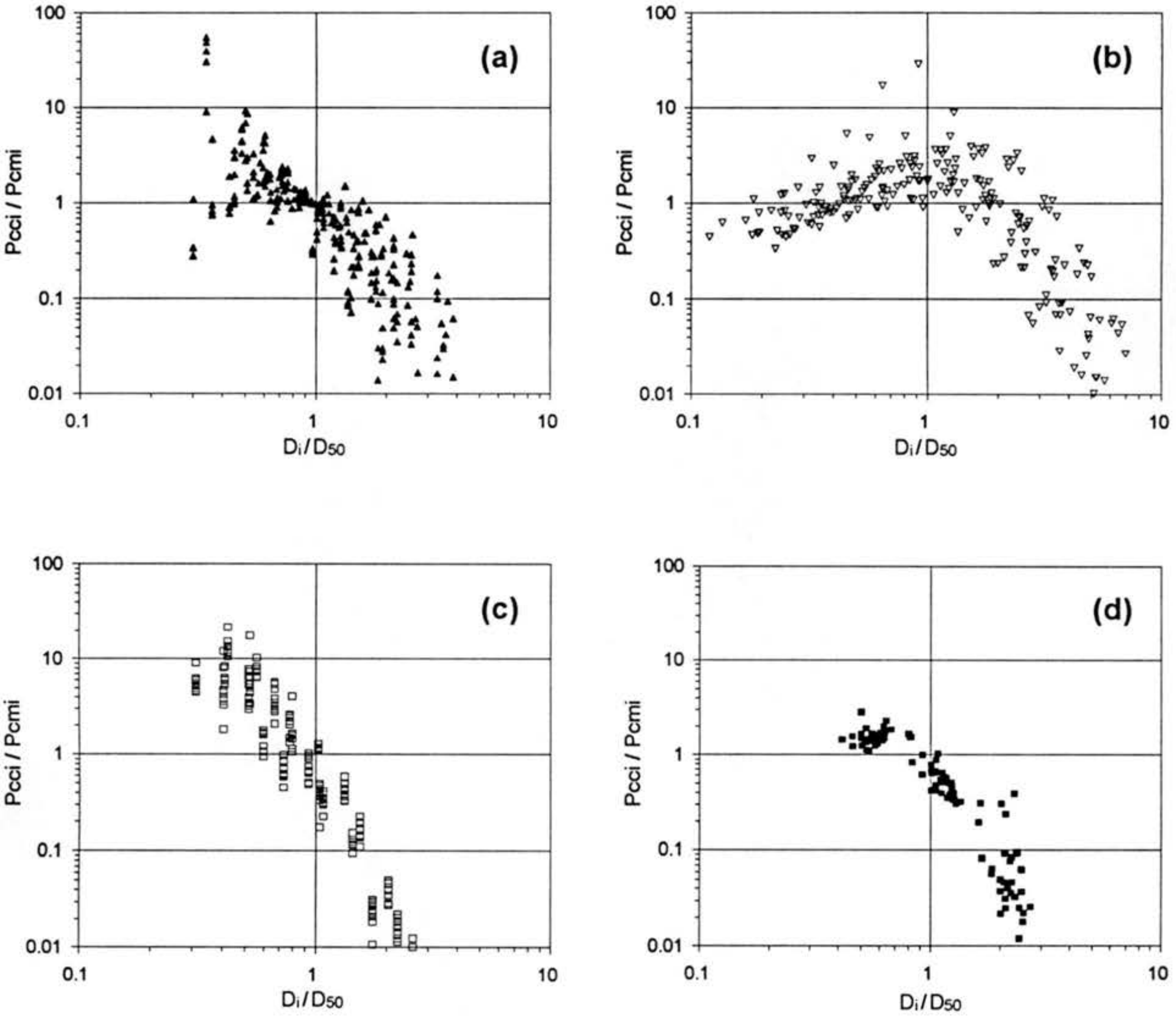

Fig. 6.40. Variation of P_{cci} / P_{cmi} versus D_i / D_{50} for the TCF Approach Using the Transport Capacity Distribution Function of Li (1988): (a) Einstein Data; (b) Einstein and Chien Data; (c) Samaga et al. Data; (d) Niobrara River and Middle Loup River Data.

6.4 VERIFICATION OF THE PROPOSED SEDIMENT TRANSPORT CAPACITY DISTRIBUTION FUNCTIONS

To verify the validity of sediment transport capacity distribution functions developed in Chapter 3, an independent data base with 48 sets of sediment transport data from flume and rivers are compiled. These data are given in Tables 6.3-6.5. The 20 sets of flume data given in Table 6.3 are derived from the laboratory experiments of White and Day (1982). It needs to be pointed out that the bed material size distribution information reported in White and Day's flume experiments are those of parent-bed material, which are generally different from the bed-surface materials. The 28 sets of river data given in Tables 6.4-6.5 include those measurements from the Rio Grande Conveyance Canal (Culbertson et al., 1972) and the Yellow River at Tuchengzi (Long and Liang, 1994). These field data contain complete flow and sediment information for each record, including the compositions for both bed material and sediment in transport.

Table 6.6 presents the statistical results for computed size fractions of bed-material load sediment in transport for the flume data of White and Day. The statistical results of mean normalized error, average geometric deviation, and discrepancy ratio indicate that the newly proposed transport distribution functions of Eq. (3.9) and (3.24) along with the function of Karim and Kennedy (1981) give the best prediction amongst all methods. It should be pointed out that the use of the size distribution from parent-bed material (instead of surface-bed material) may be favorable to the performance of Karim and Kennedy's function.

Table 6.7 gives the statistical results for computed size fractions of bed-material load sediment in transport for data of the Rio Grande Conveyance Canal and the Yellow River at

Tuchengzi. It can be seen that the mean normalized error was 51.0% and 78.7% for the newly proposed transport capacity distribution functions of Eqs. (3.9) and (3.24), respectively, while it was 65.7-183.6% for other methods. The average geometric deviation was 1.58 and 1.93 for Eqs. (3.9) and (3.24), respectively, while it was 2.75-39.6 for other methods. The percentage of data falling within the range of discrepancy ratios between 0.25 and 1.75 was 81.7% and 76.5% for Eq. (3.9) and (3.24), respectively, while it was 30.4-67.0% for other methods.

Table 6.3. Laboratory Data of White and Day (1982)

		Flow Properties					Bed Material				Transported Sediment			
Data No. (1)	Run ID (2)	Q (m^3/s) (3)	W (m) (4)	d (m) (5)	S (m/m) (6)	T (°C) (7)	D_{50}^* (mm) (8)	D_{65}^* (mm) (9)	σ_g^* (10)	s_g (11)	C_T (kg/m^3) (12)	C_T (PPM) (13)	D_{50t}^* (mm) (14)	σ_{gt}^* (15)
1	1	0.1990	2.46	0.1660	0.000680	12.0	2.065	3.470	3.887	2.65	0.0143	14.27	0.439	1.605
2	2	0.1990	2.46	0.1590	0.000770	12.0	2.065	3.470	3.887	2.65	0.0194	19.35	0.425	1.631
3	3	0.1990	2.46	0.1450	0.000790	12.0	2.065	3.470	3.887	2.65	0.0178	17.79	0.452	2.106
4	4	0.1970	2.46	0.1690	0.000660	12.0	2.065	3.470	3.887	2.65	0.0089	8.88	0.494	1.915
5	5	0.1960	2.46	0.1470	0.000890	12.0	2.065	3.470	3.887	2.65	0.0247	24.69	0.488	2.484
6	6	0.1970	2.46	0.1330	0.001090	12.0	2.065	3.470	3.887	2.65	0.0300	30.00	0.509	2.833
7	7	0.1970	2.46	0.1230	0.001700	12.0	2.065	3.470	3.887	2.65	0.0976	97.56	0.801	3.301
8	8	0.1970	2.46	0.1310	0.001530	12.0	2.065	3.470	3.887	2.65	0.0833	83.27	0.942	3.125
9	9	0.1960	2.46	0.1210	0.002490	12.0	2.065	3.470	3.887	2.65	0.1565	156.53	1.282	3.429
10	10	0.1980	2.46	0.1120	0.002890	12.0	2.065	3.470	3.887	2.65	0.4362	436.06	1.836	3.334
11	11	0.1930	2.46	0.1070	0.003660	12.0	2.065	3.470	3.887	2.65	0.8353	834.85	2.060	3.586
12	1	0.2030	2.46	0.1890	0.000445	12.0	1.745	2.273	2.983	2.65	0.0016	1.62	1.168	2.391
13	2	0.2100	2.46	0.1840	0.000446	12.0	1.745	2.273	2.983	2.65	0.0030	2.98	0.728	2.553
14	3	0.2020	2.46	0.1620	0.000722	12.5	1.745	2.273	2.983	2.65	0.0196	19.63	0.813	2.473
15	4	0.2020	2.46	0.1540	0.001616	12.0	1.745	2.273	2.983	2.65	0.0308	30.75	0.905	2.595
16	5	0.2000	2.46	0.1450	0.001769	12.0	1.745	2.273	2.983	2.65	0.0754	75.40	1.097	2.832
17	6	0.2020	2.46	0.1190	0.002262	12.0	1.745	2.273	2.983	2.65	0.7500	749.65	1.454	2.760
18	7	0.2040	2.46	0.1240	0.002188	12.0	1.745	2.273	2.983	2.65	0.6739	673.63	1.640	2.551
19	8	0.2000	2.46	0.1170	0.002614	13.0	1.745	2.273	2.983	2.65	0.8363	835.86	1.680	2.589
20	9	0.2010	2.46	0.1150	0.002987	12.0	1.745	2.273	2.983	2.65	1.0907	1089.95	1.691	2.550

Note: * — Values computed from adjusted bed material size distribution (wash load materials excluded).

Table 6.3. Laboratory Data of White and Day (1982) (continued)

Data No. (1)	Run ID (2)	D_c (mm) (16)	Size distribution of bed material*, finer than indicated diameters Grp1 (%) (17)	Grp2 (%) (18)	Grp3 (%) (19)	Grp4 (%) (20)	Grp5 (%) (21)	Grp6 (%) (22)	Grp7 (%) (23)	Grp8 (%) (24)	Grp9 (%) (25)	Grp10 (%) (26)	Grp11 (%) (27)	Grp12 (%) (28)	Grp13 (%) (29)	Grp14 (%) (30)	Grp15 (%) (31)
			0.18	**0.25**	**0.355**	**0.5**	**0.71**	**1**	**1.4**	**1.7**	**2.36**	**3.35**	**4.76**	**6.35**	**7.85**	**9.52**	**15.6 mm**
1	1	0.25	1.3	5.46	16.46	27.89	34.89	39.66	44.64	47.74	54.7	64.8	74.68	85.43	92.3	95.65	98.28
2	2	0.25	1.3	5.46	16.46	27.89	34.89	39.66	44.64	47.74	54.7	64.8	74.68	85.43	92.3	95.65	98.28
3	3	0.25	1.3	5.46	16.46	27.89	34.89	39.66	44.64	47.74	54.7	64.8	74.68	85.43	92.3	95.65	98.28
4	4	0.25	1.3	5.46	16.46	27.89	34.89	39.66	44.64	47.74	54.7	64.8	74.68	85.43	92.3	95.65	98.28
5	5	0.25	1.3	5.46	16.46	27.89	34.89	39.66	44.64	47.74	54.7	64.8	74.68	85.43	92.3	95.65	98.28
6	6	0.25	1.3	5.46	16.46	27.89	34.89	39.66	44.64	47.74	54.7	64.8	74.68	85.43	92.3	95.65	98.28
7	7	0.25	1.3	5.46	16.46	27.89	34.89	39.66	44.64	47.74	54.7	64.8	74.68	85.43	92.3	95.65	98.28
8	8	0.25	1.3	5.46	16.46	27.89	34.89	39.66	44.64	47.74	54.7	64.8	74.68	85.43	92.3	95.65	98.28
9	9	0.25	1.3	5.46	16.46	27.89	34.89	39.66	44.64	47.74	54.7	64.8	74.68	85.43	92.3	95.65	98.28
10	10	0.25	1.3	5.46	16.46	27.89	34.89	39.66	44.64	47.74	54.7	64.8	74.68	85.43	92.3	95.65	98.28
11	11	0.25	1.3	5.46	16.46	27.89	34.89	39.66	44.64	47.74	54.7	64.8	74.68	85.43	92.3	95.65	98.28
12	1	0.25	2.13	6.83	18.6	27.9	33	39.14	46.11	51.01	67.94	81.41	96.41	97.88			
13	2	0.25	2.13	6.83	18.6	27.9	33	39.14	46.11	51.01	67.94	81.41	96.41	97.88			
14	3	0.25	2.13	6.83	18.6	27.9	33	39.14	46.11	51.01	67.94	81.41	96.41	97.88			
15	4	0.25	2.13	6.83	18.6	27.9	33	39.14	46.11	51.01	67.94	81.41	96.41	97.88			
16	5	0.25	2.13	6.83	18.6	27.9	33	39.14	46.11	51.01	67.94	81.41	96.41	97.88			
17	6	0.25	2.13	6.83	18.6	27.9	33	39.14	46.11	51.01	67.94	81.41	96.41	97.88			
18	7	0.25	2.13	6.83	18.6	27.9	33	39.14	46.11	51.01	67.94	81.41	96.41	97.88			
19	8	0.25	2.13	6.83	18.6	27.9	33	39.14	46.11	51.01	67.94	81.41	96.41	97.88			
20	9	0.25	2.13	6.83	18.6	27.9	33	39.14	46.11	51.01	67.94	81.41	96.41	97.88			

Note: * - Parent-bed material.

Table 6.3. Laboratory Data of White and Day (1982) (continued)

Data No. (1)	Run ID (2)	Size distribution of transported sediment, finer than indicated diameters Grp1 (%) (32)	Grp2 (%) (33)	Grp3 (%) (34)	Grp4 (%) (35)	Grp5 (%) (36)	Grp6 (%) (37)	Grp7 (%) (38)	Grp8 (%) (39)	Grp9 (%) (40)	Grp10 (%) (41)	Grp11 (%) (42)	Grp12 (%) (43)	Grp13 (%) (44)	Grp14 (%) (45)	Grp15 (%) (46)
		0.18	**0.25**	**0.355**	**0.5**	**0.71**	**1.0**	**1.4**	**1.7**	**2.36**	**3.35**	**4.76**	**6.35**	**7.85**	**9.52**	**15.6 mm**
1	1	0.67	6.28	32.72	65.84	82.56	90.81	94.60	96.08	97.90	99.13	99.92	100.00	100.00	100.00	100.00
2	2	1.00	8.58	37.73	69.09	83.21	89.91	93.25	94.58	96.57	98.26	99.73	100.00	100.00	100.00	100.00
3	3	1.33	9.97	37.33	62.37	75.12	82.01	86.21	88.26	92.42	96.90	100.01	100.01	100.01	100.01	100.01
4	4	0.61	5.33	27.19	53.67	70.53	81.71	88.66	91.65	95.80	98.43	100.10	100.10	100.10	100.10	100.10
5	5	0.99	8.34	32.83	56.02	68.33	76.03	81.29	83.94	89.06	94.96	100.45	100.45	100.45	100.45	100.45
6	6	0.93	8.11	32.06	53.50	64.57	71.53	76.51	79.06	84.25	91.29	96.63	99.36	99.91	100.03	100.03
7	7	1.02	7.28	25.53	41.65	51.21	58.49	64.35	67.53	73.96	83.36	92.27	97.98	99.83	100.18	100.24
8	8	0.72	5.55	20.12	35.72	46.05	54.06	60.73	64.49	72.75	83.45	93.09	97.99	99.53	99.75	99.78
9	9	0.65	4.83	17.48	31.16	40.21	47.59	54.21	58.00	66.53	76.64	86.79	94.97	98.78	99.82	100.12
10	10	0.47	3.76	13.66	23.96	31.37	38.08	45.17	49.60	59.41	72.11	84.80	94.34	98.70	99.79	100.03
11	11	0.56	3.90	14.32	24.81	31.06	37.06	43.09	46.96	55.50	67.22	79.90	91.28	97.69	99.59	100.01
12	1	1.01	4.13	13.57	25.76	35.57	46.53	58.55	66.29	84.20	95.06	99.09	100.00			
13	2	1.37	7.57	25.80	42.88	53.10	62.38	70.93	76.40	88.35	95.85	99.52	100.00			
14	3	0.60	4.07	18.44	35.22	47.85	58.78	67.81	73.53	87.54	97.17	100.27	100.27			
15	4	1.77	7.86	23.56	37.88	47.30	56.65	65.83	71.73	85.62	96.23	100.00	100.00			
16	5	1.77	7.71	23.07	35.85	43.81	51.61	60.05	65.27	79.42	91.37	99.64	100.17			
17	6	1.61	6.35	17.63	27.87	35.01	43.31	52.17	58.16	73.76	89.17	99.45	100.31			
18	7	0.70	3.28	10.83	19.73	27.18	36.22	46.09	52.89	70.21	87.89	99.09	99.97			
19	8	1.16	3.77	11.55	20.38	27.67	36.32	46.02	52.48	69.04	87.22	99.28	100.40			
20	9	0.50	2.43	9.51	18.40	25.90	34.83	44.70	51.40	68.27	86.69	98.99	100.00			

Table 6.4. Rio Grande Conveyance Channel Data of Culbertson, Scott, and Bennett (1972)

Data No. (1)	Survey Date (yymmdd) (2)	Flow Properties: Q (m^3/s) (3)	W (m) (4)	d (m) (5)	S (m/m) (6)	T (°C) (7)	Bed Material: D_{50} (mm) (8)	D_{65} (mm) (9)	σ_g (10)	s_g (11)	Transported Sediment: C_T (kg/m^3) (12)	C_T (PPM) (13)	D_{50t} (mm) (14)	σ_{gt} (15)
1	650512	25.753	21.336	1.298	0.000650	15.0	0.270	-1	1.62	2.65	3.4200	3412.73	0.12	1.71
2	650512	25.753	22.860	1.374	0.000650	15.0	0.280	-1	1.75	2.65	3.4200	3412.73	0.12	1.71
3	650513	25.187	22.860	1.496	0.000650	15.0	0.210	-1	1.42	2.65	3.0200	3014.33	0.11	1.63
4	650513	25.187	20.117	1.247	0.000650	15.0	0.230	-1	1.42	2.65	3.0200	3014.33	0.11	1.63
5	650602	33.677	22.555	0.894	0.000730	17.0	0.200	-1	1.3	2.65	2.8100	2805.09	0.13	1.67
6	650603	36.507	27.432	0.887	0.000520	17.0	0.180	-1	1.34	2.65	2.9000	2894.77	0.11	1.46
7	651129	35.375	22.555	1.096	0.000660	4.0	0.180	-1	1.4	2.65	4.2200	4208.94	0.13	1.61
8	651130	35.375	22.555	1.108	0.000590	3.0	0.180	-1	1.42	2.65	4.5600	4547.09	0.16	1.63
9	660504	36.224	21.336	1.023	0.001110	18.0	0.210	-1	1.46	2.65	3.3500	3343.03	0.16	1.64

Table 6.4. Rio Grande Conveyance Channel Data of Culbertson, Scott, and Bennett (1972) (continued)

Data No. (1)	Survey Date (yymmdd) (2)	D_c (mm) (16)	Size distribution of bed material, finer than indicated diameters: Grp1 (%) (17)	Grp2 (%) (18)	Grp3 (%) (19)	Grp4 (%) (20)	Grp5 (%) (21)	Grp6 (%) (22)	Size distribution of sediment load, finer than indicated diameters: Grp1 (%) (23)	Grp2 (%) (24)	Grp3 (%) (25)	Grp4 (%) (26)	Grp5 (%) (27)	Grp6 (%) (28)
			0.062	**0.125**	**0.25**	**0.5**	**1**	**2mm**	**0.062**	**0.125**	**0.25**	**0.5**	**1**	**2mm**
1	650512	0.062	0.0	4.0	43.0	87.0	98.0	100.0	70.0	86.0	97.0	100.0	100.0	100.0
2	650512	0.062	0.0	3.0	42.0	82.0	99.0	100.0	70.0	86.0	97.0	100.0	100.0	100.0
3	650513	0.062	0.0	10.0	71.0	98.0	100.0	100.0	70.0	87.0	97.0	100.0	100.0	100.0
4	650513	0.062	0.0	9.0	61.0	97.0	100.0	100.0	70.0	87.0	97.0	100.0	100.0	100.0
5	650602	0.062	0.0	4.0	75.0	98.0	100.0	100.0	52.0	75.0	94.0	99.0	100.0	100.0
6	650603	0.062	0.0	11.0	85.0	99.0	100.0	100.0	66.0	87.0	99.0	100.0	100.0	100.0
7	651129	0.062	0.0	12.0	82.0	99.0	100.0	100.0	41.0	68.0	93.0	100.0	100.0	100.0
8	651130	0.062	0.0	12.0	84.0	99.0	100.0	100.0	33.0	53.0	87.0	100.0	100.0	100.0
9	660504	0.062	1.0	8.0	66.0	98.0	100.0	100.0	26.0	48.0	86.0	99.0	100.0	100.0

Table 6.5. Yellow River Data at Tuchengzi of Long and Liang (1994)

		Flow Properties					Bed Material				Transported Sediment			
Data No. (1)	Run ID (2)	Q (m^3/s) (3)	W (m) (4)	D (m) (5)	S (m/m) (6)	T (°C) (7)	D_{50}^* (mm) (8)	D_{65}^* (mm) (9)	σ_g^* (10)	s_g (11)	C_T (kg/m^3) (12)	C_T (PPM) (13)	D_{50t}^* (mm) (14)	σ_{gt}^* (15)
1	570828	1173.33	572.67	1.447	0.0000940	28.4	0.056	0.071	1.812	2.65	14.94	14800.97	0.042	2.301
2	570918	1316.67	578.00	1.420	0.0000840	21.2	0.058	0.071	1.787	2.65	22.49	22183.81	0.050	2.073
3	570926	1273.33	539.67	1.437	0.0000900	18.6	0.064	0.078	1.709	2.65	26.57	26141.63	0.046	2.057
4	571008	1486.67	581.33	1.427	0.0000780	15.4	0.060	0.072	1.685	2.65	25.22	24831.72	0.037	2.121
5	571018	1233.33	566.00	1.417	0.0001000	15.2	0.065	0.077	1.620	2.65	23.26	22930.04	0.054	1.966
6	571027	848.00	607.53	1.443	0.0000920	14.1	0.070	0.083	1.707	2.65	20.40	20142.26	0.064	1.831
7	571104	1180.00	545.23	1.447	0.0001000	12.2	0.064	0.076	1.669	2.65	25.96	25545.09	0.058	1.811
8	580319	480.00	298.00	1.750	0.0000960	7.6	0.055	0.068	1.813	2.65	12.05	11956.98	0.052	1.949
9	580328	432.00	292.00	1.740	0.0000920	6.6	0.055	0.068	1.688	2.65	10.16	10099.79	0.062	1.842
10	580410	964.00	282.00	1.910	0.0000970	12.4	0.061	0.073	1.607	2.65	20.68	20417.87	0.054	1.784
11	580427	446.00	279.00	1.650	0.0000940	16.4	0.055	0.066	1.670	2.65	15.06	14921.68	0.065	1.673
12	580520	996.00	429.00	1.320	0.0001000	20.3	0.057	0.069	1.692	2.65	31.17	30574.14	0.062	1.816
13	580527	293.00	410.00	0.960	0.0001400	22.3	0.069	0.080	1.403	2.65	7.31	7274.65	0.066	1.599
14	580604	88.80	333.00	0.590	0.0001600	22.8	0.069	0.079	1.331	2.65	14.42	14290.44	0.075	1.496
15	580613	252.00	431.00	1.030	0.0001100	22.8	0.062	0.075	1.759	2.65	20.44	20182.67	0.070	1.375
16	580624	161.00	352.00	0.870	0.0001200	26.2	0.068	0.079	1.521	2.65	18.38	18174.34	0.074	1.682
17	580705	392.00	398.00	1.070	0.0000800	28.0	0.058	0.072	1.725	2.65	12.98	12877.14	0.066	1.584
18	580716	3880.00	794.00	1.740	0.0001000	26.9	0.064	0.074	1.595	2.65	101.61	95561.53	0.035	2.206
19	580814	3980.00	807.00	1.820	0.0001000	22.0	0.068	0.081	1.648	2.65	59.02	56926.68	0.038	2.179

Note: * — Values computed from adjusted bed material size distribution (wash load materials excluded).

Table 6.5. Yellow River Data at Tuchengzi of Long and Liang (1994) (continued)

Data No. (1)	Run ID (2)	D_c (mm) (16)	Size distribution of bed material, finer than indicated diameters								
			Grp1 (%) (17)	Grp2 (%) (18)	Grp3 (%) (19)	Grp4 (%) (20)	Grp5 (%) (21)	Grp6 (%) (22)	Grp7 (%) (23)	Grp8 (%) (24)	Grp9 (%) (25)
			0.005	**0.01**	**0.025**	**0.05**	**0.1**	**0.25**	**0.5**	**1**	**2mm**
1	570828	0.01	0.13	1.13	10.35	42.78	87.83	99.77	100.00	100.00	100.00
2	570918	0.01	0.00	1.07	10.58	39.63	89.57	99.87	100.00	100.00	100.00
3	570926	0.01	0.10	0.77	6.54	30.12	85.50	100.00	100.00	100.00	100.00
4	571008	0.01	0.13	0.60	6.59	35.47	92.80	99.87	100.00	100.00	100.00
5	571018	0.01	0.00	0.27	4.99	25.98	88.60	100.00	100.00	100.00	100.00
6	571027	0.01	0.00	0.17	4.03	21.57	81.23	97.03	100.00	100.00	100.00
7	571104	0.01	0.00	0.00	5.64	28.82	88.47	99.93	100.00	100.00	100.00
8	580319	0.01	0.00	2.80	14.50	45.50	91.80	99.90	100.00	100.00	100.00
9	580328	0.01	1.50	1.80	5.00	44.00	92.50	99.90	100.00	100.00	100.00
10	580410	0.01	0.00	0.00	1.00	32.00	93.00	99.90	100.00	100.00	100.00
11	580427	0.01	4.70	6.30	12.00	46.00	97.80	99.90	100.00	100.00	100.00
12	580520	0.01	0.00	0.00	7.50	38.50	96.00	99.90	100.00	100.00	100.00
13	580527	0.01	0.00	0.00	1.00	16.50	88.00	99.90	100.00	100.00	100.00
14	580604	0.01	0.00	0.00	0.00	11.00	93.50	99.90	100.00	100.00	100.00
15	580613	0.01	0.00	1.00	9.60	33.00	87.50	99.90	100.00	100.00	100.00
16	580624	0.01	0.00	0.00	2.00	21.00	87.50	99.90	100.00	100.00	100.00
17	580705	0.01	0.00	1.00	4.00	40.00	87.50	99.90	100.00	100.00	100.00
18	580716	0.01	0.00	1.20	5.50	28.00	93.50	99.90	100.00	100.00	100.00
19	580814	0.01	4.50	8.00	12.50	30.00	85.00	99.90	100.00	100.00	100.00

Table 6.5. Yellow River Data at Tuchengzi of Long and Liang (1994) (continued)

Data No. (1)	Run ID (2)	Size distribution of transported sediment, finer than indicated diameters Grp1 (%) (26)	Grp2 (%) (27)	Grp3 (%) (28)	Grp4 (%) (29)	Grp5 (%) (30)	Grp6 (%) (31)	Grp7 (%) (32)	Grp8 (%) (33)	Grp9 (%) (34)
		0.005	**0.01**	**0.025**	**0.05**	**0.1**	**0.25**	**0.5**	**1**	**2mm**
1	570828	24.5	34.0	53.9	71.4	94.4	100.0	100.0	100.0	100.0
2	570918	20.9	28.5	42.7	64.1	93.0	100.0	100.0	100.0	100.0
3	570926	21.2	28.2	43.7	67.0	96.1	100.0	100.0	100.0	100.0
4	571008	17.0	25.0	46.4	74.8	97.2	100.0	100.0	100.0	100.0
5	571018	15.5	22.7	36.3	56.9	93.9	100.0	100.0	100.0	100.0
6	571027	11.4	16.5	25.8	42.1	86.9	100.0	100.0	100.0	100.0
7	571104	7.8	11.9	22.9	46.1	93.1	100.0	100.0	100.0	100.0
8	580319	5.8	11.3	27.9	53.2	97.6	99.9	100.0	100.0	100.0
9	580328	6.5	13.6	24.5	42.2	89.6	99.9	100.0	100.0	100.0
10	580410	4.9	8.3	19.8	49.6	95.6	99.9	100.0	100.0	100.0
11	580427	4.0	6.7	11.8	32.5	87.3	99.9	100.0	100.0	100.0
12	580520	14.2	19.7	28.1	46.9	88.9	99.9	100.0	100.0	100.0
13	580527	21.0	27.8	31.3	45.5	92.1	100.0	100.0	100.0	100.0
14	580604	1.5	2.0	2.4	9.9	80.3	99.8	100.0	100.0	100.0
15	580613	22.4	26.1	28.9	36.8	91.5	99.9	100.0	100.0	100.0
16	580624	24.6	27.4	29.5	39.3	82.0	99.9	100.0	100.0	100.0
17	580705	7.5	11.0	16.4	31.5	91.0	99.9	100.0	100.0	100.0
18	580716	22.7	33.2	55.6	78.2	97.0	99.9	100.0	100.0	100.0
19	580814	33.2	43.6	60.9	79.1	98.4	100.0	100.0	100.0	100.0

Table 6.6 Comparison between Computed and Measured Size Fractions of Sediment in Transport (*Bed-Material Load*) for the 20 Sets of Flume Data from White and Day (1982)

Fractional Bed-Material Load Computation Method	Data in Range of Discrepancy Ratio, R_i (%)				Mean Normalized Error, MNE (%)	Average Geometric Deviation, AGD	No. of Data Points
	0.75-1.25	0.5-1.5	0.25-1.75	0.5-2.0			
(1)	(2)	(3)	(4)	(5)	(6)	(7)	(8)
a) Direct computation by size fraction approach							
Einstein's equation (1950)	4.7	8.0	14.6	12.7	187.3	4083.0	212
Laursen's equation (1958)	25.5	39.2	46.7	45.8	76.7	8.09	212
Toffaleti's equation (1968)							
b) BMF approach using							
Engelund and Hansen's equation (1967)	20.8	49.1	78.3	57.1	75.8	1.99	212
Ackers and White's equation (1973)	27.8	43.4	60.8	49.5	76.3	2.85	212
Yang's equation (1973)	30.2	56.6	64.2	62.7	60.1	4.03	212
Karim's modified BMF method (1998)	17.5	42.9	51.9	47.6	648.2	7.21	212
c) TCF approach using							
Function of Karim and Kennedy (1981)	50.5	78.3	82.1	83.0	162.4	1.62	212
Function of Li (1988)	2.0	5.2	9.9	7.1	130.1	117.1	212
Proposed function of Eq. (3.9)	34.0	64.2	78.8	73.6	66.4	1.89	212
Proposed function of Eq. (3.24)	32.1	63.7	77.8	69.8	86.1	1.92	212

Table 6.7. Comparison between Computed and Measured Size Fractions of Sediment in Transport (*Bed-Material Load*) for the 28 Sets of Data from Rio Grande Conveyance Canal and Yellow River at Tuchengzi.

Fractional Bed-Material Load Computation Method	Data in Range of Discrepancy Ratio, R_i (%)				Mean Normalized Error, MNE (%)	Average Geometric Deviation, AGD	No. of Data Points
	0.75-1.25	0.5-1.5	0.25-1.75	0.5-2.0			
(1)	(2)	(3)	(4)	(5)	(6)	(7)	(8)
a) Direct computation by size fraction approach							
Einstein's equation (1950)	9.6	25.2	41.7	37.4	593.0	14.64	115
Laursen's equation (1958)	25.4	35.7	52.2	47.8	78.0	4.30	115
Toffaleti's equation (1968)	14.8	22.6	41.7	32.2	108.3	5.49	115
b) BMF approach using							
Engelund and Hansen's equation (1967)	22.6	45.2	67.0	54.8	66.7	2.28	115
Ackers and White's equation (1973)	9.6	19.1	35.7	27.0	179.3	8.39	115
Yang's equation (1973)	20.0	37.4	60.9	49.6	84.1	2.75	115
Karim's modified BMF method (1998)	17.4	27.0	42.6	34.8	115.7	6.62	115
c) TCF approach using							
Function of Karim and Kennedy (1981)	8.7	17.4	30.4	23.5	183.6	39.60	115
Function of Li (1988)	22.6	43.5	57.4	54.8	65.7	3.81	115
Proposed function of Eq. (3.9)	45.2	67.0	81.7	79.1	51.0	1.58	115
Proposed function of Eq. (3.24)	27.0	52.2	76.5	64.4	78.7	1.93	115

CHAPTER 7

SUMMARY AND CONCLUSIONS

7.1 SUMMARY

In this dissertation, a new method for predicting fractional transport rates of bed-material load in sand-bed channels is presented. The proposed method is developed based on the concept of the transport capacity fraction (TCF) approach expressed by Eq. (2.8). The bed-material concentration for a given size fraction is obtained by weighting the bed-material concentration, C_t, with the newly developed transport capacity distribution function, P_{ci}, from Eqs. (3.9) or (3.24). The first transport capacity distribution function given by Eq. (3.9) depends on relative fall velocity. The associated coefficients are given by Eqs. (3.12)-(3.14). The second transport capacity distribution function given by Eq. (3.24) depends on relative diameters. The associated coefficients are given by Eqs. (3.25)-(3.27). The procedure and a detailed example problem showing the use of the proposed method are provided.

For the computation of bed-material concentrations, the effect of size gradations on the transport of sediment mixtures is investigated in detail. First, Eq. (4.3) is proposed for predicting the median diameter, D_{50t}, of bed-material load. Then, the effect of size gradations on the transport of sediment mixtures is demonstrated by the use of Engelund and Hansen's transport function and Yang's unit stream power function. To compensate for the size gradation effect, the median diameter, D_{50t}, is proposed for use as the representative size for bed-material load computations. For the existing bed-material load equations, an equivalent diameter, D_e, expressed by Eq. (4.6), is proposed. This equivalent diameter, which is related to D_{50t}, is incorporated into the Engelund and Hansen, Ackers and White, and Yang formulas for the computation of bed-material concentrations.

A comprehensive comparison and evaluation of the proposed fractional load computation method with various existing fractional transport methods is conducted based on the available flume and field data. Statistical analysis and graphical comparisons are utilized to qualitatively and quantitatively demonstrate the performance and variations in different methods.

Sources of data and their flow and sediment properties used in the analysis are summarized as follows:

1) *Data for the development and verification of fractional bed-material load computation method*

For the development of new transport capacity distribution functions of Eqs. (3.9) and (3.24), a data base with 118 sets of flume and field data containing a total of 891 points is collected from different sources available in the literature. Each set of data contains a complete record for flow and sediment information, including the size distributions of bed material and transported sediments, pertaining to each measurement. This data base is limited to sand sizes with median diameter in the range of 0.10 to 0.90 mm, geometric standard deviation of bed material in the range of 1.30 to 3.0, flow discharge in the range of 0.0056 to 16.06 m^3/s, flow velocity in the range of 0.49 to 1.41 m/s, flow depth in the range of 0.056 to 0.58 m, and slope in the range of 0.00093 to 0.013. A summary of these data is given in Table 3.1, and detailed information for each data set are provided in Tables 3.2-3.6.

In the verification of the proposed transport capacity distribution functions, an independent data base with 48 sets of flume and field data, which contain a total of 327 data points, was compiled. This independent data base covers flow and sediment conditions with median diameter of 0.055-2.06 mm, geometric standard deviation of 1.30-3.89, flow discharge of 0.19 - 3980.0 m^3/s, flow velocity of 0.44 - 2.81 m/s, flow depth of 0.11-1.91 m, and slope of 0.000078-0.0037. Detailed data information are provided in Tables 6.3-6.5.

2) *Data for the analysis and verification of median diameters of sediment in transport and the effect of size gradations on the transport of sediment mixtures*

In the development of a prediction equation for median diameters of bed-material load and the analysis of the effect of size gradations on the transport of sediment mixtures, the 118 sets of data collected for the development of transport capacity distribution functions plus another 280 sets of flume data from CSU were used. For verifying the variation of median diameters of sediment in transport with size gradations, an independent database with 124 sets of flume and field data were compiled. These independent data cover flow and sediment conditions with median diameter of 0.055-2.10 mm, geometric standard deviation of 1.25-4.06, flow discharge of 0.0037-3980, flow velocity of 0.19-2.81, flow depth of 0.062-1.91, and slope of 0.000078-0.0039.

7.2 CONCLUSIONS

The following conclusions are drawn from this study:

1. Research on fractional sediment transport of nonuniform sediment mixtures can be classified into four categories: direct computation by size fraction approach; shear stress correction approach; the BMF approach; and the TCF approach. This

classification is very useful for the analysis and understanding of the problem. The TCF approach relates the fractional transport rate to the bed-material transport capacity and to the transport capacity distribution function. It computes sediment transport rate corresponding to each size group by weighting the bed-material concentration with the transport capacity distribution function. Through the use of the TCF formulations given by Eq. (2.8), discrepancies in computing bed-material load due to the distribution and number of class intervals can be avoided. Also due to the form of Eq. (2.8), errors made in fractional transport computations (e.g., extremely high transport rate for finest fractions) are limited.

2. The transport capacity distribution function, P_{ci}, in the TCF approach can be related to both hydraulic conditions and sediment properties. By introducing proper parameters in the determination of P_{ci}, the effects due to the presence of other size fractions in sediment mixtures on the transport of a given size fraction can be reflected. The literature review shows that the sheltering and exposure correction factor is mainly related to relative sediment sizes (D_i/D_{50}, D_i/D_a, D_i/D_A, D_i/D_u, D_i/D_n, etc.), size gradation (M, σ_g), and flow intensity (V/V_*, d/D_{50}, etc.). This understanding is essential for incorporating the sheltering and exposure effects in the formulations of transport capacity distribution function, P_{ci}.

3. The proposed transport capacity distribution functions are derived from combinations of theoretical derivation and physical considerations. The first function of Eq. (3.9) depends on fall velocity, which is derived from the unit stream power theory and the concepts of the TCF approach and the bed material fraction (BMF) approach. The second function of Eq. (3.24) depends on relative diameter, which is derived from

Engelund and Hansen's transport relations and the concepts of the TCF approach and the BMF approach. The sheltering and exposure effects are considered in both functions by including a second term in their derivations.

4. Fractional bed-material concentration (C_{ti}) comparisons indicate that the proposed method gives the best predictions for the118 sets of flume and field data (containing 891 points) used in the comparison. By using the Yang equation with D_e and the newly proposed transport capacity distribution functions of Eqs. (3.9) and (3.24), 78% and 77% of data can be accounted for within the range of discrepancy ratios between 0.25 and 1.75 (up from 36.0-68.5% for other methods), respectively. The discrepancy ratios for the proposed method are normally distributed and concentrated around the perfect agreement.

5. Transport capacity fraction (P_{ci}) comparisons using the118 sets of flume and field data indicate that the proposed method gives the best predictions for the data used in the comparison. 79% of data can be accounted for within the range of discrepancy ratios between 0.25 and 1.75 (compared to 46-70% for other methods) by the use of the proposed transport capacity distribution functions of Eqs. (3.9) and (3.24). A close agreement between computed and measured values is obtained for all ranges of P_{cmi} values using both Eqs. (3.9) and (3.24). Overall, the Einstein method underpredicts the transport rate for finer sizes and overpredicts for the coarser size fractions, while the other methods overestimate the finer fractions and underestimate the coarser fractions. An independent test using another 48 sets of flume and filed data (327 data points) shows that the proposed method ranks at the top among all the methods compared.

6. The size composition of sediment in transport is different from the size composition of bed-surface material. The median diameter of sediment in transport is generally finer than the median diameter of bed material, which results from selective transport of grains by flow. The median size of bed-material load, D_{50t}, can be predicted by Eq. (4.3), which is a function of not only median size of bed material, but also the size gradation of bed material and flow intensity. The relative median size of sediment in transport, D_{50t}/D_{50}, decreases as size gradation increases, and the relationship between them can be represented by Eq. (4.4).

7. Considering the physical processes governing the transport of sediment mixtures, the geometric standard deviation, σ_g, which represents the range of particle sizes present in the bed material, is found to be a significant additional parameter. For the same flow condition and the same D_{50}, the sediment size in transport and the transport rate of sediment mixtures are different for different sediment size gradations. For a given flow condition and median bed-material size, as the size gradation increases, the size of sediment in transport decreases, resulting in higher sediment transport rates.

8. The median diameter D_{50t} (equivalent diameter, D_e, for the existing bed-material load formulas) is a better indicator for nonuniform bed material. Using D_{50t} (D_e) will produce a more accurate prediction of bed-material discharge for nonuniform sediment mixtures.

9. The effects of bed material size gradations on transport of sediment mixtures cannot be reflected appropriately by a single fixed size, such as D_{35} or D_{50}. Bed-material load formulas such as those developed by Engelund and Hansen, Ackers and White, and Yang are based on a single representative size of bed material and may generate

considerable scatter when applied to nonuniform sediment mixtures. By introducing D_e, which is related to D_{50t}, into bed-material load computations for the 118 data sets, the improvement in the range of discrepancy ratios between 0.25 and 1.75 was from 73% to 89% for the Engelund and Hansen formula, from 74% to 82% for the Ackers and White formula, and from 83% to 98% for the Yang formula. Independent verification using 54 sets of CSU flume data also shows significant improvement in bed-material load computations by the use of D_e.

7.3 RECOMMENDATIONS

Among the numerous research topics which are recommended for future studies, the author would like to concentrate on the following subjects:

1. Applicability of the transport capacity distribution functions proposed in the present study should be tested for a wider range of flow and sediment conditions, including highly graded bed material and large natural rivers.
2. The conceptual model and formulations proposed in this study should be extended to studies on the fractional transport of gravel bed material, where the sheltering and exposure effect are more pronounced. If necessary, the effective shear stress concept should be included.
3. Partial transport processes should be taken into account in the formulations of transport capacity distribution function in cases where the sediment particles are not fully mobilized.
4. The proposed method for fractional bed-material load computation should be incorporated into numerical models to simulate the change of bed composition and

hydraulic sorting for sand-bed materials.

5. Research for predicting bed-material transport rate for sand-bed materials by the use of predicted median diameters of sediment in transport as representative size should be conducted.

REFERENCES

Ackers, P. and White, W. R. (1973). "Sediment Transport: New Approach and Analysis," Journal of Hydraulic Division, ASCE, Vol. 99, No. HY11, pp. 2041-2060.

Alonso, C. V. (1980). "Selecting a Formula to Estimate Sediment Transport Capacity in Nonvegetated Channels," CREAMS - *A Field Scale Model for Chemicals, Runoff, and Erosion from Agriculture Management System*, Conversation Research Report, No. 26, W. G. Knisel, ed., U. S. Department of Agriculture, Washington D. C., pp. 426-439.

ASCE Task Committee on Relations between Morphology of Small Streams and Sedimentation of the Hydraulics Division (1982). "Relationships between Morphology of Small Streams and Sediment Yield," Journal of Hydraulics Division, ASCE, Vol. 108, No. 11, pp. 1328-1365.

Ashida, K. and Michiue, M. (1973). "Study on Bed Load Transport Rate in Open Channel Flows," International Symposium on River Mechanics, IAHR, Bangkok, Thailand, pp. A36-1-12.

Bridge, M. and Bennett, S. J. (1992). "A Model for the Entrainment and Transport of Sediment Grains," Water Resources Research, Vol. 28, No. 2, pp. 337-363.

Brownlie, W. R. (1981). "Prediction of Flow Depth and Sediment Discharge in Open Channels," W. M. Keck Laboratory of Hydraulics and Water Resources, California Institute of Technology, Pasadena, Calif., 232 pp.

Colby, B. R. and Hembree, C. H. (1955). "Computations of Sediment Discharge, Niobrara River near Cody, Nebraska," U.S. Geological Survey Water Supply Paper 1357.

Culbertson, J. K., Scott, C. H., and Bennett, J. P. (1972). "Summary of Alluvial-Channel Data From Rio Grande Conveyance Channel, New Mexico, 1965-69," U. S. Geological Survey Professional Paper 562-J.

Diplas, P. (1987). "Bedload Transport in Gravel-Bed Streams," Journal of Hydraulic Engineering, ASCE, Vol. 113, No. 3, pp. 277-292.

Dorough, W. G., Holly, F. M., and Wei, T. (1988). "IALLUVIAL Sediment Routing

Model," Twelve Selected Computer Stream Sedimentation Models Developed in the United States, Edited by Shou-shan Fan, Interagency Ad Hoc Sedimentation Work Group, Subcommittee on Sedimentation, Interagency Advisory Committee on Water Data, Federal Energy Regulatory Commission, pp.79-94.

Dou, G., Zhao, S., and Huang, Y. (1987). "A Study on Two Dimensional Mathematical Model of Total Load Transport in Streams," Proc. of the National Symp. on the Mathematical Model of Sediment Transport (in Chinese), Wuhan, China.

Einstein, H. A. (1944). "Bed Load Transportation in Mountain Creek," Technical Paper No. 55, Soil Conservation Service, United States Department of Agriculture.

Einstein, H. A. (1950). "The Bed Load Function in Open Channel Flows," Technical Bulletin No.1026, United States Department of Agriculture, Soil Conservation Service.

Einstein, H. A. and Chien, N. (1953). "Transport of Sediment Mixtures with Large Ranges of Grain Sizes," MRD Sediment Series No.2, U.S. Army Engineer Division, Missouri River, Corps of Engineers, Omaha, Neb.

Einstein, H. A. (1978). "Sediment Transport Data in Laboratory Flumes," International Research and Training Center on Erosion and Sedimentation, Publication Circular No.2, Beijing, China.

Egiazaroff. I. V. (1965). "Calculation of Nonuniform Sediment Concentrations," Journal of Hydraulic Division, ASCE, Vol. 91. No. HY4, pp. 225-247.

Engelund, F. and Hansen, E. (1967). "A Monograph on Sediment Transport in Alluvial Streams," Danish Technical Press (Teknish Forlag).

Garde, R. J. and Ranga Raju, K. G. (1985). "Mechanics of Sediment Transportation and Alluvial Steam Problems," Second Edition, John Wiley & Sons, Inc. New York, p. 237.

Guy, H. P., Simons, D. B., and Richardson, E. V. (1966). "Summary of Alluvial Channel Data from Flume Experiments, 1956-1961," U.S. Geological Survey Professional Paper 462-I.

Han, Q. W. (1973). "Preliminary Studies on the Non-Equilibrium Transport of Sediment in Reservoir," Report on Sedimentation in Reservoirs, Wuhan, China (in Chinese), pp. 145-168.

Han, Q. W. (1980). "A Study on the Non-Equilibrium Transport of Suspended Load," Proceedings of the International Symposium on River Sedimentation, Beijing, China, Vol. 2, pp. 793-802.

Hayashi, T., Ozaki, S., and Ichibashi, T. (1980). "Study on Bedload Transport of Sediment Mixtures," Proc. 24th Japanese Conference on Hydraulics.

Holly, F. M. (1988). "CHARIMA and SEDICOUP Codes for Riverine-Bed Simulation," Twelve Selected Computer Stream Sedimentation Models Developed in the United States, Edited by Shou-shan Fan, Interagency Ad Hoc Sedimentation Work Group, Subcommittee on Sedimentation, Interagency Advisory Committee on Water Data, Federal Energy Regulatory Commission, pp. 263-352.

Holly, F. M. and Karim, M. F. (1986). "Simulation of Missouri River Bed Degradation," Journal of Hydraulic Engineering, ASCE, Vol. 112, No. 6, pp. 497-517.

Holly, F. M. and Rahuel J. L. (1990). "New Numerical/Physical Framework for Mobile-Bed Modeling," Journal of Hydraulic Research, Vol. 28, No. 4, pp. 401-416.

Hsu, S. M. and Holly, F. M. (1992). "Conceptual Bed-Load Transport Model and Verification for Sediment Mixtures," Journal of Hydraulic Engineering, ASCE, Vol. 118, No. 8, pp. 1135-1152.

Hubbel, D. W. and Matejka, D. Q. (1959). "Investigation of Sediment Transportation, Middle Loup River at Dunning, Nebraska," U.S. Geological Survey Water Supply Paper 1476.

Julien P. Y. (1995). "Erosion and Sedimentation," Cambridge University Press, London, England, pp. 204-205.

Karim, M. F. and Kennedy, J. F. (1981). "Computer-Based Predictors for Sediment Discharge and Friction Factor of Alluvial Streams," Iowa Institute of Hydraulic Research Report No. 242, University of Iowa, Iowa City, Iowa.

Karim, M. F. and Kennedy, J. F. (1982). "IALLUVIAL: A Computer-Based Flow- and Sediment-Routing for Alluvial Stream and Its Application to the Missouri River," Iowa Institute of Hydraulic Research Report No. 250, University of Iowa, Iowa City, Iowa.

Karim, M. F. (1985). "IALLUVIAL: Analysis of Sediment Continuity and Application to the Missouri River," Iowa Institute of Hydraulic Research Report No. 292, University of Iowa, Iowa City, Iowa.

Karim, M. F. (1998). "Bed Material Discharge Prediction for Nonuniform Bed Sediments," Journal of Hydraulic Engineering, ASCE, Vol. 124, No. 6, pp. 597-604.

Kircher, J. E. (1983). "Interpretation of Sediment Data for The South Platte River in Colorado and Nebraska, and the North Platte and Platte Rivers in Nebraska," U.S. Geological Survey Professional Paper 1277-D.

Laursen, E. M. (1958). "The Total Sediment Load of Streams," Journal of Hydraulic Division, ASCE, Vol. 84, No. HY1, pp. 1-36.

Li, Y., (1988). "A Study on the Computation of Two Dimensional Deformations in Streams," Sediment Research (in Chinese), No. 1.

Long, Y., and Liang, G. (1994). "Data Base of Sediment Transport in the Yellow River." Technical Report No. 94001, Institute of Hydraulic Research, Yellow River Conservation Commission, Zhengzhou, P. R. China, 15 pp. (in Chinese).

Meyer-Peter, E. and Müller, R. (1948). "Formula for Bed Load Transport," Proc. 2nd. Meeting, Intern. Assoc. Hyd. Res., Vol. 6.

Misri, R. L., Garde, R. J., and Ranga Raju, K. G. (1984). "Bed Load Transport of Coarse Nonuniform Sediment," Journal of Hydraulic Engineering, ASCE, Vol. 110, No. 3, pp. 312-328.

Molinas, A., and Yang, C. T. (1986). "Computer Program User's Manual for GSTARS (Generalized Stream Tube model for Alluvial River Simulation)," U.S. Department of the Interior, Bureau of Reclamation, Engineering and Research Center, Denver, Colorado, 142 pp.

Molinas, A. (1990). "User's Manual for BRI-STARS (Bridge Stream Tube Model for Alluvial River Simulation)," National Cooperative Highway Research Program, Project No. HR 15-11, Transportation Research Board, Washington, D.C.

Molinas, A., and Trent, R. (1991). "BRI-STARS - BRIdge Stream Tube model for Alluvial River Simulation," Proceedings of the 5th Interagency Sedimentation Conference, Sedimentation Committee of the Water Resources Council.

Molinas, A. (1993). "BRI-STARS Model for Alluvial River Simulation," Hydraulic Engineering, Proceedings of the 1993 National Conference, ASCE.

Molinas, A., and Wu, B. (1997). "Non-equilibrium Sediment Transport Modeling of Sanmenxia Reservoir," Energy and Water: Sustainable Development, Proceedings of Theme D, the 27th Congress of International Association for Hydraulic Research, San Francisco, California, pp.126-131.

Molinas, A. and Wu, B. (1998). "Effect of Size Gradation on Transport of Sediment Mixtures," Journal of Hydraulic Engineering, ASCE, Vol. 124, No. 8, pp. 786-793.

Nordin, C, F. (1989). "Application of Engelund-Hansen Sediment Transport Equation in Mathematical Models", Fourth International Symposium on River Sedimentation, Beijing, China, pp. 611-616.

Paintal, A. S. (1971). "Stochastic Model for Bed Load Transport," Journal of Hydraulic Research, IAHR, Vol. 9, No. 4, pp. 527-554.

Parker, G., Klingeman, P. C., and McLean, D. G. (1982). "Bedload and Size Distribution in Paved Gravel-Bed Streams," Journal of Hydraulic Division, ASCE, Vol. 108, No. HY4, pp. 544-571.

Parker, G. (1990). "Surface-Based Bedload Transport Relationship for Gravel Rivers," Journal of Hydraulic Research, Vol. 28, No. 4, pp. 417-436.

Patel, P. L. and Ranga Raju, R. G. (1996). "Fractionwise Calculation of Bed Load Transport," Journal of Hydraulic Research, IAHR, Vol. 34, No. 3, pp. 363-379.

Pemberton, E. L. (1972). "Einstein's Bedload Function Applied to Channel Design and Degradation," Ch. 16 in Sedimentation, Symposium to Honor Prof. H. A. Einstein, Edited and Published by H. W. Shen, Fort Collins, Colorado.

Proffitt, G. J. and Sutherland, A. J.(1983). "Transport of Nonuniform Sediment," Journal of Hydraulic Research, IAHR, Vol. 21, No. 1, pp. 33-43.

Qu, X., Wu, B., Zhang, Q., and Han, Q. (1994). "Preliminary Study on One-Dimensional Model of Reservoirs on the Yellow River," Journal of the Yellow River (in Chinese), No. 1, Yellow River Press, Zhengzhou, China.

Rahuel, J. L., Holly, F. M., Chollet, J. P., Belleudy, P. J., and Yang, G. (1989). "Modeling of Riverbed Evolution for Bedload Sediment Mixtures," Journal of Hydraulic Engineering, ASCE, Vol. 115, No. 11, pp. 1521-1542.

Raudkivi, A. J. (1990). "Loose Boundary Hydraulics," Third Edition, Pergamon Press, Oxford, England.

Ribberink, J. S. (1987). "Mathematical Modeling of One-Dimensional Morphological Change in Rivers with Non-Uniform Sediment," Communication of Hydraulic and Geotechnical Engineering, Report No. 87-2, Delft University Technology.

Samaga, B. R., Ranga Raju, K. G., and Garde, R. J. (1986a). "Bed Load Transport of Sediment Mixtures," Journal of Hydraulic Engineering, ASCE, Vol. 112, No. 11, pp. 1003-1018.

Samaga, B. R., Ranga Raju, K. G., and Garde, R. J. (1986b). "Suspended Load Transport of Sediment Mixtures," Journal of Hydraulic Engineering, ASCE, Vol. 112, No.11, pp. 1019-1035.

Shen, H. W., and Rao, C. X. (1991). "Transport of Uniform and Non-uniform Sediment Sizes," Proceedings of the Fifth Federal Interagency Sedimentation Conference, Vol. I, Las Vegas, Nevada, 4-162-169.

Simons, D. B., and Sentürk, F. (1992). "Sediment Transport Technology: Water and Sediment Dynamics," Revised Edition, Water Resources Publications, Littleton, Colorado.

Smart, G. M, and Jaeggi, M. N. R. (1983). "Sediment Transport on Steep Slopes," Mitteilungen der Versuchsanstalt für Wasserbau, Hydrologie und Glaziologie, Nr. 64, Zürich.

Stevens, H. H. and Yang, C. T. (1989). "Summary and Use of Selected Fluvial Sediment-Discharge Formulas," U. S. Geological Survey Water Resources Investigations Report 89-4026, Denver, Colorado.

Taylor, B. D. and Vanoni, V. A. (1972). "Temperature Effects in High Transport, Flat-Bed Flows," Journal of Hydraulics Division, ASCE, Vol. 98, No. HY12, pp. 2191-2206.

Toffaleti, F. B. (1968). "A Procedure for Computation of the Total River Sand and Detailed Distribution, Bed to Surface." Technical Report No. 5, Committee on Channel Stabilization, U. S. Army Corps of Engineers Waterways Experiment Station, Vicksburg, Miss., 177pp.

Toffaleti, F. B. (1969). "Definitive Computations of Sand Discharge in River." Journal of Hydraulic Division, ASCE, Vol. 95, No. HY1, pp. 225-246.

Thomas, W. A. (1982). "Mathematical Modeling of Sediment Movement." Gravel-Bed Rivers, Fluvial Processes, Engineering and Management, Edited by R. D. Hey, J. C. Bathurst, and C. R. Thorne, John Wiley and Sons, pp. 487-511.

U. S. Corps of Engineers (1977). "HEC-6 Scour and Deposition in Rivers and Reservoirs, User's Manual," Hydrologic Engineering Center, Davis, CA.

U. S. Inter-Agency Committee on Water Resources, Subcommittee on Sedimentation (1957). "Some Fundamentals of Particle Size Analysis," Report 12 of A Study of Methods Used in Measurement and Analysis of Sediment Loads in Streams, 55 pp.

van Rijn, L. C. (1984). "Sediment Transport, Part II: Suspended Load Transport," Journal of Hydraulic Engineering, ASCE, Vol. 110, No. 11, pp. 1613-1641.

Vanoni, V. A. and Brooks, N. H. (1957). "Laboratory Studies of the Roughness and Suspended Load of Alluvial Streams," Report No. E-68, Sedimentation Laboratory, California Institute of Technology, Pasadena, California.

Vanoni, V. A. and Hwang, L. S. (1967). "Relation between Bed Forms and Friction in Streams," Journal of Hydraulics Division, ASCE, Vol. 93, No. 3, pp. 121-144.

Vetter, M. (1989). "Total Sediment Transport in Open Channel," Report No. 26 of the Institute of Hydrology, University of the German Federal Army (Translated from "Gesamttransport von Sedimenten in offenen Gerinnen" by U. S. Bureau of Reclamation, May 1989).

Vischer, D. (1992). Proceedings of the International Grain Sorting Seminar, October 21-26, 1991, Centro Stefano Francscini, Monte Verità, Ascona, Switzerland.

Wang, S., Zhang. R. (1990). "Experimental Study on Transport Rate of Graded Sediment," International Conference on River Flood Hydraulics, Edited by W. R. White, John Wiley & Sons Ltd, pp. 299-306.

Wang, S., Zhang, R., and Hui, Y. (1995). "New Equations of Sediment Transport Rate," International Journal of Sediment Research, IRTCES, Vol. 10, No. 3, pp. 1-18.

Wang, S., Cheng, J. and Hui, Y. (1998). "Research on Transport Capacity of Nonuniform Sediment in Open Channels," Journal of Hydraulic Engineering, Chinese Hydraulic Engineering Society, No. 1, 1998, Beijing, China, pp. 1-9 (in Chinese).

White, W. R., Milli, H., and Crabbe, A. D. (1975). "Sediment Transport Theories: A Review," Proc. Instn. Civ. Engrs., Part 2, 59, pp. 265-292.

White, W. R. and Day, T. J. (1982). "Transport of Graded Gravel Bed Material." Gravel-Bed Rivers, Fluvial Processes, Engineering and Management, Edited by R. D. Hey, J. C. Bathurst, and C. R. Thorne, John Wiley and Sons, pp. 181-223

Wilcock, P. R. and McArdell, B. W. (1997). "Partial Transport of a Sand/Gravel Sediment," Water Resources Research, Vol. 33, No. 1, pp. 235-245.

Wilcock, P. R. (1997). "The Components of Fractional Transport Rate," Water Resources Research, Vol. 33, No. 1, pp. 247-258.

Wu, B. (1992a). "A Review on the Research of Sediment Transport." Technical Report No. 92068, Institute of Hydraulic Research, Yellow River Conservation Commission, Zhengzhou, P. R. China, 31 pp. (in Chinese).

Wu, B. (1992b). "Development and Application of Numerical Sediment Transport Models in the Yellow River." Technical Report No. 92075, Institute of Hydraulic Research, Yellow River Conservation Commission, Zhengzhou, P. R. China, 51 pp. (in Chinese).

Wu, B., and Long, Y. (1992). "Comparison and Modification of Sediment Transport Equations in the Yellow River," Proceedings of the First National Symposium on River Sedimentation, November (in Chinese), Beijing, China.

Wu, B., and Long, Y. (1993). "Amendments of Sediment Transport Equations in the Yellow River," Journal of Yellow River (in Chinese), No. 7, Yellow River Press, Zhengzhou, China.

Wu, B. and Molinas, A. (1996). "Modeling of Alluvial River Sediment Transport," Proceedings of the International Conference on Reservoir Sedimentation, Vol. I, Edited by M. L. Albertson, A. Molinas, and R. Hotchkiss, Colorado State University, Fort Collins, Colorado, USA, pp. 281-325.

Wu, B. and Molinas, A. (1998). "SedWin (Visually Interactive Sediment Transport Model for Windows 95/98)," Hydrau-Tech, Inc., Fort Collins, Colorado.

Yang, C. T. (1973). "Incipient Motion and Sediment Transport," Journal of Hydraulic Division, ASCE, Vol. 99, No. HY10, pp. 1679-1704.

Yang, C. T. and Molinas, A. (1982). "Sediment Transport and Unit Stream Power Function," Journal of Hydraulic Division, ASCE, Vol. 108, No. HY6, pp. 774-793.

Yang, C. T., and Wan, S. (1991). "Comparisons of Selected Bed-Material Load Formulas," Journal of Hydraulics Engineering, ASCE, Vol. 117, No. 8, pp. 973-811.

Yang, C. T., Molinas, A., and Wu, B. (1996). "Sediment Transport in the Yellow River," Journal of Hydraulic Engineering, ASCE, Vol. 122, No. 5, pp.237-244.

Yang, C. T. (1996). "Sediment Transport Theory and Practice," The McGraw-Hill Companies, Inc., New York.

Zhang, Q., and Wu, B. (1993). "Numerical Modeling of Sediment Transport in the Lower Yellow River," Journal of Sediment Research (in Chinese), No. 1, Beijing, China.